

# NANOSPAIN 2008

## NANOIBERIAN CONFERENCE

BRAGA PORTUGAL - APRIL 14 - 18 2008



FCT Fundação para a Ciência e a Tecnologia  
MINISTÉRIO DA CIÊNCIA, TECNOLOGIA E ENSINO SUPERIOR



Universidade do Minho

INL

International Baseline Nanotechnology Laboratory

During the last two decades, a revolutionary scientific new age, based on the capacity to observe, characterize, manipulate and organize matter in the nanometric scale, is appearing. In this scale, physics, chemistry, materials science, computational theory, and engineering converge towards the same theoretical principles and experimental findings that are basically governed by the laws of the Quantum Mechanics. Nanotechnology involves these interdisciplinary knowledge areas and methodologies in order to study, manufacture and characterize functional structures with dimensions of tens of nanometers.

In 2008, Spain and Portugal (through their respective networks NanoSpain and PortugalNano) decided to join efforts in order that NanoSpain2008 event facilitate the dissemination of knowledge and promote interdisciplinary discussions not only in Spain but among the different groups from Southern Europe. Other objectives will also be to enhance industrial participation and permit considering the situation of Nanoscience and Nanotechnology in the south of Europe.

In 2008, this event will therefore be organised in collaboration with 3 networks:

- **NanoSpain** (Spain): 240 Spanish groups with around 2000 researchers in total - one of the widest Spanish scientific networks
- **PortugalNano** (Portugal): 188 Portuguese groups
- **C'Nano Grand Sud Ouest** (France): 50 labs and more than 500 researchers

In order to organise the various sessions and to select contributions, the meeting will be structured in the following thematic lines, but interactions among them will be promoted:

1. NanoBiotechnology/Nanomedicine
2. NanoMaterials
3. NanoElectronics/Molecular Electronics
4. NanoChemistry
5. Nanomagnetism
6. NanoPhotonics/NanoOptics
7. Nanotubes
8. NEMS/MEMS
9. Scanning Probe Microscopies (SPM)
10. Infrastructure & Scientific Policy
11. Simulation at the nanoscale



Thematic parallel sessions will also be organised to enhance information flow between participants and in particular:

- Exchange information of current work in specific research areas
- Solve particular technological problems
- Look for areas of common ground between different technologies
- Provide contributions to specific reports

The following Thematic Sessions will be organised:

1. NanoBiotechnology (Coordinators: Jesus M. De la Fuente & Elena Martínez)
2. NanoFabrication (Coordinators: Francesc Pérez-Murano & Fernando Briones)
3. Industrial (Coordinators: José Luís Viviente & Emilio Prieto)
4. NanoChemistry (Coordinators: Jaume Veciana & Nora Ventosa)
5. NanoOptics & NanoPhotonics (Coordinators: Juan José Sáenz & Antonio García Martín)
6. Nanocomposites (Coordinator: Carlos Bernardo)

Finally, thanks must be directed to the staff of all organising institutions whose hard work has helped the smooth organisation and planning of this conference.

## THE ORGANISING COMMITTEE



## NanoSpain2008 Platinum Sponsors

 <p>MINISTERIO DE EDUCACIÓN Y CIENCIA</p>	<p><b>FCT</b> Fundação para a Ciência e a Tecnologia          MINISTÉRIO DA CIÊNCIA, TECNOLOGIA E ENSINO SUPERIOR Portugal</p>
--	--

## NanoSpain2008 Sponsors



## Organising Committee

<b>Xavier Bouju</b>	CEMES-CNRS & C'Nano Grand Sud-Ouest (France)
<b>Fernando Briones</b>	CNM/IMM-CSIC (Spain)
<b>Susana Cardoso</b>	INESC-MN and Instituto Superior Técnico (IST) (Portugal)
<b>Virginia Chu</b>	INESC-MN (Portugal)
<b>Antonio Correia*</b>	Fundación Phantoms (Spain)
<b>Pedro Echenique</b>	Donostia International Physics Center (Spain)
<b>Luis Melo</b>	Fundação para a Ciência e a Tecnologia (Portugal)
<b>Jesús Pérez Conde</b>	Universidad Publica de Navarra (Spain)
<b>Emilio Prieto</b>	Centro Español de Metrologia - CEM (Spain)
<b>Juan José Sáenz</b>	Universidad Autónoma de Madrid (Spain)
<b>Josep Samitier</b>	PCB (Parc Científic de Barcelona) / UB (Universidad de Barcelona) (Spain)
<b>Helena Soares</b>	Instituto Gulbenkian de Ciência and Escola Superior de Tecnologia da Saúde de Lisboa (Portugal)

## Local Organising Committee

<b>Pedro Alpuim</b>	Universidade do Minho (Portugal)
<b>Carlos A. Bernardo</b>	International Iberian Nanotechnology Laboratory - INL (Portugal)
<b>José Rivas</b>	Universidad de Santiago de Compostela (Spain) / INL (Portugal)

## Advisory Board

<b>Sabino Azcarate</b>	Tekniker (Spain)
<b>Mário Barbosa</b>	IBMC/INEB (Portugal)
<b>Carlos Bernardo</b>	INL (Portugal)
<b>Pedro Brogueira</b>	IST (Portugal)
<b>Maria Celeste do Carmo</b>	I3N/Universidade de Aveiro (Portugal)
<b>Jaime Colchero</b>	Universidad de Murcia (Spain)
<b>João Pedro Conde</b>	IST and INESC-MN (Portugal)
<b>Margarida Costa</b>	Universidade de Coimbra (Portugal)
<b>José Covas</b>	Universidade do Minho (Portugal)
<b>Pedro Echenique</b>	Donostia International Physics Center (Spain)
<b>Guilherme Ferreira</b>	Universidade do Algarve (Portugal)
<b>Elvira Fortunato</b>	CENIMAT/I3N (Portugal)
<b>Paulo Freitas</b>	INESC-MN, IST and INL (Portugal)
<b>Rogério Gaspar</b>	Universidade de Lisboa (Portugal)
<b>Javier Méndez</b>	ICMM-CSIC (Spain)
<b>Rodolfo Miranda</b>	Universidad Autónoma de Madrid (Spain)
<b>Pablo Ordejon</b>	Universidad Autónoma de Barcelona (Spain)
<b>Fernando Palacio</b>	Universidad de Zaragoza (Spain)
<b>José Maria Pitarke</b>	CIC nanoGUNE Consolider (Spain)
<b>Emilio Prieto</b>	Centro Español de Metrología (Spain)
<b>Rui Reis</b>	3Bs Research Group / IBB (Portugal)
<b>José Rivas</b>	Universidad de Santiago de Compostela (Spain) / INL (Portugal)
<b>João Rocha</b>	CICECO (Portugal)
<b>Juan José Sáenz</b>	Universidad Autonoma de Madrid (Spain)
<b>Josep Samitier</b>	Parc Científic de Barcelona / UB (Spain)
<b>Conchita Solans</b>	Instituto de Investigaciones Químicas y Ambientales de Barcelona (Spain)
<b>Jaume Veciana</b>	Instituto de Ciencia de Materiales de Barcelona (CSIC) (Spain)
<b>José Luís Viviente</b>	Fundación Inasmet (Spain)

## Technical Organising Committee

<b>Carmen Chacon</b>	Fundación Phantoms (Spain)
<b>Maria Teresa Fernandez</b>	Fundación Phantoms (Spain)
<b>José Luís Roldán</b>	Fundación Phantoms (Spain)
<b>Soraya Serrano</b>	Fundación Phantoms (Spain)

\* Contact person: Antonio Correia – [antonio@phantomsnet.net](mailto:antonio@phantomsnet.net)



## Exhibitors



**Nanotec Electrónica** is a company devoted to the design, construction and development of **Scanning Probe Microscopes** and related devices. It is well known that nanotechnology is currently one of the most promising fields in technology. For both fundamental and technological reasons, nanoscience will be the cornerstone of research in coming years. Scanning Probe Microscopes are the main tool used to explore the wonderful nanoscopic world.

Nanotec Electrónica is now distributing **siesta**, a well known linear-scaling density-functional method. This distribution is only for non academic institutions. For further information about this software package, please [contact us](#).

While Nanotec Electrónica is mainly oriented towards scientific market, we sustain strong connections with the industrial world. Our microscopes cover a very wide range of applications.

If you have any questions, or want any information about Nanotec Electrónica, please contact us at:

Centro Empresarial Euronova 3  
Ronda de Poniente, 2  
Edificio 2 - 1ª Planta - Oficina A  
28760 Tres Cantos (Madrid) **SPAIN**  
Fax: +34-918 043 348  
<http://www.nanotec.es>



### Solutions for Nanoscale Surface Analysis

With excellent know-how in the new and fast growing fields of nanoscience and materials science, **Schaefer Techniques** has become a leading supplier of reliable scientific equipments. The strength of our European Group lies in our capability to propose you the most comprehensive range of **Scanning Probe Microscopes**: from the easy-to-use AFM or STM to the custom UHV system as a total solution for surface analysis research. With **RHK, NANOSURF & QUESANT**, we have concentrated our efforts in providing you very innovative instruments such as Turnkey UHV STM/AFM system, Cryogenic STM/AFM, universal SPM controller & software, portable AFMs, low-cost educational systems, unique AFM/SECM Dual Modes combination, ambient universal SPM with plug-in probe modules or interesting options like nanolithography and liquid cell. The available key **modes** in this product line are: STM, Contact AFM, Intermittent Contact AFM, Phase contrast, Spreading Resistance, EC-AFM/STM, SECM (Scanning ElectroChemical Microscopy), MFM, EFM, SCM and LFM. **Additional techniques** for surface science complete our SPM solutions: optical profilers, topomicroscopes, LEED/AES systems, ion guns & thin film properties measurement devices. Thanks to our highly qualified team of engineers based in Europe, we are today in position to recommend the optimum system that will meet your **specific requirements** and bring you all the technical support you need. This includes project definition, technical specifications & validation tests. purchasing, training : and after sales.

**Schaefer Techniques Sarl**  
1, rue du Ruisseau Blanc  
ZA de Lunézy  
91620 Nozay - France  
Phone: +33 (0)1 64 49 63 50  
Fax: +33 (0)1 69 01 12 05  
E-mail : [info@schaefer-tech.com](mailto:info@schaefer-tech.com)  
WEB : [www.schaefer-tech.com](http://www.schaefer-tech.com)

Holding:  
**SCHAEFER Holding AG**  
Group Members:  
**SCHAEFER Technologie GmbH (Germany)**  
**SCHAEFER-TEC AG (Switzerland)**

DIAS DE SOUSA, started its activities in 1983 and signed its first exclusive contract to distribute nanotechnology equipment in Portugal with Topometrix exactly 10 years later in June 1992. It has organized the first conference in Portugal about Scanning Probe Microscopy between the 14th and the 16th of September of that year (1992).

Dias de Sousa has also been the first and as far as we know the only company in Portugal which developed with the Universidade Nova de Lisboa, starting in September 1997, a liquid cell for SNOM, being the Director of this 3-year Praxis Project in cooperation with that University.

Today after 25 years of activity and with its unique history in Portugal in the nanotechnology world, DIAS DE SOUSA became a leading distributor of scientific and analytical instrumentation in Portugal, working with world class manufacturers in this area as exclusive distributor for Portugal, like Skyscan, Bruker Group, etc. We highlight of course our Iberian responsibilities in the exclusive distribution for Spain and Portugal of the most talented and reliable manufacturer of nanotechnology instrumentation: NT-MDT. NT-MDT enjoys an 18-year history dedicated to this field having developed SPM's from the simple equipment for education to the most sophisticated and complete system for scientific research, industry and nanotechnology centres.

Dias de Sousa and NT-MDT are certified companies following ISO 9001:2000 since 2003 and 2005 respectively. NT-MDT has received in 2006 one prestigious R&D 100 award for its famous NTEGRA SPM based systems.

DIAS DE SOUSA - Instrumentação Analítica e Científica SA  
Rua dos Jasmins, Nº 541  
Parque Industrial do Batel  
2890-189 Alcochete  
Portugal  
Tel: +351 219 533 120  
Fax: +351 219 533 129  
General E-Mail: [ds@dias-de-sousa.pt](mailto:ds@dias-de-sousa.pt)  
Website: [www.dias-de-sousa.pt](http://www.dias-de-sousa.pt)



ScienTec is specialized in the distribution of rigorously selected scientific equipments dedicated to near field surface analysis : AFM, STM, SNOM, Optical Interferometry...

ScienTec objectively studies your individual needs, advises you and proposes the right product for your application, from our product range. We can provide a specific service, with dedicated engineers for after-sales follow-up and support. ScienTec has the in-house expertise to analyse your problem and resolve it, by designing solutions using products and accessories from our range of electronics, optics, mechanics and data processing.

Molecular Imaging is dedicated to providing innovative scanning probe microscopy (SPM) solutions for all academic research and industrial applications. The new PicoPlus microscope is the "all-in-one" solution for applications such as biology, polymers, nanomaterials, electrochemistry...etc, and integrates a number of imaging techniques, such as Scanning Tunneling Microscopy (STM), Low Current STM, Contact Atomic Force Microscopy (AFM), MacMode AFM, including phase imaging, acoustic AC AFM, Lateral Force Microscopy, Current-Sensing AFM, Pulsed Force Mode (PFM), Magnetic Force Microscopy (MFM)...etc.

Phase Shift is a manufacturer of 3D non-contact surface metrology instruments. The MicroXAM optical interferometer allows to measure step heights, roughness, waviness, flatness and microstructures etc..., and it is dedicated to many applications such as biomedical optics, hard disks and magnetic media, general optics, semi conductors, polymers, MEMS...etc.

Please contact us at [info@scientec.fr](mailto:info@scientec.fr) or visit our web page [www.scientec.fr](http://www.scientec.fr) for more information.



**TELSTAR INSTRUMAT, S.L.** develops high technology instrumentation sales for research and industry, offering suitable technological tools adapted to each application, in order to improve the scientific researches or productive processes of our clients. In these last few years, TELSTAR INSTRUMAT has strengthened its activities representing leading companies in Spain & Portugal in the following applications:

- Surface and material characterisation
- Vacuum and cryogenics instrumentation and technology
- Radiometry and photometry
- Particle counting

**TELSTAR INSTRUMAT, S.L.** counts amongst its customers the principal Official Organisation Investigation Centres and private customers in the microelectronic, aerospace, automotive, optical, food and pharmaceutical industries and in innovative fields such as biotechnology and nanofabrication.

Some of our principals that are specifically of interest for the attendees to this conference are listed below:

- Veeco Instruments (SPM, Optical and Mechanical Profilers)
- Micromaterials Ltd (Nanoindentation Systems)
- SPECS GmbH (Surface Analysis, AFM-STM in UHV)

The company's head office is in Sant Cugat del Vallès (Barcelona) and it also has a branch office in Madrid.

Telstar Instrumat, S.L.  
Avda. Alcalde Barnils, 70, 3ª Planta  
08174 Sant Cugat del Vallès (Spain)  
Tel. +34 935 442 320  
Fax. +34 935 442 911

C/ Benisoda, 3  
28042 Madrid  
Tel. +34 913 717 511  
Fax. +34 917 477 538  
Web: [www.telstar-instrumat.com](http://www.telstar-instrumat.com)  
E-mail: [comercial@telstar-instrumat.com](mailto:comercial@telstar-instrumat.com)



**FEI COMPANY**

**OLYMPUS**  
Your Vision. Our Future



**MAB**

MAB INDUSTRIAL S.L.U.

### Microscopy in all dimensions

With more than thirty years providing optical microscopy solutions to Material Science applications in the fields of research and inspection, MAB Industrial offers innovative instruments for nanotechnology in **Confocal Laser Scanning Microscopy (CLSM)** and **Scanning Electron Microscopy (SEM)**. The **Olympus LEXT** system extends the capabilities of light microscopy into a three dimensional laser confocal metrology system with fast and reliable measurement results. LEXT obtains 3D images in one click for real-time, high precision non-contact surface measurements (step height, roughness, waviness, particle analysis, etc.). It offers the capability to merge real color information to the image and unique observation methods like laser confocal Differential Interference Contrast (DIC) for the detailed inspection of the tiniest unevenness on a surface. **FEI Company** has recently launched the **PHENOM** Imaging Tool, a table-top SEM offering a BSE magnification of 20kX and instant sample loading for superb image quality and high throughput, bridging the gap between optical and electron microscopy. In addition, MAB Industrial distributes **Olympus Soft Imaging Solutions (SIS)** high resolution cameras and image analysis software for almost every TEM microscope in the market to increase the performance and to reduce operating costs.

MAB Industrial, S.L.U.  
Córcega 117  
08029 Barcelona - Spain  
P: +34 93 430 83 01  
F: +34 93 419 58 79

Please contact us at [info@mabindustrial.es](mailto:info@mabindustrial.es) for further information.

E-Mail: [mabindustrial@mab.es](mailto:mabindustrial@mab.es)  
WEB: [www.mabindustrial.es](http://www.mabindustrial.es)



**BIOMETA** was set up in 1998. Its activities are centred on the supply of products and services for research laboratories, industrial quality control and clinical diagnostic. The offices at Parque Tecnológico de Asturias centralize the main services: commercial department, warehouse and technical service. There is an spacious application laboratory where training courses take place quite often, as well as seminars and demos. In order to give the customer the best service there are commercial branches spreaded over the Spanish territory: Vigo, Bilbao, Barcelona, Valencia, Sevilla and Madrid, where the technical service is located as well. The current staff is formed by 21 people, most of them with a high degree and wide experience. Materials Science is one of the most relevant fields in which Biometa participates.

The following are some of the most important companies settled in the nano-field and represented by Biometa in Spain:

- **PSIA**: Atomic Force Microscopes able to measure in True Non Contact mode.
- **Hysitron**: Nanoindenters designed to specifically indent in the nano-range and able to perform in-situ SPM images.

Other important companies represented by Biometa are:

**BUEHLER**: Metallography / **GALDABINI**: Universal Testing Machine / **LENTON**: Camera and Tube furnaces up to 1800°C **RETSCH**: Grinding of samples. Particle size analysis / **FLUXANA**: Sample preparation and accessories for XRF / **PARR**: Combustion calorimeters. Laboratory reactors

**Biometa** Parque Tecnológico de Asturias, Parcela 38, 33428 Llanera, Asturias, España (Spain)

Tel.: +34-902-24-43-43

Fax: +34-985-26-91-69

E-mail: [info@biometa.es](mailto:info@biometa.es)

WEB: <http://www.biometa.es/>



Alava Ingenieros Group has an history of more than 35 years in Instrumentation Distribution, focused on products for Measurement, Calibration, Simulation, Recording, and Analysis.. We act on the Iberian market, with Alava Ingenieros for the Spanish market and branch company MRA Instrumentação for Portugal. Our main markets are Industry in general, Education and I&D, Communications, Defence, Surveillance, etc.

Alava Ingenieros and MRA Instrumentação officially distribute in Spain and Portugal manufacturers of Test and Measurement Instruments which are leaders on their fields, like [www.tsi.com](http://www.tsi.com), instrument manufacturer for **Ultrafine Particles** applications. In Nanotechnology world, TSI has a complete product range of **Nanoparticle Aerosol monitors** and **Nanoparticle Surface Area Monitors**. Also, we are focused on other related applications like: Inhalation toxicology, Aerosol Research, Particle Characterization, Atmospheric Aerosols, Particle sizing & counting, Environmental studies, Particle generation & characterization, Flow and Particle diagnostics, Laboratory environmental controls, Life Science research, Pharmaceutical research, Spray diagnostics, powder characterization , Calibration and testing, Cleanroom certification and testing, Combustion gases, Combustion research, Diesel emissions.

Alava Ingenieros  
Edificio Antalia. C/Albasanz, 16.  
28037 Madrid  
España  
Tel: +34.91 567 97 00  
Fax: +34.91 570 26 61  
e-mail: [alava@alava-ing.com](mailto:alava@alava-ing.com)  
[www.alava-ing.es](http://www.alava-ing.es)

MRA Instrumentação  
Taguspark  
Edifício Ciência II, 1-B  
2740-120 Porto Salvo  
Portugal  
Tel.: +351.214217472  
Fax: +351.214218188  
e-mail: [mra@mra.pt](mailto:mra@mra.pt)  
[www.mra.pt](http://www.mra.pt)



Innovation is nothing new at M.T.Brandão, it's been our major concern for nearly 25 years. M.T.Brandão was set up in 1984 and centered its activities on the supply of rigorously selected scientific equipments and services for R&D Laboratories, Industrial Quality Control and counts amongst its customers Investigation Centres and Private Companies in the Chemical and Petrochemical Industries, Automotive, Optical, Food, Beverages and Pharmaceutical Industries...

Little more than two decades later, M.T.Brandão provides specific services, with dedicated engineers for after-sales follow-up and support. M.T.Brandão has the in-house expertise to analyse each problem and give it an individual solution.

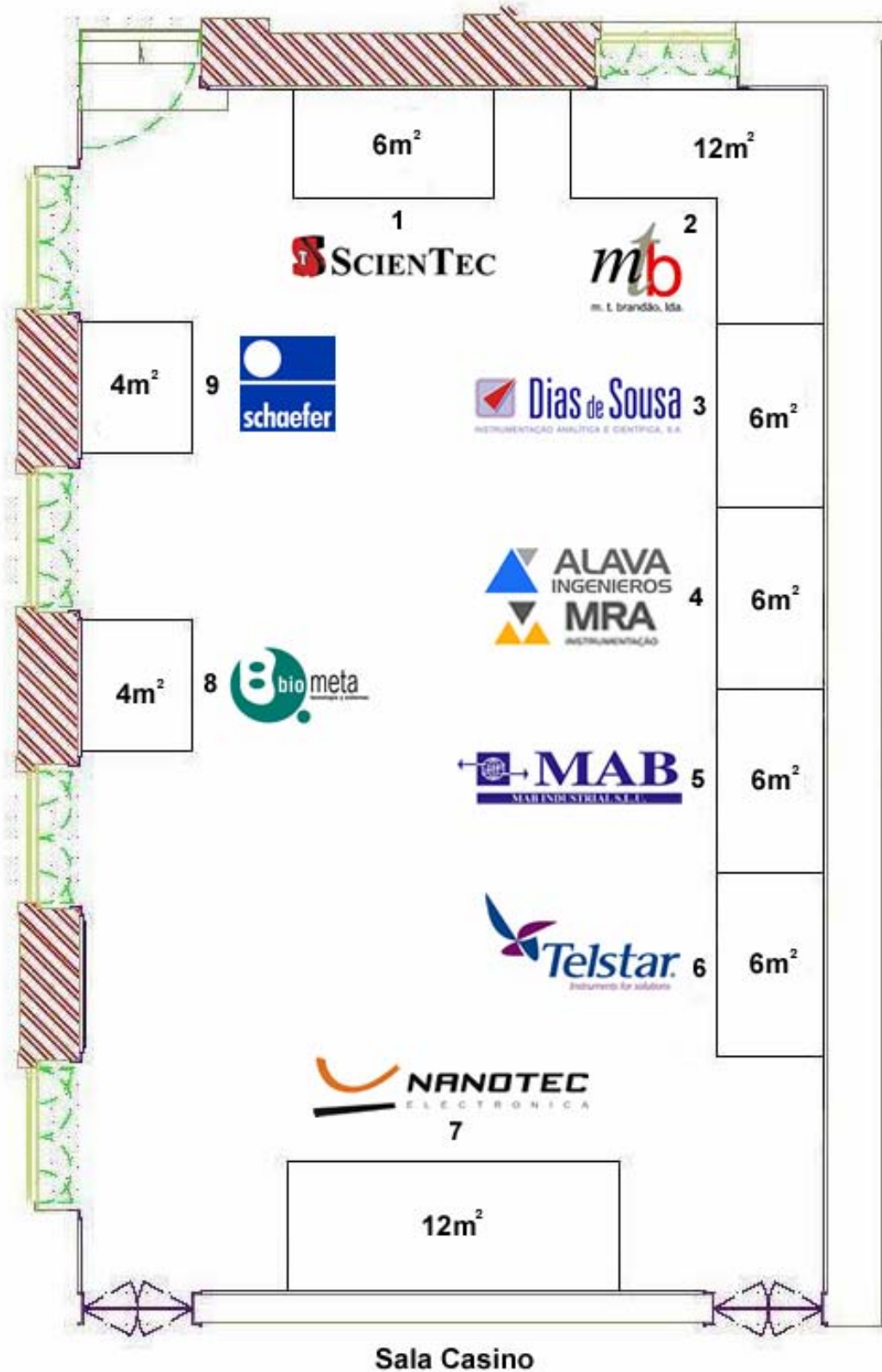
M.T.Brandão has strengthened its activities representing leading companies such as:

- **Spectra-Physics** : Diode Pump Lasers, UltraFast Lasers, Tunable Lasers, Amplifiers
- **Newport**: Vibration Control, Motion Control, Opto-Mechanics, Optics, Photonics Instrumentation
- **Anton Paar**: Small Angle X-ray Scattering , SURPASS
- **FRT** : Optical Surface Measuring Systems –Roughness, Profile, Topography, Contour

M.T.Brandão products and services assist customers all over Portugal. You'll find more information about us at [www.mtbrandao.com](http://www.mtbrandao.com).

M.T.Brandão, S.A.  
Rua de Serralves, 599  
4150-708 Porto  
Portugal  
Tel: +351 226 167 370  
Fax: +351 226 167 379  
General e-mail: [mtb@mtbrandao.com](mailto:mtb@mtbrandao.com)  
Website: [www.mtbrandao.com](http://www.mtbrandao.com)

# Exhibition Floor Plan



Tools for Nanotech™

# Solutions for enhanced performance



FEI's Tools for Nanotech™, featuring focused ion- and electron-beam technologies, deliver 3D characterization, analysis and modification capabilities with resolution down to the sub-Ångström level. With R&D centers in North America, Europe and Asia, and sales and service operations in more than 50 countries around the world, FEI is bringing the nanoscale within the grasp of leading researchers and manufacturers and helping to turn some of the biggest ideas of this century into reality.





**NANOSPAIN2008**  
**SCIENTIFIC PROGRAMME**



<b>SCIENTIFIC PROGRAMME</b>	
<b>Monday April 14, 2008</b>	
10h00-13h00	<b>Registration</b>
13h00-14h30	<b>Light Lunch (Buffet)</b>
14h30-14h40	<b>Opening Ceremony</b>
<i>(Session: Nanochemistry) - Chairman: Jaume Veciana</i>	
14h40-15h20	<b>Trevor Douglas</b> (Montana State University, USA)
<b>(page 11)</b>	"Virus capsids: constrained organic architectures for nanomaterials synthesis"
15h20-15h40	<b>Inhar Imaz</b> (Nanosfun- Institut català de nanotecnologia, Spain)
<b>(page 69)</b>	"Functional Metal-Organic Nanoparticles"
15h40-16h00	<b>Marta Mas-Torrent</b> (ICMAB - CSIC, Spain)
<b>(page 83)</b>	"Self-assembly of polychlorotriphenylmethyl organic radicals on surfaces"
16h00-16h20	<b>Joao Rocha</b> (University of Aveiro, CICECO, Portugal)
<b>(page 99)</b>	"Photoluminescent Microporous Lanthanide Silicates and Metal-Organic Frameworks"
16h20-17h00	<b>Sebastien Lecommandoux</b> (ENSCP - University of Bordeaux, France)
<b>(page 21)</b>	"Block copolymer self-assembly: a powerful tool for the design of new smart biomimetic nano-carriers"
17h00-17h30	<b>Coffee Break – Poster Session &amp; Instrument Exhibition</b>
<i>(Session: Modelling) - Chairman: Juan José Saenz</i>	
17h30-18h10	<b>Emilio Artacho</b> (Cambridge University, UK)
<b>(page 5)</b>	"First-principles calculations of manganite surfaces and interfaces for spintronics"
18h10-18h30	<b>Juan Maria Garcia Lastra</b> (Universidad del País Vasco, Spain)
<b>(page 55)</b>	"Effect of Chemisorbed Molecules on the Transport Properties of a (6,6) Carbon Nanotube"
18h30-18h50	<b>Fernando Cruz</b> (Imperial College London, UK)
<b>(page 47)</b>	"Equilibrium and Transport Properties of Small Alkanes and Alkenes Confined in Single-Walled Carbon Nanotubes"
18h50-19h10	<b>Pedro García Mochales</b> (Universidad Autónoma de Madrid, Spain)
<b>(page 59)</b>	"Formation of stable pentagonal nanowires under stretching on FCC metals"
20h30	<b>Welcome Reception (Braga Center)</b>



<b>SCIENTIFIC PROGRAMME</b>	
<b>Tuesday April 15, 2008</b>	
<b>(Session: Nanophotonics) - Chairman: Niek van Hulst</b>	
08h30-09h10	<b>Tobias J. Kippenberg</b> (Max-Planck Institute of Quantum Optics, Germany)
<b>(page 17)</b>	"Cooling of a micro-mechanical oscillator using radiation-pressure induced dynamical backaction "
09h10-09h30	<b>Xavier Borrise</b> (CNM, Spain)
<b>(page 37)</b>	"Plasmon confinement in V-groove waveguides fabricated by NanoImprint Lithography"
09h30-09h50	<b>Antonio Garcia Martin</b> (IMM - CSIC, Spain)
<b>(page 57)</b>	"Magneto-plasmonic materials: tuning magneto-optics with plasmons"
09h50-10h10	<b>Luis Carlo</b> (University of Aveiro, Portugal)
<b>(page 41)</b>	"Self-organization, photoluminescence and emergence in amide-functionalized organic/inorganic hybrids"
10h10-10h30	<b>Sergio Pereira</b> (University of Aveiro - CICECO, Portugal)
<b>(page 91)</b>	"Controlled integration of nanocrystals on the surface of group III-nitride light-emitting epitaxial heterostructures"
11h00-11h30	<b>Coffee Break – Poster Session &amp; Instrument Exhibition</b>
<b>(Session: Scientific Policy &amp; Infrastructure) - Chairman: Carlos Bernardo</b>	
11h30-11h45	<b>José Maria Pitarke</b> (Asociación CIC nanoGUNE, Spain)
<b>(page 95)</b>	"CIC nanoGUNE Consolider, the big challenge of the small"
11h45-12h00	<b>Rodolfo Miranda</b> (UAM & IMDEA Nanociencia, Spain)
<b>(page 87)</b>	"IMDEA-Nanociencia: A new Institute devoted to research in Nanoscience and Nanotechnology in Madrid"
12h00-12h15	<b>Ramón Torrecillas</b> (CINN-CSIC, Spain)
	"Nanoscience Institute in Asturias"
12h15-12h35	<b>José Rivas Rey</b> (INL, Portugal & USC, Spain)
<b>(page 97)</b>	"The International Iberian Nanotechnology Laboratory Facts, Prospects and Strategic Goals"
12h35-12h55	<b>Magrit Hanbucken</b> (Direction Générale de la Recherche et de l'Innovation (DGRI), France)
<b>(page 63)</b>	"A glance at the French networks supporting nanoscience and nanotechnology"
12h55-13h15	<b>Luis Melo</b> (FCT, Portugal)
<b>(page 85)</b>	"Nano Activity in Portugal"
13h15-15h00	<b>Lunch (Buffet) – Poster Session &amp; Instrument Exhibition</b>
15h00-17h30	Thematic Parallel Sessions
	<b>Nanobiotechnology – Chairmen: Jesus M. De la Fuente &amp; Elena Martinez</b>
	<b>Nanofabrication – Chairmen: Francesc Perez Murano &amp; Fernando Briones</b>
	<b>Industrial – Chairmen: Jose-Luis Viviente &amp; Emilio Prieto</b>
	<b>Nanochemistry – Chairmen: Jaume Veciana &amp; Nora Ventosa</b>
	<b>NanoPhotonics &amp; NanoOptics – Chairmen: Juan Jose Saenz &amp; Antonio Garcia Martin</b>
	<b>Nanocomposites – Chairman: Carlos Bernardo</b>
17h30-20h00	<b>Poster Session / Coffee Break &amp; Instrument Exhibition</b>
20h00	<b>Dinner (Buffet) – Poster Session &amp; Instrument Exhibition</b>
21h30	<b>Jazz Session – “Six at Seven” Jazz group</b>



<b>Programme – NanoBiotechnology Thematic Session – Tuesday April 15, 2008</b>	
15h00-15h30	<b>Josep Samitier</b> (IBEC, Spain)
<b>(page 185)</b>	"Nanobiotechnology and nanomedicine in Spain"
15h30-15h45	<b>Elisa Elizondo Sáez de Vicuña</b> (ICMAB-CSIC, Spain)
<b>(page 139)</b>	"Compressed Fluid Based Technologies for the Preparation of Drug Delivery Systems"
15h45-16h00	<b>Irene Fernandez-Cuesta</b> (CNM, Spain)
<b>(page 143)</b>	"Interdigitated nanoelectrodes for sensing: fabrication and characterization"
16h00-16h15	<b>Elvira Fortunato</b> (FCT-UNL, Portugal)
<b>(page 145)</b>	"DNA detection using amorphous silicon sensors with gold nanoparticles"
16h15-16h30	<b>Joana Loureiro</b> (INESC-MN, Portugal)
<b>(page 161)</b>	"Integrated platform for Stem Cells separation/counting"
16h30-16h45	<b>Luisa Pedro</b> (University of Algarve, Portugal)
<b>(page 177)</b>	"Protein nanoparticles for molecular therapy: Molecular construction of SIVp17/HIV1p6 nanoparticles and assembly in animal cell cultures"
16h45-17h15	<b>Paulo Freitas</b> (INESC-MN, IST and INL, Portugal)
<b>(page 147)</b>	
17h15-17h30	<b>Conclusion</b>

<b>Programme – NanoFabrication Thematic Session – Tuesday April 15, 2008</b>	
15h00-15h05	<b>Jose Maria de Teresa</b> (ICMA-CSIC, Spain)
	"Information about dissemination and networking on Nanofabrication in Spain"
15h05-15h35	<b>Javier Tamayo</b> (IMM-CSIC, Spain)
<b>(page 191)</b>	"Nanomechanical Devices: Ultrasensitive sensors of molecular recognition and conformational changes of biomolecules."
15h35-16h05	<b>Pedro Brogueira</b> (IST, Portugal)
<b>(page 127)</b>	
16h05-16h20	<b>Amelia Barreiro</b> (CIN2, Spain)
<b>(page 121)</b>	"Nanotube based thermal motors: sub-nanometer motion of cargoes driven by thermal gradients"
16h20-16h35	<b>Juan de la Figuera</b> (Instituto de Quimica-Fisica Rocasolano, Spain)
<b>(page 137)</b>	"Nanoscale periodicity in stripe-forming systems at high temperature – the Au/W(110) system"
16h35-16h50	<b>Ivan Fernandez</b> (IMM - CSIC, Spain)
<b>(page 141)</b>	"Parallel nanogap fabrication with nanometer size control using III-V semiconductor epitaxial technology"
16h50-17h05	<b>Daniel Garcia Sanchez</b> (CIN2, Spain)
<b>(page 151)</b>	"Mechanical detection of the vibrations of Carbon Nanotube and Graphene Resonators"
17h05-17h20	<b>Gonzalo Gonçalves</b> (FCT-UNL/CENIMAT-I3N, Portugal)
<b>(page 155)</b>	"High mobility indium zinc oxide deposited by rf magnetron sputtering at room temperature"
17h20-17h35	<b>Steve Reyntjens</b> (FEI Company, Netherlands)
<b>(page 183)</b>	"Novel tools for NanoPrototyping using Dualbeam™ FIB/SEM"
17h35-17h45	<b>Discussion &amp; Conclusion</b>

<b>Programme – Industrial Thematic Session – Tuesday April 15, 2008</b>	
15h00-15h20	<b>Emilio Prieto</b> (CEM, Spain)
<b>(page 179)</b>	"Standardization in Nanotechnologies. The AENOR Spanish Group GET15 and its role within ISO and CEN"
15h20-15h40	<b>Jun Xiao</b> (CETR, USA)
<b>(page 195)</b>	"Scanning Nano-Metrology of ultra thin films"
15h40-16h20	<b>Julio Santarén</b> (TOLSA S.A., Spain)
<b>(page 187)</b>	"DOMINO Project: A Challenging Adventure from the Spanish Industry into the Nanoworld"
16h20-16h30	<b>Martin Hernandez-Palacios</b> (Aliter, Spain)
	"Nanotechnology Master Overview"
16h30-17h00	(Acciona, Spain) – speaker to be defined
17h00-17h30	<b>Discussion &amp; Conclusion</b>

<b>Programme – NanoChemistry Thematic Session – Tuesday April 15, 2008</b>	
15h00-15h30	<b>Roberto Otero</b> (Universidad Autónoma de Madrid, Spain)
<b>(page 175)</b>	"1D ZnO Chains as the Spinal Cord of Adsorbed Metalloporphyrin Nanotubes Linked by Water Ligands"
15h30-16h00	<b>Jose Martinho</b> (IST and IN, Portugal)
16h00-16h15	<b>Suzana M Andrade</b> (Instituto Superior Técnico, Portugal)
<b>(page 119)</b>	"Nanometric aggregates of a covalent porphyrin dimer followed by Fluorescence Correlation Spectroscopy in aqueous buffered solution"
16h15-16h30	<b>Ernesto Brunet</b> (Universidad Autónoma de Madrid, Spain)
<b>(page 129)</b>	"The Role of Porous Materials in the Efficient Storage of Hydrogen"
16h30-16h45	<b>Rodolfo Miranda</b> (Universidad Autónoma de Madrid, Spain)
<b>(page 165)</b>	"Preferential nucleation, molecular distortion, charge transfer, and elastic effects in the self-assembly of TCNQ on Cu(100)"
16h45-17h00	<b>José V. García Ramos</b> (Instituto de Estructura de la Materia. CSIC, Spain)
<b>(page 153)</b>	"SERS on Functionalized Silver Nanostructures: Towards the Detection of Single Molecules in Hot Spots"
17h00-17h15	<b>Miguel Monge</b> (Universidad de La Rioja, Spain)
<b>(page 167)</b>	"Silver nanoparticles and gold metallodendrimers: from molecular precursors to nanomaterials"
17h15-17h30	<b>Erwan Rauwel</b> (University of Aveiro and CICECO, Portugal)
<b>(page 181)</b>	"Non-Aqueous Sol-Gel Routes Applied to Atomic Layer Deposition"
17h30-17h40	<b>Discussion &amp; Conclusion</b>

<b>Programme – NanoPhotonics &amp; NanoOptics Thematic Session – Tuesday April 15, 2008</b>	
15h00-15h30	<b>Niek van Hulst</b> (ICFO – the Institute of Photonic Sciences, Spain)
<b>(page 193)</b>	"NanoAntennas - Controlling Single Molecule Excitation and Emission"
15h30-15h45	<b>Senentxu Lanceros-Mendez</b> (University of Minho, Portugal)
<b>(page 157)</b>	"Tunable Fabry-Perot Optical Filter with a Resonant Cavity"
15h45-16h00	<b>Alvaro Blanco</b> (ICMM - CSIC, Spain)
<b>(page 123)</b>	"Self-assembled disorder"
16h00-16h15	<b>Luis Froufe</b> (ICMM - CSIC, Spain)
<b>(page 149)</b>	"Single molecule fluorescence decay rate statistics in disordered media"
16h15-16h30	<b>Mauricio Calvo</b> (Instituto de Ciencias de Materiales de Sevilla, Spain)
<b>(page 133)</b>	"Nanoparticle based One-Dimensional Photonic Crystals"
16h30-16h45	<b>Reinhard Schwarz</b> (Instituto Superior Técnico, Portugal)
<b>(page 189)</b>	"Interface analysis techniques on nanoscale dimension in flexible solar cells"
16h45-17h30	<b>Discussion &amp; Conclusion</b>

<b>Programme – Nanocomposites Thematic Session – Tuesday April 15, 2008</b>	
15h00-15h30	<b>José A. Covas</b> (I3N /Univ. Minho, Portugal)
<b>(page 135)</b>	"Preparing nanocomposites via melt processing: current difficulties and perspectives"
15h30-16h00	<b>Salazar Norkis</b> (Universidad Simón Bolívar, Venezuela)
<b>(page 171)</b>	"PMMA-Organic Bentonite Nanocomposites from the Exfoliation-Adsorption Technique and their Characterization by FTIR, XRD, TEM, TSDC & DSC"
15h45-16h00	<b>Luis Cadillon</b> (I3N /Univ. Aveiro, Portugal)
<b>(page 131)</b>	"Introduction of polypyrrol nanoparticles in cement paste to improve the physical properties"
16h00-16h15	<b>N.M. Neves</b> (IBB/3B's - University of Minho, Portugal)
<b>(page 169)</b>	"Biodegradable Polymeric Microfibres Reinforced with Nanofibres for Biomedical Applications"
16h15-16h30	<b>Marc Obiols-Rabasa</b> (CSIC - IIQAB, CIBER-BBN, Spain)
<b>(page 173)</b>	"Rheological studies on polymeric nanoparticle dispersions stabilized by a polyfructose-derivative surfactant"
16h30-16h45	<b>João M. Maia</b> (I3N - University of Minho, Portugal)
<b>(page 163)</b>	"Direct Numerical Simulation of Carbon Nanofibre Composites Under Shear Flow"
16h45-17h00	<b>Senentxu Lanceros-Mendez</b> (University of Minho, Portugal)
<b>(page 159)</b>	"Polymer based Electro-active Micro- and Nano-composites"
17h00-17h15	<b>João Borges</b> (Universidade Nova de Lisboa, Portugal)
<b>(page 125)</b>	"Electrospun Nanofibers as Potential Reinforcements for Composites"
17h15-17h30	<b>Discussion of the main problems that are still to be overcome to make viable the commercial exploitation of Nanocomposites &amp; Conclusion</b>

<b>SCIENTIFIC PROGRAMME</b>	
<b>Wednesday April 16, 2008</b>	
<i>(Session: C'Nano GSO) - Chairman: Xavier Bouju</i>	
08h30-09h00	<b>Jean-Pierre Aime</b> (Université Bordeaux I, France)
<b>(page 29)</b>	"Aquitaine, Midi-Pyrénées, Languedoc-Roussillon A single network for three regions promoting Nanoscience and Nanotechnology in the South-West of France"
09h00-09h20	<b>Jean-Roch Huntzinger</b> (Université Montpellier 2/CNRS, France)
<b>(page 67)</b>	"Atomic force microscopy and Raman analysis of exfoliated graphene on SiC"
09h20-09h40	<b>Angel Rubio</b> (Universidad del País Vasco, Spain)
<b>(page 101)</b>	"Dimensionality effects in the optics of BN nanostructures: applications for optoelectronic devices"
09h40-10h00	<b>Francesc Pérez-Murano</b> (Centro Nacional de Microelectrónica (CNM-IMB, CSIC), Spain)
<b>(page 93)</b>	"CMOS integrated nanomechanical mass sensors: determination of evaporation rate of femtoliter droplets"
10h00-10h20	<b>Myrtil Kahn</b> (Laboratoire de Chimie de Coordination, UPR8241 CNRS, France)
<b>(page 71)</b>	"Experimental evidence of the existence in solution of organizations of ZnO nanoparticles synthesized by organometallic method using dynamic light scattering"
10h20-10h40	<b>Daniel Sanchez-Portal</b> (Donostia International Physics Center (DIPC) / CSIC, Spain)
<b>(page 103)</b>	"Carbon Nanostructures: Optical Properties from TDDFT Studies and Complex Magnetic Behaviour of Substitutional Transition Metal Impurities"
10h40-11h00	<b>Caroline Bonafos</b> (CEMES-CNRS, France)
<b>(page 35)</b>	"White electroluminescence from C- and Si-rich thin silicon oxides"
11h00-11h30	<b>Poster Session / Coffee Break &amp; Instrument Exhibition</b>
<i>(Session: C'Nano GSO) - Chairman: Jean-Pierre Aime</i>	
11h30-11h50	<b>Ross Brown</b> (IPREM, Pau, France)
<b>(page 39)</b>	"Mapping molecular diffusion in nano-channel systems by tracking individual fluorescent molecules"
11h50-12h10	<b>Jordi Hernandez-Borrell</b> (IN2UB-UB, Spain)
<b>(page 65)</b>	"Towards insertion of a transmembrane protein into supported planar bilayers: preliminary studies"
12h10-12h30	<b>Marie-Hélène Delville</b> (University of Sciences and Technology of Bordeaux, France)
<b>(page 51)</b>	"Towards multifunctional core-shell nanoparticles for biological applications"
12h30-12h50	<b>Yannick Guari</b> (Université Montpellier, France)
<b>(page 61)</b>	"Synthesis and studies of coordination polymer nanoparticles"
12h50-13h10	<b>Philippe Serp</b> (Toulouse University, France)
<b>(page 105)</b>	"MWCNT activation and its influence on the catalytic performance of Pt/MWCNT catalysts for selective hydrogenation"
13h10-13h30	<b>Guyhaine Clavel</b> (University of Aveiro - CICECO, Portugal)
<b>(page 43)</b>	"Nonaqueous sol-gel routes to diluted magnetic semiconductors"
13h30-14h30	<b>Lunch (Buffet) – Poster Session &amp; Instrument Exhibition</b>
<i>(Session: Nanoelectronics/Molecular Electronics) - Chairman: Fernando Briones</i>	
14h30-15h10	<b>André Gourdon</b> (CEMES-CNRS, France)
<b>(page 15)</b>	"Molecular Devices for Single Molecule STM Experiments"
15h10-15h30	<b>Elena Laukhina</b> (CIBER-BBN, Spain)
<b>(page 75)</b>	"Conducting nanocomposite organic films for plastic pressure sensors and electronic circuits"
15h30	<b>Departure to O'Porto (Visit)</b>
21h00	<b>Conference Dinner</b>



<b>SCIENTIFIC PROGRAMME</b>	
<b>Thursday April 17, 2008</b>	
<i>(Session: NEMS / Nanometrology) - Chairman: Emilio Prieto</i>	
09h30-10h10 <b>(page 9)</b>	<b>Robert H. Blick</b> (University of Wisconsin-Madison, USA) "Self-Excitation in Nano-Electromechanical Systems"
10h10-10h50 <b>(page 7)</b>	<b>Rob H. Bergmans</b> (NMI Van Swinden Laboratorium B.V, The Netherlands) "Nanometrology and its role in the development of nanotechnology; an overview of the state of the art and an outlook on future developments by the European National Metrology Institutes"
10h50-11h10 <b>(page 79)</b>	<b>Pedro Martins</b> (Universidade do Minho, Portugal) "Electroactive $\beta$ -PVDF Polymer as Fluidic Acoustic Mixer for Lab-on-a-Chip Applications"
11h10-11h40	<b>Coffee Break – Poster Session &amp; Instrument Exhibition</b>
<i>(Session: SPM) - Chairman: Adriana Gil</i>	
11h40-12h20 <b>(page 25)</b>	<b>Mervyn Miles</b> (University of Bristol, UK) "High Speed AFM – Contact & Non-contact"
12h20-12h40 <b>(page 81)</b>	<b>Daniel Maspoch</b> (Institut Català de Nanotecnologia, Spain) "Dip-Pen Nanolithography: "Writing" Molecules, Biological Entities and Nanomaterials at the Nanometer Scale"
12h40-13h00 <b>(page 109)</b>	<b>Amadeo L. Vazquez de Parga</b> (Universidad Autonoma de Madrid, Spain) "Graphene on Ru(0001): Spatially resolved electronic structure"
13h00-13h20 <b>(page 73)</b>	<b>Andrei Kholkin</b> (University of Aveiro, Portugal) "Nanoscale Characterization of Ferroelectric Materials via Piezoresponse Force Microscopy"
13h20-15h00	<b>Lunch (Buffet) – Poster Session &amp; Instrument Exhibition</b>
<i>(Session: NanoBio/Nanomedicine) - Chairman: Elena Martinez</i>	
15h00-15h20 <b>(page 45)</b>	<b>Eugenia Cruz</b> (INETI /UNFAB and iMed.UL, Portugal) "Nanoliposomes as Tolls for the Treatment of Infectious Diseases"
15h20-15h40 <b>(page 31)</b>	<b>Antonio Almeida</b> (Universidade de Lisboa, Portugal) "Production and Immune Response Characterisation of S. equi Antigens Encapsulated in Surface Modified Polymeric Nanoparticles"
15h40-16h00 <b>(page 77)</b>	<b>Maria Teresa Martinez</b> (Instituto de Carboquimica, Spain) "Electronic detection of DNA hybridization"
16h00-16h20 <b>(page 49)</b>	<b>Ana Luisa Daniel da Silva</b> (University of Aveiro - CICECO, Portugal) "Magnetic polysaccharide nanospheres with potential for biomedical applications: preparation via a reverse miniemulsion method"
16h20-17h10	<b>Poster-Flash Contributions</b>
17h10-20h00	<b>Poster Session / Coffee Break &amp; Instrument Exhibition</b>
20h00	<b>Dinner (Buffet) – Poster Session &amp; Instrument Exhibition</b>
21h30	<b>Baroque Concert – Bom Jesus Church</b>

**Poster Flash Contributions - Thursday April 17, 2008**

<b>Monica Gonzalez</b> (Instituto de Carboquimica, Spain)	<b>NanoBiotechnology</b>	"Non-specific adsorption of biomolecules on single-walled carbon nanotubes"
<b>Maria Moros</b> (Instituto de Nanociencia de Aragón, Spain)	<b>NanoBiotechnology</b>	"Cell response against water stable magnetic nanoparticles obtained by thermal decomposition procedure"
<b>Sara Puertas</b> (Instituto de Carboquimica, Spain)	<b>NanoBiotechnology</b>	"Biofunctionalitation of Magnetic Nanoparticles for Immunomagnetic Biosensors"
<b>Jose M. Gonzalez</b> (Instituto de Carboquimica, Spain)	<b>NanoChemistry</b>	"Carbon nanotubes dispersion towards polymer integration"
<b>Alejandro Anson</b> (Instituto de Carboquimica, Spain)	<b>Nanomaterials</b>	"Separation of Argon and Oxygen by Adsorption on a Titanosilicate Molecular Sieve"
<b>Joao Gomes</b> (CeNTI - Centre for Nanotechnology and Smart Materials, Portugal)	<b>Nanotubes</b>	"Carbon Nanofibre-poly(vinylidene fluoride) nanocomposite: effect of the carbon nanofibres concentration on the $\alpha$ to $\beta$ phase transformation and the degree of crystallinity"
<b>Merce Pacios</b> (Universitat de Barcelona, Spain)	<b>Nanotubes</b>	"Amperometric (bio)sensors based on carbon nanotubes"
<b>Samuel Sanchez</b> (Universitat de Barcelona, Spain)	<b>Nanotubes</b>	"Characterization and enhancement of electrochemical properties of MWCNT/polysulfone composite modified screen-printed electrodes"
<b>Luis Goncalves</b> (University of Minho, Portugal)	<b>NEMS / MEMS</b>	"Thermoelectric thin-films for microcoolers and energy scavenging microsystems"
<b>Enrique Sahagun</b> (Universidad Autonoma de Madrid, Spain)	<b>SPM</b>	"Adhesion hysteresis in Dynamic Atomic Force Microscopy"

**SCIENTIFIC PROGRAMME****Friday April 18, 2008****(Session: Nanomagnetism) - Chairman: Jose-Luis Costa Kramer**

08h30-09h10	<b>Mathias Kläui</b> (University of Konstanz, Germany)
<b>(page 19)</b>	"Current-induced domain wall dynamics"
09h10-09h30	<b>Andreas Berger</b> (CIC nanoGUNE Consolider, Spain)
<b>(page 33)</b>	"Magnetic Characterization of Nano-scale Granular Materials"
09h30-09h50	<b>Luis Fernandez Barquin</b> (Universidad de Cantabria, Spain)
<b>(page 29)</b>	"Size versus Disorder effects in the electronic properties of nanosized intermediate valence metals"
09h50-10h10	<b>Nuno Joao Oliveira Silva</b> (ICMA - CSIC, Spain)
<b>(page 107)</b>	"Magnetic and structural properties of iron oxyhydroxynitrate nanoparticles"
10h10-10h40	<b>Coffee Break – Poster Session &amp; Instrument Exhibition</b>

**(Session: Nanomaterials) - Chairman: Luis Melo**

10h40-11h20	<b>Oscar L. Malta</b> (Universidade de Pernambuco, Brazil)
<b>(page 23)</b>	"The chemical bond overlap plasmon as a tool for quantifying covalency in optical solid state materials"
11h20-11h40	<b>Jone Zabaleta</b> (ICMAB - CSIC, Spain)
<b>(page 113)</b>	"Self-assembling and guided self-organization of oxide nanostructures from chemical solutions"
11h40-12h00	<b>Marc Georg Willinger</b> (University of Aveiro, Portugal)
<b>(page 111)</b>	"EELS in the TEM: chemical information at the nanometer scale"
12h00-12h20	<b>Mikhail Zheludkevich</b> (CICECO/DECV, Portugal)
<b>(page 115)</b>	"Self-healing coatings with multi-level protection based on active nanocontainers"
12h20-12h40	<b>Maria Conceicao Paiva</b> (Institute for Polymers and Composites, Portugal)
<b>(page 89)</b>	"Chemical Functionalisation of Carbon Nanotubes for the Dispersion in Polymer Matrices"
12h40-13h20	<b>Daisuke Fujita</b> (National Institute for Materials Science (NIMS), Japan)
<b>(page 13)</b>	"Low-dimensional Surface Nanostructures studied by Scanning Tunneling Microscopy"
13h40-13h45	<b>Concluding Remarks / NanoSpain2009 announcement</b>



## Keynote Contributions (Index)

<b>Emilio Artacho</b> (Cambridge University, UK)	<b>p.5</b>
<i>"First-principles calculations of manganite surfaces and interfaces for spintronics"</i>	
<b>Rob H. Bergmans</b> (NMI Van Swinden Laboratorium B.V, The Netherlands)	<b>p.7</b>
<i>"Nanometrology and its role in the development of nanotechnology; an overview of the state of the art and an outlook on future developments by the European National Metrology Institutes"</i>	
<b>Robert H. Blick</b> (University of Wisconsin-Madison, USA)	<b>p.9</b>
<i>"Self-Excitation in Nano-Electromechanical Systems"</i>	
<b>Trevor Douglas</b> (Montana State University, USA)	<b>p.11</b>
<i>"Virus capsids: constrained organic architectures for nanomaterials synthesis"</i>	
<b>Daisuke Fujita</b> (National Institute for Materials Science (NIMS), Japan)	<b>p.13</b>
<i>"Low-dimensional Surface Nanostructures studied by Scanning Tunneling Microscopy"</i>	
<b>André Gourdon</b> (CEMES - CNRS, France)	<b>p.15</b>
<i>"Molecular Devices for Single Molecule STM Experiments"</i>	
<b>Tobias J. Kippenberg</b> (Max-Planck Institute of Quantum Optics, Germany)	<b>p.17</b>
<i>"Cooling of a micro-mechanical oscillator using radiation-pressure induced dynamical backaction"</i>	
<b>Mathias Kläui</b> (University of Konstanz, Germany)	<b>p.19</b>
<i>"Current-induced domain wall dynamics"</i>	
<b>Sébastien Lecommandoux</b> (ENSCP - University of Bordeaux, France)	<b>p.21</b>
<i>"Block copolymer self-assembly: a powerful tool for the design of new smart biomimetic nano-carriers"</i>	
<b>Oscar L. Malta</b> (Universidade de Pernambuco, Brazil)	<b>p.23</b>
<i>"The chemical bond overlap plasmon as a tool for quantifying covalency in optical solid state materials"</i>	
<b>Mervyn Miles</b> (University of Bristol, UK)	<b>p.25</b>
<i>"High Speed AFM – Contact &amp; Non-contact"</i>	



## Oral Contributions (Index)

<b>Jean-Pierre Aimé</b> (Université Bordeaux I, France) - CNANO-GSO	<b>p.29</b>
<i>"Aquitaine, Midi-Pyrénées, Languedoc-Roussillon A single network for three regions promoting Nanoscience and Nanotechnology in the South-West of France"</i>	
<b>Antonio Almeida</b> (Universidade de Lisboa, Portugal) - NanoBiotechnology	<b>p.31</b>
<i>"Production and Immune Response Characterisation of S. equi Antigens Encapsulated in Surface Modified Polymeric Nanoparticles"</i>	
<b>Andreas Berger</b> (CIC nanoGUNE Consolider, Spain) - Nanomagnetism	<b>p.33</b>
<i>"Magnetic Characterization of Nano-scale Granular Materials"</i>	
<b>Caroline Bonafos</b> (CEMES-CNRS, France) - CNANO-GSO	<b>p.35</b>
<i>"White electroluminescence from C- and Si-rich thin silicon oxides"</i>	
<b>Xavier Borrise</b> (CNM, Spain) - Nanophotonics	<b>p.37</b>
<i>"Plasmon confinement in V-groove waveguides fabricated by NanoImprint Lithography"</i>	
<b>Ross Brown</b> (IPREM6ECP, France) - CNANO-GSO	<b>p.39</b>
<i>"Mapping molecular diffusion in nano-channel systems by tracking individual fluorescent molecules"</i>	
<b>Luís Carlos</b> (Universidade de Aveiro, Portugal) - Nanophotonics	<b>p.41</b>
<i>"Self-organization, photoluminescence and emergence in amide-functionalized organic/inorganic hybrids"</i>	
<b>Guyhaine Clavel</b> (University of Aveiro - CICECO, Portugal) - CNANO-GSO	<b>p.43</b>
<i>"Nonaqueous sol-gel routes to diluted magnetic semiconductors"</i>	
<b>Eugenia Cruz</b> (INETI /UNFAB and iMed.UL, Portugal) - NanoBiotechnology	<b>p.45</b>
<i>"Nanoliposomes as Tolls for the Treatment of Infectious Diseases"</i>	
<b>Fernando Cruz</b> (Imperial College London, UK) - Simulation at the Nanoscale	<b>p.47</b>
<i>"Equilibrium and Transport Properties of Small Alkanes and Alkenes Confined in Single-Walled Carbon Nanotubes"</i>	
<b>Ana Luisa Daniel-Da-Silva</b> (University of Aveiro and CICECO, Portugal) - NanoBiotechnology	<b>p.49</b>
<i>"Magnetic polysaccharide nanospheres with potential for biomedical applications: preparation via a reverse miniemulsion method"</i>	
<b>Marie-Hélène Delville</b> (University of Bordeaux, France) - CNANO-GSO	<b>p.51</b>
<i>"Towards multifunctional core-shell nanoparticles for biological applications"</i>	
<b>Luís Fernández Barquin</b> (Universidad de Cantabria, Spain) – Nanomagnetism	<b>p.53</b>
<i>"Size versus Disorder effects in the electronic properties of nanosized intermediate valence metals"</i>	
<b>Juan Maria García Lastra</b> (Universidad del País Vasco, Spain) – Nanotubes	<b>p.55</b>
<i>"Effect of Chemisorbed Molecules on the Transport Properties of a (6,6) Carbon Nanotube"</i>	
<b>Antonio Garcia-Martin</b> (IMM-CSIC, Spain) – Nanophotonics	<b>p.57</b>
<i>"Magneto-plasmonic materials: tuning magneto-optics with plasmons"</i>	
<b>Pedro García-Mochales</b> (Universidad Autónoma de Madrid, Spain) – Simulation at the Nanoscale	<b>p.59</b>
<i>"Formation of stable pentagonal nanowires under stretching on FCC metals"</i>	

<b>Yannick Guari</b> (Université Montpellier, France) - CNANO-GSO	<b>p.61</b>
<i>"Synthesis and studies of coordination polymer nanoparticles"</i>	
<b>Magrit Hanbucken</b> (Direction Générale de la Recherche et de l'Innovation (DGRI), France) - Scientific Policy	<b>p.63</b>
<i>"A glance at the french networks supporting nanoscience and nanotechnology"</i>	
<b>Jordi Hernández-Borrell</b> (IN2UB-UB, Spain) - CNANO-GSO	<b>p.65</b>
<i>"Towards insertion of a transmembrane protein into supported planar bilayers: preliminary studies"</i>	
<b>Jean-Roch Huntzinger</b> (Université Montpellier 2/CNRS, France) – CNANO-GSO	<b>p.67</b>
<i>"Atomic force microscopy and Raman analysis of exfoliated graphene on SiC"</i>	
<b>Inhar Imaz</b> (Nanosfun- Institut català de nanotecnologia, Spain) – NanoChemistry	<b>p.69</b>
<i>"Functional Metal-Organic Nanoparticles"</i>	
<b>Myrtil Kahn</b> (Laboratoire de Chimie de Coordination, CNRS, France) – CNANO-GSO	<b>p.71</b>
<i>"Experimental evidence of the existence in solution of organizations of ZnO nanoparticles synthesized by organometallic method using dynamic light scattering"</i>	
<b>Andrei Kholkin</b> (University of Aveiro, Portugal) – SPM	<b>p.73</b>
<i>"Nanoscale Characterization of Ferroelectric Materials via Piezoresponse Force Microscopy"</i>	
<b>Elena Laukhina</b> (CIBER-BBN, Spain) - Molecular Electronics	<b>p.75</b>
<i>"Conducting nanocomposite organic films for plastic pressure sensors and electronic circuits"</i>	
<b>Maria Teresa Martinez</b> (Instituto de Carboquímica, Spain) – NanoBiotechnology	<b>p.77</b>
<i>"Electronic detection of DNA hybridization"</i>	
<b>Pedro Martins</b> (Universidade do Minho, Portugal) - NEMS / MEMS	<b>p.79</b>
<i>"Electroactive <math>\beta</math>-PVDF Polymer as Fluidic Acoustic Mixer for Lab-on-a-Chip Applications"</i>	
<b>Daniel Maspoch</b> (Institut Català de Nanotecnologia, Spain) – SPM	<b>p.81</b>
<i>"Dip-Pen Nanolithography: "Writing" Molecules, Biological Entities and Nanomaterials at the Nanometer Scale"</i>	
<b>Marta Mas-Torrent</b> (ICMAB - CSIC, Spain) – NanoChemistry	<b>p.83</b>
<i>"Self-assembly of polychlorotriphenylmethyl organic radicals on surfaces"</i>	
<b>Luis Melo</b> (Fundação para a Ciência e a Tecnologia , Portugal) - Scientific Policy	<b>p.85</b>
<i>"Nano Activity in Portugal"</i>	
<b>Rodolfo Miranda</b> (UAM - IMDEA Nanociencia, Spain) - Scientific Policy	<b>p.87</b>
<i>"IMDEA-Nanociencia: A new Institute devoted to research in Nanoscience and Nanotechnology in Madrid"</i>	
<b>Maria Conceição Paiva</b> (Institute for Polymers and Composites, Portugal) – NanoMaterials	<b>p.89</b>
<i>"Chemical Functionalisation of Carbon Nanotubes for the Dispersion in Polymer Matrices"</i>	
<b>Sergio Pereira</b> (CICECO University of Aveiro, Portugal) - Nanophotonics	<b>p.91</b>
<i>"Controlled integration of nanocrystals on the surface of group III-nitride light-emitting epitaxial heterostructures"</i>	
<b>Francesc Perez-Murano</b> (CNM-IMB, CSIC, Spain) - CNANO-GSO	<b>p.93</b>
<i>"CMOS integrated nanomechanical mass sensors: determination of evaporation rate of femtoliter droplets"</i>	
<b>Jose Maria Pitarke</b> (CIC nanoGUNE Consolider, Spain) - Scientific Policy	<b>p.95</b>

<i>"CIC nanoGUNE Consolider, the big challenge of the small"</i>	
<b>Jose Rivas Rey</b> (INL, Portugal & USC, Spain) - Scientific Policy	<b>p.97</b>
<i>"The International Iberian Nanotechnology Laboratory Facts, Prospects and Strategic Goals"</i>	
<b>Joao Rocha</b> (University of Aveiro, CICECO, Portugal) – NanoChemistry	<b>p.99</b>
<i>"Photoluminescent Microporous Lanthanide Silicates and Metal-Organic Frameworks"</i>	
<b>Angel Rubio</b> (Universidad del País Vasco, Spain) - CNANO-GSO	<b>p.101</b>
<i>"Dimensionality effects in the optics of BN nanostructures: applications for optoelectronic devices"</i>	
<b>Daniel Sanchez Portal</b> (Donostia Internacional Physics Center / CSIC, Spain) – CNANO-GSO	<b>p.103</b>
<i>"Carbon Nanostructures: Optical Properties from TDDFT Studies and Complex Magnetic Behaviour of Substitutional Transition Metal Impurities"</i>	
<b>Philippe Serp</b> (Toulouse University, France) – CNANO-GSO	<b>p.105</b>
<i>"MWCNT activation and its influence on the catalytic performance of Pt/MWCNT catalysts for selective hydrogenation"</i>	
<b>Nuno Joao Oliveira Silva</b> (ICMA - CSIC, Spain) – Nanomagnetism	<b>p.107</b>
<i>"Magnetic and structural properties of iron oxyhydroxynitrate nanoparticles"</i>	
<b>Ramón Torrecillas</b> (CINN-CSIC, Spain)	-
<i>"Nanoscience Institute in Asturias"</i>	
<b>Amadeo L. Vázquez de Parga</b> (Universidad Autónoma de Madrid, Spain) – SPM	<b>p.109</b>
<i>"Graphene on Ru(0001): Spatially resolved electronic structure"</i>	
<b>Marc-Georg Willinger</b> (University of Aveiro, Portugal) – NanoMaterials	<b>p.111</b>
<i>"EELS in the TEM: chemical information at the nanometer scale"</i>	
<b>Jone Zabaleta</b> (ICMAB - CSIC, Spain) – NanoMaterials	<b>p.113</b>
<i>"Self-assembling and guided self-organization of oxide nanostructures from chemical solutions"</i>	
<b>Mikhail Zheludkevich</b> (CICECO/DECV, Portugal) – NanoMaterials	<b>p.115</b>
<i>"Self-healing coatings with multi-level protection based on active nanocontainers"</i>	



## Oral Contributions – Parallel Sessions (Index)

<b>Suzana M. Andrade</b> (Instituto Superior Técnico, Portugal) – NanoChemistry	<b>p.119</b>
<i>"Nanometric aggregates of a covalent porphyrin dimer followed by Fluorescence Correlation Spectroscopy in aqueous buffered solution"</i>	
<b>Amelia Barreiro</b> (CIN2, Spain) – NanoFabrication	<b>p.121</b>
<i>"Nanotube based thermal motors: sub-nanometer motion of cargoes driven by thermal gradients"</i>	
<b>Alvaro Blanco</b> (ICMM-CSIC, Spain) – NanoPhotonics	<b>p.123</b>
<i>"Self-assembled disorder"</i>	
<b>João Borges</b> (Universidade Nova de Lisboa, Portugal) – NanoComposites	<b>p.125</b>
<i>"Electrospun Nanofibers as Potential Reinforcements for Composites"</i>	
<b>Pedro Brogueria</b> (Instituto Superior Técnico, Portugal) – NanoFabrication	<b>p.127</b>
<b>Ernesto Brunet</b> (Universidad Autónoma de Madrid, Spain) – NanoChemistry	<b>p.129</b>
<i>"The Role of Porous Materials in the Efficient Storage of Hydrogen"</i>	
<b>Luis Cadillon</b> (I3N-Universidade de Aveiro, Portugal) – NanoComposites	<b>p.131</b>
<i>"Introduction of polypyrrol nanoparticles in cement paste to improve the physical properties"</i>	
<b>Mauricio Calvo</b> (Instituto de Ciencias de Materiales de Sevilla, Spain) – NanoPhotonics	<b>p.133</b>
<i>"Nanoparticle based One-Dimensional Photonic Crystals"</i>	
<b>José A. Covas</b> (I3N-Universidade de Aveiro, Portugal) – NanoComposites	<b>p.135</b>
<i>"Preparing nanocomposites via melt processing: current difficulties and perspectives"</i>	
<b>Juan de la Figuera</b> (Instituto de Química-Física Rocasolano, Spain) – NanoFabrication	<b>p.137</b>
<i>"Nanoscale periodicity in stripe-forming systems at high temperature – the Au/W(110) system"</i>	
<b>Elisa Elizondo Sáez de Vicuña</b> (ICMAB - CSIC, Spain) - NanoBiotechnology	<b>p.139</b>
<i>"Compressed Fluid Based Technologies for the Preparation of Drug Delivery Systems"</i>	
<b>Ivan Fernández</b> (IMM-CSIC, Spain) – NanoFabrication	<b>p.141</b>
<i>"Parallel nanogap fabrication with nanometer size control using III-V semiconductor epitaxial technology"</i>	
<b>Irene Fernández-Cuesta</b> (CNM, Spain) – NanoBiotechnology	<b>p.143</b>
<i>"Interdigitated nanoelectrodes for sensing: fabrication and characterization"</i>	
<b>Elvira Fortunato</b> (FCT-UNL, Portugal) – NanoBiotechnology	<b>p.145</b>
<i>"DNA detection using amorphous silicon sensors with gold nanoparticles"</i>	
<b>Paulo Freitas</b> (INESC-MN, IST and INL, Portugal) – NanoBiotechnology	<b>p.147</b>
<b>Luis Froufe</b> (ICMM-CSIC, Spain) – NanoPhotonics	<b>p.149</b>
<i>"Single molecule fluorescence decay rate statistics in disordered media"</i>	
<b>Daniel García Sánchez</b> (CIN2, Spain) – NanoFabrication	<b>p.151</b>
<i>"Mechanical detection of the vibrations of Carbon Nanotube and Graphene Resonators"</i>	
<b>José V. García Ramos</b> (Instituto de Estructura de la Materia. CSIC., Spain) - NanoChemistry	<b>p.153</b>
<i>"SERS on Functionalized Silver Nanostructures: Towards the Detection of Single Molecules in Hot Spots"</i>	

<b>Gonzalo Gonçalves</b> (FCT-UNL/CENIMAT-I3N, Portugal) – NanoFabrication	<b>p.155</b>
<i>"High mobility indium zinc oxide deposited by rf magnetron sputtering at room temperature"</i>	
<b>Senentxu Lanceros-Mendez</b> (University of Minho, Portugal) – NanoPhotonics	<b>p.157</b>
<i>"Tunable Fabry-Perot Optical Filter with a Resonant Cavity"</i>	
<b>Senentxu Lanceros-Mendez</b> (University of Minho, Portugal) – NanoComposites	<b>p.159</b>
<i>"Polymer based Electro-active Micro- and Nano-composites"</i>	
<b>Joana Loureiro</b> (INESC-MN, Portugal) – NanoBiotechnology	<b>p.161</b>
<i>"Integrated platform for Stem Cells separation/counting"</i>	
<b>João M. Maia</b> (I3N-Universidade de Aveiro, Portugal) – NanoComposites	<b>p.163</b>
<i>"Direct Numerical Simulation of Carbon Nanofibre Composites Under Shear Flow"</i>	
<b>Jose Martinho</b> (IST and IN, Portugal) – NanoChemistry	-
<b>Rodolfo Miranda</b> (Universidad Autónoma de Madrid , Spain) – NanoChemistry	<b>p.165</b>
<i>"Preferential nucleation, molecular distortion, charge transfer, and elastic effects in the self-assembly of TCNQ on Cu(100)"</i>	
<b>Miguel Monge</b> (Universidad de La Rioja, Spain) – NanoChemistry	<b>p.167</b>
<i>"Silver nanoparticles and gold metallodendrimers: from molecular precursors to nanomaterials"</i>	
<b>N.M. Neves</b> (IBB/3B's- University of Minho, Portugal) – NanoComposites	<b>p.169</b>
<i>"Biodegradable Polymeric Microfibres Reinforced with Nanofibres for Biomedical Applications"</i>	
<b>Salazar Norkis</b> (Universidad Simón Bolívar, Venezuela) – NanoComposites	<b>p.171</b>
<i>"PMMA-Organic Bentonite Nanocomposites from the Exfoliation-Adsorption Technique and their Characterization by FTIR, XRD, TEM, TSDC &amp; DSC"</i>	
<b>Marc Obiols-Rabasa</b> (CSIC - IIQAB, CIBER-BBN, Spain) – NanoComposites	<b>p.173</b>
<i>"Rheological studies on polymeric nanoparticle dispersions stabilized by a polyfructose-derivative surfactant"</i>	
<b>Roberto Otero</b> (Universidad Autónoma de Madrid, Spain) – NanoChemistry	<b>p.175</b>
<i>"1D ZnO Chains as the Spinal Cord of Adsorbed Metalloporphyrin Nanotubes Linked by Water Ligands"</i>	
<b>Luisa Pedro</b> (University of Algarve, Portugal) – NanoBiotechnology	<b>p.177</b>
<i>"Protein nanoparticles for molecular therapy: Molecular construction of SIVp17/HIV1p6 nanoparticles and assembly in animal cell cultures"</i>	
<b>Emilio Prieto</b> (CEM, Spain) – Industrial	<b>p.179</b>
<i>"Standardization in Nanotechnologies. The AENOR Spanish Group GET15 and its role within ISO and CEN"</i>	
<b>Erwan Rauwel</b> (University of Aveiro and CICECO, Portugal) – NanoChemistry	<b>p.181</b>
<i>"Non-Aqueous Sol-Gel Routes Applied to Atomic Layer Deposition"</i>	
<b>Steve Reyntjens</b> (FEI Company , Netherlands) – NanoFabrication	<b>p.183</b>
<i>"Novel tools for NanoPrototyping using Dualbeam™ FIB/SEM"</i>	
<b>Josep Samitier</b> (IBEC, Spain) – NanoBiotechnology	<b>p.185</b>
<i>"Nanobiotechnology and nanomedicine in Spain"</i>	
<b>Julio Santaren</b> (TOLSA S.A., Spain) – Industrial	<b>p.187</b>
<i>"DOMINO Project: A Challenging Adventure from the Spanish Industry into the Nanoworld"</i>	

<b>Reinhard Schwarz</b> (Instituto Superior Técnico, Portugal) – NanoPhotonics	<b>p.189</b>
<i>"Interface analysis techniques on nanoscale dimension in flexible solar cells"</i>	
<b>Javier Tamayo</b> (IMM-CSIC, Spain) – NanoFabrication	<b>p.191</b>
<i>"Nanomechanical Devices: Ultrasensitive sensors of molecular recognition and conformational changes of biomolecules."</i>	
<b>Niek Van Hulst</b> (ICFO, Spain) – NanoPhotonics	<b>p.193</b>
<i>"NanoAntennas - Controlling Single Molecule Excitation and Emission"</i>	
<b>Jun Xiao</b> (CETR, USA) – Industrial	<b>p.195</b>
<i>"Scanning Nano-Metrology of ultra thin films"</i>	



## Alphabetical Order

<b>Jean-Pierre Aime</b> (Université Bordeaux I, France) - CNANO-GSO	<b>ORAL</b>	<b>p.29</b>
<i>"Aquitaine, Midi-Pyrénées, Languedoc-Roussillon A single network for three regions promoting Nanoscience and Nanotechnology in the South-West of France"</i>		
<b>Antonio Almeida</b> (Universidade de Lisboa, Portugal) - NanoBiotechnology	<b>ORAL</b>	<b>p.31</b>
<i>"Production and Immune Response Characterisation of S. equi Antigens Encapsulated in Surface Modified Polymeric Nanoparticles"</i>		
<b>Suzana M. Andrade</b> (Instituto Superior Técnico, Portugal) - NanoChemistry	<b>ORAL Parallel Session</b>	<b>p.119</b>
<i>"Nanometric aggregates of a covalent porphyrin dimer followed by Fluorescence Correlation Spectroscopy in aqueous buffered solution"</i>		
<b>Emilio Artacho</b> (Cambridge University, UK) - Theory & Modelling	<b>INVITED</b>	<b>p.5</b>
<i>"First-principles calculations of manganite surfaces and interfaces for spintronics"</i>		
<b>Amelia Barreiro</b> (CIN2, Spain) – NanoFabrication	<b>ORAL Parallel Session</b>	<b>p.121</b>
<i>"Nanotube based thermal motors: sub-nanometer motion of cargoes driven by thermal gradients"</i>		
<b>Andreas Berger</b> (CIC nanoGUNE Consolider, Spain) - Nanomagnetism	<b>ORAL</b>	<b>p.33</b>
<i>"Magnetic Characterization of Nano-scale Granular Materials"</i>		
<b>Rob H. Bergmans</b> (NMI Van Swinden Laboratorium B.V, The Netherlands) - Nanometrology	<b>INVITED</b>	<b>p.7</b>
<i>"Nanometrology and its role in the development of nanotechnology; an overview of the state of the art and an outlook on future developments by the European National Metrology Institutes"</i>		
<b>Alvaro Blanco</b> (ICMM-CSIC, Spain) – NanoPhotonics	<b>ORAL Parallel Session</b>	<b>p.123</b>
<i>"Self-assembled disorder"</i>		
<b>Robert H. Blick</b> (University of Wisconsin-Madison, USA) - NEMS	<b>INVITED</b>	<b>p.9</b>
<i>"Self-Excitation in Nano-Electromechanical Systems"</i>		
<b>Caroline Bonafos</b> (CEMES-CNRS, France) - CNANO-GSO	<b>ORAL</b>	<b>p.35</b>
<i>"White electroluminescence from C- and Si-rich thin silicon oxides"</i>		
<b>João Borges</b> (Universidade Nova de Lisboa, Portugal) – NanoComposites	<b>ORAL Parallel Session</b>	<b>p.125</b>
<i>"Electrospun Nanofibers as Potential Reinforcements for Composites"</i>		
<b>Xavier Borrise</b> (CNM, Spain) - Nanophotonics	<b>ORAL</b>	<b>p.37</b>
<i>"Plasmon confinement in V-groove waveguides fabricated by NanoImprint Lithography"</i>		
<b>Pedro Brogueria</b> (Instituto Superior Técnico, Portugal) – NanoFabrication	<b>ORAL Parallel Session</b>	<b>p.127</b>
<b>Ross Brown</b> (IPREM6ECP, France) - CNANO-GSO	<b>ORAL</b>	<b>p.39</b>
<i>"Mapping molecular diffusion in nano-channel systems by tracking individual fluorescent molecules"</i>		

<b>Ernesto Brunet</b> (Universidad Autonoma de Madrid, Spain) – NanoChemistry	<b>ORAL Parallel Session</b>	<b>p.129</b>
<i>"The Role of Porous Materials in the Efficient Storage of Hydrogen"</i>		
<b>Luis Cadillon</b> (I3N-Universidade de Aveiro, Portugal) – NanoComposites	<b>ORAL Parallel Session</b>	<b>p.131</b>
<i>"Introduction of polypyrrol nanoparticles in cement paste to improve the physical properties"</i>		
<b>Mauricio Calvo</b> (Instituto de Ciencias de Materiales de Sevilla, Spain) – NanoPhotonics	<b>ORAL Parallel Session</b>	<b>p.133</b>
<i>"Nanoparticle based One-Dimensional Photonic Crystals"</i>		
<b>Luis Carlos</b> (Universidade de Aveiro, Portugal) - Nanophotonics	<b>ORAL</b>	<b>p.41</b>
<i>"Self-organization, photoluminescence and emergence in amide-functionalized organic/inorganic hybrids"</i>		
<b>Guyhaine Clavel</b> (University of Aveiro - CICECO, Portugal) - CNANO-GSO	<b>ORAL</b>	<b>p.43</b>
<i>"Nonaqueous sol-gel routes to diluted magnetic semiconductors"</i>		
<b>Jose A. Covas</b> (I3N-Universidade de Aveiro, Portugal) – NanoComposites	<b>ORAL Parallel Session</b>	<b>p.135</b>
<i>"Preparing nanocomposites via melt processing: current difficulties and perspectives"</i>		
<b>Eugenia Cruz</b> (INETI /UNFAB and iMed.UL, Portugal) - NanoBiotechnology	<b>ORAL</b>	<b>p.45</b>
<i>"Nanoliposomes as Tolls for the Treatment of Infectious Diseases"</i>		
<b>Fernando Cruz</b> (Imperial College London, UK) - Simulation at the Nanoscale	<b>ORAL</b>	<b>p.47</b>
<i>"Equilibrium and Transport Properties of Small Alkanes and Alkenes Confined in Single-Walled Carbon Nanotubes"</i>		
<b>Ana Luisa Daniel-Da-Silva</b> (University of Aveiro and CICECO, Portugal) - NanoBiotechnology	<b>ORAL</b>	<b>p.49</b>
<i>"Magnetic polysaccharide nanospheres with potential for biomedical applications: preparation via a reverse miniemulsion method"</i>		
<b>Juan de la Figuera</b> (Instituto de Quimica-Fisica Rocasolano, Spain) – NanoFabrication	<b>ORAL Parallel Session</b>	<b>p.137</b>
<i>"Nanoscale periodicity in stripe-forming systems at high temperature – the Au/W(110) system"</i>		
<b>Marie-Hélène Delville</b> (University of Bordeaux, France) - CNANO-GSO	<b>ORAL</b>	<b>p.51</b>
<i>"Towards multifunctional core-shell nanoparticles for biological applications"</i>		
<b>Trevor Douglas</b> (Montana State University, USA) - Nanochemistry	<b>INVITED</b>	<b>p.11</b>
<i>"Virus capsids: constrained organic architectures for nanomaterials synthesis"</i>		
<b>Elisa Elizondo Sáez de Vicuña</b> (ICMAB - CSIC, Spain) - NanoBiotechnology	<b>ORAL Parallel Session</b>	<b>p.139</b>
<i>"Compressed Fluid Based Technologies for the Preparation of Drug Delivery Systems"</i>		
<b>Ivan Fernández</b> (IMM-CSIC, Spain) – NanoFabrication	<b>ORAL Parallel Session</b>	<b>p.141</b>
<i>"Parallel nanogap fabrication with nanometer size control using III-V semiconductor epitaxial technology"</i>		

<b>Luis Fernandez Barquin</b> (Universidad de Cantabria, Spain) – Nanomagnetism	<b>ORAL</b>	<b>p.53</b>
<i>"Size versus Disorder effects in the electronic properties of nanosized intermediate valence metals"</i>		
<b>Irene Fernández-Cuesta</b> (CNM, Spain) – NanoBiotechnology	<b>ORAL Parallel Session</b>	<b>p.143</b>
<i>"Interdigitated nanoelectrodes for sensing: fabrication and characterization"</i>		
<b>Elvira Fortunato</b> (FCT-UNL, Portugal) – NanoBiotechnology	<b>ORAL Parallel Session</b>	<b>p.145</b>
<i>"DNA detection using amorphous silicon sensors with gold nanoparticles"</i>		
<b>Daisuke Fujita</b> (National Institute for Materials Science (NIMS), Japan) - SPM/Nanomaterials	<b>INVITED</b>	<b>p.13</b>
<i>"Low-dimensional Surface Nanostructures studied by Scanning Tunneling Microscopy"</i>		
<b>Paulo Freitas</b> (INESC-MN, IST and INL, Portugal) – NanoBiotechnology	<b>ORAL Parallel Session</b>	<b>p.147</b>
<b>Luis Froufe</b> (ICMM-CSIC, Spain) – NanoPhotonics	<b>ORAL Parallel Session</b>	<b>p.149</b>
<i>"Single molecule fluorescence decay rate statistics in disordered media"</i>		
<b>Juan Maria García Lastra</b> (Universidad del País Vasco, Spain) – Nanotubes	<b>ORAL</b>	<b>p.55</b>
<i>"Effect of Chemisorbed Molecules on the Transport Properties of a (6,6) Carbon Nanotube"</i>		
<b>Antonio Garcia-Martin</b> (IMM-CSIC, Spain) – Nanophotonics	<b>ORAL</b>	<b>p.57</b>
<i>"Magneto-plasmonic materials: tuning magneto-optics with plasmons"</i>		
<b>Pedro García-Mochales</b> (Universidad Autonoma de Madrid, Spain) – Simulation at the Nanoscale	<b>ORAL</b>	<b>p.59</b>
<i>"Formation of stable pentagonal nanowires under stretching on FCC metals"</i>		
<b>Daniel García Sánchez</b> (CIN2, Spain) – NanoFabrication	<b>ORAL Parallel Session</b>	<b>p.151</b>
<i>"Mechanical detection of the vibrations of Carbon Nanotube and Graphene Resonators"</i>		
<b>José V. García Ramos</b> (Instituto de Estructura de la Materia. CSIC., Spain) - NanoChemistry	<b>ORAL Parallel Session</b>	<b>p.153</b>
<i>"SERS on Functionalized Silver Nanostructures: Towards the Detection of Single Molecules in Hot Spots"</i>		
<b>Gonzalo Gonçalves</b> (FCT-UNL/CENIMAT-I3N, Portugal) – NanoFabrication	<b>ORAL Parallel Session</b>	<b>p.155</b>
<i>"High mobility indium zinc oxide deposited by rf magnetron sputtering at room temperature"</i>		
<b>André Gourdon</b> (CEMES - CNRS, France) - Molecular Electronics	<b>INVITED</b>	<b>p.15</b>
<i>"Molecular Devices for Single Molecule STM Experiments"</i>		
<b>Yannick Guari</b> (Université Montpellier, France) - CNANO-GSO	<b>ORAL</b>	<b>p.61</b>
<i>"Synthesis and studies of coordination polymer nanoparticles"</i>		
<b>Magrit Hanbucken</b> (Direction Générale de la Recherche et de l'Innovation (DGRI), France) - Scientific Policy	<b>ORAL</b>	<b>p.63</b>
<i>"A glance at the french networks supporting nanoscience and nanotechnology"</i>		

<b>Jordi Hernández-Borrell</b> (IN2UB-UB, Spain) - CNANO-GSO	<b>ORAL</b>	<b>p.65</b>
<i>"Towards insertion of a transmembrane protein into supported planar bilayers: preliminary studies"</i>		
<b>Jean-Roch Huntzinger</b> (Université Montpellier 2/CNRS, France) – CNANO-GSO	<b>ORAL</b>	<b>p.67</b>
<i>"Atomic force microscopy and Raman analysis of exfoliated graphene on SiC"</i>		
<b>Inhar Imaz</b> (Nanosfun- Institut català de nanotecnologia, Spain) – NanoChemistry	<b>ORAL</b>	<b>p.69</b>
<i>"Functional Metal-Organic Nanoparticles"</i>		
<b>Myrtil Kahn</b> (Laboratoire de Chimie de Coordination, CNRS, France) – CNANO-GSO	<b>ORAL</b>	<b>p.71</b>
<i>"Experimental evidence of the existence in solution of organizations of ZnO nanoparticles synthesized by organometallic method using dynamic light scattering"</i>		
<b>Andrei Kholkin</b> (University of Aveiro, Portugal) – SPM	<b>ORAL</b>	<b>p.73</b>
<i>"Nanoscale Characterization of Ferroelectric Materials via Piezoresponse Force Microscopy"</i>		
<b>Tobias J. Kippenberg</b> (Max-Planck Institute of Quantum Optics, Germany) - Nanophotonics	<b>INVITED</b>	<b>p.17</b>
<i>"Cooling of a micro-mechanical oscillator using radiation-pressure induced dynamical backaction"</i>		
<b>Mathias Kläui</b> (University of Konstanz, Germany) - Nanomagnetism	<b>INVITED</b>	<b>p.19</b>
<i>"Current-induced domain wall dynamics"</i>		
<b>Senentxu Lanceros-Mendez</b> (University of Minho, Portugal) – NanoPhotonics	<b>ORAL Parallel Session</b>	<b>p.157</b>
<i>"Tunable Fabry-Perot Optical Filter with a Resonant Cavity"</i>		
<b>Senentxu Lanceros-Mendez</b> (University of Minho, Portugal) – NanoComposites	<b>ORAL Parallel Session</b>	<b>p.159</b>
<i>"Polymer based Electro-active Micro- and Nano-composites"</i>		
<b>Elena Laukhina</b> (CIBER-BBN, Spain) - Molecular Electronics	<b>ORAL</b>	<b>p.75</b>
<i>"Conducting nanocomposite organic films for plastic pressure sensors and electronic circuits"</i>		
<b>Sebastien Lecommandoux</b> (ENSCP - University of Bordeaux, France) - Nanochemistry	<b>INVITED</b>	<b>p.21</b>
<i>"Block copolymer self-assembly: a powerful tool for the design of new smart biomimetic nano-carriers"</i>		
<b>Joana Loureiro</b> (INESC-MN, Portugal) – NanoBiotechnology	<b>ORAL Parallel Session</b>	<b>p.161</b>
<i>"Integrated platform for Stem Cells separation/counting"</i>		
<b>João M. Maia</b> (I3N-Universidade de Aveiro, Portugal) – NanoComposites	<b>ORAL Parallel Session</b>	<b>p.163</b>
<i>"Direct Numerical Simulation of Carbon Nanofibre Composites Under Shear Flow"</i>		
<b>Oscar L. Malta</b> (Universidade de Pernambuco, Brazil) - Nanomaterials	<b>INVITED</b>	<b>p.23</b>
<i>"The chemical bond overlap plasmon as a tool for quantifying covalency in optical solid state materials"</i>		

<b>Maria Teresa Martinez</b> (Instituto de Carboquímica, Spain) – NanoBiotechnology	<b>ORAL</b>	<b>p.77</b>
<i>"Electronic detection of DNA hybridization"</i>		
<b>Pedro Martins</b> (Universidade do Minho, Portugal) - NEMS / MEMS	<b>ORAL</b>	<b>p.79</b>
<i>"Electroactive <math>\beta</math>-PVDF Polymer as Fluidic Acoustic Mixer for Lab-on-a-Chip Applications"</i>		
<b>Daniel Maspoch</b> (Institut Català de Nanotecnologia, Spain) – SPM	<b>ORAL</b>	<b>p.81</b>
<i>"Dip-Pen Nanolithography: "Writing" Molecules, Biological Entities and Nanomaterials at the Nanometer Scale"</i>		
<b>Marta Mas-Torrent</b> (ICMAB - CSIC, Spain) – NanoChemistry	<b>ORAL</b>	<b>p.83</b>
<i>"Self-assembly of polychlorotriphenylmethyl organic radicals on surfaces"</i>		
<b>Luis Melo</b> (Fundação para a Ciência e a Tecnologia , Portugal) - Scientific Policy	<b>ORAL</b>	<b>p.85</b>
<i>"Nano Activity in Portugal"</i>		
<b>Mervyn Miles</b> (University of Bristol, UK) - SPM	<b>INVITED</b>	<b>p.25</b>
<i>"High Speed AFM – Contact &amp; Non-contact"</i>		
<b>Rodolfo Miranda</b> (Universidad Autónoma de Madrid , Spain) – NanoChemistry	<b>ORAL Parallel Session</b>	<b>p.165</b>
<i>"Preferential nucleation, molecular distortion, charge transfer, and elastic effects in the self-assembly of TCNQ on Cu(100)"</i>		
<b>Rodolfo Miranda</b> (UAM-IMDEA Nano, Spain) - Scientific Policy	<b>ORAL</b>	<b>p.87</b>
<i>"IMDEA-Nanociencia: A new Institute devoted to research in Nanoscience and Nanotechnology in Madrid"</i>		
<b>Miguel Monge</b> (Universidad de La Rioja, Spain) – NanoChemistry	<b>ORAL Parallel Session</b>	<b>p.167</b>
<i>"Silver nanoparticles and gold metallodendrimers: from molecular precursors to nanomaterials"</i>		
<b>N.M. Neves</b> (IBB/3B's- University of Minho, Portugal) – NanoComposites	<b>ORAL Parallel Session</b>	<b>p.169</b>
<i>"Biodegradable Polymeric Microfibrils Reinforced with Nanofibrils for Biomedical Applications"</i>		
<b>Salazar Norkis</b> (Universidad Simón Bolívar, Venezuela) – NanoComposites	<b>ORAL Parallel Session</b>	<b>p.171</b>
<i>"PMMA-Organic Bentonite Nanocomposites from the Exfoliation-Adsorption Technique and their Characterization by FTIR, XRD, TEM, TSDC &amp; DSC"</i>		
<b>Marc Obiols-Rabasa</b> (CSIC - IIQAB, CIBER-BBN, Spain) – NanoComposites	<b>ORAL Parallel Session</b>	<b>p.173</b>
<i>"Rheological studies on polymeric nanoparticle dispersions stabilized by a polyfructose-derivative surfactant"</i>		
<b>Roberto Otero</b> (Universidad Autónoma de Madrid, Spain) – NanoChemistry	<b>ORAL Parallel Session</b>	<b>p.175</b>
<i>"1D ZnO Chains as the Spinal Cord of Adsorbed Metalloporphyrin Nanotubes Linked by Water Ligands"</i>		

<b>María Conceição Paiva</b> (Institute for Polymers and Composites, Portugal) – NanoMaterials	<b>ORAL</b>	<b>p.89</b>
<i>"Chemical Functionalisation of Carbon Nanotubes for the Dispersion in Polymer Matrices"</i>		
<b>Luisa Pedro</b> (University of Algarve, Portugal) – NanoBiotechnology	<b>ORAL Parallel Session</b>	<b>p.177</b>
<i>"Protein nanoparticles for molecular therapy: Molecular construction of SIVp17/HIV1p6 nanoparticles and assembly in animal cell cultures"</i>		
<b>Sergio Pereira</b> (CICECO University of Aveiro, Portugal) - Nanophotonics	<b>ORAL</b>	<b>p.91</b>
<i>"Controlled integration of nanocrystals on the surface of group III-nitride light-emitting epitaxial heterostructures"</i>		
<b>Francesc Perez-Murano</b> (CNM-IMB, CSIC, Spain) - CNANO-GSO	<b>ORAL</b>	<b>p.93</b>
<i>"CMOS integrated nanomechanical mass sensors: determination of evaporation rate of femtoliter droplets"</i>		
<b>Jose Maria Pitarke</b> (CIC nanoGUNE Consolider, Spain) - Scientific Policy	<b>ORAL</b>	<b>p.95</b>
<i>"CIC nanoGUNE Consolider, the big challenge of the small"</i>		
<b>Emilio Prieto</b> (CEM, Spain) – Industrial	<b>ORAL Parallel Session</b>	<b>p.179</b>
<i>"Standardization in Nanotechnologies. The AENOR Spanish Group GET15 and its role within ISO and CEN"</i>		
<b>Erwan Rauwel</b> (University of Aveiro and CICECO, Portugal) – NanoChemistry	<b>ORAL Parallel Session</b>	<b>p.181</b>
<i>"Non-Aqueous Sol-Gel Routes Applied to Atomic Layer Deposition"</i>		
<b>Steve Reyntjens</b> (FEI Company , Netherlands) – NanoFabrication	<b>ORAL Parallel Session</b>	<b>p.183</b>
<i>"Novel tools for NanoPrototyping using Dualbeam™ FIB/SEM"</i>		
<b>Jose Rivas Rey</b> (INL, Portugal & USC, Spain) - Scientific Policy	<b>ORAL</b>	<b>p.97</b>
<i>"The International Iberian Nanotechnology Laboratory Facts, Prospects and Strategic Goals"</i>		
<b>Joao Rocha</b> (University of Aveiro, CICECO, Portugal) – NanoChemistry	<b>ORAL</b>	<b>p.99</b>
<i>"Photoluminescent Microporous Lanthanide Silicates and Metal-Organic Frameworks"</i>		
<b>Angel Rubio</b> (Universidad Pais Vasco, Spain) - CNANO-GSO	<b>ORAL</b>	<b>p.101</b>
<i>"Dimensionality effects in the optics of BN nanostructures: applications for optoelectronic devices"</i>		
<b>Josep Samitier</b> (IBEC, Spain) – NanoBiotechnology	<b>ORAL Parallel Session</b>	<b>p.185</b>
<i>"Nanobiotechnology and nanomedicine in Spain"</i>		
<b>Daniel Sanchez Portal</b> (Donostia Internacional Physics Center / CSIC, Spain) – CNANO-GSO	<b>ORAL</b>	<b>p.103</b>
<i>"Carbon Nanostructures: Optical Properties from TDDFT Studies and Complex Magnetic Behaviour of Substitutional Transition Metal Impurities"</i>		

<b>Julio Santaren</b> (TOLSA S.A., Spain) – Industrial	<b>ORAL Parallel Session</b>	<b>p.187</b>
<i>"DOMINO Project: A Challenging Adventure fro the Spanish Industry into the Nanoworld"</i>		
<b>Reinhard Schwarz</b> (Instituto Superior Técnico, Portugal) – NanoPhotonics	<b>ORAL Parallel Session</b>	<b>p.189</b>
<i>"Interface analysis techniques on nanoscale dimension in flexible solar cells"</i>		
<b>Philippe Serp</b> (Toulouse University, France) – CNANO-GSO	<b>ORAL</b>	<b>p.105</b>
<i>"MWCNT activation and its influence on the catalytic performance of Pt/MWCNT catalysts for selective hydrogenation"</i>		
<b>Nuno Joao Oliveira Silva</b> (ICMA - CSIC, Spain) – Nanomagnetism	<b>ORAL</b>	<b>p.107</b>
<i>"Magnetic and structural properties of iron oxyhydroxynitrate nanoparticles"</i>		
<b>Javier Tamayo</b> (IMM-CSIC, Spain) – NanoFabrication	<b>ORAL Parallel Session</b>	<b>p.191</b>
<i>"Nanomechanical Devices: Ultrasensitive sensors of molecular recognition and conformational changes of biomolecules."</i>		
<b>Niek Van Hulst</b> (ICFO, Spain) – NanoPhotonics	<b>ORAL Parallel Session</b>	<b>p.193</b>
<i>"NanoAntennas - Controlling Single Molecule Excitation and Emission"</i>		
<b>Amadeo L. Vazquez de Parga</b> (Universidad Autonoma de Madrid, Spain) – SPM	<b>ORAL</b>	<b>p.109</b>
<i>"Graphene on Ru(0001): Spatially resolved electronic structure"</i>		
<b>Marc-Georg Willinger</b> (University of Aveiro, Portugal) – NanoMaterials	<b>ORAL</b>	<b>p.111</b>
<i>"EELS in the TEM: chemical information at the nanometer scale"</i>		
<b>Jun Xiao</b> (CETR, USA) – Industrial	<b>ORAL Parallel Session</b>	<b>p.195</b>
<i>"Scanning Nano-Metrology of ultra thin films"</i>		
<b>Jone Zabaleta</b> (ICMAB - CSIC, Spain) – NanoMaterials	<b>ORAL</b>	<b>p.113</b>
<i>"Self-assembling and guided self-organization of oxide nanostructures from chemical solutions"</i>		
<b>Mikhail Zheludkevich</b> (CICECO/DECV, Portugal) – NanoMaterials	<b>ORAL</b>	<b>p.115</b>
<i>"Self-healing coatings with multi-level protection based on active nanocontainers"</i>		





## ABSTRACTS





## INVITED CONTRIBUTIONS



## FIRST-PRINCIPLES CALCULATIONS OF MANGANITE SURFACES AND INTERFACES FOR SPINTRONICS

Emilio Artacho<sup>§</sup>

*Department of Earth Sciences, University of Cambridge, Cambridge CB2 3EQ, UK*

Lanthanum-strontium manganites,  $\text{La}_{1-x}\text{Sr}_x\text{MnO}_3$  (LSMO), are materials that display an enormously rich phase diagram by varying temperature and composition,  $x$ , with phases displaying behaviours as interesting as colossal magnetoresistance. For  $x \sim 1/3$  the material behaves as a ferromagnetic half metal, that is, with the Fermi level within a gap in the minority-spin density of states, and thus total spin polarisation of carriers at the Fermi level. It is an attractive material for spintronics, where the spin degree of freedom of the electrons is manipulated. Any such manipulation involves interfacing this material with others, which is the topic of this talk. In particular, an experimental group at Cambridge built nano-magnetoresistive devices by bridging a carbon nanotube (CNT) between two LSMO electrodes, and obtained remarkable magnetoresistance characteristics [1]. LSMO used as source and drain of electrons allow a much higher conduction through the device when both electrodes have their magnetisations aligned, while the conductance drops very substantially if they are counter-aligned. The electrons injected into the CNT have a high degree of spin polarisation, which barely alters when travelling along the CNT, given the very low spin-flip probability in the tube. If the drain electrode presents a gap for these carriers the resistance is high. The relative magnetisation orientation can be controlled easily with an external magnetic field, giving the desired magnetoresistive coupling.

The electronic characterisation of the LSMO-CNT interface prompted by these experiments, and performed by first-principles simulations [1], offered intriguing results, which made us turn back to the bare LSMO surface [2]. A detailed study has been performed on the  $\text{MnO}_2$ -terminated (001) surface by means of density-functional calculations, showing clear indications of a latent ferroelastic phase, of a ferrodistorive kind analogous to the ferroelectric phase in  $\text{BaTiO}_3$ . This phase is stabilised close to the surface, triggered by a surface buckling of Mn atoms outwards at the surface layer. This buckling is a canonical instability originated by the high density of states induced by a surface state, and thus hardly surprising. It is the subsurface propagation of the Mn off-centering in the respective O octahedra which is remarkable. It amounts to  $\sim 0.1 \text{ \AA}$  close to the surface. Its decay length into the bulk cannot be determined from the calculations, except that it is longer than  $\sim 10 \text{ \AA}$ , determined by the thickness of the slab used in the calculations. The off-centring order parameter competes with the octahedral tilting order parameter in the bulk of the material, as shown by a suppression of the tilt towards the surface. The characterisation of this phase and its possible implications for this and other interfaces will be discussed.

<sup>§</sup>Work done in collaboration with JM Pruneda, V Ferrari, R Rurali, PB Littlewood and NA Spaldin.

[1] LE Hueso, JM Pruneda, V Ferrari, G Burnell, JP Valdés-Herrera, BD Simons, PB Littlewood, E Artacho, A Fert & ND Mathur, *Nature* **445**, 410 (2007).

[2] JM Pruneda, V Ferrari, R Rurali, PB Littlewood, NA Spaldin and E Artacho, *Phys. Rev. Lett.* **99**, 226101 (2007).



# NANOMETROLOGY AND ITS ROLE IN THE DEVELOPMENT OF NANOTECHNOLOGY; AN OVERVIEW OF THE STATE OF THE ART AND AN OUTLOOK ON FUTURE DEVELOPMENTS BY THE EUROPEAN NATIONAL METROLOGY INSTITUTES

*R.H. Bergmans,*

*NMi Van Swinden Laboratorium, P.O. Box 654, 2600 AR Delft, The Netherlands*

[Rbergmans@nmi.nl](mailto:Rbergmans@nmi.nl)

In order to ensure that results in nanotechnology can be compared quantitatively and parts are interchangeable, the measurements made must be traceable. This means that standards should be used which are linked through a traceable chain to the corresponding SI-unit, i.e., the Meter, the Kelvin, ... , of the measurand. Due to the quite different nature of nanotechnology the conventional standards, measurement methods and instrumentation are no longer sufficient or cannot reach the desired uncertainty/accuracy. Therefore there is a need for a new branch of metrology, the so-called nanometrology. This is a multidisciplinary kind of metrology since it is not limited to a particular SI-unit. The presentation will focus on the traceability of dimensional quantities, such as length, size, shape, and roughness.

The role of our institute just like other National Metrology Institutes (NMIs) is to provide this traceability of measurements to (inter)national standards thereby making measurements quantitatively comparable and trade possible. For these reason NMIs develop and improve standards to fulfill the needs of their national industry and society. Since there is international trade there exist also an international metrological infrastructure. The CIPM (Committee international the Poids et Measure) is the worldwide link between the NMIs. It gets its authority from "The convention of the Metre", a diplomatic treaty between fifty-one nations. Further every region in the world has is own linking body. For Europe this is EURAMET. One of the tasks of the CIPM and its working groups, in cooperation with the regional bodies, is to establish the degree of equivalence between national measurement standards of the NMIs and to provide mutual recognition of the calibration certificates issued by the NMIs. This is done by reviews of the NMIs as well as by carrying out comparisons on artifacts and standards.

Also for nanometrology the equivalence between the NMIs needs to be established. One of the differences between nanometrology and "classical metrology" are the huge investments in money and man-hours by the NMIs that are necessary to keep up with the demands of industry and science. It is therefore no longer possible for every NMI to develop the necessary standards and measuring instruments individually. For this reason in 2001 an "Initiative on nanometrology" was started by EURAMET. As part of this Initiative an inventory of the efforts and visions of the NMIs was made in 2002-2003 and in 2006 a roadmap for nanometrology was set-up. The main challenges we identified in this roadmap are:

- a. Nanoparticle standards
- b. Scanning probe microscopy to support nanotechnology
- c. Displacement metrology at the nanometre scale
- d. 2D- and 3D-instrumentation with nm uncertainty

In this presentation the current state of the art in nanometrology will be given. The main instruments such as the metrological Atomic Force Microscope will be presented, see figure 1. Focus will be on the metrological nature of these instruments as compared to most instruments on the market. Comparisons in nanometrology on physical standards will be presented, showing the need for traceability as well as demonstrating what is currently possible.

Based on the nanometrology roadmap and the key challenges the European NMIs are currently setting-up joint projects to take the next steps in getting traceable standards, measurements and instruments for nanotechnology. Important issues here are:

- Probe sample interactions in AFM, Scanning Electron Microscopy (SEM) and optical Scatterometry. These measurement techniques have fundamentally different probe sample interaction effects. This limit the agreement of the measurement results as well as the full potential of the individual techniques.
- The need for new physical standards, especially for nanoparticles. Here standards and procedures for determining size, shape and distribution need to be developed with an accuracy of better than 1 nm.
- New means and methods for the traceable characterisation of crucial dimensions relevant to industrial, economic and scientific development
- New traceability routes. The traceability of length measurements is currently exclusively assured by optical interferometry. Today's applications in nano- and semiconductor-technology ask for resolutions far beyond the nanometre. So new ways and standards to provide traceability at the atomic scale will be explored.

An overview of these developments and joint projects will be presented.

### Figures:

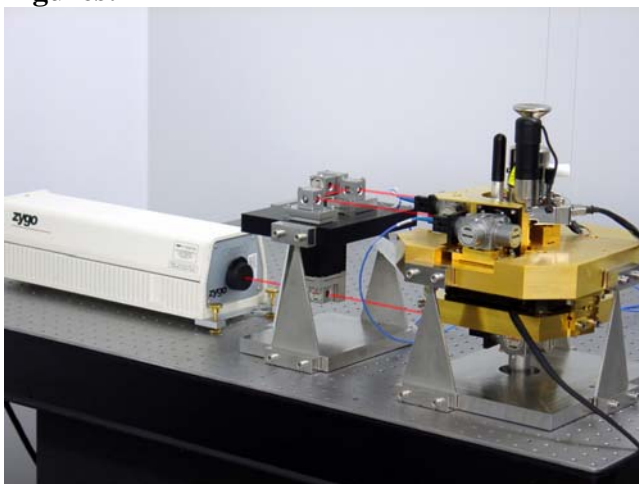


Figure 1: Overview of a metrological AFM set-up at NMi VSL. The measurement system is a 3 axes laserinterferometer. The beam from the laser source (left) is split into 3 beams (middle section) and fed into the interferometer optics (right).

## SELF-EXCITATION IN NANO-ELECTROMECHANICAL SYSTEMS

Robert H. Blick, Hyun-Seok Kim, Chulki Kim, and Hua Qin  
 University of Wisconsin-Madison, Electrical & Computer Engineering,  
 1415 Engineering Drive, Madison, WI 53706, USA. [blick@engr.wisc.edu](mailto:blick@engr.wisc.edu)

In this talk I want to give an overview of mechanically mediated electron transport in nano-electromechanical systems (NEMS). One aspect will cover self-excitation in NEMS: self-excitation is a mechanism, which is ubiquitous for electromechanical power devices such as electrical generators. This is conventionally achieved by making use of the magnetic field component in electrical generators, where a good example are the overall visible wind farm turbines. In other words, a static force, like wind acting on the rotor blades, can generate a resonant excitation at a certain mechanical frequency. This mechanical resonance is then usually transformed into electrical energy.

For nanomechanical systems such a self-excitation mechanism is highly desirable as well, since it can generate mechanical oscillations at radio frequencies by simply applying a DC bias voltage. This is of great importance for low-power signal communication devices and detectors, as well as for nanomechanical computing [1]. For a particular nanomechanical system – the single electron shuttle – this effect was predicted some time ago by & Gorelik *et al.* [2]. Here, we use a nano-electromechanical single electron transistor (NEMSET) to demonstrate first mechanical mixing and then self-excitation for both the soft and hard regime, respectively [3,4]. The ability to use self-excitation in nanomechanical systems may enable the detection of radiation via rectification, the discovery of quantum mechanical backaction effects in direct tunneling, and macroscopic quantum tunneling in NEMS.

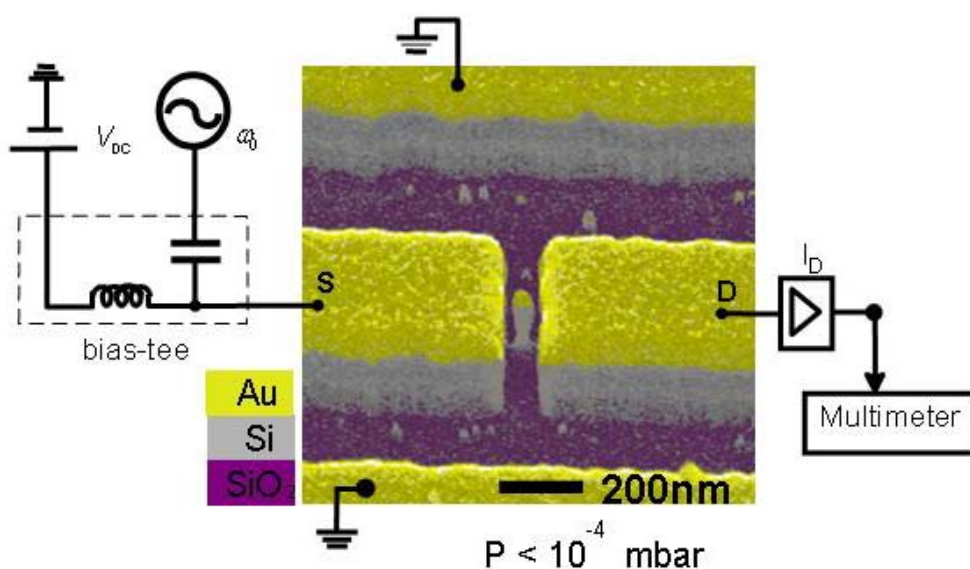


**Fig. 1.** Nanopyllar between source and drain electrode for probing mechanical electron shuttling. The devices are fabricated in silicon-on-insulator materials with a metalized top layer.

**References:**

- [1] Robert H. Blick, Hua Qin, Hyun-Seok Kim, and Robert Marsland, *New J. Phys.* **9**, 241 (2007).
  - [2] L.Y. Gorelik, A. Isacson, M.V. Voinova, B. Kasemo, R.I. Shekhter, and M. Jonson, *Phys. Rev. Lett.* **80**, 4526 (1998).
  - [3] H.-S. Kim, H. Qin, M.S. Westphall, L.M. Smith, and R.H. Blick, *Applied Physics Letters* **91**, 143101(2007).
  - [4] H.-S. Kim, H. Qin, and R.H. Blick, submitted to *Nature Nanotechnology*.
-

## VIRUS CAPSIDS: CONSTRAINED ORGANIC ARCHITECTURES FOR NANOMATERIALS SYNTHESIS

Trevor Douglas, Center for BioInspired Nanomaterials, Montana State University, Bozeman, Montana USA.

In nature, proteins orchestrate the formation of elaborate inorganic ‘biomineralized’ structures. The single-celled algae, *Emiliana huxleyi*, form intricate calcium carbonate ( $\text{CaCO}_3$ ) structures called coccoliths (Figure 1A) whereas synthetic preparations of  $\text{CaCO}_3$  result in a far more limited range of morphologies, by comparison. Coccolith formation is controlled by proteins that direct the nucleation and assembly of crystallites into intricate 3D assemblies. The degree of control exhibited by this and other natural biomineral systems is an inspiration for material scientists.

Viral capsids are also naturally occurring, intricate assemblies that serve to house, protect, and deliver nucleic acid genomes to specific host cells. Their structures must be robust enough to survive diverse conditions yet sufficiently dynamic to release their genome into host cells. Proteins are the building blocks of viral capsids and protein-protein interactions dictate their 3D structure. Typically, protein motifs on the interior are involved in packaging nucleic acid whereas those on the exterior are involved with cell recognition and attachment. Viral capsids devoid of their nucleic acid genomes can be thought of as “nanocontainers” [1]. The diversity of these nanocontainers is seemingly endless, since viruses are ubiquitous with life. An illustration of this functional organic architecture is the *Sulfolobus* turreted icosahedral virus (STIV), isolated from the acidic hot ( $>90^\circ\text{C}$ ) springs of Yellowstone National Park (YNP), which presents elaborate turret-like structures on its exterior [2] (Figure 1B). Both the coccolith and the archaeal virus are examples of naturally occurring 3D assemblies whose architecture is dictated by protein. Inspired by nature, we have selected a bio-mimetic approach to nanomaterials synthesis utilizing protein cage architectures to serve as size constrained reaction vessels and chemical building blocks [3-5].

Protein cage architectures, 10-100 nm diameter, are self-assembled hollow spheres derived from viruses and other biological cages including heat shock proteins (Hsp), DNA binding proteins from starved cells (Dps), and ferritins. These architectures play critical and biological roles and are similar in that they are all essentially proteinaceous containers with three distinct surfaces (interior, exterior, and subunit interface) to which one can impart synthetic function by design. Through a combination of genetic and chemical modifications the cages can be used to direct the nucleation of specific inorganic phases, the covalent attachment of organics, and the packaging of polymers in a size constrained manner. This has resulted in the formation of materials with novel magnetic, catalytic and therapeutic properties. This presentation will highlight the demonstrated utility of protein cage architectures in

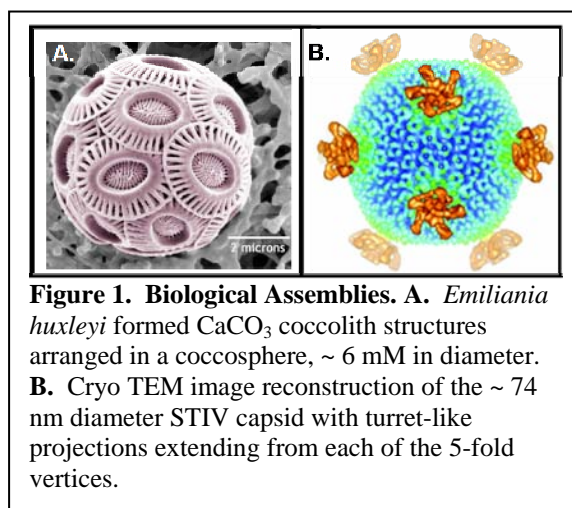
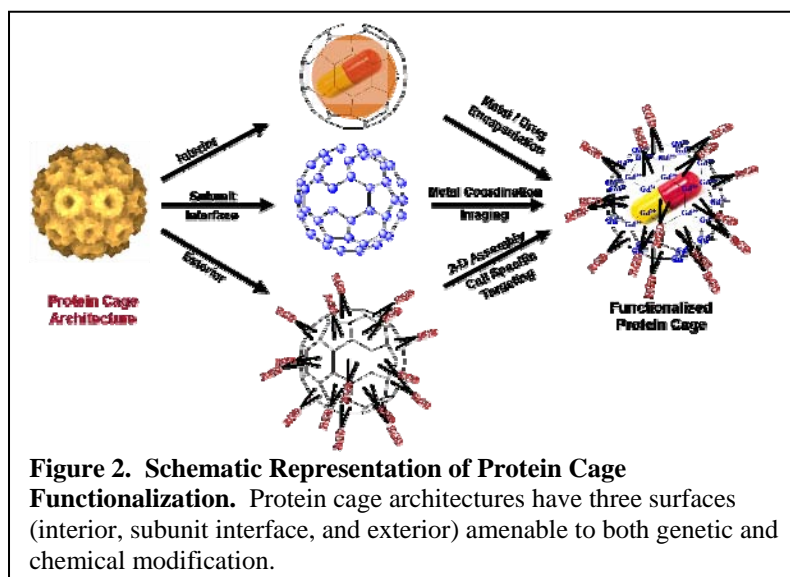


**Figure 1. Biological Assemblies.** A. *Emiliana huxleyi* formed  $\text{CaCO}_3$  coccolith structures arranged in a coccosphere, ~ 6  $\mu\text{m}$  in diameter. B. Cryo TEM image reconstruction of the ~ 74 nm diameter STIV capsid with turret-like projections extending from each of the 5-fold vertices.

nanotechnology with applications including magnetic nanoparticle synthesis and the development of targeted therapeutic and imaging delivery agents [6-10] (Figure 2).



## References

1. Douglas, T. and M. Young, *Viruses: Making friends with old foes*. Science, 2006. **312**(5775): p. 873-875.
2. Rice, G., et al., *The structure of a thermophilic archaeal virus shows a double-stranded DNA viral capsid type that spans all domains of life*. Proc Natl Acad Sci U S A, 2004. **101**(20): p. 7716-20.
3. Klem, M., M. Young, and T. Douglas, *Biomimetic magnetic nanoparticles*. Materials Today, 2005: p. 28-37.
4. Douglas, T., M. Allen, and M. Young, *Self-assembling Protein Cage Systems and Applications in Nanotechnology*, in *Polyamides and Complex Proteinaceous Materials I*, S.R. Fahnstock and A. Steinbuechel, Editors. 2002, Wiley-VCH: Weinheim. p. 517.
5. Douglas, T. and M. Young, *Host-guest encapsulation of materials by assembled virus protein cages*. Nature (London), 1998. **393**(6681): p. 152-155.
6. Allen, M.A., et al., *Paramagnetic Viral Nanoparticles as Potential High-Relaxivity Magnetic Resonance Contrast Agents*. Magnetic Resonance in Medicine, 2005. **54**: p. 807-812.
7. Bulte, J.W.M., et al., *Magnetodendrimers allow endosomal magnetic labeling and in vivo tracking of stem cells*. Nature Biotechnology, 2001. **19**(12).
8. Douglas, T., et al., *Protein Engineering of a Viral Cage for Constrained Nano-Materials Synthesis*. Advanced Materials, 2002. **14**(6): p. 415-418.
9. Flenniken, M.L., et al., *Melanoma and lymphocyte cell-specific targeting incorporated into a heat shock protein cage architecture*. Chemistry & Biology, 2006. **13**: p. 161-170.
10. Liepold, L.O., et al., *Viral capsids as MRI contrast agents* Magnetic Resonance in Medicine, 2007. **58**: p. 871-879.

## LOW-DIMENSIONAL SURFACE NANOSTRUCTURES STUDIED BY SCANNING TUNNELING MICROSCOPY

Daisuke Fujita<sup>\*1,2</sup> and Keisuke Sagisaka<sup>1,2</sup>

<sup>1</sup> International Center for Materials Nanoarchitectonics, World Premier International Research Center,

<sup>2</sup> Advanced Nano Characterization Center, National Institute for Materials Science (NIMS)

1-2-1 Sengen, Tsukuba, Ibaraki 305-0047, Japan

\*[fujita.daisuke@nims.go.jp](mailto:fujita.daisuke@nims.go.jp)

With a further miniaturization of functional devices for information technology, novel nanoprobe technology for fabrication, manipulation and characterization of low-dimensional surface nanostructures with atomic-scale resolution has been highly required. Such a novel nanometer-scale processing tool with multiple functions plays an important role in the interdisciplinary research on materials nano-architectonics. Here our recent achievements in the application of scanning tunneling microscopy and spectroscopy (STM/STS) to atomic-scale fabrication, manipulation and characterization in ultrahigh vacuum (UHV) and at low temperatures (LT) are presented.

Firstly, exploration of the true ground state and the reversible phase manipulation on Si(001) reconstructed surfaces will be discussed using high resolution LT-UHV STM/STS. Although the Si(001) wafer has been the most important substrate material in semiconductor industry and nano-electronics, and its surface has been extensively and intensively studied for decades, the ground state of Si(001) surface at LT, having the most stable atomic-configuration, has been a matter of controversy in surface physics for the decade [2]. As schematically shown in Fig.1, there have been various papers reporting the observation of different surface structures for the ground state of Si(001) surfaces (static (2×1), dynamic (2×1), c(4×2) and p(2×2)) using various surface analysis methods such as LT-STM, LT noncontact-AFM and LT-LEED. It should be noted that the reconstruction on Si(001) surfaces involve dimerization, which creates the unique one-dimensional property of this surface. The dimerization removes one of the two dangling bonds (DB) associated to each atom on the bulk terminated surfaces. Further reconstruction can be characterized by dimer buckling, opening up an energy gap between the two remaining DBs. As a result, the remaining DBs form filled and empty states at the Si(001) surface.

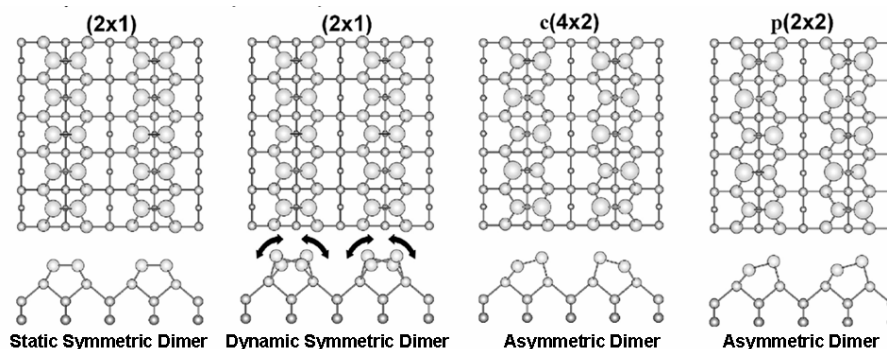


Fig. 1. The proposed atomic configurations on Si(001) at low temperatures (< 50K).

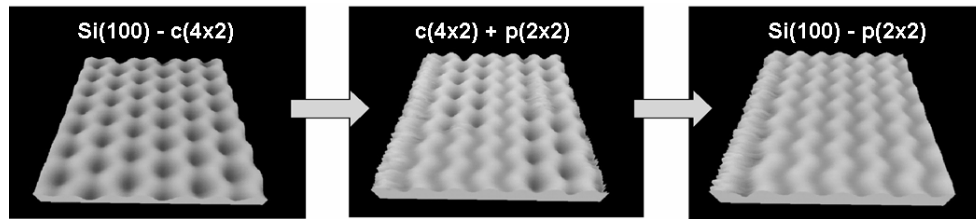


Fig. 2 Reversible phase manipulation between the ground state  $c(4 \times 2)$  and quasi-ground state  $p(2 \times 2)$ .

Our LT-STM analysis has discarded the  $(2 \times 1)$  cases first. Furthermore, it has clarified that the emergence of  $p(2 \times 2)$  and the flip-flop dimers at LT is generated by an STM scan at a specific bias voltage, and is not the intrinsic nature of the Si(001) surface [2]. The injection of tunneling electrons or holes into a particular surface state plays an important role in the surface phase modification. Finally we have discovered how to manipulate the surface phases between  $c(4 \times 2)$  and  $p(2 \times 2)$  by controlling the tunneling conditions (Fig.2). From such findings, we concluded that the ground state of Si(001) is  $c(4 \times 2)$  phase [3].

The empty DB state, which is located in the bulk band gap, reveals dispersive in the direction of the dimer row, and may be regarded as one-dimensional (1D) electronic state. LT-STM/STS observations clearly show a 1D electronic characteristic along the dimer row [4]. Taking advantage of STM atom manipulation, we have succeeded in the fabrication of an artificial 1D quantum well on a single Si dimer row by depositing tungsten atom dots from STM tips [5]. The energy-resolved imaging ( $dI/dV$ ) shows wave patterns of different amplitudes and oscillation periods as the sample bias is varied. These results clarify that the DB state is confined between the artificial potential barriers and it behaves as a 1D quantum well (QW). The observed differential conductance (LDOS) images in Fig.3 shows that 1D confinement in the artificial QW can be explained by a parabolic potential well. These results clearly prove that the atomic scale 1D electronic states can be artificially fabricated and analyzed by high resolution LT-STM/STS techniques.

Finally, recent new findings on the artificial atomic structure fabricated on Si(111)- $(7 \times 7)$  surfaces at LT will be presented.

Based on the combination of STM nano-processing capability and advanced physical fields, we expect to promote the novel nanomaterials research by the nano-architectonics principle.

### Acknowledgements

This work was supported by *World Premier International Research Center Initiative (WPI Initiative)*, MEXT, Japan.

### References

- [1] Uda T, Shigekawa H, Sugawara Y, Mizuno S, Tochihara H, Yamashita Y, Yoshinobu J, Nakatsuji K, Kawai H, Komori F, *Prog. in Surf. Sci.*, 76 (2004) 147.
- [2] Sagisaka K, Fujita D and Kido G, *Phys. Rev. Lett.* **91** (2003) 146103.
- [3] Sagisaka K. and Fujita D, *Phys. Rev. B* **71** (2005) 235327.
- [4] Sagisaka K. and Fujita D, *Phys. Rev. B* **71** (2005) 245319 .
- [5] Sagisaka K. and Fujita D, *Appl. Phys. Lett.* 88 (2006) 203118.

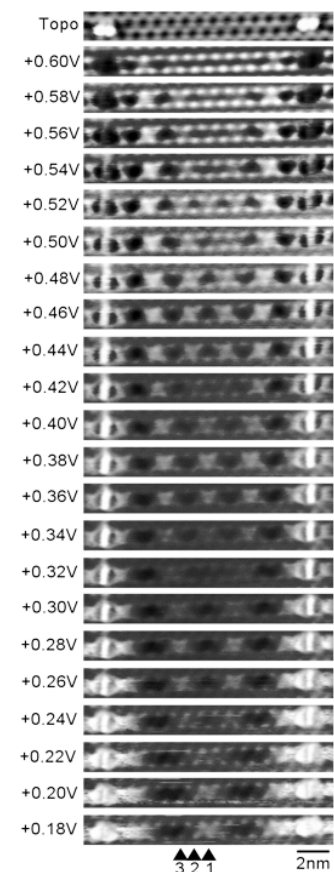


Fig. 3 Top: STM topography image of QW fabricated on a single Si(001) dimer row. Others: Differential conductance ( $dI/dV$ ) images for various sample bias voltages.

## MOLECULAR DEVICES FOR SINGLE MOLECULE STM EXPERIMENTS

*André Gourdon*

*NanoSciences Group, CEMES-CNRS, Toulouse (France)*

[gourdon@cemes.fr](mailto:gourdon@cemes.fr)    [www.cemes.fr/GNS](http://www.cemes.fr/GNS)

Scanning probe microscopy in ultra-high vacuum nowadays allows very precise experiments at the single molecule level [1]. We have designed and synthesized series of molecules finely tuned for studying molecule-substrate interactions, molecular mechanics, contact conductance or molecular switching.

In this talk, I will introduce molecular moulds able to perform and stabilize nanoelectrodes, molecular devices designed to trap and move metallic atoms [2], to perform switching and conformational changes [3] or to demonstrate a rack-and-pinion mechanism (Figure below) [4]. Current work on molecular orbital imaging will also be presented [5].

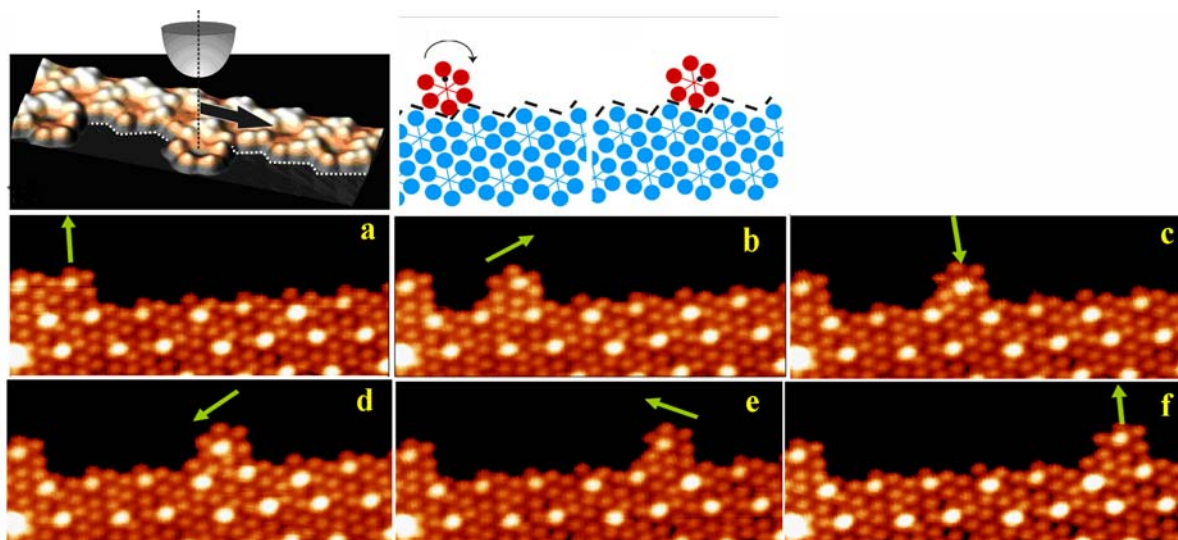


*Figure: A fully controlled rotation of a single molecule in a rack-and-pinion system. The arrow shows the orientation of a quasi six-fold symmetry molecule with respect to the 2D crystal step-edge.*

### References:

- 1 F. Moresco and A. Gourdon, *Proc. Natl. Acad. Sci. USA* 8809 (2005) 102.
- 2 L. Gross, K.-H. Rieder, F. Moresco, S. Stojkovic, A. Gourdon and C. Joachim, *Nature Materials* 892 (2005) 4.
- 3 L. Grill, K.-H. Rieder, and F. Moresco, S. Stojkovic, A. Gourdon, and C. Joachim *Nanoletters* 12(6), (2006) 2685.
- 4 F. Chiaravalloti, L. Gross, K.-H. Rieder, S. M. Stojkovic, A. Gourdon, C. Joachim, and F. Moresco *Nature Materials* 6 (2007) 30.
- 5 C. J. Villagomez Ojeda, T. Zambelli, S. Gauthier, A. Gourdon, C. Barthes, S. Stojkovic, C. Joachim. *Chem. Phys. Letters* 450 (2007) 107.

*Supports from the CNRS, and the EU through the IST projects CHIC and Pico-Inside are gratefully acknowledged.*



# COOLING OF A MICRO-MECHANICAL OSCILLATOR USING RADIATION-PRESSURE INDUCED DYNAMICAL BACKACTION

T.J. Kippenberg<sup>1</sup>

<sup>1</sup>Max-Planck-Institute of Quantum Optics, 85748 Garching, Germany

<sup>2</sup>Department of Applied Physics, California Institute of Technology, Pasadena, CA91125 USA

## Abstract:

We demonstrate how dynamical backaction of radiation pressure can be exploited for *passive* laser-cooling of high-frequency (>50 MHz) mechanical oscillation modes of ultra-high-finesse optical microcavities from room temperature to 11 K.

©2007 Optical Society of America

**OCIS codes:** (140.3320) Laser cooling; (230.3990) Microstructure devices; (270.2500) Fluctuations, relaxations, and noise; (190.3100) Instabilities and Chaos

For more than three decades, *dynamical backaction* in the form of radiation pressure has been predicted to give rise to intricate coupled dynamics of the optical modes of a high-finesse cavity and the mechanical modes of its boundaries [1]. In particular, if the mechanical oscillation period is comparable to the cavity's photon lifetime, and the cavity is pumped with a red-detuned laser, the Brownian motion of the mechanical mode can be reduced, corresponding to an effective temperature reduction or cooling.

In this contribution, we report on the first the experimental observation of this phenomenon using very high-finesse toroidal silica microresonators[2]. These structures (Fig. 1A) possess whispering gallery type optical modes (with photon lifetimes up to 500 ns) while simultaneously exhibiting micro-mechanical resonances in the radio-frequency domain. Here we study the interaction of the intracavity light with the ~60 MHz radial breathing mode of the cavity, which has a Q-factor of about 3000 in ambient atmosphere. Due to the curved nature of the dielectric cavity, the circulating photons exert a radial force on the cavity sidewalls, thereby coupling the optical and modes as reported in prior work. [3-5] Consequently, this system is equivalent in its description to a Fabry P erot cavity with a movable mirror (Fig. 1B). Owing to the resonator's optical photon lifetime being similar to the mechanical oscillation period, these devices operate in a regime where cavity retardation effects cannot be neglected, which has previously enabled the study of radiation pressure induced oscillations [3-5] in an experimental setting.

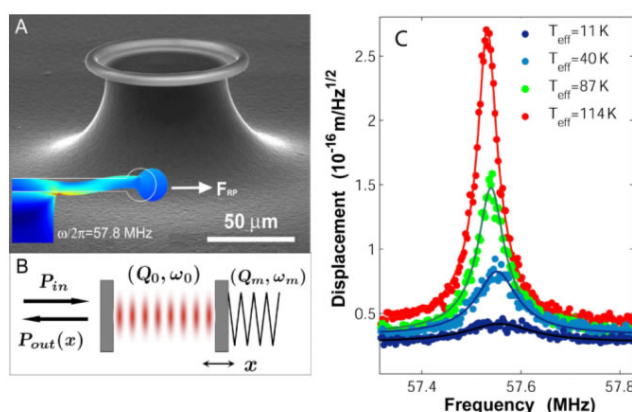


Fig. 1. (A): Scanning electron micrograph of a toroid microcavity on a chip. Inset: Finite element simulation showing the stress (color coded) and strain of the 57.8-MHz breathing mode of the device. The strain is exaggerated for clarity. Note that radiation pressure exerts a radial force owing to total internal reflection of the confined light. (B) Fabry-P erot equivalent diagram of the experiment. (C) Cooling of the mechanical mode as induced by a red-detuned 972nm laser at power levels of 0.25, 0.75, 1.25, 1.75 mW (red to blue curves). The effective temperature, as inferred from the modified mechanical damping, could be reduced down to 11 K.

Cooling (Fig. 1C) is achieved when the cavity is excited with a red-detuned laser with respect to the cavity resonance. A reduction in the displacement fluctuations (as monitored in the transmission signal of the cooling laser itself) is clearly observed, with a concomitant increase of the mechanical linewidth due to the additional dissipation of the mechanical mode which is introduced by the cooling laser. For the maximum applied power of ~2 mW (at 972 nm), a reduction to an effective temperature of 11 K was observed.

By solving the equations of motion of the coupled optomechanical system using a perturbative approach, we were able to deduce analytical expressions for the radiation pressure force, cooling rates, mechanical resonance frequency shift and damping modification. In a series of experiments, very good quantitative agreement with these predictions was observed, constituting first evidence that the origin of the observed effect is indeed a radiation-pressure induced, cavity-delayed back-action of the displacement readout on the mechanical mode. In particular, a drastic change in the dynamics of the system is observed when changing no parameter except the (independently measured) optical cavity linewidth to values below twice the mechanical resonance frequency. In this regime, the resonance frequency shift is reversed for small detunings and has an additional pair of zeros for a specific laser detuning (Fig.2), indicating a purely viscous radiation pressure force. We note that this regime has not been entered by other recently reported cooling experiments[6, 7].

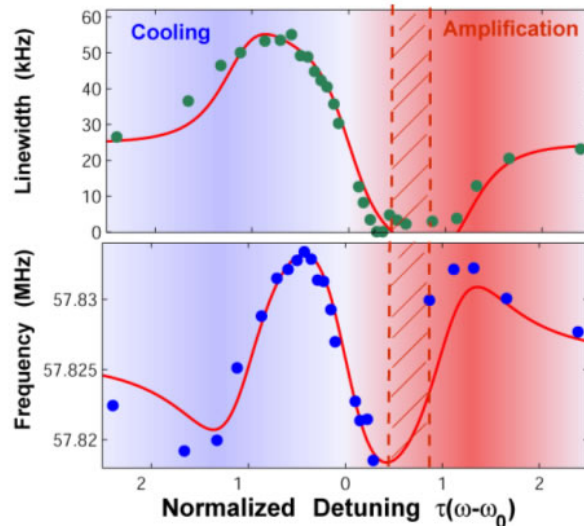


Fig. 2. Mechanical linewidth (upper panel) and resonance frequency (lower panel) of the 57.8 MHz radial breathing mode as a function of (normalized) detuning when the laser is tuned over a 50 MHz-wide optical resonance. For  $(\omega - \omega_0) < 0$ , the resonance is being cooled. Solid lines are theoretical predictions based on our model.

Finally response measurements were carried out, where a strong, modulated pump laser drives the different nonlinearities present in the cavity (thermal effects, Kerr effect, radiation-pressure induced displacement), while a weaker probe laser reads out the induced resonance frequency shift. This has allowed to assess the contributions of thermal effects to the observed cooling to be on the 1% level.

We believe our result constitutes an important step towards the long-sought aim of cooling a micro-mechanical oscillator to its motional ground-state.

#### References

1. Braginsky, V.B. and F.Y. Khalili, *Quantum Measurement*. 1992: Cambridge University Press.
2. Schliesser, A., P. Del Haye, N. Nooshi, K. Vahala, and T.J. Kippenberg, *Cooling of a Micro-Mechanical Oscillator Using Radiation-Pressure Induced Dynamical Backaction*. 2006. **(to be published)**.
3. Carmon, T., H. Rokhsari, L. Yang, T.J. Kippenberg, and K.J. Vahala, *Temporal behavior of radiation-pressure-induced vibrations of an optical microcavity phonon mode*. Physical Review Letters, 2005. **94**(22).
4. Kippenberg, T.J., H. Rokhsari, T. Carmon, A. Scherer, and K.J. Vahala, *Analysis of Radiation-Pressure Induced Mechanical Oscillation of an Optical Microcavity*. Physical Review Letters, 2005. **95**: p. 033901.
5. Rokhsari, H., T.J. Kippenberg, T. Carmon, and K.J. Vahala, *Radiation-pressure-driven micro-mechanical oscillator*. Optics Express, 2005. **13**(14): p. 5293-5301.
6. Gigan, S., et al., *Self-cooling of a micromirror by radiation pressure*. Nature, 2006. **444**(7115): p. 67-70.
7. Arcizet, O., P.F. Cohadon, T. Briant, M. Pinard, and A. Heidmann, *Radiation-pressure cooling and optomechanical instability of a micromirror*. Nature, 2006. **444**(7115): p. 71-74.

## CURRENT-INDUCED DOMAIN WALL DYNAMICS

M. Kläui

Fachbereich Physik, Universität Konstanz, Universitätsstr. 10, D-78457 Konstanz, Germany

When combining transport with magnetic materials on the nanoscale, a range of exciting and novel phenomena emerge. Due to the interaction of the current with the magnetization, the spin transfer torque effect leads to current-induced domain wall motion (CIDM) [1-3], which we study in detail. In CIDM, electrons transfer angular momentum and thereby push a domain wall [1-3]. We have comprehensively investigated this effect and observed that this interaction is strongly dependent on the temperature [3] and the wall spin structure [2]. So far, primarily current pulses have been employed to investigate domain wall displacements and strongly stochastic behaviour has been observed.

More reproducible behaviour is found if AC currents are used to excite domain wall oscillations, which are inherently reproducible. To generate a domain wall oscillator a restoring force is necessary, which can be provided by a constriction that generates an attractive potential well for a domain wall, which then acts as a quasiparticle [4]. The depth of the potential well, was found to increase with decreasing constriction width, and the well width was found to extend far beyond the physical size of the constriction [4].

To fully characterize the pinning potential, the curvature has to be determined in addition to the width and the depth. To study the curvature, the resonance frequency of the domain wall has to be ascertained and to this end, we inject AC currents with variable frequency into the structure shown in Fig. 1 (a) [5]. We then measure the depinning field as a function of the injected microwave frequency as shown in Fig. 2 (a) (blue squares) for a transverse wall (Fig. 1 (b)). We observe a dip of the depinning field at a resonance frequency of about 1.3 GHz even for low current densities of  $10^{10}$  A/m<sup>2</sup> and the eigenmode consists of the whole wall moving. Next we consider a pinned vortex wall (Fig. 1 (c)) and a strong dip in the depinning field is observed at around 800 MHz (Fig. 2 (b), blue squares). Here the eigenmode consists of the vortex core oscillation. To obtain the resonance frequencies at variable fields we employ a DC homodyne detection scheme:

As the domain wall oscillates, the resistance of the magnetic structure is modulated due to the anisotropic magnetoresistance in phase with the domain wall position. If the quasiparticle happens to be excited at the resonance frequency, the varying resistance will rectify the injected high frequency current and a DC voltage is developed across the structure. We plot the DC response for the vortex wall pinned at the constriction in Fig. 2 (b) (red line). We see a dispersion-like signal with a change in the sign exactly at the resonance frequency, which allows us to determine the resonance from the DC signal. For the transverse wall the expected signal is much weaker since the oscillation has a smaller amplitude, as visible from the smaller change in the depinning field compared to the vortex wall and this is also reflected in the smaller DC signal (Fig. 2 (a) (red line)).

The domain wall resonance frequency was measured for different external magnetic fields and was found to increase with increasing field so that we can conclude that the potential well curvature can be engineered by varying the external field [5].

To directly determine the potential  $U(x)$  we can use the power dependence of the resonance frequency [5]. From the resonance frequency as a function of the power, we obtain the oscillation period and, since the energy of an oscillator is proportional to the square of the driving force, also as a function of the energy in the system. From the energy dependence of the oscillation period we can for the first time directly determine  $U(x)$  as shown in Fig. 2 (c) with the absolute width of the potential well determined as described in [4]. The blue dots are calculated from the measured oscillator periods and the red line indicates the parabolic part of the potential well. As expected the domain wall potential flattens far away from the origin, indicating a non-harmonic (non-linear) contribution [5].

Very recently the relation between the non-adiabaticity parameter  $\beta$  and the damping constant  $\alpha$  were investigated using pulse-induced wall displacement and periodic transformations between vortex and transverse walls were observed, which yield that  $\beta$  does not equal  $\alpha$ .

## References

- [1] C. Marrows, *Adv. Phys.* **54**, 585 (2007)  
 [2] A. Yamaguchi et al., *Phys. Rev. Lett.* **92**, 077205 (2004); M. Kläui et al., *Appl. Phys. Lett.* **83**, 105 (2004); *Phys. Rev. Lett.* **94**, 106601 (2005); *Phys. Rev. Lett.* **95**, 26601 (2005)  
 [3] M. Laufenberg et al., *Phys. Rev. Lett.* **97**, 46602 (2006); F. Junginger et al. *Appl Phys. Lett.* **90**, 132506 (2007)  
 [4] M. Kläui et al., *Phys. Rev. Lett.* **90**, 97202 (2003), *Appl. Phys. Lett.* **87**, 102509 (2005).  
 [5] D. Bedau et al., *Phys. Rev. Lett.* **99**, 146601 (2007); D. Bedau et al. (unpublished); L. D. Landau and E. M. Lifshitz *Theoretical Physics Course – Mechanics*.  
 [6] L. Heyne et al., *Phys. Rev. Lett.* **100**, 66603 (2008)

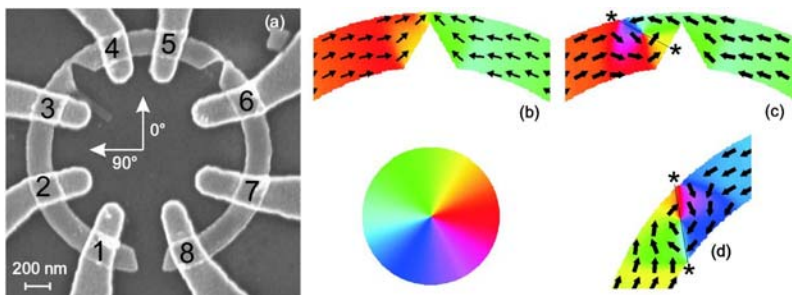


Fig. 1: (a) SEM image of the device used with the AC current injected between contacts 3 and 4. Micromagnetic simulations of a pinned transverse wall (b), pinned vortex wall (c) and a free vortex wall (d).

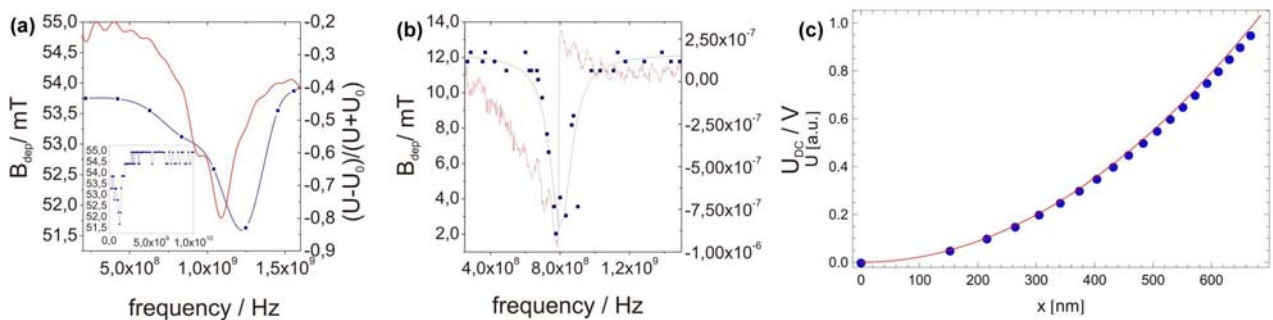


Fig. 2: Depinning field (blue squares) and DC signal (red line) for a transverse wall (a) and a vortex wall (b). In (c) the potential  $U(x)$  is directly determined and a non-harmonic contribution is found.

## **BLOCK COPOLYMER SELF-ASSEMBLY: A POWERFUL TOOL FOR THE DESIGN OF NEW SMART BIOMIMETIC NANO- CARRIERS**

*Willy Agut, Charles Sanson, Daniel Taton, Alain Soum, Jean-François Le Meins, Christophe Schatz, and Sébastien Lecommandoux\**  
*Laboratoire de Chimie des Polymères Organiques (LCPO), UMR5629 CNRS, ENSCPB-  
Université Bordeaux 1, 16, Avenue Pey-Berland, Pessac 33607, France*  
[lecommandoux@enscpb.fr](mailto:lecommandoux@enscpb.fr)

In which manner can polymers be useful for biological applications? The main physical characteristic of a polymer chain is its length, which can largely exceed the micrometer range. This unique feature is responsible of the establishment of short and long range interactions tunable by the choice of the chemical nature of the monomer i.e. the repetitive unit. Such interactions can lead to the formation of small objects with well-defined shapes such as particles, vesicles or micelle-like structures. Medical interest of these objects is infinite if we consider them at a nanoscopic scale. Indeed, these polymeric systems can be synthesized at this scale in such a manner that they are able to carry a drug or a biomolecule having a therapeutic interest, to reach a biological target (organs, cells or tissues), to overcome the chemical and/or biological degradation and to release the encapsulated molecules in a triggered or controlled fashion.

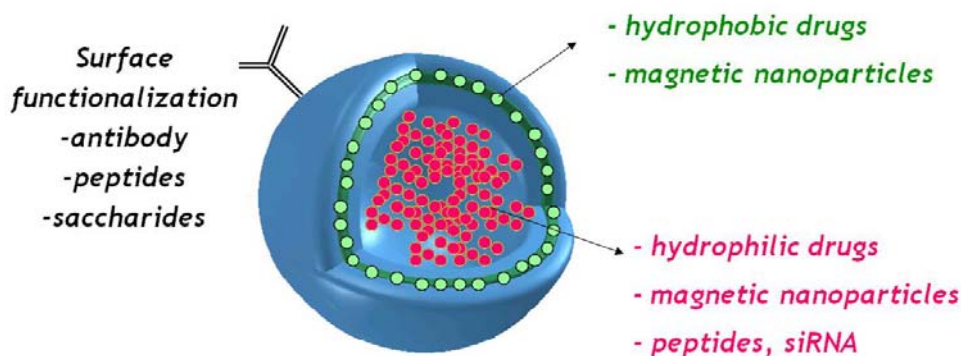
Our strategy concerns the design of self-assembled nanostructures from weak interactions. Playing with the so-called weak interactions (electrostatic, Van der Waals, hydrogen bonds, hydrophobic effect) allows to mimic the interactions found in biological media and to create objects having a high plasticity, a reversible mechanism of assembly and a high affinity with biomolecules. Naturally occurring polymers, biodegradable polymers and polypeptide-based copolymers are mainly used in regards to their known biocompatibility and biodegradability. The formation of nanoparticles in the range 10-200 nm, such as micelles and vesicles from these copolymers was undertaken and the encapsulation/delivery of various molecules (drug, peptides, and magnetic particles) was investigated as well.

The self-assembly of well-defined polypeptide-based diblock copolymers into micelles and vesicles is presented. The stimuli-responsive behavior of polypeptides to pH and ionic strength is used to produce stimuli-responsive nanoparticles with a control size and shape.<sup>1</sup> Results focusing on polymersomes<sup>1,2</sup> will be detailed by means of static and dynamic light scattering analysis, UV circular dichroism, NMR and small angle neutron scattering experiments. Systems that are able to form vesicles with a narrow size distribution at basic and acid pH going through an intermediate state of single molecule will also be detailed.<sup>2</sup> In addition, the encapsulation of iron oxide nanoparticles into these vesicles, forming hybrid supramolecular hollow objects with a magnetic membrane, which deformation under an applied magnetic field will be evidenced.<sup>3</sup> These multi-responsive nanoparticles, with a structure and physical characteristics similar to viral capsids, are particularly interesting for encapsulation and delivery purpose at a controlled pH or under a specific magnetization (Figure 1).<sup>4,5</sup> Finally, recent results on the preparation of such polymersomes, fully biocompatible and biodegradable poly(trimethylene carbonate)-*b*-poly(glutamic acid)<sup>6</sup> and multi-responsive (pH, temperature)<sup>7</sup> polymersomes poly(dimethylaminoethylmethacrylate)-*b*-poly(glutamic acid)<sup>8</sup> will be described. Different projects are currently under development in collaboration with biologists and medecists using this strategy for the delivery of drug and genes in the central nervous system or for the treatment of motor neuron diseases.

## References:

- [1] (a) F. Chécot, S. Lecommandoux, Y. Gnanou, H.-A. Klok *Angewandte Chemie Int. Ed.* **2002**, *41*, 1339. (b) F. Chécot, S. Lecommandoux, H.-A. Klok, Y. Gnanou *European Physical Journal E* **2003**, *10*, 25. (c) J. Babin, J. Rodriguez-Hernandez, S. Lecommandoux, H.-A. Klok, M.-F. Achard *Faraday Discussion* **2005**, *128*, 179. (d) F. Chécot, A. Brûlet, J. Oberdisse, Y. Gnanou, O. Mondain-Monval, S. Lecommandoux, *Langmuir* **2005**, *21*, 4308.
- [2] [J. Rodríguez-Hernández, S. Lecommandoux](#), *JACS* **2005**, *127*, 2026.
- [3] S. Lecommandoux, O. Sandre, F. Chécot, J. Rodriguez-Hernandez, R. Perzynski *Adv. Mat.* **2005**, *17*, 712.
- [4] Y. Gnanou and S. Lecommandoux, *Bioforum Europe* **2004**, *8*(5), 38.
- [5] (a) <http://www.physorg.com/news73581022.html>. (b) Technical Insights, Frost & Sullivan, High-Tech Materials Alert, sept 4, 2006. (c) <http://medicalphysicsweb.org/medphys/Articles/ViewArticle.do?channel=research&articleId=26378>.
- [6] C. Sanson, C. Schatz, A. Soum, J.-F. Le Meins, S. Lecommandoux, in prep.
- [7] W. Agut, A. Brûlet, D. Taton, S. Lecommandoux *Langmuir* **2007**, *23*, 11526.
- [8] W. Agut, D. Taton, S. Lecommandoux, *Macromolecules* **2007**, *40*, 5653.

**Figure 1: block copolymer vesicles, a versatile and multi-functional platform for drug-delivery and diagnosis.**



## THE CHEMICAL BOND OVERLAP PLASMON AS A TOOL FOR QUANTIFYING COVALENCY IN OPTICAL SOLID STATE MATERIALS

**O. L. Malta<sup>\*1</sup>, R. T. Moura Jr<sup>1</sup>, R. L. Longo<sup>1</sup> and M. Lalic<sup>2</sup>**

<sup>1</sup>*Departamento de Química Fundamental-CCEN-UFPE. Cidade Universitária,  
Recife-PE, 50670-901, Brasil*

<sup>2</sup>*Departamento de Física, Universidade Federal de Sergipe. São Cristóvão, Sergipe,  
Brazil*

Correlations between the characteristics of the chemical bond and the properties of matter have long been the subject of intense investigation. In an attempt to get deeper insights on covalency in the special case of lanthanide compounds, we have introduced the concepts of chemical bond overlap polarizability (OP) and ionic specific valence (ISV) [1]. Several consequences of these concepts have been then explored and tested in different systems from diatomic to complex molecules and solids. Among these consequences are the definition of a quantitative covalent fraction scale and a description of ligand field effects in terms of a contact potential that may be treated non phenomenologically when the charge factors, appearing in the Simple Overlap Model, are identified with the ligating atoms ionic specific valences [1,2]. The OP and ISV concepts have also been explored in a more general context. Relevant questions can be raised on possible relationships between macroscopic properties of materials and these concepts. Thus, for example, a good correlation has been found between the non-linear index of refraction ( $n_2$ ) and the OP [3]. A proposal in which the overlap region is regarded as a localized plasmon-like charge distribution - the chemical bond overlap plasmon (CBOP) - characterized by the OP, has raised the question on the possibility of absorption and inelastic scattering of radiation, above the first ionization threshold, by the overlap region [4]. Predicted CBOP oscillator strengths, scattering and electron energy loss cross sections for solid alkali-halides and aluminum oxides are considerably high and could be measured experimentally. These spectroscopic quantities depend on the OP and ISV, and are suggested as a useful tool for quantifying covalency in optical materials.

[1] O.L.Malta, H.J.Batista, L.D.Carlos, Chem. Phys. 282, 21 (2002).

[2] L.D.Carlos, O.L.Malta, R.Q.Albuquerque, Chem. Phys. Letters 415, 238 (2005).

[3] R.Q.Albuquerque, Doctorate Thesis, Departamento de Química Fundamental-UFPE, Recife-PE, Brazil, July 2004.

[4] O.L.Malta, Chem.Phys.Letters 406, 192 (2005).

CNPq , RENAMI ,

IMMC

-----  
\*e-mail : oscar@renami.com.br



## HIGH SPEED AFM – CONTACT & NON-CONTACT

Loren Picco, Massimo Antognozzi, David Engledew, Arturas Ulcinas, Peter Dunton,  
Mervyn Miles

H.H. Wills Physics Laboratory  
IRC in Nanotechnology  
University of Bristol  
Tyndall Avenue,  
Bristol,  
U.K.

High-speed AFM imaging is important for many applications not least in biology where the ability to follow processes occurring in the millisecond regime at the molecular level is a major goal. High-speed imaging also allows greater areas of specimen to be examined in a given time, and it allows the patterning of surfaces over useful areas on a practical timescale for the creation of nanostructures. In recent years, Ando *et al.* [1] reported major achievements in high-speed tapping mode AFM. Here we will briefly present two alternative AFM techniques for achieving high-speed imaging.

The first of these methods for high-speed AFM imaging uses standard AFM cantilevers not operated in AC mode [2]. The specimen was either mounted on the resonant scanner or on a flexure stage capable of scanning at up to 40kHz. The AFM cantilever probe is brought into continuous contact with the specimen and the topographic structure derived for the deflection of the cantilever. A piezo stack provided the slow scan. Imaging at video rate is routinely achieved even on soft biological or organic molecules materials [3]. Damage to specimens resulting from this high-speed contact-mode imaging is surprisingly very considerably less than would be caused at normal speeds. Even samples having relatively large height differences such as hydrated human chromosomes have been imaged in liquid. Further recent developments of the instrument allow imaging >1000 frames per second [3].

The second new high-speed technique presented here is a non-contact force microscopy. It is recognized that non-contact imaging in liquid is of importance in biomolecular systems in order to cause the least distortion of the sample in an environment that is close to the natural state. Non-contact FM AFM techniques [4] have recently made a major step forward to attain these capabilities. The further challenge of high speed must be met in order to achieve the goal of following many biomolecular processes *in situ*. In the work presented here, we show a newly developed non-contact transverse dynamic force microscopy (TDFM) technique with the potential for high-speed imaging. TDFM has for many years been known to offer high-resolution imaging on delicate biological specimens in air or liquid in a non-contact mode, and these recent development, reported here, are a proof of concept of its capability as a high-speed imaging technique with the potential to image at video rate and beyond in a non-contact mode. TDFM approach curves show features associated with the ordering of water molecules above the sample. A demonstration of the 3D imaging of the water structure above a sample surface using the new version of TDFM will be presented. The visualization of local water structure in biomolecular systems is a dream for the understanding of structure formation and processes at the molecular level.

## References:

- [1] see, for example, T Ando, *et al. Jap. J. Appl. Phys. Part 1* **45** (2006) 1897-190
- [2] ADL Humphris, MJ Miles, & JK Hobbs, *Applied Physics Letters* **86** (2005) art no. 034106.
- [3] LM Picco, *et al. Nanotechnology* **18** (2007) Art. No. 044030.
- [4] T Fukuma *et al.*, *Appl Phys Lett* **87** (2005) 034101.



## ORAL CONTRIBUTIONS



## AQUITAINE, MIDI-PYRÉNÉES, LANGUEDOC-ROUSSILLON A SINGLE NETWORK FOR THREE REGIONS PROMOTING NANOSCIENCE AND NANOTECHNOLOGY IN THE SOUTH-WEST OF FRANCE

*J.-P. Aimé\**, *C. Bernard\**, *X. Bouju\*\**, *J.-L. Sauvajol\*\*\**

\* *C'Nano GSO, CPMOH, Université Bordeaux I*  
*351 cours de la Libération, 33405 Talence Cedex, France*

[jp.aime@cnanogso.org](mailto:jp.aime@cnanogso.org)

\*\* *C'Nano GSO, CEMES-CNRS*  
*29 rue Jeanne Marvig, 31055 Toulouse Cedex 4, France*

\*\*\* *C'Nano GSO, LCVN, Université Montpellier 2*  
*Place Eugène Bataillon, 34095 Montpellier Cedex 5, France*

French C'Nano networks are recent regional initiatives that bring together the scientific community active in nanoscience and nanotechnology. They include a large number of researchers, professors and research engineers that advance on the same front with the knowledge and skills essential for development of nanotechnology (4100 full-time equivalents, permanent and non-permanent). [C'Nano GSO](#) (South West of France, red on the map) gathers together three regions: Aquitaine (Bordeaux), Midi-Pyrénées (Toulouse) and Languedoc-Roussillon (Montpellier), and is part of the network across France (see map below): C'Nano NO (North West, green), C'Nano IdF (Ile de France, blue), C'Nano GE (East, yellow) and C'Nano RA (Rhône-Alpes, orange).



As many networks focused on the development of nanoscience and nanotechnology (see for instance the recent report from National Nanoscience Initiative in USA), C'Nano GSO acts on three main fields: fundamental research, teaching and training, transfer and reinforcing partnerships with company. In more details the following list of goals:

- Promote activities on nanoscience and nanotechnology throughout the French South-West area ;
- Promote the emergence of unifying themes;
- Share tools and equipment performance;
- Build partnerships with national regions and European countries;
- Develop effective partnerships with industry;
- Participate to training at any level;
- Keep inform general public on developments in nanoscience and nanotechnology.

The most prominent research themes in the South West are:

- *Nanomaterials and molecules*

Metallic nanoparticles, quantum wells and dots, self-assembled systems, organic nano-fibres, carbon nanotubes, bio-inspired materials, molecular motors, supramolecular biocomplexes, molecular machines

- *Near field techniques, spectroscopy and imaging on nano-objects*

STM, AFM, Raman spectroscopy, photothermal and femto-second spectroscopy, near-field optics, plasmonics

- *Nano-probes, nano-manipulation and nano-machines, nanomechanics*

Nano-bio-sensors, nanofluidics, MEMS-NEMS (Micro-Nano-Electro-Mechanical Systems)

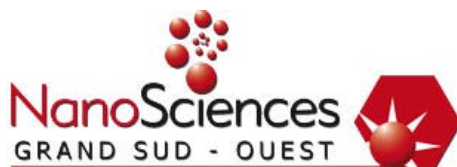
As part of its training component, the C'Nano GSO is building an inter-regional Master (MSc) degree between the three regions constituting the GSO (Aquitaine, Midi-Pyrénées and Languedoc-Roussillon). This MSc degree will be devoted to nanoscience and nanotechnology. A working group has been created to define the body of an education for physicists, chemists and biologists.

The working group seeks to an action towards our Spanish colleagues to share a MSc “nano” with Spain. The action is supported both by the Spanish and France agencies.

Through partnerships with industry, C'Nano GSO is working in close collaboration with a Transregional Collective Action Nanomaterials, called [ACT Nano](#). This action has been set up by the French industrial agency to speed up the dissemination of technology “nanomaterials” in the industrial fabric and its acquisition by small-scale businesses. ACT Nano completes C'Nano providing a transfer dimension and technological research partnership with small-scale businesses in the field of nanomaterials.

C'Nano GSO seeks to improve partnerships between France, Spain and Portugal based on strong scientific links between European South-West countries and C'Nano GSO. Next to the special C'Nano GSO session at the 2008 NanoSpain conference (Braga, Portugal, 14-18 Avril), will take place a Franco-Spanish conference in November 2008 (November, 3<sup>rd</sup>-6<sup>th</sup>, in Bordeaux, France) to launch collaborations between Spain and C'Nano GSO. Moreover, the goal of the inter-regional MSc degree dedicated to nanoscience and nanotechnology is to be extended to Spain to share training and teaching capacities.

<http://www.cnanogso.org>



# PRODUCTION AND IMMUNE RESPONSE CHARACTERISATION OF S. EQUI ANTIGENS ENCAPSULATED IN SURFACE MODIFIED POLYMERIC NANOPARTICLES

31

*António J. Almeida*<sup>1</sup>, *L.M.D. Gonçalves*<sup>1</sup>, *S. Pandit*<sup>2</sup>, *H.O. Alpar*<sup>2</sup> and *H. Florindo*<sup>1,2</sup>

<sup>1</sup> *iMed.UL, Faculty of Pharmacy, University of Lisbon, Lisbon Portugal*

<sup>2</sup> *Centre for Drug Delivery Research, School of Pharmacy, University of London, London, UK*  
[aalmeida@ff.ul.pt](mailto:aalmeida@ff.ul.pt)

**INTRODUCTION:** Strangles is a bacterial infection of Equidae family that affects the nasopharynx and draining lymph nodes, caused by *Streptococcus equi* subspecies *equi*, a Lancefield group C streptococcus [1]. It causes suppurative nasopharyngitis and lymphadenopathy, with a long convalescent period [1, 2]. Although *S. equi* is sensitive to some antibiotics, most of the treatments are ineffective and prevention is the key. Since the 1980s new vaccines against strangles have been developed but limited efficacy has been attested [2]. As biodegradable nanoparticles have enormous potential as antigen carriers for the induction of systemic and local immunity, the aims of the present study were to produce surface modified polycaprolactone (PCL) and polylactic acid (PLA) nanoparticles, produced with cationic (glycochitosan) or anionic (sodium alginate or polyvinyl alcohol) polymers, and absorption enhancers (spermine and oleic acid), as *S. equi* carriers for the induction of both systemic and local protective immunity in a mice model.

**EXPERIMENTAL:** PCL (42.5kDa) and PLA (2kDa) nanoparticles were prepared by the double emulsion (w/o/w) solvent evaporation method described elsewhere [3]. Particle size and surface charge were determined (laser scattering) and morphology was observed using scanning electron microscopy (SEM). The amount of protein encapsulated per unit weight of nanoparticles was measured using the BCA protein assay (Pierce). Protein integrity throughout encapsulation was assessed by SDS-PAGE.

*In vivo* studies involved six groups of female BALB/c mice (25g; n=4/group), which were immunized on day 1 and boosted on day 29, with 50µl of solution containing *S. equi* antigen equivalent to 10µg of SeM, either free or encapsulated in nanoparticles (Table 1).

**Table 1.** Vaccines and delivery route of immunized mice.

Set	Groups	Route
A	SeM encapsulated PLA particles	i.m.
B	Ext. encapsulated PLA particles	i.m.
C	Ext. encapsulated PLA particles	i.n.
D	Ext. encapsulated PCL particles	i.n.

Blood samples were collected at appropriate times after immunization and, by week 12, all animals were ethically sacrificed, their lungs were washed and spleens aseptically removed. The levels of anti-*S. equi* specific IgG, IgG1, IgG2a and IgA were assessed by indirect ELISA. The spleen cells were co-cultured with soluble antigen and interleukin concentrations (IL-2, IL-4, IL 6 and IFN-γ) were quantified using ELISA.

**RESULTS AND DISCUSSION:** The nanoparticles presented a spherical and smooth surface under SEM (Fig.1). The encapsulation efficiency varied from 30.4% to 95.4 %. The SDS-PAGE analysis showed that antigen integrity was maintained. Vaccination of sets A and B induced a strong increase of serum IgG levels (Fig. 2). Differences between IgG2a level were statistically significant, except those induced by GCs/set B. Negatively charged formulations induced significantly higher IgG and IgG2a levels. Simultaneously, differences were observed in serum antibody levels of animals vaccinated with bacterial extract encapsulated in PLA and PCL particles, when compared to the free form of the antigen.

Overall, the results from the IgG subclass titers obtained in all four sets of particles indicates generation of Th1/Th2 mixed response. Differences observed in IL2 and IFN- $\gamma$  induced by formulations A and B were statistically significant. Levels of IL2 were not different when comparing spermine formulations C and D. Formulation C induced IFN- $\gamma$  levels statistically higher when comparing with D. Interleukin levels induced by formulations C and D were lower than those obtained in groups treated with formulations A and B. Moreover, the efficacy of vaccines to prevent strangles seems to be dependent on the induction of a mucosal immune response. Nasal mucosal antibody response (IgA) was statistically higher in animals immunized with formulations C than with D.

**CONCLUSIONS:** PCL and PLA nanoparticles are potential vaccine carriers with strong immunoadjuvant properties for the effective delivery of *S. equi* antigens.

## References:

- [1] Flock M, Jacobsson K, Frykberg L, Hirst TR, Franklin A, Guss B, Flock JI, Infect. Immun. **72** (2004) 3228-3236.
- [2] Hamlen HJ, Timoney J, Bell RJ, JAVMA **204** (1994) 768-775.
- [3] Conway BR, Alpar HO, Eur J Pharm Biopharm **42** (1996) 42-48.

## Figures

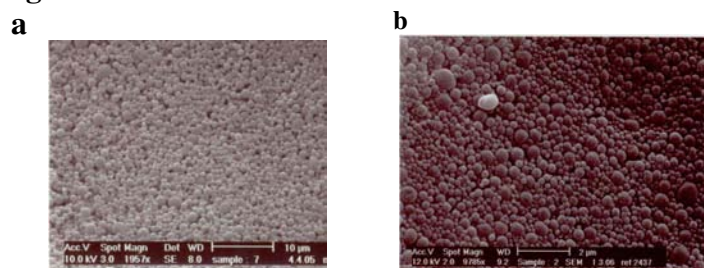


**Fig. 1.** SEM micrographs of antigen-containing nanoparticles: a) PCL-chitosan; b) PLA-chitosan.

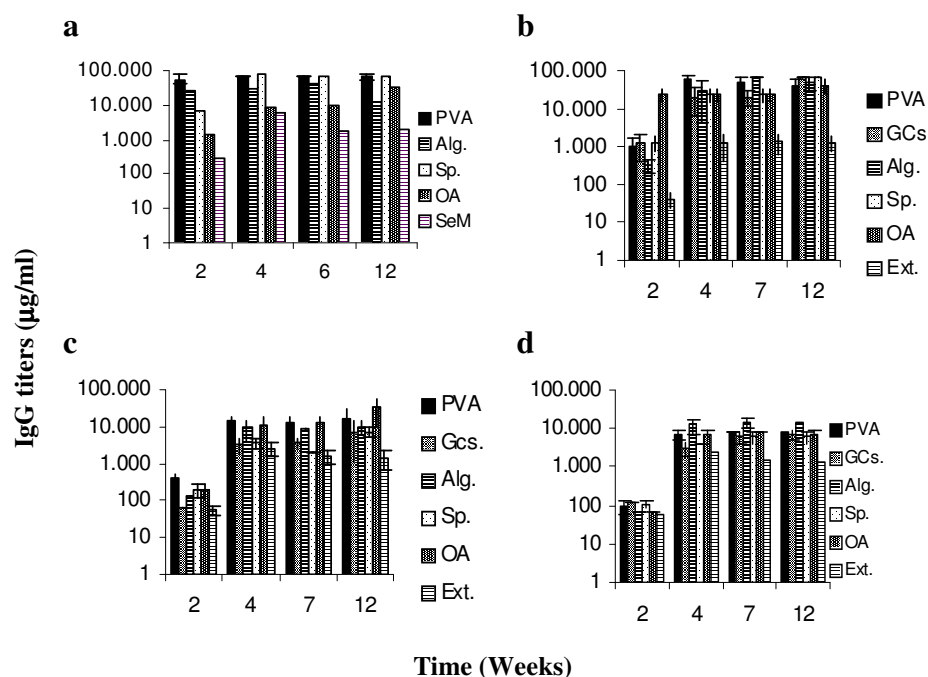


**Fig. 2.** Systemic immune response to: 1-i.m. administrated a) SeM free or encapsulated, b) Ext. free or encapsulated in PLA nanoparticles; 2-i.n. administrated Ext. free or encapsulated in c) PLA or d) PCL nanoparticles (n=4, mean $\pm$ sd).

## Acknowledgements:

This work was supported by Fundação para a Ciência e Tecnologia, Portugal (SFRH/BD/14300/2003; POCI/BIO/59147/2004; PPCDT/BIO/59147/2006).

## MAGNETIC CHARACTERIZATION OF NANO-SCALE GRANULAR MATERIALS

*O. Hovorka<sup>1</sup>, Y. Liu<sup>2</sup>, K. A. Dahmen<sup>2</sup>, and A. Berger<sup>1</sup>*

<sup>1</sup>*CIC nanoGUNE Consolider, E-20009 Donostia – San Sebastián, Spain*

<sup>2</sup>*Department of Physics, University of Illinois at Urbana-Champaign, Urbana, IL 61801, USA*  
*a.berger@nanogune.eu*

Progress in the Nano-Sciences during the past decade opened up new pathways for developing materials with enhanced electronic or other properties. Their potential applications are wide-spread, such as semiconductor electronics, spintronics, photonic devices, sensors for molecular recognition in chemistry and biology to name a few. Despite the tremendous progress in recent years, however, substantial challenges remain to be resolved before many of these nanotechnologies can reach their anticipated potential. Hereby, one needs to recognize that further advancement inevitably relies on the availability of characterization methodologies that allow for optimization of materials design and processing as well as for gaining a fundamental understanding of underlying scientific phenomena and concepts.

As an example of such materials characterization challenges, we have studied issues related to nano-scale granular materials, such as the ones used for the purpose of information storage in hard disk drives (HDD). To achieve today's product level technology, magnetic grains of only 6-10 nanometer diameter have to be utilized with further technical progress requiring even smaller functional particles. In turn, the already achieved technology requires methodologies that allow for a sufficiently accurate and time-efficient magnetic characterization of the about 100 trillions magnetic grains in a typical last-generation laptop computer HDD [1].

In recent years, numerous attempts have been made to develop a reliable and efficient characterization methodology capable of extracting all relevant information about the recently introduced perpendicular magnetic recording (PMR) media [2, 3]. Specifically, the magnetization switching field distribution was found to be a crucial material property and the so-called  $\Delta H$ -method (Fig. 1) has been the most reliable technique for its determination so far [2, 3]. However, as all other available methods today, also the  $\Delta H$ -method has its limits of applicability, and an all-around satisfactory technique is yet to be developed. Correspondingly, the main goal of the present work is to estimate the range of applicability of the  $\Delta H$ -method. For our computational analysis, we used a previously devised realistic model [4, 5], in which PMR media are viewed as a planar assembly of magnetic single domain nano-grains. Magnetization reversal of each grain is described by a rectangular hysteresis loop with a randomly chosen switching field in accordance with an overall representative switching field distribution. Every grain interacts with its nearest neighbors via ferromagnetic exchange interactions of strength  $J_{\text{ex}}$  and with all other grains on the lattice via the distance-dependent dipolar interaction of strength  $J_{\text{dp}}$ . Correspondingly, the interaction constants  $J_{\text{ex}}$  and  $J_{\text{dp}}$  as well as the switching field distribution determine the hysteresis loop behavior.

We observe, using this computational model of nano-scale granular PMR-media, that the simultaneous presence of exchange and dipolar interactions between individual grains generally allows for a precise determination of the intrinsic switching field distribution (Fig. 2). The method's reliability is due to the fact that the two types of interactions have opposite signs, which partially suppresses the correlation of the magnetic reversal in neighboring particles. Otherwise, the particle interaction would wash out the individual character of the magnetic grains and make the characterization in terms of single grain properties impossible. However, due to the existence of this compensation effect it appears impossible to separate the different interaction contributions from each other by means of the  $\Delta H$ -method, and this

fact seems to even hold for  $\Delta H$ -dataset analysis schemes that go beyond the presently used mean-field approximation.

Work at UIUC is supported by NSF through grants DMR 03-14279 and the Materials Computation Center DMR 03-25939(ITR). Work at nanoGUNE is supported by the Department of Industry, Trade and Tourism of the Basque Government and the Provincial Council of Gipuzkoa under the ETORTEK Program, Project IE06-172, as well as from the Spanish Ministry of Science and Education under the Consolider-Ingenio 2010 Program, Project CSD2006-53.

## References:

- [1] J. Markoff, "Hitachi achieves storage record for disc drives", NY Times, 2005.
- [2] A. Berger, Y. H. Xu, B. Lengsfeld, Y. Ikeda and E. E. Fullerton, IEEE Trans. Mag., **41** (2005) 3178.
- [3] A. Berger, B. Lengsfeld, and Y. Ikeda, J. Appl. Phys., **99** (2006) 08E705.
- [4] Y. Liu, K. A. Dahmen, and A. Berger, accepted for publication in Phys. Rev. B.
- [5] Y. Liu, K. A. Dahmen, and A. Berger, J. Appl. Phys., **103** (2008) 07F504.

## Figures:

Fig. 1: Major hysteresis loop (solid line) and two recoil loops (dotted lines).  $\Delta H$  is the field difference between the major and a given recoil loop for the same magnetization  $M$  value.  $\Delta H(M, \Delta M)$  data are then compared with the analytical solutions of the mean-field model to determine the intrinsic switching field distribution [2, 3].

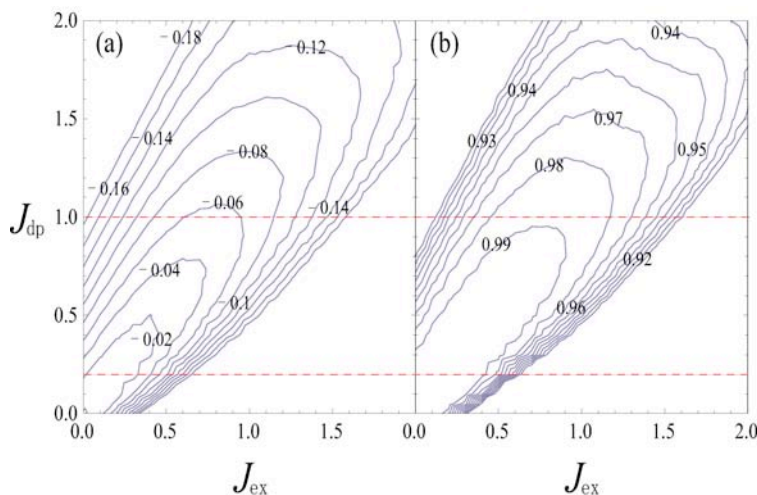
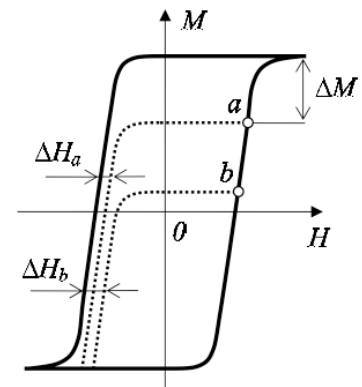


Fig. 2: Contour plots of the data analysis quality and accuracy of the  $\Delta H$ -method as a function of  $J_{ex}$  and  $J_{dp}$ . (a) difference between the recovered value and the input parameter for the variance of the switching field distribution. (b) Multiple correlation coefficient  $R^2$  of the least-squares fit to the mean-field model. The dotted horizontal lines indicate the range  $0.2 < J_{dp} < 1.0$  applicable to real recording materials.

## WHITE ELECTROLUMINESCENCE FROM C- AND SI-RICH THIN SILICON OXIDES

*O. Jambois, B. Garrido, P. Pellegrino, Josep Carreras, and A. Pérez-Rodríguez*  
 EME, Departament d'Electrónica, IN2UB, Universitat de Barcelona, Martí i Franquès 1,  
 08028 Barcelona, Spain

*J. Montserrat*

*Instituto de Microelectrónica de Barcelona (IMB-CNM, CSIC), Bellaterra 08193, Barcelona, Spain*

*C. Bonafos, G. BenAssayag, and S. Schamm*

*Nanomaterials Group, CEMES-CNRS, 29 rue J. Marvig, 31055 Toulouse, France*

[blas@el.ub.es](mailto:blas@el.ub.es), [bonafos@cemes.fr](mailto:bonafos@cemes.fr)

During the last decade, intense investigations have been devoted to the development of an efficient silicon-based optically active material that could enable integration of photonics with Si microelectronics. For example, silicon nanocrystals (Si-ncs) embedded in SiO<sub>2</sub> emit in the red and near infrared spectral regions. In this system, light emission has been attributed to quantum confinement or surface states [1–3]. Recently, a few studies have reported broad photoluminescence (PL) in the whole visible domain, by doping Si-rich SiO<sub>2</sub> layers with carbon [4, 5]. Blue electroluminescence (EL) emission from such a material has been already reported [6] but efficient EL covering the whole visible spectrum has still to be developed. White light sources compatible with Si technology are interesting for several applications, such as biological and chemical sensors, that need a broad spectral detection, optical interconnectors, or colour display.

Some years ago, we have reported white PL of 400 nm thick SiO<sub>2</sub> layers by co-implanting Si and C [5]. The PL spectrum is the convolution of emission bands located in the red, green, and blue spectral regions. The structural and optical studies attributed the red band to Si-ncs, observed by TEM. The blue and green bands are linked to C-related nanophase such as SiC- or graphitic-like nanoaggregates, detected by Raman spectroscopy and XPS analysis. Furthermore, the green band shows lifetimes of the order of 50–100 ps [7] which gives interest to this system for telecommunication applications where fast modulation is required. This material looks very promising as a CMOS compatible light source once electrical excitation is achieved. This work reports the observation of white EL achieved by adapting the Si and C implantation procedure previously developed [5] for thick materials to thin SiO<sub>2</sub> films (40 nm). Reduction of the thickness of the active layer is required to allow injection and conduction of electrical charge across the dielectric layer at relatively low voltages.

The samples have been prepared by sequential implantation of Si<sup>+</sup> and C<sup>+</sup> in a 40 nm thick SiO<sub>2</sub> layer grown by dry oxidation at 1000 °C on a *p*-type (100) Si wafer. A uniform profile of 10 at. % Si excess in SiO<sub>2</sub> has been obtained by means of a four step implantation including low energy implant (for more details see ref. 8). Subsequently, a single C<sup>+</sup> ion implantation was carried out to a nominal dose of 10 at. % at the peak, i.e., equal to the Si excess. The C implant energy was selected to locate the distribution at the centre of the Si rectangular profile to block the out-diffusion of C, and to favour the formation of SiC and C compounds in the implanted layer. A sample without C<sup>+</sup> implantation was also fabricated as a reference sample. To synthesize the Si and C nanophases, the samples were annealed in a N<sub>2</sub> atmosphere at 1100 °C for some hours. Metal-oxide-semiconductor structures were fabricated by a standard photolithographic process. For the gate electrode, a semitransparent 100 nm thick *n*-type polycrystalline silicon contact was deposited. The device was polarized by applying a negative voltage on the gate, allowing injection of electrons from the gate and hole injection from the *p*-type substrate. EL excitation has been obtained using an Agilent 8114A pulse generator, and the collected signal was processed with a Stanford Research SR830 lock-in amplifier. Current-voltage (*I*-*V*) characteristics were measured using an HP4140B pico-amperimeter. For the structural characterization, Energy filtered transmission electron microscopy (EFTEM) was performed on a field emission TEM, FEI Tecnai™ F20 microscope operating at 200 kV, equipped with a corrector for spherical aberration and the last generation of the Gatan imaging filter series.

Fig. 1. shows PL measurements from both the Si and C implanted sample and the reference sample (without C). The latter shows a PL band centred at 760 nm, characteristic of the light emission coming from Si-nc. For the former spectrum, the two Gaussian peak deconvolution shows that in addition to the band due to the Si-ncs, another band appears, attributed to the C-containing nano-aggregates, similarly to what was observed in thicker layers in previous work [5]. In inset, an EFTEM picture from this sample shows that the active layer in this sample is separated in three regions. The two regions at the border are pure Si-nc embedded in SiO<sub>2</sub>, and no C has been detected inside. In the region between the two Si-nc layers a C-rich region is detected, and no Si-nc are observed.

EL has been observed for both samples. The spectra are represented in Fig. 2, from the onset voltage of EL up to breakdown voltage. For both samples, the EL is visible by naked eye. The overall EL power efficiency has been estimated to be around  $10^{-4}$  %. A significant improvement of the external quantum efficiency can be attained by optimizing the transparency of the gate electrode in our devices. In both samples of the present work, the red EL band from Si-nc can be easily identified. Moreover, appearance of bands at higher energies is clearly observed, leading to a white EL. Even though it is difficult to assign the exact microstructural origin of the broad white EL, we can state that this latter is the sum of the emission from Si-nc and from C-related complexes in the matrix. Electrical characterization of both samples was performed in forward polarization. Further details are reported in Ref. 8. For voltage larger than 20 V, the  $I$ - $V$  curve shows a Fowler-Nordheim dependence. This mechanism is related to the tunnel injection of carriers in the conduction band of the oxide through a triangular shaped barrier. This suggests that the excitation of the luminescent centres is produced by impact ionization.

In conclusion, very thin Si- and C-rich layers have been synthesized by high dose ion beam synthesis. The use of low energy implants has allowed growing a uniform distribution of light emitting nanoparticles. The C-related centres give rise to a significant luminescent contribution in the high energy region of the visible spectrum. Together with the well known red light coming from the Si-ncs, this leads to a white to the eye characteristic emission. The electro-optical characterization of these systems has allowed demonstrating the existence of an intense, white EL emission, which correlates with the PL behavior. Radiative impact ionization of the emitting centers is proposed as the main mechanism responsible for the EL emission. In a further work, we also demonstrated an improve of the power efficiency of at least one order of magnitude, by shifting the distribution of the C-related centres toward the interface region with the substrate and by exciting the Si and C-rich nanoparticles under pulsed excitation conditions [9].

#### References:

- [1] A. G. Cullis and L. T. Canham, *Nature* **353** (1991) 335.
- [2] B. Garrido, M. Lopez, C. Garcia, A. Pérez-Rodríguez, J. R. Morante, C. Bonafos, M. Carrada, and A. Claverie, *J. Appl. Phys.* **91** (2002) 798.
- [3] P. M. Fauchet, *Mater. Today* **8** (2005) 26.
- [4] L. Rebohle, T. Gebel, H. Fröb, H. Reuther, and W. Skorupa, *Appl. Surf. Sci.* **184** (2001) 156.
- [5] A. Pérez, O. González, B. Garrido, P. Pellegrino, J. R. Morante, C. Bonafos, M. Carrada and A. Claverie, *J. Appl. Phys.* **94** (2003) 254.
- [6] T. Gebel, L. Rebohle, J. Sun, and W. Skorupa, *Physica E* **16** (2003) 366.
- [7] P. Pellegrino, A. Pérez-Rodríguez, B. Garrido, O. González-Varona, J. R. Morante, S. Marcinkevicius, A. Galeckas, and J. Linnros, *Appl. Phys. Lett.* **84** (2004) 25.
- [8] O. Jambois, B. Garrido, P. Pellegrino, J. Carreras, A. Pérez-Rodríguez, J. Montserrat, C. Bonafos, G. BenAssayag, S. Schamm *Appl. Phys. Letters* **89** (2006) 253124.
- [9] O. Jambois, Josep Carreras, A. Pérez-Rodríguez, B. Garrido, C. Bonafos, S. Schamm, G. Ben Assayag, *Appl. Phys. Lett.* **91** (2007) 211105.

#### Figures:

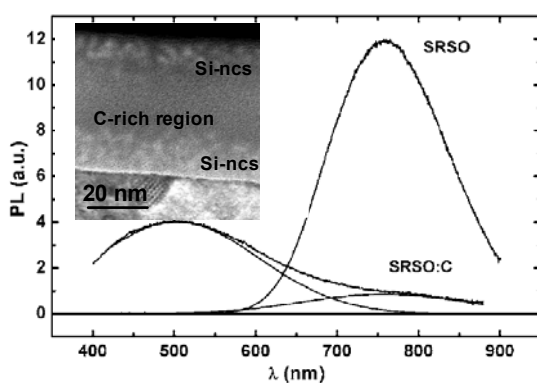


FIG. 1. PL spectra of the the Si and C implanted (SRSO:C) and reference (Si-only, SRSO) samples. Inset shows the EFTEM image of the layer.

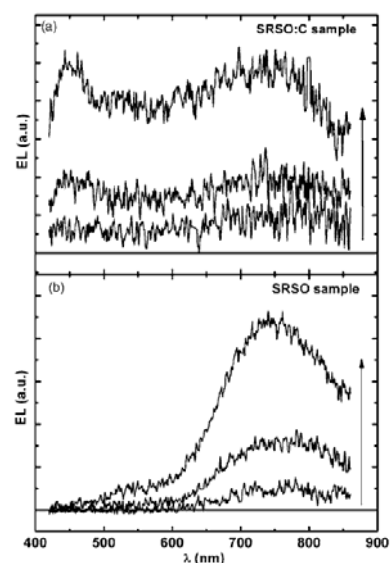


Fig. 2: EL of (a) Si and C implanted and (b) reference (Si only) samples.

## PLASMON CONFINEMENT IN V-GROOVE WAVEGUIDES FABRICATED BY NANOIMPRINT LITHOGRAPHY

Irene Fernandez-Cuesta<sup>1</sup>, Rasmus Bundgaard Nielsen<sup>2</sup>, Dominique Heinis<sup>3</sup>, Alexandra Boltasseva<sup>4</sup>, Xavier Borrísé<sup>1</sup>, Niek van Hulst<sup>3</sup>, Francesc Pérez-Murano<sup>1</sup> and Anders Kristensen<sup>2</sup>.

<sup>1</sup> CNM-IMB - Centro Nacional de Microelectrónica – Institut de Microelectrónica de Barcelona (CSIC) Campus de la Universitat Autònoma de Barcelona. 08193-Bellaterra. Spain  
e-mail: [Irene.Fernandez@cnm.es](mailto:Irene.Fernandez@cnm.es)

<sup>2</sup> MIC – Department of Micro and Nanotechnology, Technical University of Denmark (DTU) Building 345 East, Ørstedes Plads, DK-2800 Kongens Lyngby, Denmark

<sup>3</sup> ICFO – Institut de Ciències Fotòniques, Castelldefells, Barcelona, Spain

<sup>4</sup> COM – Department of Communications, Optics and Materials, Technical University of Denmark, Building 345v, Ørstedes Plads, DK-2800 Kongens Lyngby, Denmark

Surface plasmon polaritons (SPPs), are quasi two-dimensional electromagnetic waves propagating along a dielectric-metal interface. SPPs modes bounded to a subwavelength structure are also called channel plasmon polaritons (CPPs). Recently, v-shape grooves made in noble metal film have demonstrated plasmon coupling in the bottom of the groove, allowing light guiding in subwavelength structures with low propagation losses [1]. The structures used for this demonstration were made in silver by Focused Ion Beam (FIB), resulting in a sharp v-groove, but showing rough sidewalls. FIB is suitable for single groove fabrication, but not for large volume applications, (i.e., biosensors).

In this work we present a process for the fabrication of the v-grooves in metal, based on **NanoImprint Lithography (NIL)** [2]. The process allows parallel fabrication of integrated devices: the v-groove and two deep channels, where the optical fibers are placed for optical characterization. The process is described in Figure 1: (a) the stamp (4 inch) is designed and fabricated in silicon; the grooves have been made by anisotropic wet etching of silicon (KOH), resulting in v-grooves with an angle of 70° and smooth sidewalls. Each stamp contains grooves with different lengths (from 100 μm to 500 μm), and different widths (5 μm to 12 μm). (b), the stamp is imprinted in PMMA. (c), a 200 nm thick film of **gold** is evaporated on the PMMA structures. (d) a UV sensitive polymer (Ormocomp®) is cast onto the gold, and cured with UV light, so it can be the support for the thin gold film. (e) The PMMA sheet is dissolved, in acetone, whereby the smooth grooves in the silicon stamps are replicated in the gold film, as shown finally in (f). Figure 2, (a) and (b), show two examples of the devices based in v-grooves, fabricated in gold on the transparent substrate.

Figure 3 shows results of SNOM characterization, using an interferometric photon scanning tunneling microscope (PSTM). The light was launched with an incident angle of 45° at the beginning of the groove. Figure 3 (a) is a topographical image of the groove, (b) is the light intensity in that area. Comparison between (a) and (b) leads to the conclusion that there is an intensity enhancement in the bottom and in the top corners of the groove. This result agrees with simulations presented by Bozhevolnyi et al. in [3], where the field distribution inside the groove has been simulated for different geometries, showing that for wider grooves, the coupling happens also in the corners.

Phase mapping [4] allows measuring the wavelength of the SPPs and CPPs that propagate in the structures. The wavelength inside the groove (CPP) has been measured to be different to the one propagating on the gold surface outside the groove (SPP). Further more, changing the incident wavelength, the dispersion curve can be represented for SPPs and CPPs in this sample, and be compared to the one at air. Both dispersion curves are non-linear, as expected, and the slope for SPPs and CPPs curves are different, leading to the conclusion that plasmon confinement is possible in v-grooves made with this method.

[1] S. I. Bozhevolnyi, V. S. Volkov, E. Devaux, T. W. Ebbesen, Phys. Rev. Lett. **95**, 046802 (2005)

[2] I. Fernandez-Cuesta, R. B. Nielsen, A. Boltasseva, X. Borrísé, F. Pérez-Murano and A. Kristensen, J. Vac. Sci. Technol. B **25**(6), (2007)

[3] Moreno, E., et al., Optics Letters, **31**(23): p. 3447-3449 (2006)

[4] N. S. L. M., J. P. Korterik, et al. Journal of Lightwave Technology **19**(8): 1169-1176 (2001)

Figures:

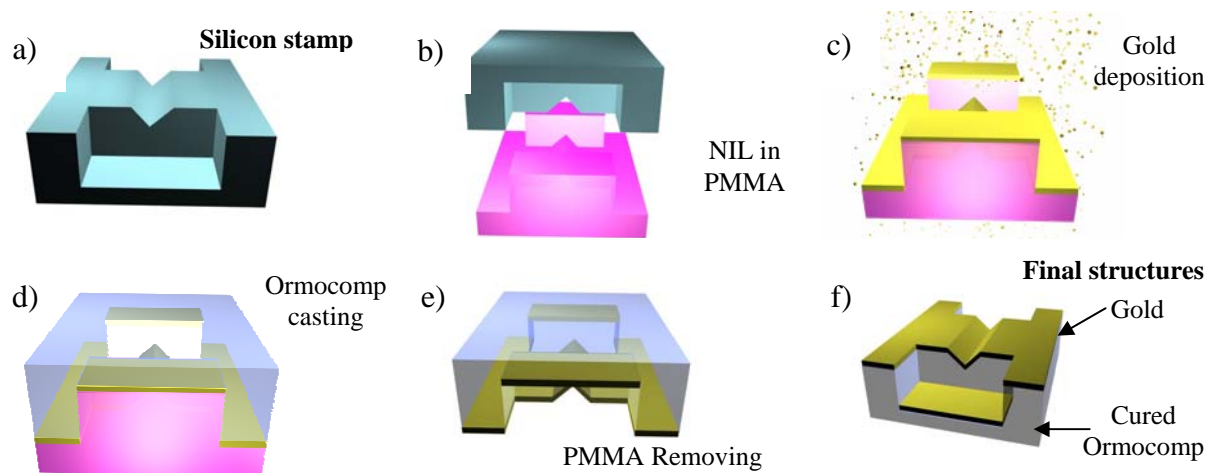


**Figure 1. Scheme of the fabrication process:** (a) silicon stamp, containing the v-grooves. (b) NanoImprint process, to transfer the features to PMMA. (c) a 200 nm thick film of gold is deposited on the PMMA structures. (d) casting of a UV curable polymer (Ormocomp, by micro resist technology) on the structures, and UV curing. (e) PMMA is dissolved in acetone. (f) scheme of the final structures, showing the same geometry of the initial stamp, but made in gold on top of Ormocomp.

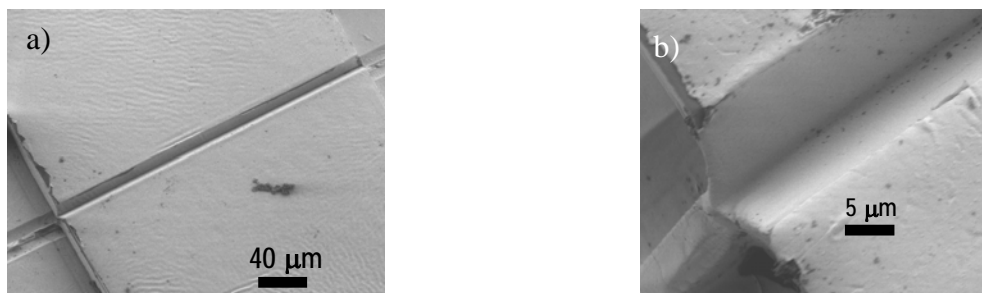


**Figure 2. SEM images of the structures fabricated in gold** (figure 1 f). (a), the groove and the deep channels. (b) a detail of the v-groove, showing the smoothness of the sidewalls.

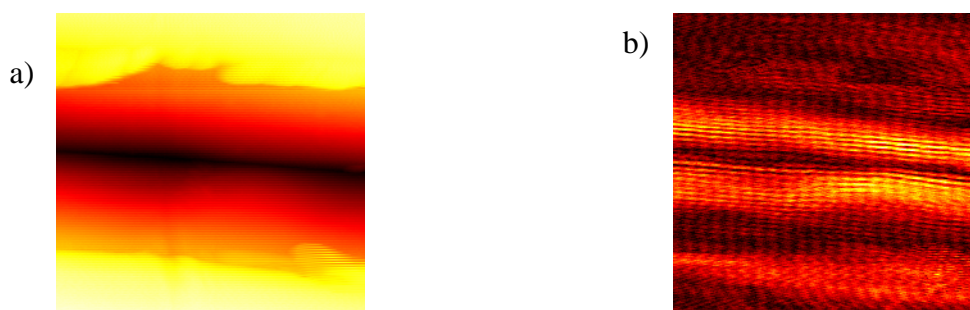


**Figure 3. Results of SNOM characterization.** (a) shows to the topography of the v-groove; (b) represents the field intensity. Light is shown to be confined mainly in the bottom of the groove, and also in the edges.

## MAPPING MOLECULAR DIFFUSION IN NANO-CHANNEL SYSTEMS BY TRACKING INDIVIDUAL FLUORESCENT MOLECULES

*R. Brown<sup>1</sup>, J. Kirstein<sup>2</sup>, C. Jung<sup>2</sup>, B. Platschek<sup>2</sup>, T. Bein<sup>2</sup>, C. Bräuchle<sup>2</sup>,  
C. Cantau<sup>1</sup>, T. Pigot<sup>1</sup>, S. Lacombe<sup>1</sup>*

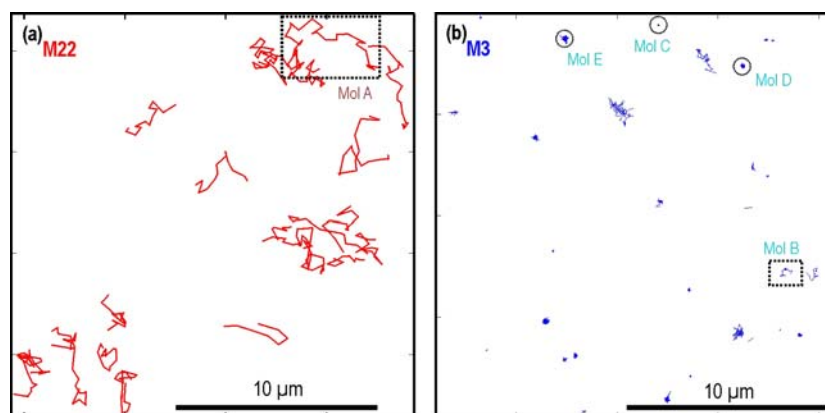
<sup>1</sup>*IPREM-ECP, umr5254 CNRS-UPPA, Hélioparc, 64053 Pau Cedex 9, France*

<sup>2</sup>*Dept. Chemie/CeNS, LMU-München, Butenandstr. 11, 81377 München, Germany*  
[ross.brown@univ-pau.fr](mailto:ross.brown@univ-pau.fr)

Sol-gel derived hybrid materials have great potential in many areas, including sensors, laser materials, molecular sieves, catalysis and photocatalysis. For example, dye-doped silica xerogel monoliths have oxidative and disinfectant properties due to photosensitised production of singlet oxygen on exposure to visible light in air[1]. It is therefore important to understand the dynamics of the organic phase, often a large dye molecule, in the pore system of the host. Immediate questions are the rates of translational and rotational diffusion, physical trapping and chemical tethering to the host material, clustering, and the homogeneity and isotropy of these phenomena throughout the material. Well established techniques for characterising porous materials, such as N<sub>2</sub> adsorption porosimetry are not fully relevant to the dynamics of the much larger dye molecules. Techniques such as PFG NMR may be difficult to deploy and may require considerable assumptions to extract dynamical information from the recorded data. One would like to be able to follow directly the motion of the large organic molecules in the pore system.

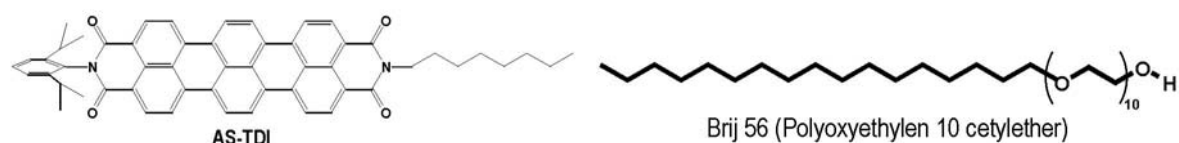
In single particle tracking, usually performed with an epifluorescence microscope, individual particles are tracked from frame to frame in a video recording. Particle tracking is slower (ms-minutes), than in fluorescence correlation spectroscopy ( $\mu$ s)[2], but much more informative, and requires no previous assumptions about the diffusive process.

We present data on tracking individual fluorescent dye molecules in amorphous silica xerogel monoliths[3] with different porosities, and in templated, spin-cast silica thin films[4]. Diffusion in the amorphous xerogels is faster in materials with wider pores. More surprising is dynamical trapping in regions of size 50nm-1 $\mu$ m. Furthermore, a tenfold spatial heterogeneity of the diffusion coefficient on micron lengthscales is also revealed by this technique.

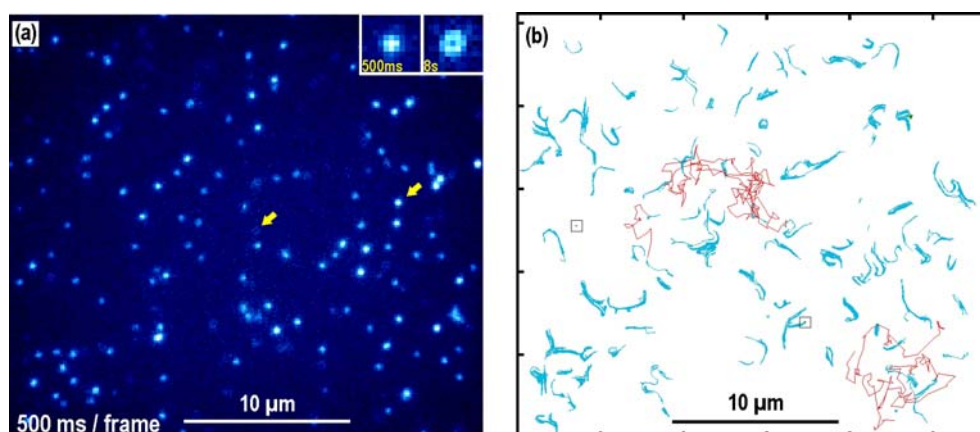


*Sample single molecule tracks (streptocyanine dye) in amorphous silica xerogel monoliths with (a) wide, 22nm and (b) narrow (3nm) pores.*

Diffusion of the dye in templated silica thin films clearly maps the topology and practical connectivity of channels in domains of different mesophases and molecules passing between them or escaping and re-entering to and from the surface. It also reveals dynamical heterogeneities, both between different parts of the sample and within the same spot.



*Terrylene diimide dye and Brij 56 template.*



(a) Epifluorescence video frame of single terrylene diimide molecules in a Brij56- templated silica thin film, in which a hexagonal and a lamellar mesophase happen to coexist. The doughnut-shaped diffraction spot in the lamellar phase shows molecular orientation parallel to the optical axis. (b) Tracks of individual molecules in the mesophases are qualitatively and quantitatively different: oriented diffusion in bundles of channels in the hexagonal phase (blue), isotropic, much slower motion in the lamellar phase (box), isotropic fast diffusion at the sample surface (red).

## References:

- [1] C. Cantau, T. Pigot, N. Manoj, E. Oliveros, S. Lacombe, *ChemPhysChem* **8** (2007) 2344.
- [2] Y. Fu, F. ye, W. G. Sanders, M. M. Collinson, D. A. Higgins, *J. Phys Chem. B* **110** (2006) 9164
- [3] C. Hellriegel, J. Kirstein, C. Bräuchle, V. Latour, T. Pigot, R. Olivier, S. Lacombe, R. Brown, V. Guieu, C. Payraastre, A. Izquierdo, P. Mocho, *J. Phys Chem. B* **108** (2004) 14699.
- [4] J. Kirstein, B. Platschek, C. Jung, R. Brown, Th. Bein, C. Bräuchle, *Nature Mat.* **6** (2007) 303.

## SELF-ORGANIZATION, PHOTOLUMINESCENCE AND EMERGENCE IN AMIDE-FUNCTIONALIZED ORGANIC/INORGANIC HYBRIDS

L. D. Carlos<sup>1</sup>, S. C. Nunes<sup>2</sup>, V. de Zea Bermudez<sup>2</sup>, R. A. Sá Ferreira<sup>1</sup>, J. M Pacheco<sup>3</sup>

<sup>1</sup>*Departamento de Física and CICECO, Universidade de Aveiro, 3810-193 Aveiro, Portugal*

<sup>2</sup>*Departamento de Química, Universidade de Trás-os-Montes e Alto Douro and CQ-VR, Quinta de Prados, Apartado 1013, 5001-911 Vila Real, Portugal*

<sup>3</sup>*ATP-Group, CFTC and Departamento de Física, Universidade de Lisboa, Av. Prof. Gama Pinto, 2, 1649-003 Lisboa Codex, Portugal*

[lcarlos@ua.pt](mailto:lcarlos@ua.pt)

Complex structures, such as living organisms or highly structured materials, share in common the fact that their inherent complexity may be accounted for by the tangled organization of a vast number of simple units. The complex behaviour arises not necessarily due to the atomic structure of the system, but to the orderly assembly of all, or part, of its constituents [1]. Self-assembly of synthetic soft-matter components such as polymers, liquid crystals, surfactants, colloids and organic/inorganic hybrids results in regular hierarchically-organized structures [2-4]. Silsesquioxanes and organosilanes are examples in which hierarchically-ordered self-assembly architectures with well-defined morphologies at the macroscopic scale are induced by weak interactions between the organic spacers (hydrogen bonding, hydrophobic interactions and  $\pi$ - $\pi$  interactions) [4]. However, up to the present, the self-assembly of the simpler alkylsilanes has only been reported sporadically [5].

We have recently introduced a hierarchically-structured amide cross-linked alkyl/siloxane hybrid (named *mono-amidosil*, Fig. 1), where self-assembly is driven by intermolecular hydrogen bonding between amide groups; van der Waals interactions between all-*trans* alkylene chains assuming a partially interdigitated packing mode and an entropic term related to the phase separation between the alkyl chains and the siloxane nanodomains [6]. This *mono-amidosil* hybrid is the first example of a photoluminescent bilayered suprastructure displaying unique nanoscopic sensitivity. The self-organization in the *mono-amidosil* is determinant for the emergence of a thermally-actuated optical memory effect induced by a reversible order-disorder phase transition of the alkyl chains (Fig. 1) [6].

Although the relationship between structural complexity and self-assembly mechanisms has been given much consideration, the essential role played by higher organizing principles in determining emergent physical phenomena in soft-matter complex structures, has been largely unexplored.

The aim of this work is to discuss the nanoscopic (~150 nm) sensitivity of the *mono-amidosil*'s light emitted as an emergent property of the hybrid host determined by the self-organization process (induced by the reversible order-disorder phase transition of the alkyl chains). This phase transition provokes a hysteretic behaviour of the emission energy which presents a slow relaxation accurately described by a logarithmic law (typical of the time evolution of a variety of strongly interacting materials). The connection between the concepts of self-organization and emergence [7] will be also addressed.

## References:

- [1] R. B. Laughlin, D. Pines, Proc. Natl. Acad. Sci. USA, **97** (2000) 28.  
 [2] A. Von Blaaderen, Nature, **439** (2006) 545.  
 [3] K. Vallé, P. Belleville, F. Pereira, C. Sanchez, Nature Mater., **5** (2006) 107.  
 [4] J. J. E. Moreau, B. P. Pichon, M. Wong Chi Man, C. Bied, H. Pritzkow, J.-L. Bantignies, P. Dieudonné, J.-L. Sauvajol, Angew. Chem. Int. Ed., **43** (2004) 203.  
 [5] A. Shimojima, N. Umeda, K. Kuroda, Chem. Mater., **13** (2001) 3610.  
 [6] L. D. Carlos, V. de Zea Bermudez, V. S. Amaral, S. C. Nunes, N. J. O. Silva, R. A. Sá Ferreira, J. Rocha, C. V. Santilli, D. Ostrovskii, Adv. Mater., **19** (2007) 341.  
 [7] P. A. Corning, Complexity, **7** (2002) 18.

## Figures:

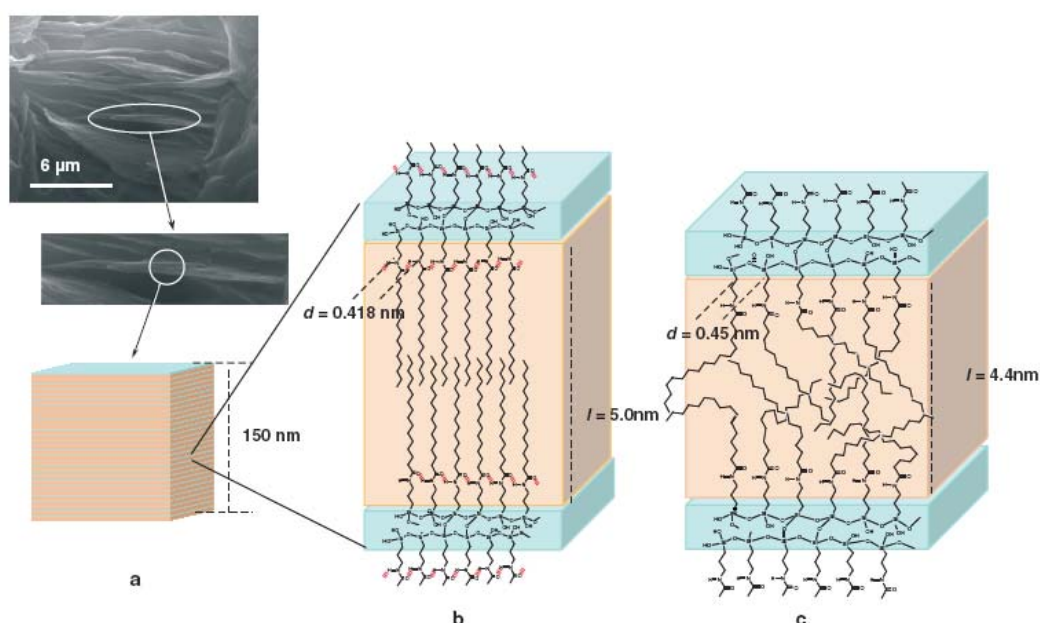


**Figure 1.** SEM image and schematic representations of the structure of mono-amidosil hybrid. a) Lateral portion of a crystallite composed of a stack of bilayers. b-c) Bilayer at room temperature and at 120 °C, respectively.

## NONAQUEOUS SOL-GEL ROUTES TO DILUTED MAGNETIC SEMICONDUCTORS

*Guylhaine Clavel<sup>1,2</sup>, Andrea Pucci<sup>1</sup>, Marc-Georg Willinger<sup>1</sup>, David Zitoun<sup>2</sup>, Nicola Pinna<sup>1</sup>*

*1 - Department of Chemistry and CICECO, University of Aveiro, 3810-193 Aveiro*

*2 - Institut Charles Gerhardt, CC15, Place Eugène Bataillon, 34095 Montpellier, France*

*pinna@ua.pt*

Nanostructured oxides play a major role in the development of functional nanoscale materials and devices. Among them, diluted magnetic semiconductors (DMS) represent an important family of materials. In an extremely quoted paper of Dietl et al., ZnO and GaN have been predicted ferromagnetic at room temperature [1]. Since 2000 a lot of controversial works were published on the subject showing that these materials show ferromagnetic behavior in function of the doping but also of the synthetic approach. A recent theoretical work predicts that transition-metal doped zirconia can be also ferromagnetic at room temperature in function of the metal dopant, its oxidation state and concentration [2].

Non-aqueous sol-gel routes are remarkably successful for the synthesis of oxide materials. Solvent assisted synthesis and especially the “benzyl alcohol route” have several advantages such as a low reaction temperature and a high crystallinity and purity of the as synthesized oxides [3,4]. We extended the “benzyl alcohol route” to the synthesis of transition metal doped oxide semiconductors[5,6]. This synthetic method enables the incorporation of several transition metal dopants into oxide matrix.

Here, we present the synthesis, the characterization and the magnetic properties of doped ZnO [5] and ZrO<sub>2</sub>[6] nanoparticles. The synthesis involves the reaction of inorganic precursors and benzyl alcohol at moderated temperature and lead to high-quality nanocrystals presenting a homogeneous distribution of the magnetic ion. Manganese doped zinc oxide as well as manganese doped zirconia, exhibit mainly a paramagnetic behavior of the diluted spins. In the case of cobalt doped zinc oxide, the magnetic properties are affected by the synthesis condition, paramagnetic or ferromagnetic behavior was obtained depending on the solvent used. The homogeneity and local environment of the magnetic ions diluted into the matrix were characterised by high resolution TEM, electron energy loss spectrometry and by electron paramagnetic resonance, which is a local probe sensitive to oxidation state, local symmetry and spin-spin interactions. After providing evidence on the homogeneity of doping and the absence of any secondary phase, the magnetic properties of the as-synthesized nanoparticles were studied using SQUID and VSM magnetometer.

### References:

- [1] T. Dietl, H. Ohno, F. Matsukura, J. Cibert, D. Ferrand, *Science* **2000**, 287, 1019.
- [2] S. Ostanin, A. Ernst, L. M. Sandratskii, P. Bruno, M. Dane, I. D. Hughes, J. B. Staunton, W. Hergert, I. Mertig, J. Kudrnovsky, *Phys. Rev. Lett.* **2007**, 98, 016101.
- [3] N. Pinna, M. Niederberger, *Angew. Chem. Intl. Ed.* **2008**, in print
- [4] N. Pinna, *J. Mater. Chem.* **2007**, 17, 2769
- [5] G. Clavel, M. Willinger, D. Zitoun, N. Pinna, *Adv. Funct. Mater.* **2007**, 17, 3159
- [6] G. Clavel, M. Willinger, D. Zitoun, N. Pinna, *Eur. J. Inorg. Chem.* **2008**, 863



## NANOLIPOSOMES AS TOOLS FOR THE TREATMENT OF INFECTIOUS DISEASES

*M. Eugénia M. Cruz, Manuela Carvalheiro, Carla Eleutério, Ana Sousa, M. Manuela Gaspar*  
*Unit of New Forms of Bioactive Agents (UNFAB)/ INETI, Estrada do Paço do Lumiar, 22*  
*1649-038 Lisbon, Portugal*  
*i-Med, Research Institute for Medicines and Pharmaceutical Sciences; Faculty of Pharmacy,*  
*Lisbon University, Av. Prof Gama Pinto, 1649-003, Lisbon, PORTUGAL*  
*eugenia.cruz@ineti.pt*

Infectious diseases (ID) represent an immense global threat, being responsible for 15 million of deaths per year worldwide. The ID caused by intracellular microorganisms, such as *M. tuberculosis*, *Leishmania*, *M. avium* and *Plasmodium sp*, are very difficult to eradicate by the conventional therapies due to the low access of drugs to the sites of infection resulting in sub-therapeutic local drug concentration. Besides, severe side effects and poor compliance have been reported, being in the origin of pathogen resistant strains and treatment failure. Therefore non conventional strategies able to modify drugs behaviour and to improve their therapeutic index are needed. One of these strategies is the association of drugs to systems able to direct them to the sites of infection, namely macrophages, instead of using “naked” (free) drugs. Nanoliposomes are the ideal systems for this purpose as they have the tendency to accumulate in macrophages, together with the incorporated drugs. This capability was exploited for the treatment of tuberculosis, *M. avium* infections and leishmaniasis, with liposomes incorporating rifamycins, aminoglycosides and dinitroanilines, respectively. We have developed different types of liposomes incorporating a rifamycin, Rifabutin (RFB) and tested in murine models of *M. tuberculosis* and *M. avium* infections. RFB incorporated in liposomes showed a superior therapeutic effect than the commercial antibiotic (free RFB) This effect has been observed either through the reduction on the number of viable colony forming units in liver, spleen and lungs as well as through histological and immunological studies [1,2].

Paromomycin (PRM) is an aminoglycoside indicated for treatment of mycobacteriosis and leishmaniasis. Biodistribution studies showed that the liposomal formulations of PRM were able to accumulate in appreciable amounts in liver, spleen and lungs, the infected organs of disseminated *M. tuberculosis* and *M. avium* , even 24 h after administration while the free PRM amounts are neglectable The therapeutic effect of PRM liposomal formulations in a model of *M. avium* infections showed the superiority of these formulations over the free drug on reducing the bacterial loads in infected organs (Figure 1).These formulations are currently on test to evaluate the activity in *M. tuberculosis* and *Leishmania* models of infection.

Dinitroanilines are herbicides that showed antiparasitic properties, namely against different strains of *Leishmania in vitro*. Its use *in vivo*, namely by parenteral route, has been limited by inappropriate properties (low water solubility and instability). Liposomal formulations of dinitroanilines were developed with success, acting liposomes as drug solvent, as stabilizing system for their storage and as drugs carriers to the sites of infection (liver and spleen). The therapeutic activity of one dinitroaniline (Trifluralin) in liposomes was assayed in a murine visceral model (*L. donovani*) of infection. As shown in Figure 2 a significant reduction of parasite loads (up to 70%), after treatment with several liposomal formulations, in comparison with the free drug was observed. No signs of toxicity after dinitroaniline liposome treatment were observed [3]. These liposomal formulations also improved the clinical condition of dogs and reduced the density of parasites [4].

### References:

- [1] Gaspar MM, Neves S, Portaels F, Pedrosa J, Silva MT, Cruz MEM., *Antimicrob Agents Chemother.* **44(9)**, (2000) 2424-30.  
 [2] Gaspar M.M., Cruz A., Penha A.F., Reymão J., Sousa A.C., Eleutério C.V., Domingues S.A., Fraga A.G., Longatto Filho A., Cruz M.E.M., Pedrosa J, *Int. J. Antimicrob. Agents* **31(1)**, (2008) 37-45.  
 [3] Cruz, MEM, Carvalho M., Jorge J, Eleutério C., Sousa A.C., Croft S., In: *Parasitologia*, **47 (Suppl.1)** (2005), 81.  
 [4] Marques C, Carvalho M, Pereira M.A, Jorge J., Cruz M.E.M., Santos-Gomes G.M., *The Veterinary Journal* (2007) (available on line [www.sciencedirect.com](http://www.sciencedirect.com)).

**Figure 1** – Therapeutic effect of PRM formulations in a *M. avium* model of infection. Influence of lipid composition on growth index in liver (grey columns), spleen (black columns) and lungs (white columns). Studied formulations: Liposomes: Lip1 - DMPC:DMPG:DSPE-PEG, Lip2-DPPC:DPPG:DSPE-PEG Lip 3 - DPPC:DPPG, Free PRM (Control - infected and non-treated mice).

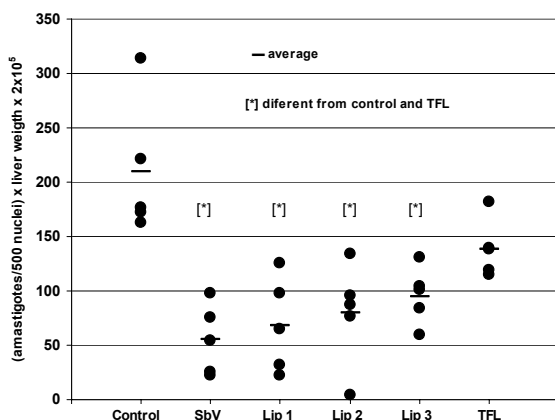
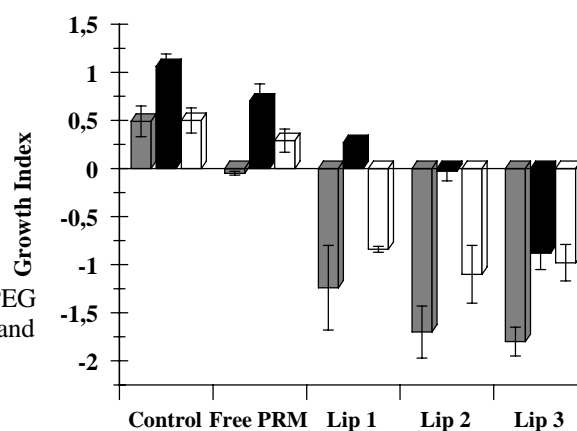


**Figure 2** – Therapeutic effect of TFL liposomal formulations in a murine Visceral model of *L. donovani*. Mice received 5 doses of 15mg/kg (in five consecutive days) of three different TFL liposomes (Lip 1 = DOPC:DOPG (7:3); Lip 2 = DSPC:Chol (4:1) and Lip 3 = PC:PG (7:3), free TFL (dissolved in ethanol) and standard drug Glucantime (15 mg Sb<sup>v</sup> /kg), by i.v. route. Negative control animals were injected with liposomes suspension medium (0.3 M trealose).

This work was partially supported by the projects: POCTI / FCB/36416/1999, POSI/SAU-FCF/58355/2004 POCTI/CVT/35249/000; POCTI/CVT/56995/2004

## EQUILIBRIUM AND TRANSPORT PROPERTIES OF SMALL ALKANES AND ALKENES CONFINED IN SINGLE-WALLED CARBON NANOTUBES.

*Fernando J. A. L. Cruz, Erich A. Müller*

*Imperial College London, Department of Chemical Engineering, London SW7 2AZ, U.K.  
e.muller@imperial.ac.uk*

In recent years it has been suggested that carbon nanotubes (CNTs) could be used as active separating agents both in carbon adsorbents and in membranes [1-3]. To efficiently use CNTs in such separation devices, it becomes essential not only to study their selectivity/equilibrium properties but also to understand the confined fluid dynamics. This work presents molecular simulation results of both the adsorption and diffusion of low molecular weight saturated (alkanes) and unsaturated (alkenes) hydrocarbons inside single-walled carbon nanotubes (SWCNTs) of different topologies.

Classical Molecular Dynamics simulations were employed to study both the adsorption and the flow dynamics. Large-scale simulations were set up where several open-ended SWCNTs were exposed to a bulk fluid in an overall canonical ensemble. The endohedral physical adsorption and non-equilibrium diffusion into the pore was monitored until steady state conditions were attained [4]. We present adsorption isotherms for both components at 300K for pressures up to 30 bar. We have seen that the adsorption is insensitive to the chirality of the nanotubes. Additionally, our results show that for the binary mixtures there is only a modest selectivity of the adsorption towards ethane. During the transient period of filling up the nanotubes we have observed a spiralling diffusion path for the molecules at low loading. This unique observation has been previously reported for water [5] and similar systems [6]. We have determined it is a property of the nanotube symmetry, as it is not seen in armchair type nanotubes.

The corresponding confined phase from the previously described simulations, containing the nanotube and the adsorbed molecules, was separated from the bulk fluid phase and replicated four times along the  $z$ -axis to produce a  $3.0 \times 3.0 \times 20.6$  nm supercell containing *ca.* 3000 graphitic carbon atoms ( $D_{eff} \approx 0.9$  nm,  $L_{eff} \approx 20.6$  nm) and the mean-squared displacement evaluated for different loadings and tube topologies, using a chiral (12,6) tube and an armchair (9,9) tube. Dynamical properties of  $C_2H_4$  and  $C_2H_6$ , both in the bulk fluid phase and confined inside SWCNTs of different symmetries, have been investigated in the regions  $0.026 \text{ mol}\cdot\text{L}^{-1} < \rho < 15.751 \text{ mol}\cdot\text{L}^{-1}$  and  $0.011 \text{ mol}\cdot\text{L}^{-1} < \rho < 14.055 \text{ mol}\cdot\text{L}^{-1}$ , respectively.

From the mean square displacement curves,  $\langle r^2 \rangle$  of confined fluids (Figure 2) [7,8], as expected, we observed a monotonical decrease of the self-diffusion coefficient with increasing density. As for the bulk fluids, an empirical correlation has been established that enabled direct comparison with experimental data; in the case of ethylene, discrepancies were found to be less than 5 %, up to  $\rho \approx 10 \text{ mol}\cdot\text{L}^{-1}$  [9]. Upon confinement inside a SWCNT, nanotube topology seems to be a relatively unimportant factor influencing the molecules dynamics, according to what has been suggested by previous studies for zig-zag and armchair symmetries [5,6]. The high-density systems confined onto a zig-zag lattice, usually exhibited a dominant Fickian-type mode of transport, although a transition seemed to occur for molecular densities  $\rho < 5.5 \text{ mol}\cdot\text{L}^{-1}$ . Below this threshold, molecules moved with a mixed mode transport, combining components from Fickian and ballistic diffusion.

This work has been supported by *E.P.S.R.C.* Grant EP/D035171/1 (UK).

## References:

- [1] Sholl, D. S.; Johnson, J. K. *Science* 2006, 312, 1003.
- [2] Majumder, M.; Chopra, N.; Andrews, R.; Hinds, B. J. *Nature* 2006, 438, 44.
- [3] Corry, B. J. *Phys. Chem. B* 2008, 112, 1427.
- [4] Cruz, F. J. A. L.; Müller, E. A. J. *Phys. Chem. C* (2008) *submitted*.
- [5] Alexiadis, A.; Kassinos, S. *Chem. Eng. Sci.* (2008) doi:10.1016/j.ces.2007.12.035.
- [6] Mao, Z.; Sinnott, S. B. *J. Phys. Chem. B* **104** (2000) 4618.
- [7] Allen, M. P.; Tildesley, D. J. *Computer Simulation of Liquids*; Clarendon Press: Oxford, 1990.
- [8] Haile, J. M. *Molecular Dynamics Simulation: Elementary Methods*; Wiley: New York, 1992.
- [9] Fernández, G. A.; Vrabc, J.; Hasse, H. *Int. J. Therm.* **26** (2005) 1389.

## Figures:

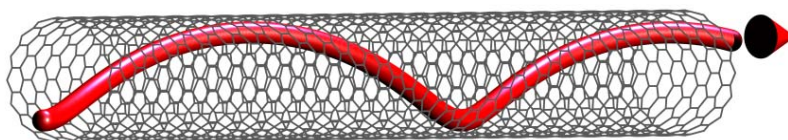


**Figure 1.** Unique spiral diffusion path inside a zig-zag (16,0) topology.

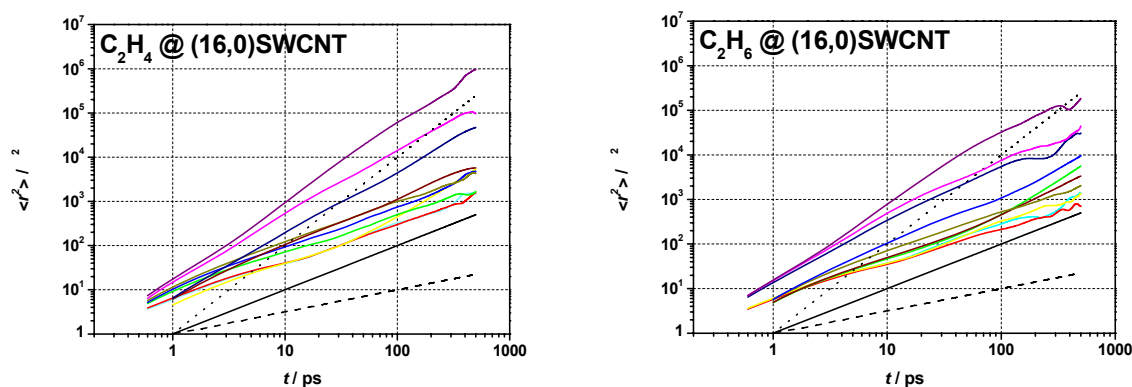


**Figure 2.** Mean squared displacement  $\langle r^2 \rangle$  for fluids confined in a (16,0) zig-zag SWCNT ( $T = 300 \text{ K}$ ). Density increases from top to bottom, respectively, from  $0.242 \text{ mol}\cdot\text{L}^{-1}$  to  $15.751 \text{ mol}\cdot\text{L}^{-1}$  ( $\text{C}_2\text{H}_4$ ) and from  $0.242 \text{ mol}\cdot\text{L}^{-1}$  to  $14.055 \text{ mol}\cdot\text{L}^{-1}$  ( $\text{C}_2\text{H}_6$ ). The different diffusion mechanisms are indicated for comparison purposes: ballistic (dotted), Fickian (straight line) and single-filed (dashed).

## MAGNETIC POLYSACCHARIDE NANOSPHERES WITH POTENTIAL FOR BIOMEDICAL APPLICATIONS: PREPARATION VIA A REVERSE MINIEMULSION METHOD

*A.L. Daniel-da-Silva, T. Trindade, B.J. Goodfellow, A.M. Gil*

*University of Aveiro, Department of Chemistry, CICECO, Campus Universitario de Santiago, 3810-193 Aveiro, Portugal*

[ana.luisa@ua.pt](mailto:ana.luisa@ua.pt)

Magnetic polymeric supports such as micro- and nanospheres have attracted increasing interest in the last few years due to their potential for applications in biology and medicine, such as cell isolation, protein immobilization, targeting drug delivery and clinical diagnosis [1]. For use in biomedical applications, magnetic polymer nanospheres need to fulfill some requirements: biocompatibility, narrow size distribution and high density of reactive surface groups for the coupling of active biomolecules. In addition, nanospheres should have high and uniformly dispersed magnetic content with superparamagnetic behavior. In our previous work [2]  $\kappa$ -carrageenan, a non-toxic sulphated polysaccharide has been successfully employed as a colloidal stabilizer in the in-situ synthesis of superparamagnetic magnetite nanoparticles, preventing their spontaneous agglomeration and conferring biocompatibility to the resulting composite. Moreover, the resulting ferrofluid, that contained magnetite nanoparticles prepared by co-precipitation within the  $\kappa$ -carrageenan under alkaline conditions, could undergo gelation under cooling conditions due to the gelling properties of this biopolymer.

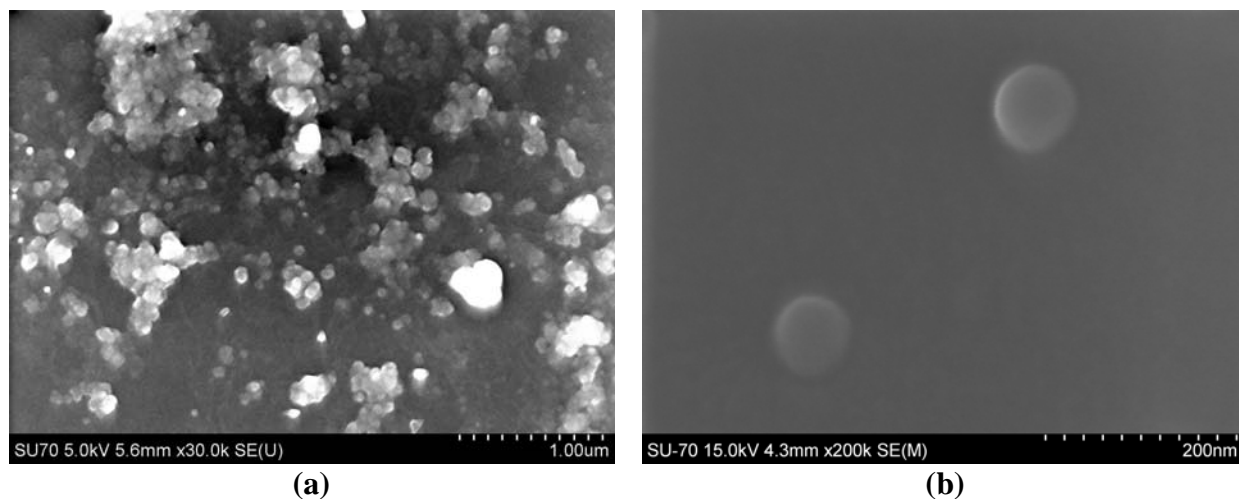
In this work, taking advantage of the ability of the ferrofluid to form gels, composite nanospheres consisting of magnetite nanoparticles embedded in a  $\kappa$ -carrageenan matrix have been prepared for the first time, using reverse miniemulsions. The reverse miniemulsions were obtained by sonication of a quaternary system comprising n-heptane as the organic phase, cetyltrimethylammonium bromide (CTAB) as surfactant and 1-butanol as the co-surfactant. The aqueous phase consisted on the ferrofluid containing the biopolymer and magnetite nanoparticles ( $d \sim 8$ nm). The stability of the miniemulsion was seen to be affected by the fine composition of the aqueous phase, namely by the concentration of alkali-metal cation added for magnetite precipitation.

Using the method outlined above, stable miniemulsions containing the magnetic polymeric fluid as aqueous phase were successfully obtained. The spherical morphology of the resulting polymer nanocomposites was confirmed by scanning electron microscopy (SEM), with particles showing an average diameter of 75 nm (Fig.1). DLS measurements have shown larger sizes than SEM probably due to some magnetic interaction of the spheres to form aggregates in solution. The control of the average size of the nanospheres was seen to be possible upon the variation of the concentration of surfactant. Furthermore, magnetic measurements have shown that magnetite nanoparticles are superparamagnetic at ambient temperature (Fig. 2).

The resulting composites are, therefore, of potential interest for several biomedical applications. Since  $\kappa$ -carrageenan forms thermoreversible gels, the controlled release of magnetic particles or loaded drugs can be envisaged by both thermal and magnetic stimuli. In addition, carrageenan can be further functionalized for the conjugation of biomolecules on the surface of the nanospheres, which is the subject of ongoing work.

### References:

- [1] U. Hafeli, W. Schutt, J. Teller, M. Zborowski, Scientific and Clinical Applications of Magnetic Carriers, Plenum, New York, 1997.
- [2] A.L.Daniel-da-Silva, T. Trindade, B.J. Goodfellow, B.F.O. Costa, R.N. Correia, A.M. Gil,

**Figures:**

**Figure 1.** SEM images of magnetic nanospheres at different magnification (a) 30,000×; (b) 200,000×.

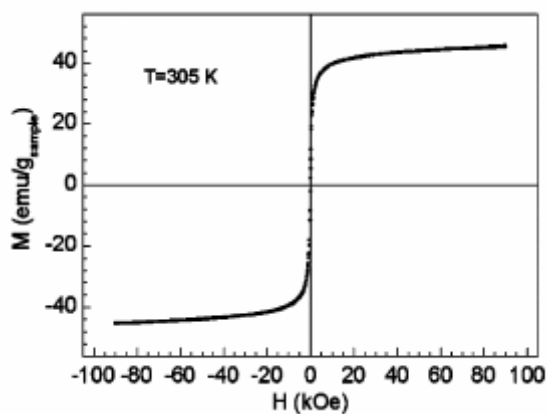


**Figure 2.** Magnetization as function of magnetic field at 305K.

## TOWARDS MULTIFUNCTIONAL CORE-SHELL NANOPARTICLES FOR BIOLOGICAL APPLICATIONS

*Marie-Hélène Delville,<sup>a,\*</sup> Sonia Pinho,<sup>a,b</sup> Stéphane Mornet,<sup>a</sup> Emeline Julie Ribot<sup>c</sup> Pierre Voisin,<sup>c</sup> Anne-Karine Bouzier-Sore,<sup>c</sup>*

<sup>a</sup> *Bordeaux Institute of Condensed Matter Chemistry, UPR CNRS 9048 / University of Sciences and Technology of Bordeaux, 87 avenue du Dr Albert Schweitzer, 33608 Pessac, France.*

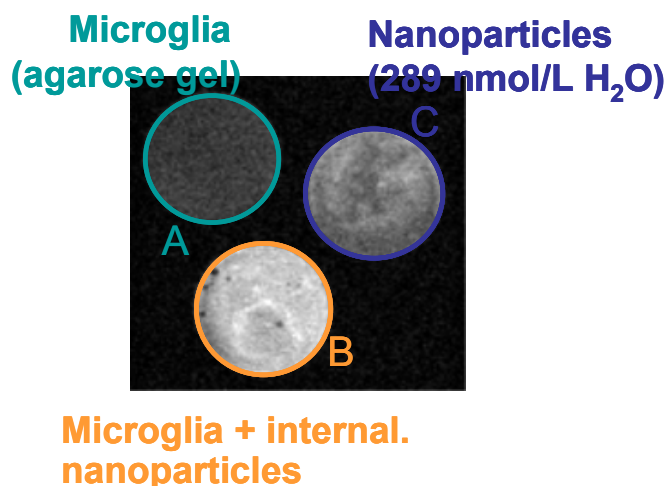
<sup>b</sup> *Department of Chemistry and Physics, University of Aveiro, CICECO, 3810-193 Aveiro, Portugal*

<sup>c</sup> *Résonance Magnétique des Systèmes Biologiques, UMR CNRS 5536, 146 rue Léo Saignat, F-33076 Bordeaux cedex France,*

[delville@icmcb-bordeaux.cnrs.fr](mailto:delville@icmcb-bordeaux.cnrs.fr)

There is therefore a real need to design multifunctional contrast agents, which can produce multiple targeting and visualization of organs or cells (detectable changes in the MR signal intensity<sup>1</sup> of the target tissue or organ by changing its MR relaxation properties and detectable optical signals for example<sup>2, 3</sup>). These contrast agents require (i) a large number of paramagnetic centers selectively bound to the target tissue and (ii) a sufficiently high molecular weight of the MRI agents in order to extend their vascular retention and thus slow their tissue clearance. For this reason, the development of biocompatible nanoparticles with an external shell of high-spin paramagnetic lanthanide contrast agents like gadolinium chelate (seven unpaired electrons), europium fluorescent probes and a superparamagnetic core, appears to be an interesting solution for targeted imaging.

Indeed, the lanthanides species are both active in the detection of the target using different techniques.  $Gd^{3+}$  nucleus generates a hypersignal with a T1 weighted sequence, even at high magnetic field and, consequently, a much easier interpretation of the MRI images. However, these low molecular weight gadolinium chelates accumulate in the extracellular space where the “blood brain barrier” breakdown has occurred. They undergo rapid diffusion through the interstitial and as well as renal elimination and therefore have the limitation of providing a time-dependent image of tumor margins. We show in this communication that the chemical grafting of such contrast agent on *metal oxide nanoparticles* can be an alternative route to change their biodistribution, with the desired half-lives, inducing their internalization by macrophages, and having a hypersignal with T1 weighted sequence (Figure 1).



4

Silica nanoparticles, for example, would be an excellent carrier for the lanthanides chelates. Silica is porous enough so that water can freely move in and out of the frame. The size of the particles will slow the rotational movement of the chelates and improve the relaxation of water. Additionally, the nontoxic silica can be easily derivatized and targeted contrast agents can be synthesized. Nanosized silica, with a size between 10 and 20 nm, are small enough to pass through the body, and above all are able to enter cells. New sets of Ln<sup>3+</sup> modified nanoparticles were synthesized and investigated for their MRI contrast agents' properties and for their ability to be internalized and allow the spatial detection of cell populations able of phagocytosis such as microglial cells. We will also present preliminary results on the introduction of a superparamagnetic oxide in the silica and study the interactions in between the shell and the core with respect to the silica shell thickness.

### References:

- <sup>1</sup> Caravan, P., Ellison, J. J., McMurry, T. J., and Lauffer, R. B. agents: *Chem. Rev.* 99, (1999)2293-2352.
- <sup>2</sup> Rocha, J.; Carlos, L. D.; Almeida Paz, F. A.; Ananias, D.; Klinowski, J. *Recent Advances in the Science and Technology of Zeolites and Related Materials*, **154C** (2004), 3028-3035
- <sup>3</sup> Voisin, Pierre; Ribot, Emeline Julie; Miraux, Sylvain; Bouzier-Sore, Anne-Karine; Lahitte, Jean-Francois; Bouchaud, Veronique; Mornet, Stephane; Thiaudiere, Eric; Franconi, Jean-Michel; Raison, Lydia; Labrugere, Christine; Delville, Marie-Helene. *Bioconjugate Chemistry* **18(4)** (2007), 1053-1063.
- <sup>4</sup> Ribot, E.; Bouzier-Sore, A.-K.; Bouchaud, V.; Miraux, S.; Delville, M.-H.; Franconi, J.-M.; Voisin, P. *Cancer Gene Therapy* **14(8)** (2007) 724-737.

## SIZE VERSUS DISORDER EFFECTS IN THE ELECTRONIC PROPERTIES OF NANOSIZED INTERMEDIATE VALENCE METALS

*L. Fernández Barquín<sup>1</sup>, D. P. Rojas<sup>1</sup>, D. Alba Venero<sup>1</sup>, J. I. Espeso<sup>1</sup>, J. Rodríguez Fernández<sup>1</sup>, M. A. Laguna Marco<sup>2,3</sup>, R. Boada<sup>2</sup>, J. Chaboy<sup>2</sup>*

<sup>1</sup>*Depto. CITIMAC, F. Ciencias, Universidad de Cantabria, Santander 39005, Spain*

<sup>2</sup>*ICMA, CSIC- Univ. Zaragoza, Zaragoza 50009, Spain*

<sup>3</sup>*Advanced Photon Source, Argonne National Laboratory, Chicago, IL, USA*

[barquinl@unican.es](mailto:barquinl@unican.es)

Nanotechnology is deeply attached to the knowledge of basic mechanisms driving the change of materials properties. For the case of magnets, the properties are drastically modified by the size of the particles and several behaviours can be found, which are object of huge attraction [1]. On the one hand, the coupling between the shell and the core of the particles may affect the superparamagnetic limit [2]. If we study the interparticle magnetic coupling, this is frequently governed by dipolar and/or RKKY interactions, which strongly affects a very important technological magnitude as anisotropy [3]. In other cases, it is the intrinsic magnetic clustered nature of the metal the origin of many magnetic properties in the border of non Fermi liquids, displaying step-like hysteresis loops in the miliKelvin range [4]. But those interesting effects are not restricted to artificial structures; for example they are also found in goethite, a very common mineral in the surface of earth, of great importance for archaeology, biosciences or geology, to cite a few areas [5]. Over the last years we have gathered some experience in dealing with these complex magnetic systems and the arising and persistent key question is whether the size or the disorder in the crystallographic structure is the main driving parameter acting in the magnetic properties. This dilemma is clearly a challenge for a broad number of scientists.

Recently we have undergone an ambitious program to study in detail the properties of Strongly Correlated Electron Systems over a certain range of particle sizes. These materials are characterized (in bulk) by a large effective electron mass, displaying in some cases exotic behaviours, such as non-Fermi liquid or Quantum Critical Points [6]. They also exhibit an interesting competition of the exchange (RKKY) and Kondo interactions, leading to magnetic-nonmagnetic crossovers that can be tuned by different physical (and chemical) parameters. Most of these systems are based in an attractive situation, specific of Ce ( $4f^1$ , one electron) and Yb ( $4f^{13}$ , one hole) atoms, which in some cases present intermediate valence [4].

In our study, we have prepared a series of alloys of  $\text{YbAl}_3$  (cubic) in different sizes from bulk to 10 nm, as estimated from Rietveld refinements of XRD data, without noticeable change in the lattice parameter ( $a = 4.2057(7) \text{ \AA}$ ). The magnetic susceptibility (2-300K) presents the typical intermediate valence behavior with a peak shifting in temperature with particle size. Also the specific heat (2-300 K) shows modifications in the usually labelled as Kondo temperature and the electronic contribution. To dig in the microscopic origin, X-ray absorption (XANES and EXAFS) were carried out in the beamline BL39XU (Spring8, Japan) and BM25A (ESRF, France) on the Yb-L<sub>II</sub> and Yb-L<sub>III</sub> edge. The short-range EXAFS Fourier transforms shows the existence of constant Yb-Yb distance (2.96  $\text{ \AA}$ ) whereas the Debye-Waller factor increased from 0.0069(22)  $\text{ \AA}^2$  (bulk alloy) to 0.0115(21)  $\text{ \AA}^2$  in samples with 10 nm. Concomitantly, the valence decreased in the XANES spectra with decreasing size. The analysis of the variations of the main parameters (valence, electronic contribution of the specific heat, Kondo temperature) is in full agreement with the size factor as a driving force and atoms in the surface (Yb<sup>2+</sup>) play an enhanced role when the ratio surface atoms/volume atoms is increased. In consequence for this case alloy in the verge of magnetism, it is the size the main parameter.

## References:

- [1] X. Battle and A. Labarta, J. Phys. D: Appl. Phys., **35** (2002) R15; S. Bader, Rev. Mod Phys **78** (2006) 1.
- [2] Q. A. Pankhurst, A. Yedra Martínez and L. Fernández Barquín, Phys. Rev. B **69** (2004) 212401.
- [3] L. Fernández Barquín, R. García Calderón, B. Farago, J. Rodríguez-Carvajal, A. Bleloch, D. McComb, R. Chater, and Q. A. Pankhurst, Phys. Rev. B **76** (2007) 172404.
- [4] N. Marcano, J. C. Gómez Sal, J. I. Espeso, L. Fernández Barquín, and C. Paulsen, Phys. Rev. B **76** (2007) 224419.
- [5] Q. A. Pankhurst, L. Fernández Barquín, J. S. Lord (to be submitted to Phys. Rev. B)
- [6] G. R. Stewart, Rev. Mod. Phys. **73** (2001) 797.
- [7] D. P. Rojas, J. I. Espeso, L. Fernández Barquín, J. Rodríguez Fernández, J. Chaboy (submitted to Phys. Rev. B).

## Figures:

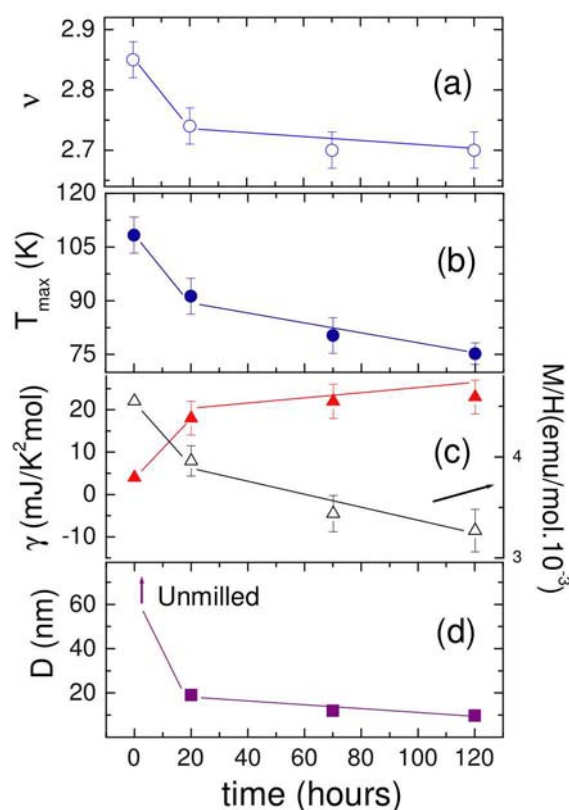


**Figure.** Milling time dependence of the mean valence  $v$ ,  $T_{max}$  of the magnetic contribution to the specific heat (b), the Sommerfeld coefficient ( $\gamma$ ) of the electronic contribution and the absolute value of the magnetic susceptibility at the maximum (c), and the size of the particles ( $D$ ) (d). The grain size of the unmilled alloy can only be suggested (arrow). An abrupt variation from unmilled to 20 hours, followed by a smooth change on going to 120 hours milled alloy is observed. Lines are guides for the eye.

## EFFECT OF CHEMISORBED MOLECULES ON THE TRANSPORT PROPERTIES OF A (6,6) CARBON NANOTUBE

*Juan María García-Lastra<sup>a</sup>, Kristian Sommer Thygesen<sup>b</sup> and Ángel Rubio<sup>a</sup>*

*<sup>a</sup>Departamento de Física de Materiales, Facultad de Químicas, Universidad del País Vasco, San Sebastián 20018, Spain.*

*<sup>b</sup>Center for Atomic-scale Materials Physics, Department of Physics, Technical University of Denmark, DK-2800 Kgs. Lyngby, Denmark  
scpgalaj@ehu.es*

We study how the electron transport properties of a (6,6) armchair carbon nanotube (CNT) are influenced by small chemisorbed molecules (H,COOH,OH,NH<sub>2</sub>,NO<sub>2</sub>). Despite the different chemical nature of the molecules, we find that they all have very similar effect on the transmission. The effect of a single adsorbate is to suppress one of the two available transport channels close to the Fermi level. When two or more adsorbates are present the conductance shows a peculiar selectivity: If both molecules are adsorbed on the same sublattice the conductance can be either 0 or 1 depending on relative position of the adsorbates. In fact, one transport channel remains fully open for any number of molecules when the adsorption sites belong to the same sublattice and satisfy a simple condition. This is shown to be due to a CNT eigenstate which vanishes simultaneously at all such sites. In contrast, when two or more molecules are adsorbed on different sublattices, the conductance shows a strong dependence on the relative positions of the molecules taking values from 0 to  $2G_0$ .



## MAGNETO-PLASMONIC MATERIALS: TUNING MAGNETO-OPTICS WITH PLASMONS

*A. García-Martín, G. Armelles, A. Cebollada, J.M. García-Martín, J.V. Anguita, J.B. González-Díaz, J.F. Torrado, X. Bendaña and E. Ferreiro*  
*Instituto de Microelectrónica de Madrid, Consejo Superior de Investigaciones Científicas, C\Isaac Newton 8 (PTM) 28760 Tres Cantos, Spain*  
[antonio@imm.cnm.csic.es](mailto:antonio@imm.cnm.csic.es)

During the last decades we have witnessed the development of a new branch in optics: plasmon optics or plasmonics. This comes from the need to develop optical components in the nanoscale and to overcome the restriction imposed by the diffraction limit. Plasmonics has already given rise to novel devices. However, in order to achieve the same state as conventional optics it will be necessary to produce active materials. These active materials are those whose optical properties can be controlled by an external agent. In our case the choice is a magnetic field. Here we will review our work on the combination of plasmons and magneto-optical activity. Firstly we will consider the system to consist in an ordered array of nickel wires and we will show that the excitation of a plasmon running along the wire gives rise to and enhancement of the magneto-optical response[1]. The use of ferromagnetic materials alone is not enough due to their broad plasmon resonance. However, the combination of magneto-optically active and noble plasmonic materials gives rise to systems with enhanced optical and MO responses. For instance, it has been shown that the MO response of Au/Co/Au trilayered systems can be enhanced when its surface plasmon resonance is excited [2], enabling to develop new high sensitivity biosensors [3]. It has also been demonstrated that an applied magnetic field modifies the propagation vector of the plasmon in continuous films[2]. However, such enhancement has been so far observed in continuous films, presenting simultaneously well defined propagating surface plasmon resonances and MO activity. A discrete, nanostructured system exhibiting localized surface plasmon resonances (LSPR) may possess two major advantages with respect to continuous structures: the strong localization of the electromagnetic field associated to these resonances around the nanostructures (i) leads to a noticeable enhancement in the MO properties [4], and (ii) could be exploited to make such a system become a promising candidate for the development of high spatial specificity magneto-plasmonic sensing devices.

Complex onion-like nanoparticles made of noble metals and ferromagnets that exhibit LSPR have been obtained using different chemical methods [5], however no MO activity has today been reported. We will show that such active nanostructures exhibiting optical and MO properties can actually be obtained [4] using lithographic techniques. The system consists of Au/Co/Au nanodisks obtained from continuous Au/Co/Au films by colloidal lithography (see figure 1). This nanostructuring gives rise to strong changes in the optical absorption properties of the system. The absorption spectra of these disks present a characteristic peak around 2 eV. The peak is due to the excitation of the LSPR of the Au/Co/Au nanodisks and its energy position can be controlled by the nanodisk shape. This excitation affects the MO response of the system, leading to a net enhancement of the signal. This can be clearly seen in figure 2, where the total MO activity (defined as the modulus of the complex Kerr rotation) of the d=110nm nanodisks normalized to that of the continuous layers is depicted. The peak observed corresponds to that observed in the absorption spectra, illustrating the effect of the LSPR on the enhancement of the MO response.

### References:

- [1] J.B. Gonzalez-Diaz et al., Adv. Mat.. **76**, (2007) 153402
- [2] J.B. Gonzalez-Diaz et al., Phys. Rev. B. **76**, (2007) 153402.
- [3] B. Sepúlveda et al. Oppt Lett.**31**, (2006) 1085.
- [4] J.B. Gonzalez-Diaz et al., Small **4**, (2008) 202
- [5] N. S. Sobal et al. Nano Letters **2**, (2002) 621;  
 Z.Ban et al J. Mater. Chem **15**, (2005) 4660;  
 J. Zhang et al. J. Phys. Chem B **110**, (2006) 7122;  
 S. Mandal et al J. Mater. Chem **17** , (2007) 372.

### Figures:

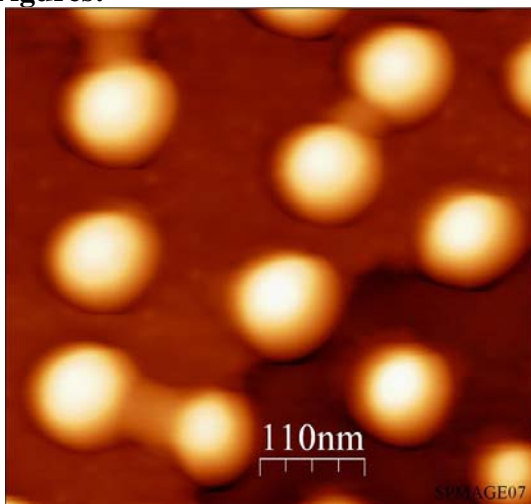


**Figure 1.** AFM image of the Au/Co/Au nanodisks fabricated by a colloidal lithography process.

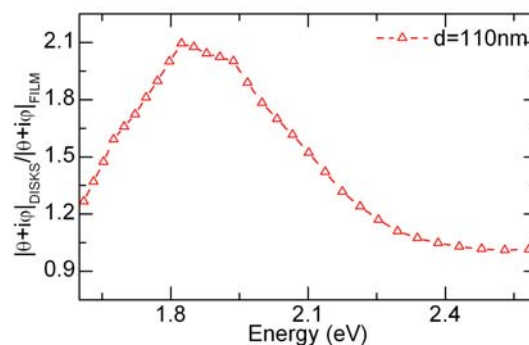


**Figure 2.** Total magneto-optical activity spectra for the 110nm diameter normalized to that of the continuous trilayer. An enhancement can be found at the same energy region of the plasmon resonance.

## FORMATION OF STABLE PENTAGONAL NANOWIRES UNDER STRETCHING ON FCC METALS

*P. García-Mochales*<sup>1,\*</sup>, *R. Paredes*<sup>2,3</sup>, *C. Guerrero*<sup>4</sup>, *S. Pelaez*<sup>3</sup>, *P.A. Serena*<sup>3</sup>

<sup>1</sup> *Dept. Física de la Materia Condensada, Facultad de Ciencias, Universidad Autónoma de Madrid, c/ Tomas y Valiente 7, Cantoblanco, E-28049-Madrid, Spain*

<sup>2</sup> *Centro de Física, Instituto Venezolano de Investigaciones Científicas, Apto. 20632, Caracas 1020A, Venezuela*

<sup>3</sup> *Instituto de Ciencia de Materiales de Madrid, Consejo Superior de Investigaciones Científicas, c/ Sor Juana Inés de la Cruz 3, Cantoblanco, E-28049-Madrid, Spain*

<sup>4</sup> *Departamento de Física, Facultad Experimental de Ciencias, La Universidad del Zulia, Maracaibo, Venezuela*

\* *pedro.garciamochales@uam.es*

Different works during the last decade have showed the formation of staggered pentagonal configurations on breaking nanowires [1-5]. These pentagonal nanowires are formed by subsequent staggered parallel pentagonal rings (with a relative rotation of  $\pi/5$ ) connected with single atoms (Fig. 1). The atomic sequence -1-5-1-5- presents a fivefold symmetry with respect the nanowire axis. This symmetry does not correspond to any crystallographic FCC nor BCC structures. The -1-5-1-5- staggered nanowire configuration may be understood in terms of a sequence of interpenetrated icosahedra. This icosahedral symmetry is very common in very small systems [6].

The formation of staggered pentagonal configurations during the stretching process has been already reported for Cu [1] and Au [2] nanowires using different Molecular Dynamic (MD) approaches. In particular the high stability of the Cu nanowire was confirmed with ab-initio calculations [3]. Pentagonal motives also appear in infinite Al and Pb nanowires obtained from MD simulated annealing methods [4]. More recently such structures have been reported for stretched Ni nanowires with different crystallographic orientations [5]. These pentagonal structures are very stable, with lengths larger of 10 Å and presenting a high plastic deformation under strain.

The aim of the present work is to carry out a statistical study of the structural evolution of FCC nanowires under stretching for a broad range of temperatures and three crystallographic stretching directions. We have carried out hundreds of MD simulations of aluminium, copper and nickel nanowires breaking processes, within the EAM approximation, following the procedure used in previous works [5, 7]. This study will confirm the existence of pentagonal nanowires, and, more important, will present the optimal set of parameters (temperature, size, crystallographic orientation) required for maximizing their occurrence probability.

The formation of pentagonal nanowires is a very anisotropic process. In fact, long pentagonal structures are relatively common for [100] and [110] stretching directions, whereas rarely occur for the [111] case. These preferred configurations have a minimum cross-section of  $S_m \sim 5$  and are unveil in computational minimum cross-section histograms  $H(S_m)$  as a very large peak at  $S_m=5$  (Fig. 2). The configurations that contribute to this peak are mainly staggered pentagonal nanowires. This type of arrangement is not seen at 4K because a larger temperature is required to explore and overcome those energy barriers leading to configurations able to develop these pentagonal chains. The probability of apparition of these structures and its stability it is reflected on the distribution function of time spent into the interval  $4.5 < S_m < 5.5$  (Fig. 3): the long tail of the distribution corresponds to very long stable pentagonal nanowires. Depending on the material, the  $S_m=5$  peak in  $H(S_m)$  increases with temperature up to certain value ( $\sim T_{\text{melting}}/3$ ), at the same time the tail of the pentagonal nanowire length distribution enlarges. At further temperatures there is a decreasing behaviour of both due to melting processes.

The present statistical study shows a protocol helpful to form these long pentagonal nanowires for different materials.

### References:

- [1] H. Mehrez and S. Ciraci, Phys. Rev. B **56**, 12622 (1997); J. C. González, V. Rodrigues, J. Bettini, L. G. C. Rego, A. R. Rocha, P. Z. Coura, S. O. Dantas, F. Sato, and D. S. Galvao, and D. Ugarte, Phys. Rev. Lett. **92**, 126102 (2004).
- [2] H. S. Park and J. A. Zimmerman, Scripta Materialia **54**, 1127 (2006).
- [3] O. Gülseren, F. Ercolessi and E. Tosatti, Phys. Rev. Lett. **80**, 2775 (1998).
- [4] P. Sen, O. Gülseren, T. Yildirim, I.P. Batra, and S. Ciraci, Phys. Rev. B **65**, 235433 (2002).
- [5] P. García-Mochales, R.Paredes, S. Peláez and P.A. Serena, Physica, Stat. Sol. (a) (accepted, 2008); P. García-Mochales, R.Paredes, S. Peláez and P.A. Serena, arXiv:0710.0645 [cond-mat.mes-hall].
- [6] N.A. Bulienkov and D.L. Tytik, Russ. Chem. Bull. Int. Ed. **50**, 1 (2001).
- [7] A. Hasmy, E. Medina, and P. A. Serena, Phys. Rev. Lett. **86**, 5574 (2001); A. Hasmy, A. J. Pérez-Jimenez, J. J. Palacios, P. García-Mochales, J. L. Costa-Krämer, M. Díaz, E. Medina, and P. A. Serena, Phys. Rev. B **72**, 245405 (2005).

### Figures:

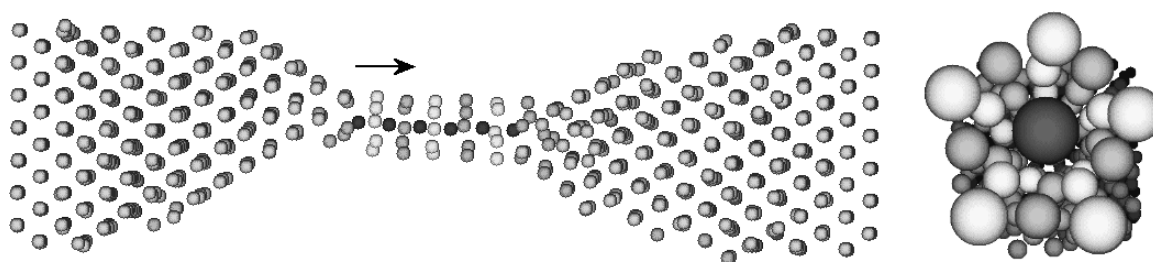


**Fig. 1:** Longitudinal (left) and cross-section (right) views of a Ni nanowire stretched along the [100] direction at 300K. The cross-section image shows a perspective view of the nanowire as seen from the position indicated on the longitudinal view. This image illustrates the appearance of staggered pentagonal structures -5-1-5-1-.

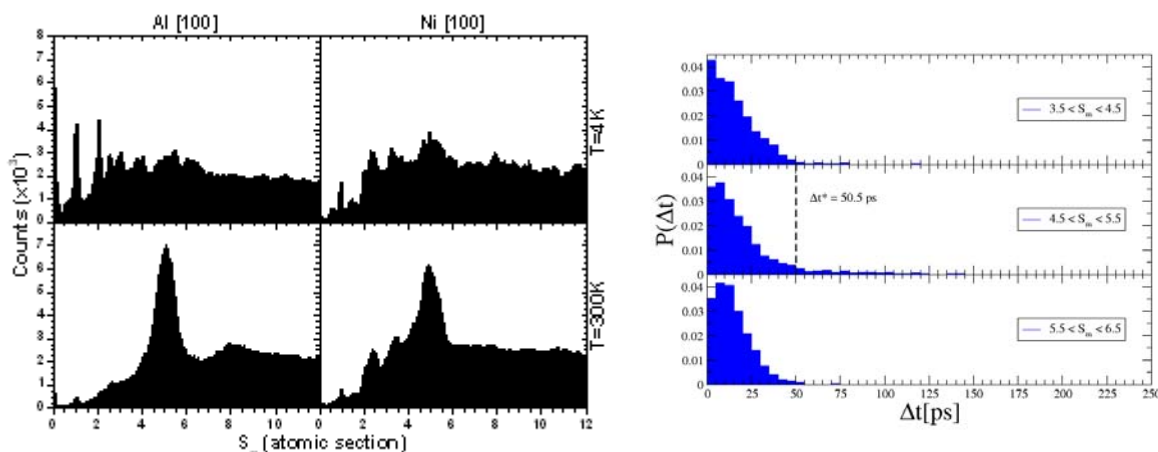


**Fig. 2:** Minimum cross section histograms  $H(S_m)$  of Aluminium and Nickel breaking nanowires stretched along [100] direction at  $T=4$  and 300K.

**Fig. 3:** Distribution function  $P(\Delta t)$  of the time spent by Ni nanowires stretched at 300K along the [110] direction within the minimum cross section interval showed in the figure.

## SYNTHESIS AND STUDIES OF COORDINATION POLYMER NANOPARTICLES.

*Yannick Guari, Benjamin Folch, Elena Chelebaeva, Joulia Larionova and Christian Guérin  
Institut Charles Gerhardt, Chimie Moléculaire et Organisation du Solide, Université  
Montpellier 2, Place Eugène Bataillon, F-34095, Montpellier, France  
[yannick.guari@univ-montp2.fr](mailto:yannick.guari@univ-montp2.fr)*

Cyano-bridged soluble coordination polymer nanoparticles were synthesized considering different approaches :

- Stable colloid solutions containing nanoparticles of cyano-bridged molecule-based magnets  $M_3[Fe(CN)_6]_2/[RMIM][BF_4]$  ( $M^{2+} = Ni, Cu, Co$ ) and  $Fe_4[Fe(CN)_6]_3/[RMIM][BF_4]$  (R = 1-butyl, BMIM and 1-decyl, DMIM) were prepared in the corresponding 1-R-3-methylimidazolium salts  $[RMIM]X$  (where X =  $BF_4, Cl, \dots$ ) which acts as both a stabilizing agent and a solvent. By varying the length of the N-alkyl chain on the imidazolium cation of  $[RMIM]^+$  and the temperature, the growing process can be controlled to produce nanoparticles of different size.[1]
- The use of silica matrixes with different pore sizes allow to afford nanocomposites incorporating nanoparticles with variable and controlled sizes.[2]
- Water-soluble coordination polymer nanoparticles core/chitosan shell were synthesized by using chitosan beads as matrixes.[3]
- The organic-phase soluble coordination polymer nanoparticles were obtained by using different stabilizing ligands such as oleic acid, oleyl amine, etc.[4]

Depending on the surrounding media, these coordination polymer nanoparticles exhibits diverse magnetic regime from superparamagnetic behaviour to spin-glass like dynamic that can be caused by a spin frustration on the surface of the nanoparticles and/or by interparticle magnetostatic interactions of variable strength.

### References:

- [1] J. Larionova, Y. Guari, H. Sayegh, Ch. Guérin, *Inorg. Chim. Acta*, **360** (2007) 3829; G. Clavel, J. Larionova, Y. Guari, Ch. Guérin, *Chem. Eur. J.*, **12** (2006) 3798.
- [2] B. Folch, Y. Guari, J. Larionova, C. Luna, C. Sangregorio, C. Innocenti, A. Caneschi, Ch. Guérin, *New J. Chem.*, **32** (2008) 273; G. Clavel, Y. Guari, J. Larionova, Ch. Guérin, *New J. Chem.*, **29** (2005) 255.
- [3] Y. Guari, J. Larionova, K. Molvinger, B. Folch, Ch. Guérin, *Chem. Commun.*, (2006) 2613.
- [4] E. Chelebaeva, Y. Guari, J. Larionova, A. A. Trifonov, Ch. Guérin, *Chem. Mater.*, **20** (2008) 1367.



**A GLANCE AT THE FRENCH NETWORKS SUPPORTING NANOSCIENCE  
AND NANOTECHNOLOGY**

Magrit Hanbucken  
Direction Générale de la Recherche et de l'Innovation (DGRI)  
France

Abstract not available



## TOWARDS INSERTION OF A TRANSMEMBRANE PROTEIN INTO SUPPORTED PLANAR BILAYERS: PRELIMINARY STUDIES

*Jordi Hernández-Borrell*<sup>§,±</sup>, *Laura Picas*<sup>§</sup>, *M. Teresa Montero*<sup>§, ±</sup>,  
*Pierre-Emmanuel Milhiet*<sup>#</sup>

<sup>§</sup>Departament de Fisicoquímica, Facultat de Farmàcia, Universitat de Barcelona (UB), and  
<sup>±</sup>Institut de Nanociència i Nanotecnologia de la Universitat de Barcelona (IN2UB) Barcelona, 08028-Spain.

<sup>#</sup>Centre de Biochimie Structurale, UMR5048 CNRS, UMR554 INSERM, Université Montpellier I et II, 34090, Montpellier, France.

[jordihernandezborrell@ub.edu](mailto:jordihernandezborrell@ub.edu)

A real paradigm or model for the secondary transport mechanism in biomembranes is the lactose permease (LacY) of *Escherichia coli* [1], a well characterized transmembrane protein that catalyzes the coupled stoichiometric translocation of  $\beta$ -galactosides and  $H^+$  across the cytoplasmic membrane. Integral membrane proteins are surrounded by a layer of phospholipids known as annular lipids, which composition and physical properties play a role in the function of the protein [2]. In physical terms, the boundary region should provide the adequate thickness to embed the protein. Basically the length of the hydrophobic domains of the protein (12 spanning  $\alpha$  helices for LacY) should match the length of the lipid bilayer membrane [3]. In regard to the interplay with membrane phospholipid it has been demonstrated that the protein is dependent on phosphatidylethanolamine (PE) presence for *in vivo* function and also for its correct folding [4,5]. Indeed, LacY has been reconstituted in a functional state only in phospholipid matrices with high levels of PE, either in the native *E. coli* polar phospholipid membrane extracts or in binary mixtures of phosphatidylglycerol (PG) and PE.

The aims of this work are two fold: (i) to investigate if there is preferential selectivity of LacY for PE and PG; and (ii) to reconstitute LacY into planar bilayers formed with PE and PG in order to visualize the annular region of the protein.

FRET experiments between a Lac Y single tryptophan mutant (w151/C154G) [6] and pyrene phospholipid derivatives were carried out to obtain information on the annular lipid composition of LacY from *E. coli*. We investigate, qualitatively, the presence of either PG or PE within the shell of adjacent boundary lipids. Thus, two pyrene derivatives were used as acceptors: 1-hexadecanoyl-2-(1-pyrenedecanoyl)-*sn*-Glycero-3-phosphoglycerol (PPDPG) and 1-hexadecanoyl-2-(1-pyrenedecanoyl)-*sn*-Glycero-3-phosphoethanolamine (PPDPE). The W151 mutant reconstituted in proteoliposomes of POPE:POPG (3:1, mol:mol) was used as the donor.

In Figure 1 the variation of the energy transfer efficiency ( $ET=1-I/I_0$ ) versus temperature, for PPDPE (solid line) and PPDPG (dotted line) (left), and the model for the process between the single tryptophan protein and the pyrene derivatives (right) are shown. PPDPE shows higher values of  $ET$  than PPDPG in all range of temperatures studied. On the other hand, the efficiency for PPDPG increases progressively as the temperature increases. These results indicate, firstly, an enrichment in PE at the vicinity of the protein, and secondly, a higher lateral mobility of PG. Assuming a single pair, the distance between the donor and the acceptor can be estimated according:  $ET = R_0^6 / R_0^6 + r^6$ . The  $r$  values for PPDPE and PPDPG were 2.6 and 2.9 nm respectively, suggesting that the first shell of the annular region may be mainly formed by PE.

Incorporation attempts of LacY into supported planar bilayers (SPBs) were performed by incubation of purified LacY in dodecylmaltoside (DDM) detergent with planar bilayers of POPE:POPG (3:1, mol:mol) previously formed and extracting the excess of detergent [7].

The effect of the detergent and  $\text{Ca}^{2+}$  presence on the stability of the SPBs was studied through AFM *in situ* observations. Figure 2 shows the effect on the bilayer of a DDM solution at the CMC in absence (2A) and presence (2B) of LacY (20 mg/ml) after 15 minutes of incubation at room temperature. Some bright spots can be seen in the SPB in presence of protein (Fig 2B). Single entities were not observed suggesting that Lac Y may be aggregated in some extension (inset in image 2B). Work is underway to unveil the annular region.

## References:

- [1] Abramson, J.; Iwata, S.; Kaback, H. (2004) *Mol. Memb. Biol.*, 21, 227-236.
- [2] Marsh, D.; Horvarth, L. I. (1998) *Biochim. Biophys. Acta*, 1376, 267-296.
- [3] Mouritsen, O. G.; Bloom, M. (1984) *Biophys. J.*, 46, 141-153.
- [4] Bogadnov, M. and Dowhan, W. (1998) *EMBO J.*, 17, 5255-5264.
- [5] Bogadnov, M.; Dowhan, W.; (1995) *J. Biol. Chem.*, 270, 732-739.
- [6] Vázquez-Ibar J. L., Guan L., Svrakic M.; Kaback H. R. (2003) *Proc. Natl. Acad. Sci. USA*, 22, 12706-11.
- [7] Milhiet, P.E.; Gubellini, F.; Berquand, A.; Dosset, P.; Rigaud, J.L.; Le Grimellec, C.; Lévy, D. (2006) *Biophys J* 91, 3268-3275.

**Figure 1**

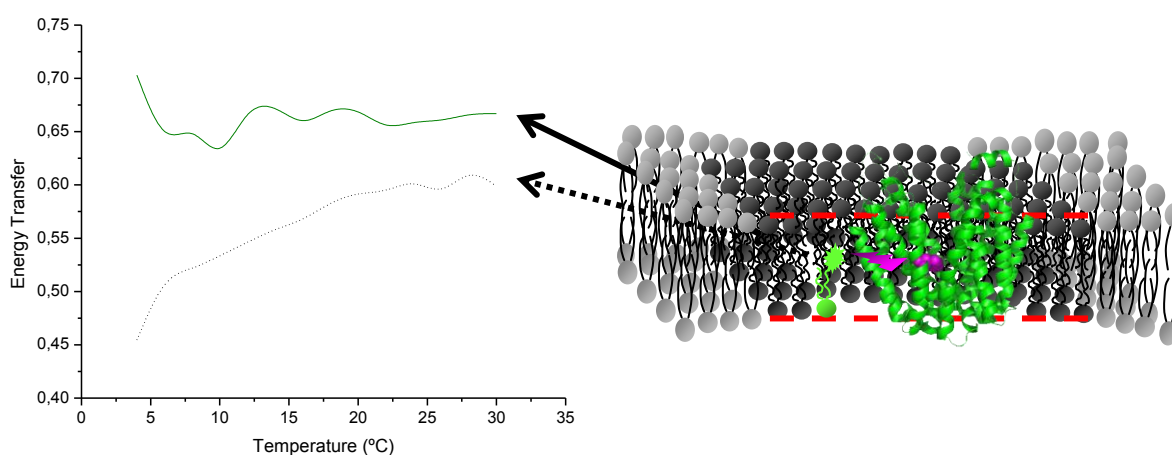
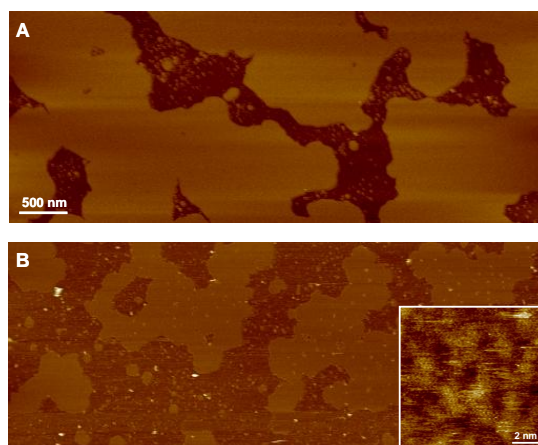


**Figure 2**



## ATOMIC FORCE MICROSCOPY AND RAMAN ANALYSIS OF EXFOLIATED GRAPHENE ON SiC

*Jean-Roch Huntzinger, Antoine Tiberj and Jean Camassel*

*GES – UMR 5650 Université Montpellier 2/CNRS, 34095 Montpellier cedex 5, France*

*Philippe Poncharal, Thierry Michel, Ahmed Zahab, and Jean-Louis Sauvajol*

*LCVN – UMR 5587 Université Montpellier 2/CNRS, 34095 Montpellier cedex 5, France*

*Nicolas Camara and Philippe Godignon*

*CNM-IMB-CSIC – Campus UAB 08193 Bellaterra, Barcelona, Spain*

[jean-roch.huntzinger@univ-montp2.fr](mailto:jean-roch.huntzinger@univ-montp2.fr)

Graphene is the single two-dimensional layer, building block of graphite. Since the recent discovery that it was possible to address a single graphene layer, its unusual electronic properties have driven an intense research activity. Epitaxial graphene layers (EGLs) grown on SiC are considered, in order to develop graphene-based electronics. Two of the biggest issues concerning this epitaxial graphene growth remain the role of the intermediate buffer layer and the control of the thickness and uniformity of layers. Towards this end, setting a rapid and non destructive investigation method to identify the existing number of graphene layers is mandatory. Since the early work of Ferrari and co-workers[1], Raman spectroscopy has become a popular characterization tool. However, up to now, there are few reports of AFM or Raman from FLGs epitaxially grown on SiC.[2-4] One could wonder whether the buffer layer in epitaxial graphene influences the Raman spectrum and the EGL devices behavior. Comparing EGLs with the intermediate system consisting in exfoliated FLGs on SiC will certainly give some clues about these questions. This communication provides a step in this direction, discussing several issues that had to be solved first.

Contrary to the case of FLGs exfoliated on oxydized silicon, anti-reflection coating that allows rapid detection of FLGs from their color under an optical microscope, there is no interference contrast on bare SiC. Nevertheless, we were able to locate several FLGs exfoliated on SiC and to show that Atomic Force Microscopy (AFM) and Raman scattering were still useful techniques to characterize FLGs on SiC.

The AFM phase image contrast is high enough to discriminate graphene covered areas from bare SiC. Then the number of graphene layers is evaluated from the measured AFM height. A single layer appears at the same level as the SiC substrate, which we attribute to different tip-graphene and tip-SiC interactions.

Then the same FLGs, ranging from 4 to 11 layers, were investigated by Raman spectroscopy. We show that through the use of a confocal setup, it is possible to reject enough substrate signal to extract the entire Raman signature (D, G and 2D bands) of the FLGs. The observed 2D bands are symmetrical, as those shown in ref [4] for epitaxial graphene. This shows that the buffer layer, present in their samples and not in ours, is not the origin of this 2D band shape. We agree with them that the most plausible explanation is that the graphene layers are not stacked in AB sequence as in highly oriented graphite. We discuss this in light of the Raman spectra of exfoliated graphene on oxydized silicon found in the recent litterature.

**References:**

- [1] A. C. Ferrari, J. C. Meyer, V. Scardaci, C. Casiraghi, M. Lazzeri, F. Mauri, S. Piscanec, D. Jiang, K. S. Novoselov, S. Roth, and A. K. Geim, *Phys. Rev. Lett.* **97** (2006) 187401.
- [2] C. Berger, Z. Song, X. Li, X. Wu, N. Brown, D. Maud, C. Naud, and W. A. de Heer, *physica status solidi (a)* **204** (2007) 1746.
- [3] G. Gu, S. Nie, R. M. Feenstra, R. P. Devaty, W. J. Choyke, W. K. Chan, and M. G. Kane, *Applied Physics Letters* **90** (2007) 253507.
- [4] C. Faugeras, A. Nerrière, M. Potemski, A. Mahmood, E. Dujardin, C. Berger, and W. A. de Heer, arXiv:0709.2538v4 [cond-mat.mes-hall] (2007).

## FUNCTIONAL METAL-ORGANIC NANOPARTICLES

**Inhar Imaz,<sup>a</sup> Daniel Ruiz-Molina,<sup>b</sup> Jordi Hernando,<sup>c</sup> Clara Rodriguez-Blanco,<sup>d</sup> Chiara Carbonera,<sup>d</sup> Javier Campo,<sup>d</sup> Fernando Luis,<sup>d</sup> Daniel Maspoch,<sup>a</sup>**

<sup>a</sup>*Institut Català de Nanotecnologia Campus UAB, 08193, Bellaterra, Spain*

<sup>b</sup>*Centro de Investigación en Nanociencia y Nanotecnología, Campus UAB, 08193, Bellaterra, Spain*

<sup>c</sup>*Departament de Química Inorgànica, Campus UAB, 08193, Bellaterra, Spain*

<sup>d</sup>*Instituto de Ciencia de Materiales de Aragón CSIC-Universidad de Zaragoza, 50009 Zaragoza, Spain.*

*e-mail: [inhar.imaz.icn@uab.es](mailto:inhar.imaz.icn@uab.es)*

Functional micro- and nanoparticles are of increasing interest in a variety of scientific fields such as storage, photonics, electronics, cell biology, biotechnology, diagnostics, nanoanalytics, and pharmaceuticals. Therefore, widespread attention has been recently paid to new strategies for fabricating particles with novel compositions and properties. Metal-organic solids are hybrid materials created by the association of metal ions and organic ligands, which have already shown a wide range of promising properties in gas sorption, sensing, catalysis, ion exchange, magnetism, optics, etc. Because of the vast range of properties, one of the actual challenges is the miniaturization of these systems to design and fabricate novel metal-organic particles nanoparticles (MONPs). To date, two possible routes to fabricating MONPs have been explored. One involves the use of microemulsion techniques, which have already enabled the synthesis of Prussian blue- and triazol-based magnetic nanoparticles, and Gd(III) nanorods that can be used as multimodal contrast enhancing agents.[1] The second is based on precipitation processes, such as antisolvent technology with supercritical fluids.[2] Based on this principle, a method consisting on both coordination polymerization and precipitation in a poor solvent has recently allowed the synthesis of colloidal amorphous particles from infinite coordination polymers that show interesting optical properties and ion-exchange capabilities.[3,4] The presented work has been inspired by the latter route, and shows that a simple precipitation process can lead to functional nanoparticles from magnetic metal-organic clusters.

In a first step, we have demonstrated how through pre-synthesized magnetic building blocks and by a simple precipitation process, magnetic metal-organic nanoparticles can be fabricated. This process consist on a direct precipitation of  $Mn_{12}O_{12}$  clusters in a mixture of acetonitrile and toluene that lead to the first example of sub-50 nm spherical  $Mn_{12}$ -based particles.[5] The integrity of these clusters is not affected in the fabrication process, and the single molecule magnet behaviour, which is typical for these well-known clusters, is maintained. Moreover, the small size as well as the amorphous character of these particles allows to obtain very important information to correlate the environment of  $Mn_{12}$  clusters (i.e. crystalline, nanostructured or amorphous character) with their magnetic properties.[6]

This approach has also been extended to other magnetic systems. The association of an electroactive building block, such as  $[Co^{III}(3,5-DBSQ)(3,5-DBCat)]$ , with the adequate bridging ligand creates the first example of nanoparticles that exhibit valence tautomeric properties.[7] As shown in Figure 1, these particles interconvert reversibly between two different magnetic states induced by a temperature modification: from the low-spin ls- $[Co^{III}(3,5-DBSQ)(3,5-DBCat)]$  to the high-spin hs- $[Co^{II}(3,5-DBSQ)_2]$  through a reversible intramolecular transfer involving the metal ion and the redox-active ligand.

In addition to the intrinsic properties of the particles, the interest of these MNOPs comes from their high capacity to encapsulate external bodies, i. e. molecules, nanoparticles, and consequently, to introduce a novel property. A detailed study of the encapsulation of fluorescent molecules and magnetic inorganic particles will be presented.

## References:

- [1] S. Vaucher, M. Li, S. Mann, *Angew. Chem. Int. Ed.*, **39**, (2000) 1793; D. Brnzei, L. Catala, C.Mathonière, W. Wernsdorfer, A.Gloter, O. Stephan, T. Mallah, *J. Am. Chem. Soc.*, **129** (2007) 3778; Guari, Y.; Larionova, J. *Chem. Commun.*, (2006) 2613; E. Coronado, J. R.Galán-Mascarós, M. Monrabal-Capilla, J. García-Martínez, P. Pardo-Ibáñez, *Adv. Mater.* **19** (2007) 1359.
- [2] Johnson, C. A.; Sharma, S.; Subramaniam, B.; Borovik, A. S. *J. Am. Chem. Soc.* 2005, **127**, 9698; M. Muntó, J. Gómez-Segura, J. Campo, M. Nakano, N. Ventosa, D. Ruiz-Molina, J. Veciana, *J. Mater. Chem.*, **16** (2006) 2612.
- [3] M. Oh, C. A. Mirkin, *Nature* **438** (2005) 651.
- [4] M. Oh, C. A. Mirkin, *Angew. Chem. Int. Ed.*, **45** (2006) 5492.
- [5] I. Imaz, F. Luis, C. Carbonera, D. Ruiz-Molina, D. Maspoch, *Chem. Commun.*, (2008) in press, DOI: 10.1039/b716071b.
- [6] C. Carbonera, I. Imaz, D. Maspoch, D. Ruiz-Molina, F. Luis, *Inorg. Chim. Acta*, Submitted.
- [7] I. Imaz, D. Maspoch, C. Rodríguez-Blanco, J.-M. Pérez-Falcón, J. Campo, D. Ruiz-Molina, *Angew. Chem. Int. Ed.*, **47** (2008) 1857.

## Figures:

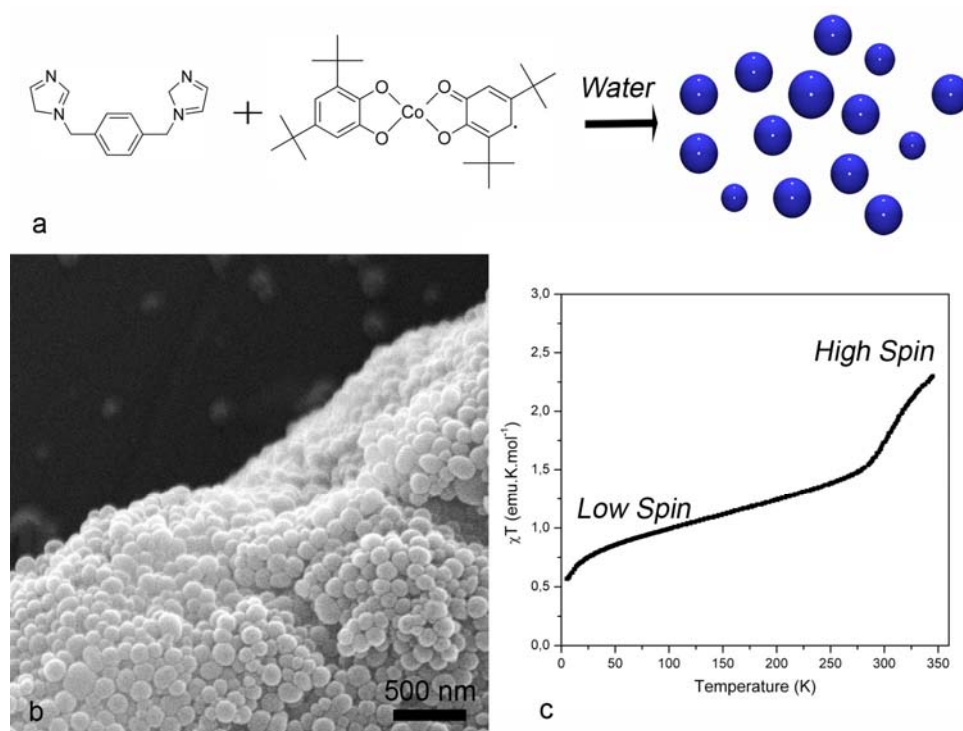


**Figure 1:** (a) Schematic illustration describing the coordination polymerization procedure followed to obtain valence tautomeric NMOPs. (b) SEM image of nanoparticles created by infinite coordination polymerization of  $[\text{Co}^{\text{III}}(3,5\text{-DBSQ})(3,5\text{-DBCat})]$  through Bix ligands. (c)  $\chi T$  values as a function of the temperature for the amorphous  $[\text{Co}^{\text{III}}(\text{Bix})(3,5\text{-DBSQ})(3,5\text{-DBCat})]$  metal-organic nanospheres

## EXPERIMENTAL EVIDENCE OF THE EXISTENCE IN SOLUTION OF ORGANIZATIONS OF ZNO NANOPARTICLES SYNTHESIZED BY ORGANOMETALLIC METHOD USING DYNAMIC LIGHT SCATTERING

Myrtil L Kahn, Carole Pagès, André Maisonnat, and Bruno Chaudret

Laboratoire de Chimie de Coordination, UPR8241 CNRS, 205 route de Narbonne, 31077 Toulouse Cedex, France.

Corresponding author: Myrtil L Kahn, Fax 0033561333179, email: myrtil.kahn@lcc-toulouse.fr

Zinc oxide is a material of particular interest because it possesses unique optical and electronic properties. It is a wide-band-gap semiconductor (3.37 eV) that is also luminescent and emerged as a good candidate for many applications. As a result ZnO stimulates research in a wide range of domains. For example, thin films of ZnO were reported to display good conductivity and high transparency in the visible region and have been envisaged as transparent electrodes for solar cells<sup>[1a]</sup> as well as gas sensors,<sup>[1b]</sup> and recently, ultraviolet lasing effect has been observed at room temperature using ZnO nanowires.<sup>[1c]</sup> These fascinating examples are based on the control of both the physical and chemical properties of the nanoparticles. Besides, it is well known that these properties depend on the synthetic method used and as a consequence, applications of nanomaterials are directly linked to the successful control of the synthetic process.

We recently developed a novel organometallic synthetic method for the preparation of crystalline ZnO nanoparticles of controlled size and shape.<sup>[2]</sup> Tendency of the nanoobjects to self-organize onto the T.E.M. grid is observed.

This contribution concerns the field of the fundamental understanding of the self-assembly of nanoparticles to form superlattices in solution. We demonstrate the existence of superlattices of nanoparticles in solution and that this formation is indeed a thermodynamic process. We also pointed out the important role of weak interactions (Van der Waals, dipolar and hydrogen bonding) for the stabilization of the superlattices.

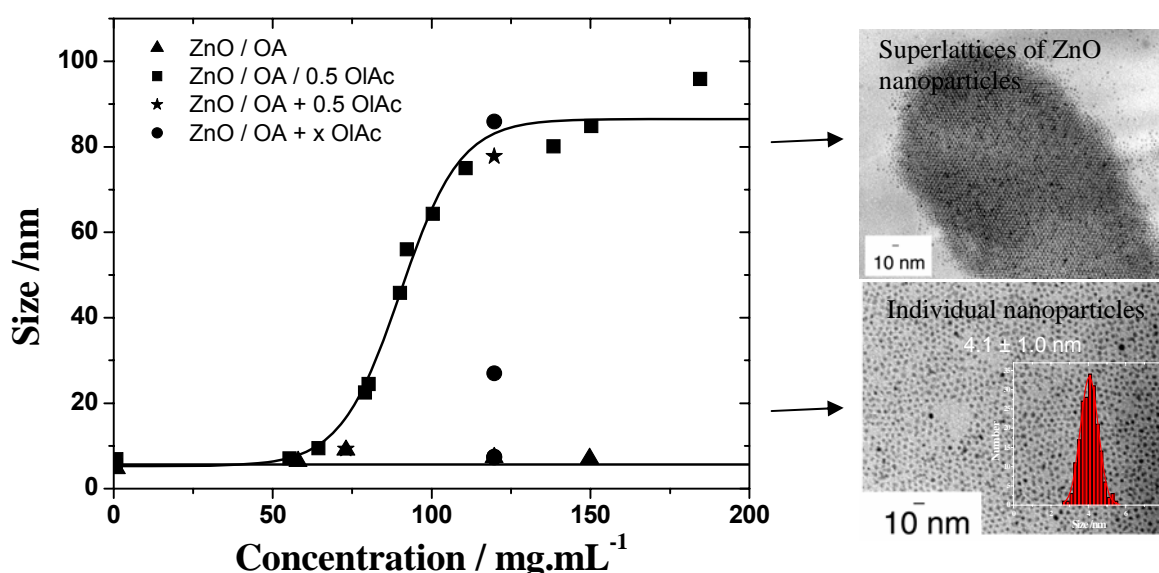


Figure 1: Variation of the size of the diffusive objects as a function of the concentration of the colloidal ZnO solutions. ▲: Colloidal solution of OA-stabilized ZnO nanoparticles; ■: Colloidal solution of OA/OIAc-stabilized ZnO nanoparticles; ●: Colloidal solution of OA-stabilized ZnO nanoparticles with a step by step addition of OIAc; ★: Colloidal solution of OA-stabilized ZnO nanoparticles with 0.5 eq of OIAc for two different concentrations.

**References:**

- [1] a- K. Westermark, H. Rensmo, H. Siegbahn, K. Keis, A. Hagfeldt, L. Ojamae, P. Persson, J. Phys. Chem. B 2002, 106, 10108; b- J. A. Rodriguez, T. Jirsak, J. Dvorak, S. Sambasivan, D. Fischer, J. Phys. Chem. B 2000, 104, 319; c- Mao, H. Feick, H. Yan, Y. Wu, H. Kind, E. Weber, R. Russo, P. Yang, Science 2001, 292, 1897.
- [2] a- M. Monge, M. L. Kahn, A. Maisonnat, B. Chaudret, Angew. Chem. Int. Ed., 2003, 42(43), 5321. b M. L. Kahn; M. Monge; A. Maisonnat; B. Chaudret, French Patent CNRS, Fr 03-042825, 2003, PCT procedure under progress; c- M. L. Kahn, M. Monge, V. Collière, F. Senocq, A. Maisonnat, B. Chaudret, *Advanced Functional Materials* 2005, 15, 458

## NANOSCALE CHARACTERIZATION OF FERROELECTRIC MATERIALS VIA PIEZORESPONSE FORCE MICROSCOPY

*A. L. Kholkin, I. K. Bdikin, D. K. Kiselev, Jingsong Liu, M. Machado, V. S. Bystrov, I. Delgado*

*Department of Ceramics and Glass Engineering & CICECO, University of Aveiro,  
3810-193 Aveiro, Portugal  
kholkin@ua.pt*

Coupling between electrical and mechanical phenomena is very often in nature. Apparently, it underpins the functionality of materials and systems as diversified as ferroelectrics and multiferroics to electroactive molecules to biological materials. In ferroelectrics, electromechanical behavior is directly linked to polarization order parameter and hence can be used to study phenomena ranging from polarization reversal mechanisms, domain wall pinning, cross-coupled phenomena in multiferroics, to direct imaging of electron-lattice coupling. It may be said that electromechanical coupling is also a key component of many electrochemical transformations, in which changes in oxidation state are associated with the variation in molecular shape and bond geometry. Electromechanical energy conversion is an integral part of processes such as triboelectricity, cavitation, and sonoluminescence. It will not be an exaggeration to say that electromechanics, along with mechanics and transport, is one of the fundamental phenomena in nature. Therefore, it forms a basis for numerous device applications, and is thus directly relevant to virtually all existing and emerging aspects of materials and nanoscience.

Recent years showed significant growth of interest towards nanoscale electromechanical phenomena originating independently in ferroelectric MEMS, biological, nano- and material science, and organic chemistry communities. The interest is stimulated both by development of nanoscience and necessity for efficient electromechanical motion and transformation at the nanoscale, and also recent emergence of scanning probe microscopy techniques capable of addressing electromechanical phenomena at a local level. As a relevant comparison, nanoscale properties are often accessible as a result of evolutionary development from macroscopic probes (e.g. interferometry or Berlincourt meter) to nanoscale, and corresponding macroscopic properties have been studied systematically since the dawn of industrial revolution. Electromechanical properties described by antisymmetric tensors averaged out in macroscopic systems and corresponding coupling coefficients are typically small ( $\sim 100$  pm/V), necessitating precise measurement tools even for macroscopic samples. These two factors resulted in limited quantitative and reproducible macroscopic studies of electromechanics even in single crystals and ceramics, recognized as important for applications (piezotransducers, SAW, sonar, ultrasonic imaging devices). Nanoscale offers a set of novel electromechanical phenomena induced by symmetry breaking at low dimensionality and by unique combination of high electric field and charge in nanovolumes that can lead to anomalous polarization reversal [1].

Ferroelectric materials are being intensively investigated due to their outstanding characteristics useful for various microelectronic devices ranging from nonvolatile ferroelectric random access (FeRAMs) memories to microelectromechanical systems (MEMS). For these applications, the nanoscale properties of ferroelectrics are of crucial importance. Since the feature size of potential devices is currently approaching to the submicron dimensions, local characterization techniques are becoming indispensable to meet the requirements of microelectronic industry. Local properties are expected to deviate from macroscopic ones due to confinement effects, lack of sufficient nucleation, and surface phenomena [2]. Piezoresponse Force Microscopy (PFM) has recently proved its usefulness for high-resolution domain imaging and local electromechanical characterization of ferroelectric materials [3].

In this presentation, the overview of the state-of-art in local ferroelectric characterization via PFM in several piezoelectric important materials (PZT, SBT, PZN-PT) will be given [4]. Local polarization switching and hysteresis [5], cross-sectional domain analysis [6] and polarization patterning [7] will be, in particular, addressed with special emphasis on the effect of PFM instrumentation on the measured properties. Based on these observations, the mechanism of local polarization reversal via PFM tip will be delineated. In the second part of the talk, the nanoscale properties of relaxor ferroelectrics will be shortly addressed. In these materials, the remanent polarization is absent at the macroscopic level due to strong disorder of ferroelectrically active ions. It will be shown that on the nanoscale the properties of relaxors are different due to symmetry breaking [8] and the material typically exhibit a clear piezoelectric contrast with the domain correlation length of the order of tens nm. Long-range order can be induced by applying small dc voltages to the tip [9]. The results confirm great potential of PFM for studying polar structures in ferroelectric and related materials.

### References:

- [1] A. L. Kholkin, I. K. Bdikin, V. V. Shvartsman, N. A. Pertsev, *Nanotechnology* **18** (2007) p. 095502.  
 [2] A. Gruverman and A. Kholkin, *Rep. Progr. Phys.* **69** (2006), pp.1-32.  
 [3] A. L. Kholkin, S. V. Kalinin, A. Roelofs and A. Gruverman in “*Scanning Probe Microscopy: Electrical and Electromechanical Phenomena at the Nanoscale*”, Eds. S. Kalinin, A. Gruverman, Springer (2007), V. 1, pp. 173-214.  
 [4] A. L. Kholkin, I. K. Bdikin, D. A. Kiselev, V. V. Shvartsman and S.-H. Kim, *J. of Electroceramics* **19** (2007), pp. 81-94.  
 [5] I. K. Bdilin, A. L. Kholkin, S. V. Kalinin and A. Morozovska, *Appl. Phys. Lett.* (submitted).  
 [6] J. S. Liu, H. Z. Zeng and A. L. Kholkin, *J. Phys. D: Appl. Phys.* **40** (2007), pp. 7053-7056.  
 [7] V. S. Bystrov, I. K. Bdikin, D. A. Kiselev, S. Yudin, V. M. Fridkin and A L Kholkin, *J. Phys. D.* **40** (2007), pp. 4571-4577.  
 [8] V. V. Shvartsman and A. L. Kholkin, *J. Appl. Phys.* **101** (2007), p. 064108.  
 [9] D. A. Kiselev, I. K. Bdikin, E. K. Selezneva, K. Bormanis, A. Sternberg and A. L. Kholkin, *J. Phys. D.* **40** (2007), pp. 7109-7112.

### Figures:

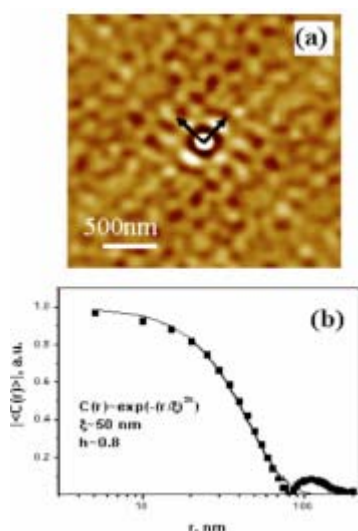


Fig. 1. Local ordering of nanodomains on the surface of disordered PLZT ceramics (a) and corresponding autocorrelation function (b).

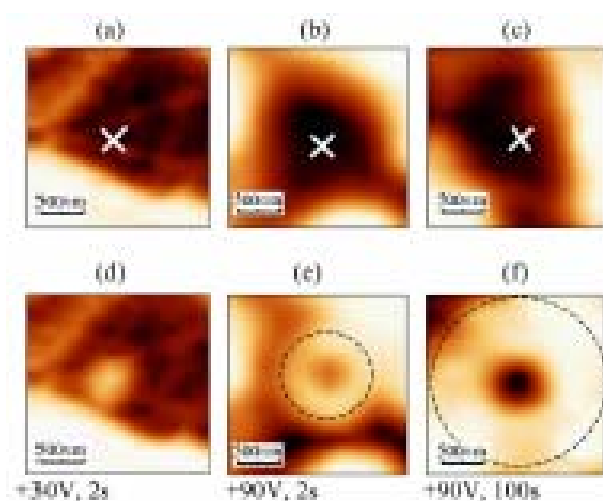


Fig. 2. Inverse polarization in PZN-PT [1]

## CONDUCTING NANOCOMPOSITE ORGANIC FILMS FOR PLASTIC PRESSURE SENSORS AND ELECTRONIC CIRCUITS

*E. Laukhina*,<sup>1,2</sup> *R. Pfattner*,<sup>2,1</sup> *M. Mas-Torrent*,<sup>2,1</sup> *V. Laukhin*,<sup>3,1</sup> *C. M. Creely*,<sup>4</sup> *D.V. Petrov*,<sup>3,4</sup>  
*C. Rovira*<sup>2,1</sup> and *J. Veciana*,<sup>2,1</sup>

<sup>1</sup>*CIBER-BBN, Barcelona, Spain*

<sup>2</sup>*Institut de Ciència de Materials de Barcelona (ICMAB-CSIC),  
 Campus UAB, 08193 Bellaterra, Spain*

<sup>3</sup>*Institució Catalana de Recerca i Estudis Avançats (ICREA), Barcelona, Spain*

<sup>4</sup>*ICFO-Institut de Ciències Fotòniques, Mediterranean Technology Park, Av. del Canal  
 Olímpic s/n 08860 Castelldefels (Barcelona), Spain  
 laukhina@icmab.es*

The processing characteristics of organic electronics make them potentially useful for electronic applications where low-cost, large area coverage and flexibility are required. In particular, there is an increasing interest in developing materials that respond to external stimulus such as pressure, temperature or gases. The conducting nanocomposite organic bilayer (BL) films offer excellent potential in plastic electronics since they combine the electrical properties of molecular organic conductors, which are sensitive to small pressure changes, with the transparency, processability and flexibility of polymers. BL films consist of a polymeric matrix with a topmost layer formed by a micro- or nanocrystalline network of a TTF-based conducting material (TTF=tetrathiafulvalene) [1] (Fig. 1).

In this work, we studied the effect of external strain on the electrical resistance of a BL film formed with the topmost layer of  $(\text{BET})_n\text{I}_x\text{Br}_{3-x}$  crystallites (BET=bis(ethylenethio)tetrathiafulvalene,  $n>2$ ,  $1\leq x\leq 3$ ). [2] The electrical resistance of the BL film demonstrates a high sensitivity to the deformation; in the single-axis deformation range 0-120  $\mu\text{m}$  the variation of resistance linearly depends on absolute strain (Fig. 2). For studied conducting nanocomposite BL films the tensosensitivity  $k = (R-R_0)/R_0\varepsilon$  ( $\varepsilon$  is relative strain,  $R_0$  is the BL film resistance without the strain,  $R$  is the resistance of the strained sample) varies in the range 5-6, which is much above the sensitivity of commonly used manganese-based sensors for which  $k$  is around 2 [3]. The tensosensitivity of BL films is governed by the type of crystallites, their orientation and the network of nano-scale contacts between them. These parameters can be controlled through the BL film preparation. The conducting nano- and microcrystalline layer of an organic molecular conductor is used as a high tensosensitive material to detect and transmit pressure data. The polymeric matrix serves as a support for the placement of the conducting layer over it. In addition, we have developed a novel technique, namely *thermochemical printing of organic conductors (TCPOC)*, for patterning the BL films. [4] The patterning is realized employing a local heat source –using a laser radiation source– since by local heating the film surface the conducting areas, formed by the TTF salts, can be converted into insulating areas, formed mainly by the neutral TTF derivatives. We further demonstrate here the potential of this novel technique for the design of electronic circuitry, components and devices (Fig. 3)

Considering their strain sensitivity, versatility and processability, the reported BL films are very promising in “*plastic electronic*” applications such as smart clothes, biomedicine or robotic interfaces.

### References:

[1] a) E. E. Laukhina, V. A. Merzhanov, S. I. Pesotskii, A. G. Khomenko, E. B. Yagubskii, J. Ulanski, M. Kryszewski, J. K. Jeszka, *Synth. Met.*, **70** (1995) 797. b) M. Mas-Torrent, E. Laukhina, C. Rovira, J. Veciana, V. Tkacheva, L. Zorina, S. Khasanov, *Adv. Funct. Mater.*,

**11**, 299 (2001). c) E. Laukhina, V. Tkacheva, S. Khasanov, L. Zorina, J. Gomez-Segura, A. Perez del Pino, J. Veciana, V. Laukhin, C. Rovira, *ChemPhysChem*, **7** (2006) 920.

[2] E. Laukhina, M. Mas-Torrent, J. Veciana, C. Rovira, V. Laukhin, Patent Appl., ES 200602887.

[3] Vishay, DMS Messtechnologie, Formel&Tabellen, Measurements Group Messtechnik, Munchen (1991).

[4] M. Mas-Torrent, E. E. Laukhina, V. Laukhin, C. M. Creely, D. V. Petrov, C. Rovira, J. Veciana, *J. Mater. Chem.*, **16** (2006) 543; Patent Application, ES 200501879.

### Figures:

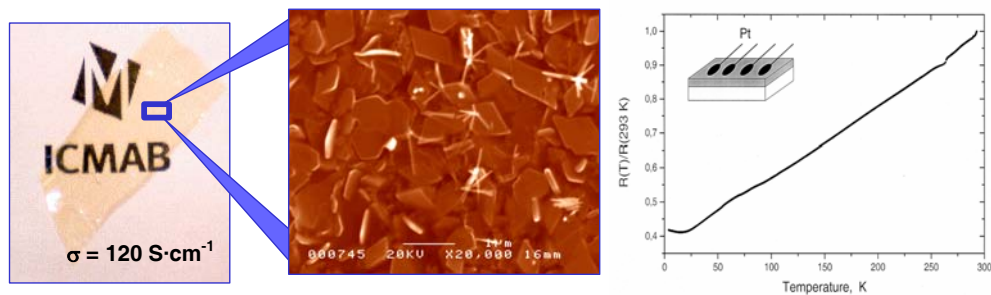


**Fig.1** View through a metal-like BL film with a surface layer of  $(\text{BETTTF})_2\text{Br}\cdot 3\text{H}_2\text{O}$  nanocrystals, SEM image of the surface layer showing the network of conducting nanocrystals, and normalized resistance of the conducting surface layer versus temperature.

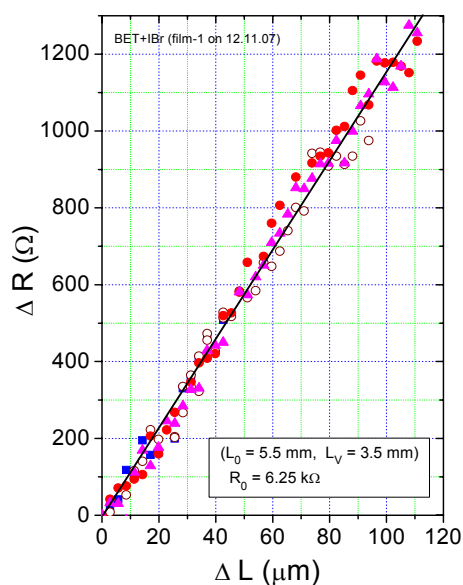


**Figure 2.** Absolute strain dependence of the resistance of the nanocomposite BL film sample at room temperature;  $\Delta R = R - R_0$ .

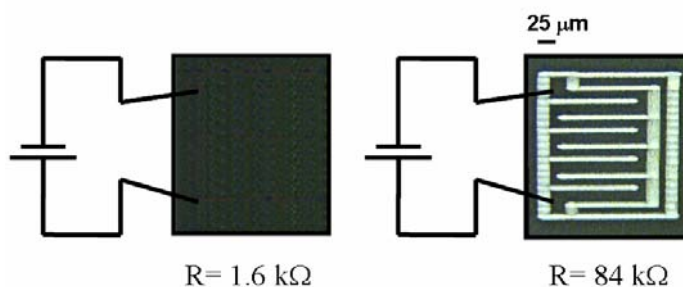


**Figure 3.** Electronic circuits in which the BL films of nanocrystals  $\beta\text{-(BET-TTF)}_{2.5}\text{I}_3$  without patterning (left) and after patterning (right) are used as micro-resistors. The light zones in the right figure correspond to the laser writing path and are insulating.

## ELECTRONIC DETECTION OF DNA HYBRIDIZATION

*MT Martínez<sup>a,e</sup>, Y. C. Tseng<sup>b</sup>, J. Bokor<sup>b</sup>, I. Loinaz<sup>c</sup>, R. Eritja<sup>d</sup>*

*<sup>a</sup>Instituto de Carboquímica, CSIC. Miguel Luesma,4 Zaragoza, Spain*

*<sup>b</sup>Electrical Engineering and Computer Science Department. Cory Hall, Berkeley CA 94720-1770 UC, California.*

*<sup>c</sup>CIDETEC P<sup>o</sup> Miramón, 196 Parque Tecn. Miramón.,20009 San Sebastián, Spain*

*<sup>d</sup>Instituto de Investigaciones Químicas y Ambientales CSIC. IIQAB-CSIC  
Jordi Girona, 18-26 , 08034-Barcelona, Spain*

*<sup>e</sup>Molecular Foundry, LBNL, One Cyclotron road, MS 67R3208-22 Berkeley, California, 94720, USA*

*mtmatinez@icb.csic.es*

The integration of biomaterials with carbon nanotubes, CNTs, has promoted an interdisciplinary field of CNT- based nanoelectronics and nanobiotechnology. The quick detection of anomalous genes responsible for a congenital disease is highly desired and the reading of the human genome has opened the possibility of early detection and diagnoses of congenital/terminal diseases. Electrical biosensors that use immobilized nucleic acids are especially promising in biosensing applications because of their potential for miniaturization and automation as well as their more simple instrumentation for on-site and point of care applications.

Here we present the label free detection of single strand DNA using a large array of CNTFET. The paper presents a methodology for avoiding no specific DNA adsorption on CNTs providing at the same time a stable binding for DNA

The DNA was covalently bonded to a polymer; poly(methylmethacrylate<sub>0.8</sub>-copolyethyleneglycolmethylmethacrylate<sub>0.1</sub>-cosuccinimidyl methacrylate) that was anchored covalently to the CNT. Using this approach and the statistically treatment of the electrical characterization data of a large array of devices, the DNA hybridization has been unequivocally detected. The changes of the electrical CNTFET characteristics upon interaction with several chemicals used for binding the DNA and upon DNA hybridization are reported.

In Figure 1, a AFM image of a SWNT joining the source and drain electrodes are shown. A schematic diagram of the reactions of the succinimidyl groups of the polymer with the amine groups of a single strand aminated DNA are presented in Figure 2. After bonding the DNA the remaining succinimidyl groups were blocked with ethanol amine before DNA hybridization.

In Figure 3 it can be seen the I/V plots corresponding to the electrical characterization before and after each of the steps. The DNA hybridization produces a shift of the I/V plot towards negative voltages and a decrease of the current for the p-type conductance what allows its electronic detection. Upon hybridization, the negatively charged backbone of target DNA is added to that of previously stacked probe. When ss DNA hybridizes with complementary DNA, three hydrogen bonding is generated for the pairing guanine-cytosine and two bonding for adenine-thymine pair. The consumption of electrons in hydrogen bonding results in smaller amount of electron transfer towards the CNT channel. This findings regarding the decrease of the source-drain current and shifts of the  $V_{th}$  to the negative values, Figure 4, are in agreement with the data reported by Star (1) working with CNTFET made with CNT networks.

### References:

[1] 7.- Star A. et al. Proc. Natl. Acad. Sci. USA (2006) 103, 4, 921-926 (2006)

## Figures:

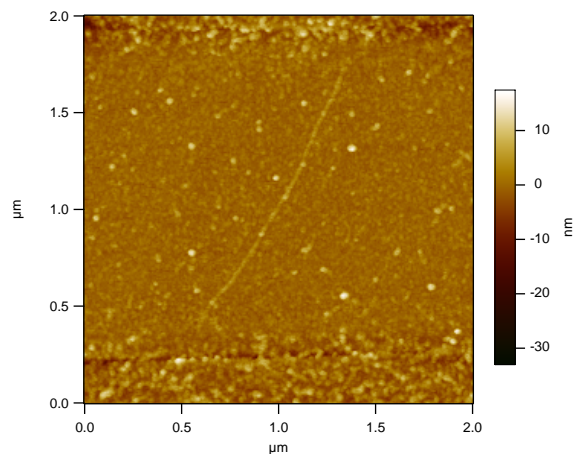


**Figure 1.- AFM images of a SWNT bonding drain and source electrodes**

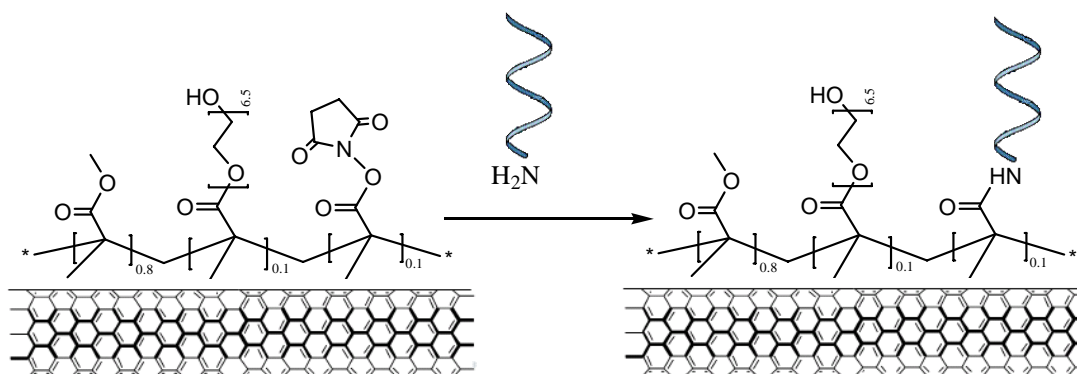


**Figure 2.- Schematic diagram of the covalent functionalization of ss DNA-NH<sub>2</sub> with the polymer bonded no-covalently with the SWNT**

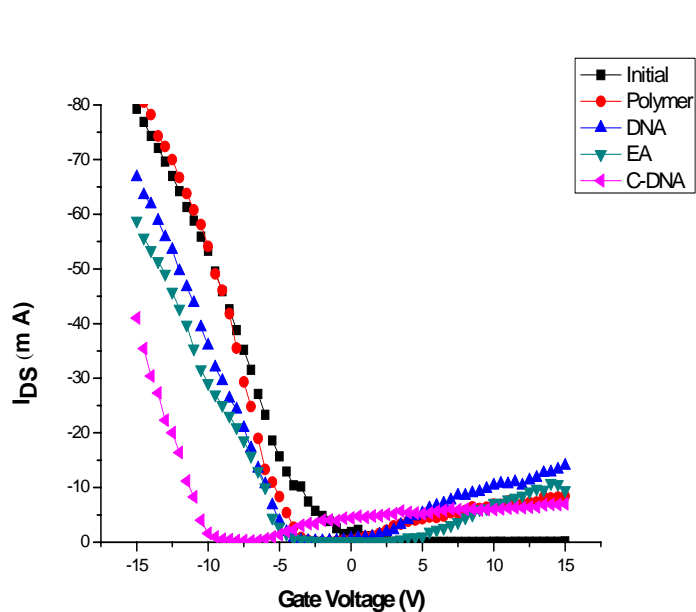


**Figure 3.- Source-Drain I/V plots evolution after depositing the chemicals and biomolecules.**

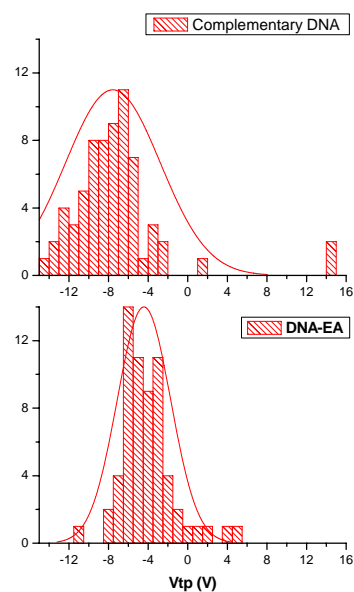


**Figure 4.- Histograms showing the changes in the V<sub>tp</sub> of the devices upon DNA hybridization.**

## ELECTROACTIVE $\beta$ -PVDF POLYMER AS FLUIDIC ACOUSTIC MIXER FOR LAB-ON-A-CHIP APPLICATIONS

*Pedro Martins\*\*<sup>1</sup>, V.F. Cardoso\*, J. Serrado Nunes\*\*, S. Lanceros-Mendez\*\*, J. H. Correia\* and G. Minas\**

*\*University of Minho, Dept. of Industrial Electronics, Campus de Azurém, 4800-058 Guimarães, Portugal*

*\*\*University of Minho, Dept. of Physics, Campus de Gualtar, 4710-057 Braga, Portugal*

*<sup>1</sup>pmartins@fisica.uminho.pt*

Ingenious micromixing systems have been developed in order to overcome the limitations of mixing microflows in microfluidic devices reaching a complete and effective mixing in short times. Several approaches have been tried. MEMS (Micro Electro Mechanical Systems) based devices have been used, such as microvalves and micropumps [1]. However, these systems increase the cost of the system, the complexity of the control system and are difficult to integrate in a single-chip. Other approaches rely in long or complex channels topologies, that can be difficult to microfabricate and can involve long mixing times, especially when the fluids diffusion coefficients are very small [2]. A different approach can be the use of acoustic waves. They have been used both to promote mixing [3] and to pump [4] fluids. One possible way to achieve these effects, is using a piezoelectric material.

This study aims to the incorporation and validation of the use of a piezoelectric polymer Poly(Vinylidene Fluoride) in its  $\beta$  phase,  $\beta$ -PVDF, in a fully-integrated disposable lab-on-a-chip for point-of-care testing and monitoring of biochemical parameters in biological fluids (Figure 1). With the deposition of the polymer underneath the microfluidics structures, acoustic microagitation can be obtained through electrical actuation, which leads to the enhancement of mixing and reaction time without moving parts.

PVDF is a semi-crystalline polymer with large scientific and technological interest due to its electroactive properties. It shows an excellent combination of processability, mechanical stress, chemical agent resistance, lightness, moldability, low-cost production and chemical inertness. It is flexible, it has a low density ( $1.97\text{g/cm}^3$ ) and it is easily produced into a thin-film. This polymer presents an unusual polymorphism in this class of materials, showing four different crystalline phases. The  $\beta$ -phase is the one which shows better properties to be applied in sensors, actuators and transducers, due to its higher piezo-, pyro- and ferroelectric properties [5]. Moreover, it can be easily processed in submicron size allowing integration in lab-on-chip systems.

Before the lab-on-a-chip device fabrication shown in Figure 1, preliminary experiments using regular cuvettes, with  $\beta$ -PVDF and its corresponding aluminum electrodes deposited on the external walls, were performed in order to validate the theoretical idea and to explore the effect of the thickness and area of the electroactive polymer on the acoustic microagitation process as well as the efficiency of the mixing. Tests were performed using two different  $\beta$ -PVDF thicknesses ( $28\ \mu\text{m}$  and  $110\ \mu\text{m}$ ) both with the same area ( $2.4\ \text{cm}^2$ ) and using two different areas ( $2.4\ \text{cm}^2$  and  $0.6\ \text{cm}^2$ ) for the same thickness ( $28\ \mu\text{m}$ ).

The evaluation of the mixing process was carried out using the Sigma Diagnostic kit (Infinity<sup>TM</sup> Uric Acid Reagent) and a standard of urine with  $15\ \text{mg/dL}$  of uric acid concentration (Sigma, 2006). Optical absorption spectrophotometry (Unicam Helios Gamma&Deta) is used as the analytical technique. The above reagent reacts with the sample of urine containing uric acid in a 50:1 ratio and produces a pink color with maximum absorption at  $495\ \text{nm}$ . The microagitation was set using sinusoidal signals of  $3.3\ \text{V}$  amplitude with  $1\ \text{kHz}$  frequency applied to the electrical contacts of the  $\beta$ -PVDF. The evolution of the reaction was studied up to a maximum absorbance of  $0.535\ \text{a. u.}$ , which is the absorbance

value of the completed mixture. All the curves (Figure 2) show similar behavior, being the main difference the time at which the total mixture is completed. This time is related directly with the reaction velocity represented by the slope of the curves. As an analysis of the results presented on Figure 2, it can be observed that faster mixtures occur when the acoustic microagitation is implemented, both with the 28  $\mu\text{m}$  and 110  $\mu\text{m}$  film thickness, regardless of the areas. Moreover, the mixing time is shorter in the case of films with smaller thickness: 257 s for the 28  $\mu\text{m}$   $\beta$ -PVDF with an area of 2.4  $\text{cm}^2$  and 304 s for the 100  $\mu\text{m}$   $\beta$ -PVDF with the same area. Furthermore, the mixing time is larger for the smaller area of the polymer: 257 s for the 28  $\mu\text{m}$   $\beta$ -PVDF with an area of 2.4  $\text{cm}^2$  and 352 s for the same thickness and with an area of 0.6  $\text{cm}^2$ .

To evaluate more qualitatively the mixing performance, an experiment was prepared in order to visualize the mixture. Two cuvettes were set for the chemical reaction between a solution of Sodium Hydroxide, Sucrose and Potassium Permanganate. In one of the cuvettes, microagitation was performed using sinusoidal signals of 10 V amplitude, with 15 MHz frequency on the  $\beta$ -PVDF transducer. Figure 3 shows the mixing differences between both cuvettes: with the application of acoustic microagitation the complete reaction time was improved in 93%. As a next step, submicron thin polymer film will be directly deposited within the lab-on-a-chip presented in Figure 1.

#### Acknowledgements:

Work supported by the Portuguese Science Foundation (grant PTDC/BIO/70017/2006).

#### References:

- [1] Cambell, C. J; Grzybowski., The Royal Society, Phil. Trans. R. Soc. Lond. A **Microfluidic mixers: from microfabricated to self-assembling devices** (2004), 362,1069-1089.
- [2] Ottino, J. M. ; Wiggins, S., Phil. Trans. R. Soc. Lond. A, **Introduction: Mixing in microfluidics**,(2004), 362, 923-935.
- [3] Bengston, M.; Laurell, T., Anal Bioanal Chem, **Ultrasonic agitation in microchannels** (2004), 378-7, 1716-1721.
- [4] Rife, J. C. et al., Sensors and Actuators B, **Miniature Valveless ultrasonic pumps and mixers** (2000) , 86, 135-140.
- [5] Sencadas, V.; Gregorio Filho, R.; Lanceros-Mendez, S.; Journal of Non-Crystalline Solids, **Processing and characterization of a novel nonporous poly(vinilidene fluoride) films in the  $\beta$  phase** (2006), Vol. 352 , 2226-2229.

#### Figures:

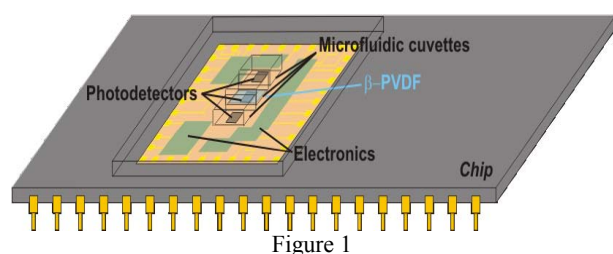


Figure 1

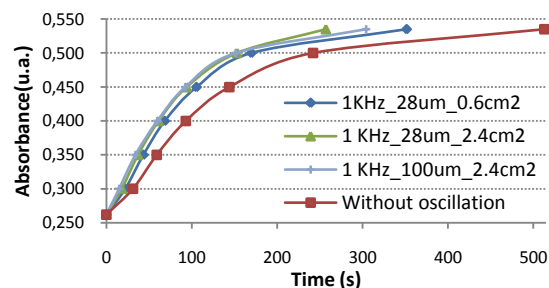


Figure 2

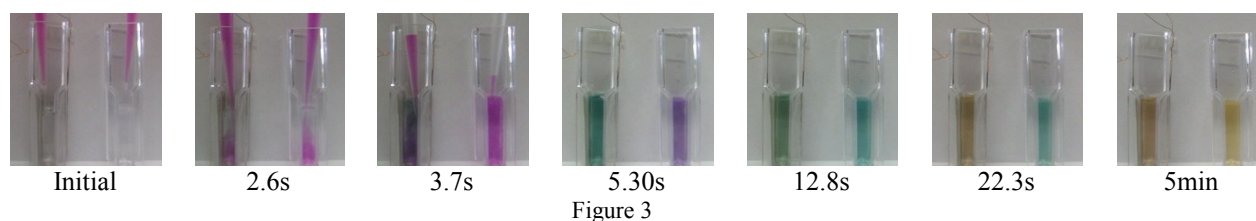


Figure 3

## DIP-PEN NANOLITHOGRAPHY: “WRITING” MOLECULES, BIOLOGICAL ENTITIES AND NANOMATERIALS AT THE NANOMETER SCALE

**Daniel Maspoch,<sup>a</sup> Elena Bellido,<sup>b</sup> Alberto Martínez,<sup>a</sup> Carlos Carbonell,<sup>a</sup> Ana Isabel Gracia,<sup>c</sup> Fernando Luis,<sup>d</sup> Daniel Ruiz-Molina.<sup>b</sup>**

<sup>a</sup>*Institut Català de Nanotecnologia;* <sup>b</sup>*Centre de Nanociència i Nanotecnologia, Campus UAB, Bellaterra 08193, Spain;* <sup>c</sup>*Instituto Universitario de Investigación de Nanociencia de Aragón;*

<sup>d</sup>*Instituto de Ciencia de Materiales de Aragón, CSIC-Universidad de Zaragoza, 50009 Zaragoza, Spain*

*E-mail: [Daniel.Maspoch.icn@uab.es](mailto:Daniel.Maspoch.icn@uab.es)*

New methods for micro- and nanofabrication are essential to scientific progress in many areas of biology, physics, chemistry, and materials science. In 1999, Mirkin's group introduced a new nanolithographic method called Dip-Pen Nanolithography (DPN).<sup>1</sup> DPN is a direct-write scanning probe-based lithography in which an AFM tip is used to deliver chemical reagents directly to nanoscopic regions of a target substrate. For example, this technique has been used to pattern alkanethiol self-assembled monolayers (SAMs) onto gold surfaces with sub-100 nm resolution and registration. To date, these nanostructures have been used as molecular templates for creating, for example, metal and semiconductor nanostructures, biological nanoarrays (including proteins, DNA, and viruses), and arrays of different nanoscale building blocks (such carbon nanotubes, nanoparticles, etc.).<sup>2,3</sup> Furthermore, DPN has allowed the direct deposition and location of proteins, DNA, polymers and nanoparticles on different surfaces.<sup>4</sup> More recently, we and other groups have been transformed this technique from a serial to a massively parallel process through the use of both one- and two-dimensional cantilever arrays.<sup>5</sup> As shown in Figure 1, any desired micro- or nanostructure can be reproduced over an area of 1 cm<sup>2</sup> by using simultaneously an array of 55.000 pens.

Recently, our group has used the direct-write capability of DPN to show that one can fabricate nanoarrays of magnetically active materials, such as ferritin proteins and Mn<sub>12</sub>O<sub>12</sub>-based clusters, at the sub-100 nm scale.<sup>6</sup> Nanoarrays of both materials have been fabricated on different surfaces, such as gold and silicon, by using parallel DPN and characterized by using several techniques, such as TOF-SIMS and FE-SEM. The direct-write capability of DPN is currently being used to direct position such arrays onto μ-SQUID devices. The precisely control on the positioning of such structures on the active areas of the μ-SQUID devices increases the sensitivity of these devices, and allows us to measure and study the magnetic properties of a small and controlled number of such proteins or clusters.

The DPN technique has also been used to directly create nanoarrays of fluorescein onto gold substrates (see Figure 2). Fluorescein is a fluorescent compound with two states featuring different optical properties after protonation/deprotonation. Therefore, its structuration on surfaces offers the possibility to design a surface molecule sensor.<sup>7</sup> The fluorescent properties of the resulting DPN-generated arrays have been investigated by confocal fluorescence microscopy, revealing a fast and a sensitive response to acid/base gas flows.

In this contribution, a general overview of the DPN technique, the recent results as well as the recent technological advances will be shown.

### References:

[1] R. D. Piner, J. Zhu, F. Xu, S. Hong, C. A. Mirkin, *Science*, **283** (1999) 661.

- [2] D. S. Ginger, H. Zhang, C. A. Mirkin, *Angew Chem. Int. Ed.*, **43** (2004) 30.  
 [3] R. A. Vega, D. Maspoch, K. Salaita, C. A. Mirkin, *Angew. Chem. Int. Ed.*, **44** (2005) 6013; Y. Wang, D. Maspoch, S. Zou, G. C. Schatz, R. E. Smalley, C. A. Mirkin, *Proc. Natl. Acad. Sci. USA*, **103** (2006) 2026.  
 [4] L. M. Demers, D. S. Ginger, S.-J. Park, Z. Li, S.-W. Chung, C. A. Mirkin, *Science*, **296** (2002) 1836.  
 [5] K. Salaita, Y. Wang, J. Fragala, R. A. Vega, C. Liu, C. A. Mirkin, *Angew. Chem. Int. Ed.*, **45** (2006) 7220.  
 [6] E. Bellido, A. Martínez, R. de Miguel, A. I. Gracia, F. Luis, D. Ruiz-Molina, D. Maspoch, in preparation.  
 [7] A. Martínez, J. Hernando, D. Maspoch, D. Ruiz-Molina, in preparation.

### Figures:

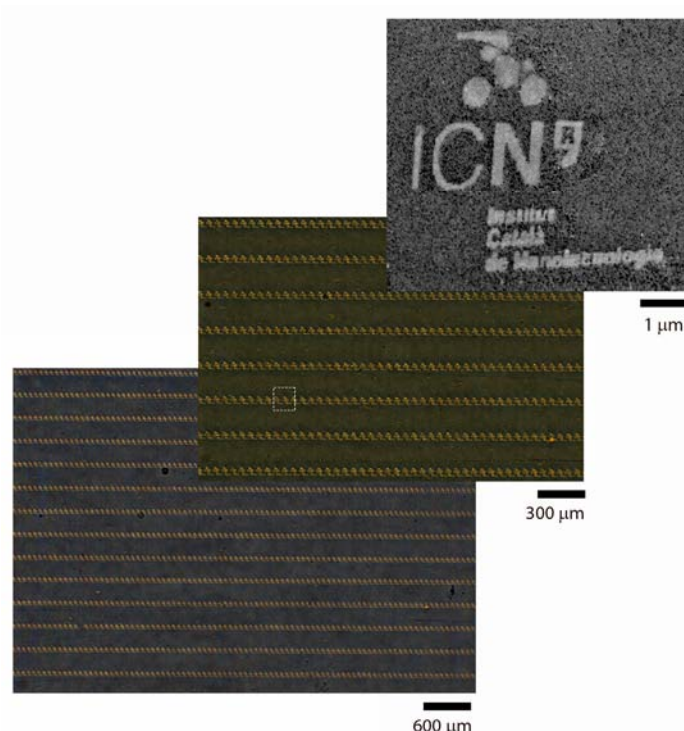


**Figure 1.** Optical image of a representative region of the substrate on which approximately 55000 duplicates of the logo of the “Institut Català de Nanotecnologia” have been generated. On top there is a high-resolution SEM image of a representative replica.

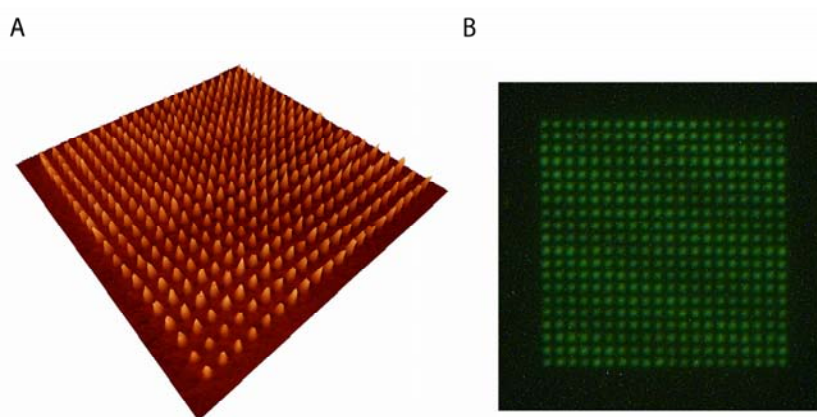


**Figure 2.** (A) 3-D AFM tapping mode image of a fluorescein nanoarray on Au surface and (B) the corresponding fluorescence image. The distance between dots is 1  $\mu\text{m}$ .

## SELF-ASSEMBLY OF POLYCHLOROTRIPHENYLMETHYL ORGANIC RADICALS ON SURFACES

*M. Mas-Torrent,<sup>a</sup> N. Crivillers,<sup>a</sup> S. Perruchas,<sup>a</sup> N. Roques,<sup>a</sup> J. Vidal-Gancedo,<sup>a</sup> J. Veciana,<sup>a</sup>  
C. Rovira,<sup>a</sup> L. Basabe-Desmonts,<sup>b</sup> B-J Ravoo,<sup>b</sup> M. Crego-Calama,<sup>b</sup> D. Reinhoudt,<sup>b</sup> S.  
Furukawa,<sup>c</sup> A. Ver Heyen,<sup>c</sup> S. De Feyter,<sup>c</sup> A. Minoia,<sup>d</sup> M. Linares<sup>d</sup> R. Lazzaroni<sup>d</sup>*

*a) Laboratory of Molecular Nanoscience and Organic Materials, Institut de Ciència de Materials de Barcelona (CSIC), Bellaterra, Campus de la UAB E-08193, Spain*

*b) Laboratory of Supramolecular Chemistry and Technology MESA+ Research Institute, University of Twente, P.O. Box 217, NL-7500 AE Enschede, The Netherlands*

*c) Department of Chemistry, Katholieke UniVersiteit LeuVen, Celestijnenlaan 200-F, 3001 Heverlee, Belgium.*

*d) Service de Chimie des Matériaux Nouveaux, Université de Mons-Hainaut, 20, Place du Parc, B-7000 Mons, Belgium.*

[mmas@icmab.es](mailto:mmas@icmab.es)

The ultimate goal of molecular bottom up approaches is to employ functional building blocks to construct nanometer scale devices addressed to specific applications. Furthermore, for practical device implementation the immobilisation of functional molecules on suitable surfaces is also often required. One powerful and versatile strategy for the modification of surfaces at the molecular level is via the preparation of self-assembled monolayers (SAMs). Here, we describe the functionalisation of SiO<sub>2</sub> and Au surfaces with polychlorotriphenylmethyl (PTM) radicals via covalent and noncovalent interactions (Fig. 1). [1-2]

The family of PTM radicals is chemically and thermally stable due to the fact that their open-shell centres are shielded by six bulky chlorine atoms.[3] These radicals are colored and also exhibit fluorescence in the red region of the spectra. More interestingly, PTM radicals are electroactive and can be easily and reversibly reduced (or oxidized) to their anionic (or cationic) species. The oxidised and reduced states show different absorption spectra than the radical and are in addition non magnetic and non fluorescent. Therefore, the preparation of SAMs functionalised with PTM radicals (PTM SAMs) on solid substrates results in multifunctional surfaces which are electrochemically, optically and magnetically active. We also demonstrate that these SAMs can be used as chemical and electrochemical redox switches with optical (absorption and fluorescence) and magnetic responses. In addition, the fabrication of surface patterns of these radical molecules has also been achieved using microcontact printing and visualized by fluorescence microscopy (Fig 2).

The self-assembly of novel PTM radicals bearing long alkyl chains at the liquid-graphite interface was also investigated. We show that the PTM hierarchical self-assembles giving rise to 3-dimensional ordered nanostructures forming double rows composed by a magnetic core of radicals surrounded by alkyl chains.

The fabrication of ordered surface nanostructures of multifunctional organic radicals represents an important step forward in the field of molecular electronics and molecular magnetism.

### References:

[1] N. Crivillers, M. Mas-Torrent, S. Perruchas, N. Roques, J. Vidal-Gancedo, J. Veciana, C. Rovira, L. Basabe-Desmonts, B-J. Ravoo, M. Crego-Calama, D. N. Reinhoudt, *Angew. Chem. Int. Ed.* **46** (2007) 2215.

[2] N. Crivillers, M. Mas-Torrent, J. Vidal-Gancedo, J. Veciana, C. Rovira, *J. Am. Chem. Soc.*, in press.

[3] M. Ballester, J. Riera, J. Castañer, C. Badia, J. M. Monso. *J. Am. Chem. Soc.* **93**, (1971). 2215.

### Figures:

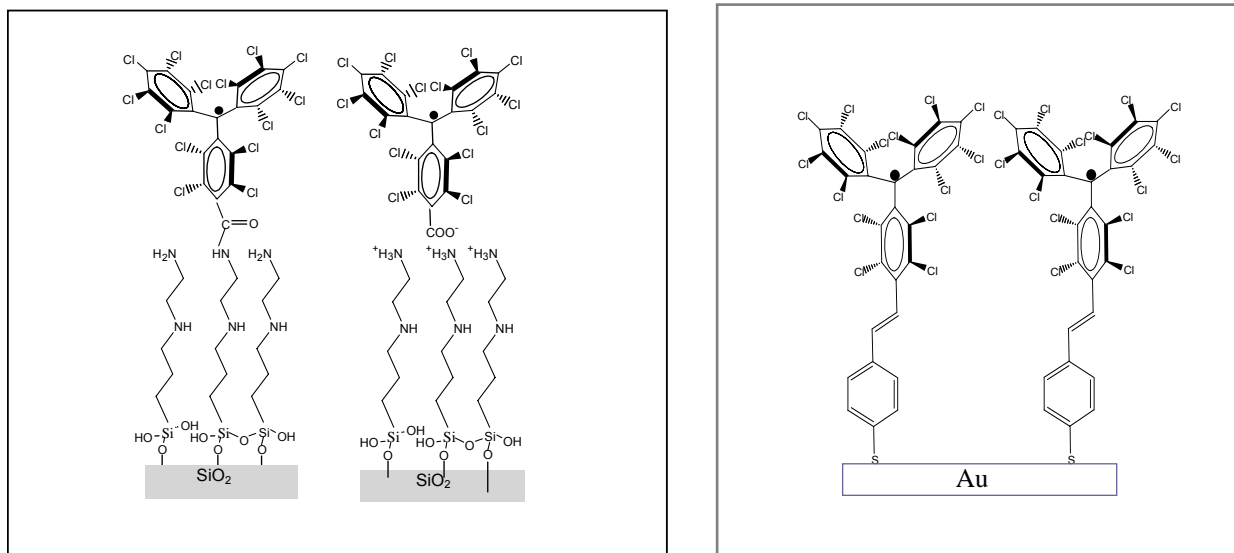


**Fig. 1** Left: PTM SAMs on SiO<sub>2</sub> prepared via covalent and noncovalent interactions Right: PTM SAMs on Au(111).

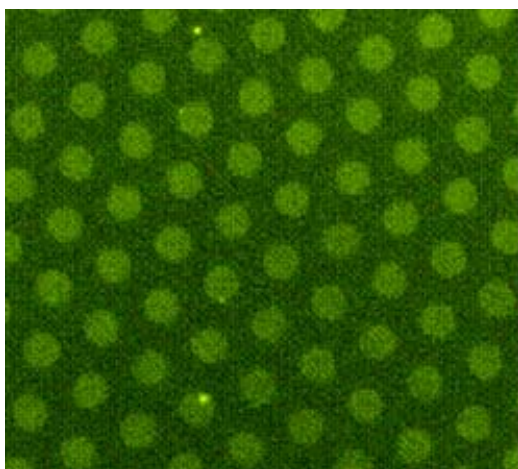


**Fig. 2** Fluorescence microscopy image of a patterned PTM SAM by microcontact printing on glass ( $\lambda_{\text{exc}}=340-370$  nm, spotsize of 10 μm).

## NANO ACTIVITY IN PORTUGAL

Luis Melo  
Fundação para a Ciência e a Tecnologia  
Portugal

Email: [luis.melo@fct.mctes.pt](mailto:luis.melo@fct.mctes.pt)

Nanotechnology has gained relevance in the last years. This is largely due to the development of the available technologies, but a very strong motivation is that most biological and chemical processes occur at nanoscale. Seeing and actuating at this scale has almost unlimited potential, in Biomedicine as well as Electronics or Materials science and technology. It is multidisciplinary in nature, as classic disciplines like Biology, Chemistry or Physics are hard to distinguish at this scale. A new class of applications is at reach if the appropriate effort is placed into Research and Development in this area.

Nanotechnology activity has been constantly gaining relevance in Portugal in the last years. Many Portuguese research Groups have shown sizeable activity, both in volume and overall quality, in Nanotechnology topics. Most of those Groups have a well-established tradition of quality research on which their move into Nanotechnology is anchored. The most active topics reflect this fact, Biochips/biosensors, Bio-nanotechnology, Nanomedicine, Nanoelectronics, Nanostructured Materials/Nanocomposites, Nanofiltration/Membranes, Semiconductor Devices, Magnetic Devices. As it would be expected for an emerging, hot topic, there are smaller, younger Groups producing quality work but in smaller volumes in other relevant topics, as SPM or Single-molecule studies and others. In order to foster the potential of Nanosciences and Nanotechnologies a considerable effort has been actively devoted to the development of this field in Portugal.

One step was the gathering of information about the activity actually taking place. This work led to the launch of PortugalNano, the Portuguese Nanoscience and Nanotechnology Network ([www.portugalnano.org](http://www.portugalnano.org)). The main purpose is to make available to all Portuguese NanoScientists information on who is doing what, including an extensive database of published work by Portuguese Groups in this field. The availability of this information should help establishing collaborations between Groups and in this way promote further advances in Nanotechnology. This initiative closely coordinates with Portuguese participation in different International and European programmes and initiatives. A bilateral collaboration with France specifically in this field is also being set up.

A very significant step into promoting Nanotechnology was the joint launch with Spain of the International Iberian Nanotechnology Laboratory (INL) to be installed in Braga, Portugal. This will be a World-class international laboratory for about 200 researchers in a first stage, and will focus onto four main topics: Nanomedicine, Nanoelectronics, Nanomanipulation and Nanorobotics, Environment Monitoring and Food Quality Control and Safety.



## IMDEA-NANOCIENCIA: A NEW INSTITUTE DEVOTED TO RESEARCH IN NANOSCIENCE AND NANOTECHNOLOGY IN MADRID

Rodolfo Miranda<sup>1,2</sup>

<sup>1</sup>*Departamento de Física de la Materia Condensada, Universidad Autónoma de Madrid.*

<sup>2</sup>*Instituto Madrileño de Estudios Avanzados en Nanociencia (IMDEA-Nanociencia)  
Cantoblanco. 28049 Madrid. Spain.*

[rodolfo.miranda@uam.es](mailto:rodolfo.miranda@uam.es) or [rodolfo.miranda@imdea.org](mailto:rodolfo.miranda@imdea.org)

IMDEA- Nanociencia is a private Foundation created by a joint initiative of the regional Government of Madrid and the Ministry of Education of the Government of Spain in February 2007. The only aim of the Foundation is to manage the Madrid Institute of Advanced Studies in Nanoscience, a new interdisciplinary research centre dedicated to the exploration of basic nanoscience and the development of applications of nanotechnology in close connection with innovative industries. The Foundation is governed by a Board of Trustees, which includes representatives of the Administration, the Academic Institutions involved (Universidad Complutense de Madrid, Universidad Autónoma de Madrid, Universidad Politécnica de Madrid, Consejo Superior de Investigaciones Científicas), industries, members of the Scientific Advisory Council, and experts in societal implications of nanoscience and technology transfer.

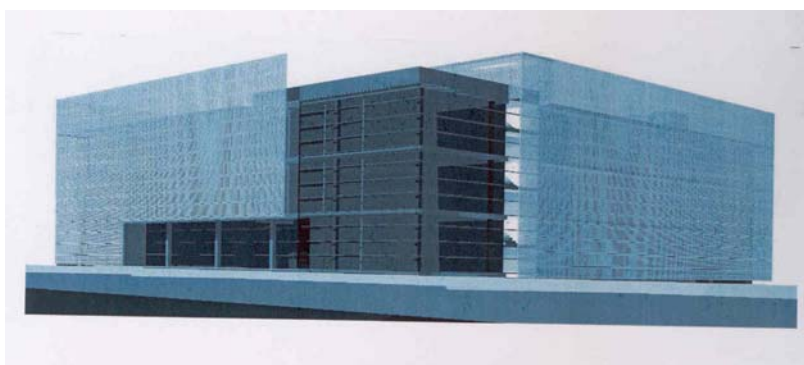
The Foundation and the Institute are located in the campus of the Universidad Autónoma de Madrid in Cantoblanco, 12 kilometres away from Madrid downtown, on the highway to the Sierra. The campus has excellent communication by public transportation with the Madrid-Barajas airport (25-30 min) and Madrid downtown (15-20 m).

The Foundation is run by a flexible, professional management structure and works for a closer interaction of scientists in the IMDEA-Nano and companies in the region of Madrid and elsewhere. The common efforts to generate joint research projects are focused into specific proposals by a qualified staff. The main tasks of the Institute are the recruitment of new scientific talent and its organization into research teams provided with first line equipment and competitive infrastructure, able to tackle specific scientific problems in basic nanoscience and certain nanotechnologies.

The scientific (Ph. D students, postdocs, junior and senior scientists), technical and administration personnel of the Institute is contracted by the Foundation through public, competitive processes, subjected to periodic scientific evaluation and salary revision.

The initial areas of research are:

- i) Molecular nanoscience (with emphasis in carbon nanostructures)
- ii) Semiconducting nanostructures for quantum information
- iii) Nanophotonics
- iv) Nanomagnetism
- v) Conductivity in nanostructures
- vi) Biomachines and manipulation of biomoléculas. Nanomedicine and biomedical application of magnetic nanoparticles
- vii) Nanolithography and nanofabrication





## CHEMICAL FUNCTIONALISATION OF CARBON NANOTUBES FOR THE DISPERSION IN POLYMER MATRICES

*Maria da Conceição Paiva<sup>1</sup>, Maria Fernanda Proença<sup>2</sup>, Carlos J. R. Silva<sup>2</sup>, Rui F. Araújo<sup>2</sup>,  
Rui M. Novais<sup>1</sup>*

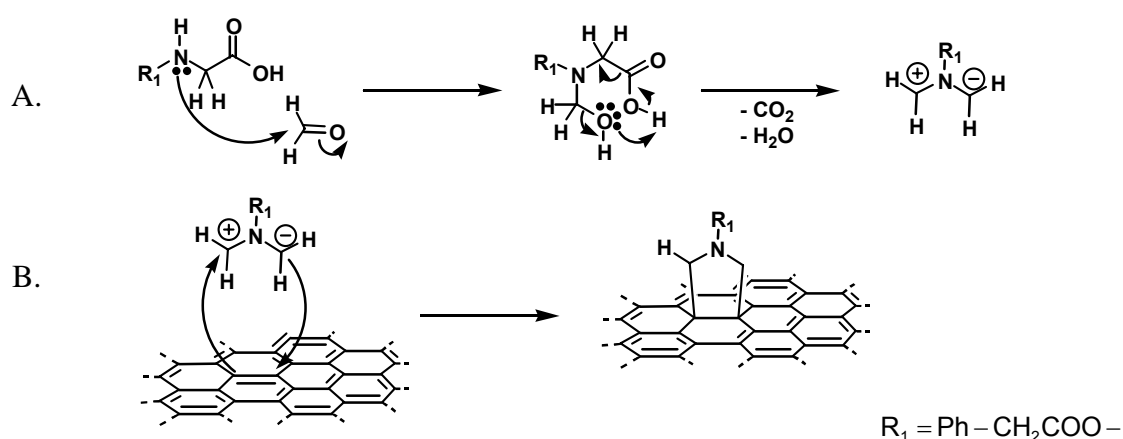
<sup>1</sup>*Institute for Polymers and Composites, Department of Polymer Engineering, University of Minho, Campus of Azurém, 4800-058 Guimarães, Portugal*

<sup>2</sup>*Department of Chemistry, University of Minho, 4710-057 Braga, Portugal*  
[mcpaiva@dep.uminho.pt](mailto:mcpaiva@dep.uminho.pt)

Carbon nanotubes (CNT) and nanofibres (CNF) exhibit unique mechanical, electric and thermal properties [1-2]. Their physical form is not convenient for most applications, demanding their combination with a matrix material. The preparation of a composite requires an efficient dispersion of the reinforcing phase and its good interaction with the matrix. However, the chemical inertness and low surface energy of the graphitic structure of the CNT and CNF makes this process difficult. Thus, the surface modification of CNT and CNF, aiming at the improvement of their interaction with other materials, is becoming an area of increasing importance. This modification can be achieved by attaching functional groups to the CNT/CNF surface [3-4] that will interact strongly with the matrix material, thus originating composites with exceptional structural properties at low reinforcement loads [5,6].

Most functionalization methods involve strong acid treatment of the CNT/CNF, producing extensive nanotube breakage. A class of functionalisation reactions that does not involve acid treatment is the direct addition to the  $\pi$ -electrons of the CNT/CNF [7,8]. These chemical reactions are less aggressive to the CNT/CNF in the sense that they do not induce high nanotube breakage, maintaining the CNT aspect ratio almost unchanged relative to the non-functionalised CNT.

The present work reports the functionalisation of CNT and CNF using two different methods. The first method is based on a Diels-Alder addition reaction (DA) of 1,3-butadiene to the CNT surface, as described in a previous work [9]. The other method is based on the addition of 1,3-dipoles to the CNT surface, generated by condensation of an  $\alpha$ -amino acid and an aldehyde [8,10], as represented in Scheme 1.



*Scheme 1.* A. Formation of the 1,3-dipole; B. Addition of the 1,3-dipole to the graphite surface.

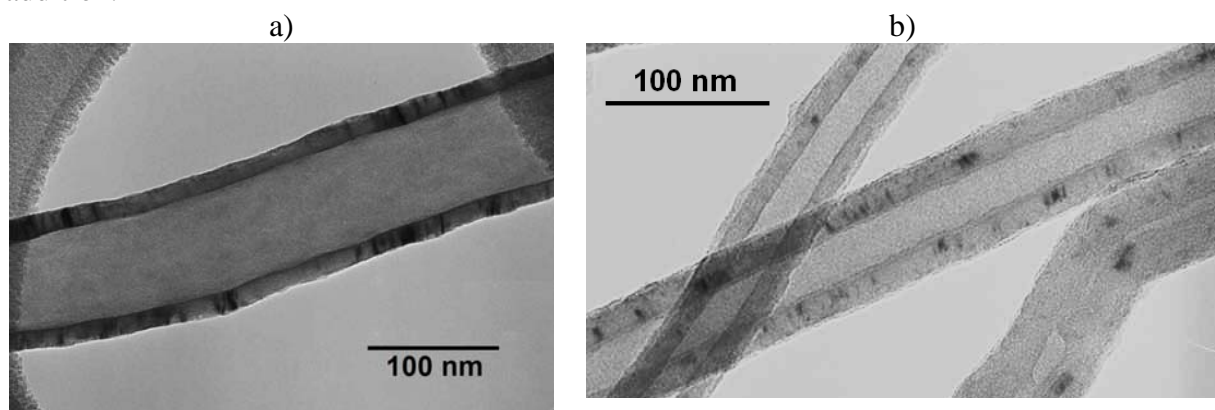
The characterisation of the CNT and CNF functionalisation was done by thermogravimetric analysis (TGA), X-ray photoelectron spectroscopy (XPS) and electron microscopy. For the CNT and CNF an increase in weight loss was observed after functionalization, measured by TGA under a constant flow of  $\text{N}_2$ , as shown in Table 1. The XPS spectra confirmed the

presence of the amine at the surface of the nanofibres functionalized by the 1,3-dipolar cycloaddition reaction. Transmission electron micrographs of the non functionalised and functionalised CNFs are shown in Figure 1. The CNF functionalised by the DA addition of butadiene, under high butadiene concentration, show a layer of a polymeric product formed at the CNF surface (Figure 1 b). The extension of this layer may be controlled by the reaction conditions.

Table 1. TGA weight loss for CNF functionalized in different conditions.

CNF treatment	Weight loss (%) $\pm$ Stand. Dev.
Untreated	$2.3 \pm 1.2$
DA reaction	$11.2 \pm 2.5$
1,3-dipolar cycloaddition reaction	$16.7 \pm 2.3$

Figure 1. TEM micrographs of CNFs: a) non-functionalised, b) functionalised by Diels-Alder addition.



Composites were prepared by mixing the CNF with polymer matrices using melt blending techniques. The analyses of the cross-sections of the composites formed showed that the distribution of the CNF through the polymer matrix was good for the non-functionalised and functionalised CNF in both matrices. The functionalised fibres were well wet by the matrix polymer, while the non-functionalised CNF showed poor wetting by the matrix.

**Acknowledgments:** The authors acknowledge the financial support from FCT (Portuguese Foundation for Science and Technology) through the project POCI/QUI/59835/2004.

### References:

- [1] Baughman R H, Zakhidov A A, de Heer W A, *Science*, 297 (2002) 787-792.
- [2] Mamalis A G, Vogtländer L O G, Markopoulos A, *Precision Eng*, 28 (2004) 16-30.
- [3] Bahr J L, Tour J M, *J Mater Chem*, 12 (2002) 1952-1958.
- [4] Tasis D, Tagmatarchis N, Georgakilas V, Prato M, *Chem Eur J*, 9 (2003) 4000-4008.
- [5] Thostenson E T, Li C, Chou T-W, *Compos Sci Tech*, 65 (2005) 491-516.
- [6] Paiva M C, Zhou B, Fernando K A S, Lin Y, Kennedy J M and Sun Y-P, *Carbon*, 42 (2004) 2849-2854.
- [7] K. Balasubramanian and M. Burghard, *Small*, 1, 2 (2005), 180 –192.
- [8] V. Georgakilas, K. Kordatos, M. Prato, D. M. Guldi, M. Holzinger and A. Hirsch, *J. Am. Chem. Soc*, 124, 5 (2002), 760-761.
- [9] F. M. Fernandes, R. Araújo, M. F. Proença, C. J. R. Silva, M. C. Paiva, *Journal of Nanoscience and Nanotechnology*, 7 (2007) 3514-3518.
- [10] Rui Araújo, M. C. Paiva, M. F. Proença, Carlos J. R. Silva, *Composites Science and Technology*, 67 (2007) 806-810.

## CONTROLLED INTEGRATION OF NANOCRYSTALS ON THE SURFACE OF GROUP III-NITRIDE LIGHT-EMITTING EPITAXIAL HETEROSTRUCTURES

*S. Pereira\**, *M. Martins* and *T. Trindade*  
*CICECO, Universidade de Aveiro, 3810-193 Aveiro, Portugal*

*D. Zhu* and *C. J Humphreys*  
*Materials Science and Metallurgy, University of Cambridge, Pembroke Street, Cambridge*  
*CB2 3QZ, UK*  
*I. M. Watson*  
*Institute of Photonics, SUPA, University of Strathclyde, Glasgow, G4 0NW, UK*

[spereira@ua.pt](mailto:spereira@ua.pt)

Currently an extensive range of colloidal nanocrystals (NCs) can be readily produced by diverse chemical methods. These nanomaterials present novel physical properties and can be regarded as building blocks to the nanofabrication of smaller, energy efficient and faster devices. However to form a functional device with reasonable complexity, these nano-building blocks have to be conveniently arranged and connected. This requires incorporation into an interconnectable, electrically and/or optically active framework. Such endeavour is a key challenge in nanoscience and nanotechnology. Here we address this via a novel and inexpensive approach that exploits the spontaneous formation of nanoscale inverted hexagonal pits (IHPs) at the surface of In-containing III-nitride epitaxial heterostructures.

We demonstrate that these morphological features, which can be designed with a suitable size, depth and density, can effectively organize and control the incorporation of NCs at the surface of efficient light emitting devices. Nanoengineering of the relative sizes of NCs and IHPs allows the number of NCs incorporated into each hexagonal pit to be controlled precisely.

Although the selective incorporation of virtually any kind of NCs into the IHPs is possible due to interfacial capillarity forces acting during the deposition method, as a proof of concept, this work will focus on the nanomanipulation of Au nanocrystals with sizes ranging from 30 to ~5 nm. It will be shown that each nano-pit can accommodate either individual NCs, or well-defined “clusters” of NCs. Controlled self-assembly, with areal densities up to  $10^9/\text{cm}^2$ , was achieved with precisions below the limits of conventional lithographic techniques, over macroscopic length scales.

The successful integration with nanometer-scale control of colloidal NCs onto the surface of III-nitride semiconductor heterostructures will bring together the benefits of *bottom-up* and *top-down* approaches towards the creation and control of nanostructures. As complementary realms of activity, the combination of both methodologies will certainly contribute to the achievement of novel functional nanodevices, and also give new scientific insights of a more

fundamental kind. In this context, new properties may arise through the exploitation of cross-coupling effects, namely by the unrivalled versatility of wet chemistry to produce a wide range of nanomaterials, to be combined with the ease of charge injection and the high efficiency of light emission of group III-N bipolar devices. Such synergetic incorporation also opens the way to investigate and tailor the physical properties of elementary NC clusters, down to isolated individual NCs, as well as the coupling of elementary excitations (e.g. electronic, photonic and plasmonic) between the nitride framework and the nanoscale building blocks.

### References:

S. Pereira, Tito Trindade, Manuel A. Martins, Ian M. Watson, Diane Zhu and Colin J. Humphreys “Controlled integration of nanocrystals in inverted hexagonal nano-pits at the surface of light-emitting heterostructures” *Adv. Mater.*, **2008**, *20*, -cover story-

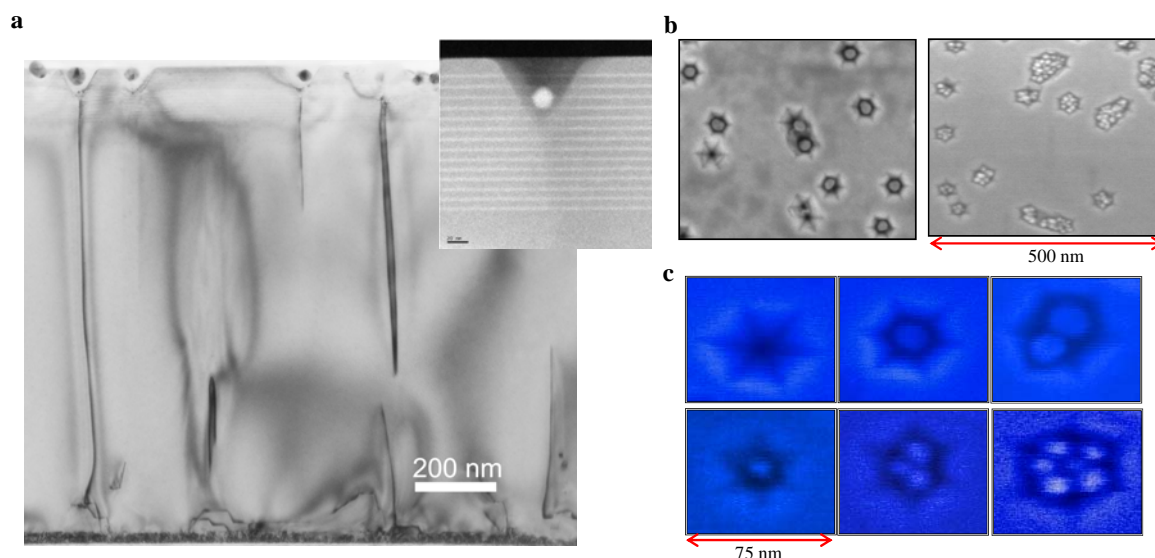


**Figure 1:** Cross section TEM and plane view SEM images showing effective selective incorporation of Au NCs into the IHPs.

**a)** Bright field TEM micrograph showing the nitride heterostructure from the sapphire interface up to the surface, where the Au NCs are incorporated inside the IHPs. The higher magnification inset shows a STEM-HAADF micrograph of the InGaN/GaN MQW region near a pit. An isolated Au NC can be observed in detail. The 14-wells forming the MQW can also be observed. In this TEM imaging mode the contrast is strongly dependent on the atomic number  $Z$  of the atoms encountered by the incident probe. The Au NC is the brightest feature ( $Z_{\text{Au}}=79$ ) while the InGaN well regions also appear brighter than the GaN barriers and cap layer ( $Z_{\text{In}}=49$ ,  $Z_{\text{Ga}}=31$ ).

**b)** Plane view SEM micrographs demonstrating selective incorporation of NC inside the Pits for Au nanoparticles with sizes of  $\sim 30\text{nm}$  (left) and  $\sim 5\text{ nm}$  (right).

**c)** The upper panel shows an empty nano-pit in detail, a  $\sim 30\text{ nm}$  Au NC inside a IHP and a NC dimmer. The lower panel shows NC assemblies with increasing complexity using  $\sim 15\text{ nm}$  NCs; namely 1 NC per pit, 4 NCs (only 3 visible) forming a tetrahedron and finally a 3-monolayer NC “lattice” with 5 NCs visible at the surface.

## CMOS INTEGRATED NANOMECHANICAL MASS SENSORS: DETERMINATION OF EVAPORATION RATE OF FEMTOLITER DROPLETS

*J. Arcamone<sup>1</sup>, T. Ondarçuhu<sup>2</sup>, E. Dujardin<sup>2</sup>, G. Rius<sup>1</sup>, and F. Pérez-Murano<sup>1</sup>*

<sup>1</sup>*CNM-IMB (CSIC), Campus UAB, 08193 Bellaterra, Spain. [Francesc.Perez@cnm.es](mailto:Francesc.Perez@cnm.es)*

<sup>2</sup>*Nanosciences group, CEMES-CNRS, 29 rue Jeanne Marvig, 31055 Toulouse, France*

*[Francesc.Perez@cnm.es](mailto:Francesc.Perez@cnm.es)*

During recent years, the need of methods to manipulate very small liquid quantities has emerged, leading to the development of nanofluidics or nanodispensing [1] techniques. At these scales, evaporation processes become important. However, previous comprehensive studies of evaporation are limited to microliter droplets [2]. We address here the question of the validity of the macroscopic models at micro and nano scales (sub-femtoliter range). We present the use of CMOS integrated nanomechanical resonators [3] to determine with high precision the change in mass of liquid droplets with time. We have studied [4] the evaporation of droplets with diameters in the one micron range, what corresponds to volumes of femtoliters, nine orders of magnitude smaller than previously published data.

The nanomechanical resonator is a polysilicon quad-beam resonator (QBR) defined by electron-beam lithography on pre-fabricated CMOS substrates. It provides high mass sensitivity together with large active area for convenient droplet deposition. Because its resonance spectrum is detected using a capacitive scheme, QBR are monolithically integrated with CMOS circuitry (fig.1) for signal amplification and parasitic capacitance reduction. Prior to the evaporation experiments, QBR are calibrated by successive loading of silica beads using a micro-manipulator. The obtained mass resolution is three orders of magnitude better than commercial quartz crystal microbalances

Dispensing of droplets is based on the NADIS technique described in [1]. Commercial AFM tips are modified by FIB milling to allow loading liquid and dispensing of droplets through a hole of 300 nm in diameter milled at the tip apex. Droplets with diameters ranging from 1 to 5  $\mu\text{m}$  were reproducibly deposited on the resonators (fig.2).

During evaporation, we monitored the resonance frequency shift of the QBR (fig.3). Using a calibration curve, the temporal evolution of the droplets mass was determined down to 10 fg (10 attoliters volume) for glycerol droplets with initial volumes ranging from 0.2 fL to 20 fL. The droplet mass decreases nonlinearly, with a slowing down of the evaporation rate with time. This behaviour, is well described by macroscopic model which predicts, in constant contact angle mode, a decrease of the droplet mass with evaporation time with a power law  $2/3$  [2]. The linear decrease of  $m^{2/3}$  as a function of time (figure 4) together with the fact that the total evaporation time depends on the initial weight  $m_0$  at power  $2/3$  (inset of figure 4), indicates that the macroscopic laws remains valid down to these scales.

This work is partially financed by the European Commission within the project NaPa (NMP4-CT-2003-500120). The content of this work is the sole responsibility of the authors.

### References:

- [1] A. Fang, E. Dujardin, and T. Ondarçuhu., *NanoLett.*, vol. 6, pp. 2368-2374, 2006.
- [2] R.G Picknett et al, *J. Col. Int. Sci.*, 61, pp. 336-350, 1977.
- [3] J. Arcamone et al, in *Tech. Digest of IEEE IEDM'06 conference*, pp. 525-528, 2006.
- [4] J. Arcamone, E. Dujardin, G. Rius, F. Perez-Murano, T. Ondarçuhu. *J. Phys. Chem. B.* 111(45), 13020-13027, (2007)

## Figures:

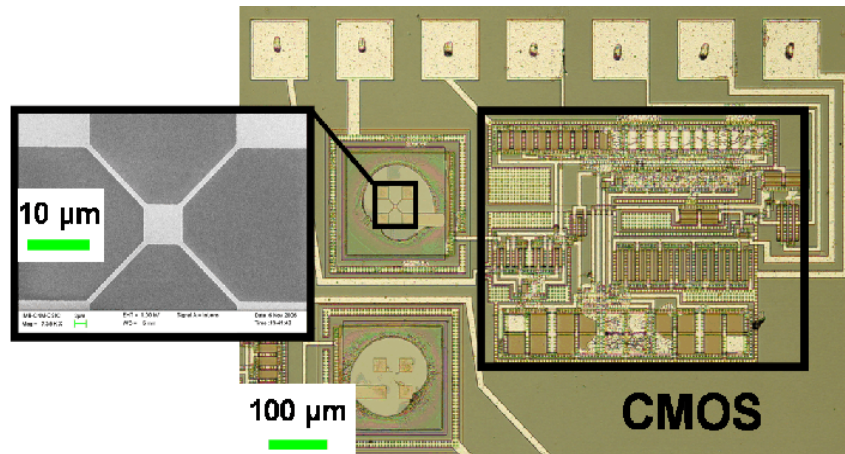


**Figure 1.** Optical image of a Quad-Beam resonator (QBR) monolithically integrated into CMOS circuitry. The polySi structural layer is electrically connected to the input of the circuit that acts as a trans-impedance amplifier. The inset shows a SEM image of a QBR defined after CMOS fabrication by e-beam lithography and subsequent Al lift-off, pattern transfer to polysilicon by RIE and release wet etching. The device has the following dimensions: central plate ( $6 \times 6 \mu\text{m}^2$ ), beams width and length: 600 nm and 13.5  $\mu\text{m}$ , thickness: 500 nm.

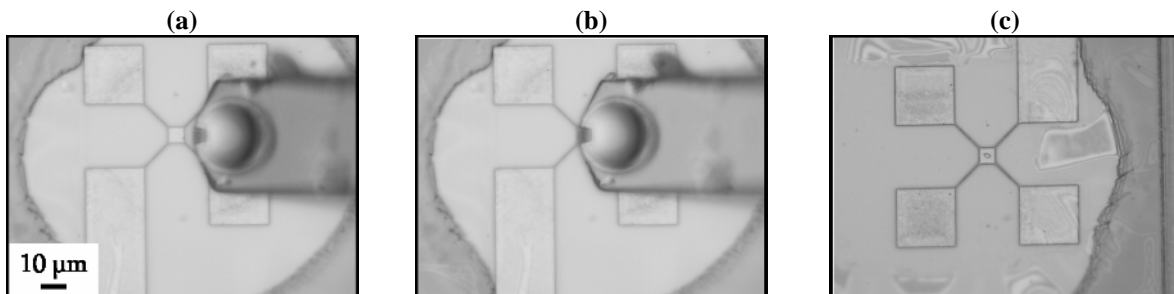


**Figure 2.** Top view of a nanodispensing probe. (a) the tip, pre-loaded with a liquid, is approached; (b) it is aligned with a QBR adjusting its position with the control table; (c) final image of the deposited droplet on the QBR central plate.

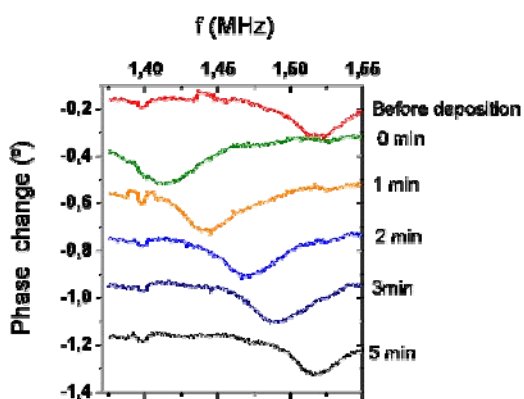


**Figure 3.** Evolution of the resonance frequency of a QBR as a function of the evaporation time (unloaded resonance frequency  $\approx 1.52$  MHz) during the evaporation of a micron-sized droplet. After complete evaporation, the resonance frequency turns back to its unloaded value. A phase offset has been added to each curve to make easier the visualization of the temporal evolution

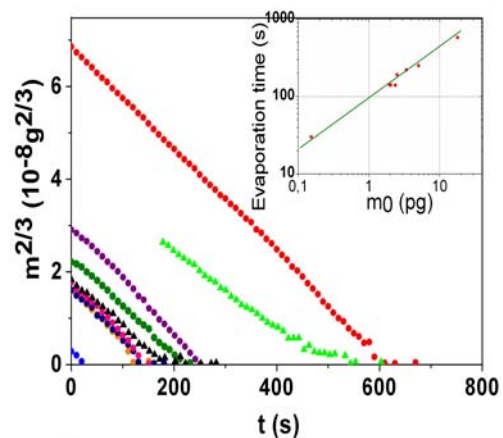


**Figure 4.** Temporal evolution of the droplet mass at a power 2/3 for the same data as in fig. 5. All the droplets exhibit a linear trend with the same slope. The inset is a plot of the total evaporation time of as a function of the initial mass

## **CIC nanoGUNE CONSOLIDER, THE BIG CHALLENGE OF THE SMALL**

J. M. Pitarke

CIC nanoGUNE, Mikeletegi Pasealekua 56, E-20009 Donostia

The Department of Industry, Trade, and Tourism of the Basque Government has recently launched a so-called nanoBASQUE2015 strategy designed for the development of a new industrial sector in the Basque Country that would be enabled by nanotechnology. In the framework of this initiative and the Spanish Consolider-Ingenio program, a new R&D center (the Nanoscience Cooperative Research Center nanoGUNE) has been created with the mission of addressing both basic and applied nanoscience world-class research for the competitive growth of the Basque Country. In this talk, I intend to give an overview of the current status of this challenging project, which we call 'the big challenge of the small' not only because it refers to the science of the small but also because it represents a big challenge for a small but successful country that is currently aiming at becoming an innovation reference in Europe.



## THE INTERNATIONAL IBERIAN NANOTECHNOLOGY LABORATORY FACTS, PROSPECTS AND STRATEGIC GOALS

*José Rivas, Carlos A. Bernardo, Paulo P. Freitas*  
*INL, Av. Dos Congregados 100, 4710-229, Braga, PORTUGAL*

*office@iinl.orgl*

### 1 - Facts and Prospects

INL – the International Iberian Nanotechnology Laboratory was created by decision of the governments of Portugal and Spain in November 2005. At the time it was decided that it would function as an international research organization in the field of nanoscience and nanotechnology (N&N). With its statutes already approved in both countries, INL has a legal framework similar to that of other international laboratories located in Europe like CERN, ESO or EMBL.

During 2006 and 2007, INL went through its first stages, with the creation of an installation commission, and an international advisory board, and the definition of the initial strategic areas of research. The first facility concepts were discussed with specialized design teams in the second half of 2007 and, in January 2008, a Basis of Design (BoD) was chosen as the starting point for the design of its future campus. The campus was designed to house up to 200 researchers and associated staff, in state-of-the-art facilities. The first phase, to be completed until 2010, will include a main scientific building and a residence for staff and visiting professors. At a later stage, an incubator and a science outreach building will be added. Fig.1 shows a physical model of the future facilities, after completion of phases 1 and 2. In the second half of 2007 the first phase of a PhD grant program where INL financed PhD stipends in Nanotechnology topics in selected Portuguese and Spanish research institutions was launched. January 2008 also saw the laying down of the symbolic first stone of the future campus, in a ceremony, in Braga, presided by the Prime Minister of Portugal and the President of the Government of Spain.

Besides high quality personnel and installations, cutting-edge scientific instruments are the most important ingredient of any international laboratory. INL will include the following central laboratory facilities.

#### *Central Micro and Nanofabrication Clean room*

This facility will be built around a class 100 clean room (ca. 450m<sup>2</sup> useful area in phase 1, with expansion to 600m<sup>2</sup> in Phase 2) with dedicated bays for nanolithography (10nm minimum features, e-beam and nanoimprint), and optical lithography (direct write laser and mask aligners). The nanolithography bay is designed for stringent EMI requirements (< 40nT, from 1Hz to 80Hz) and VCE vibration standards. Apart from standard deposition/etch, wet process and thermal treatment, and characterization bays, the clean room will include a separated bay for biochemical assays and process steps, and an isolated bay for special material processing.

#### *Central Scanning Probe Microscopy Laboratory*

This laboratory will support SPM activity from standard imaging to advanced applications. A small number of standard SPMs will be available for regular imaging. An advanced facility, especially intended for biological/ biochemical applications, will provide SPM coupled with confocal optical microscopy. There will also be one SPM especially intended for the development of new techniques, supported by standard test and measuring equipment.

#### *Central Biology and Biochemistry (CBB) facility*

CBB will provide support for biology and biochemistry research groups. It will have equipment for FPLC/HPLC protein purification, spectrophotometry/ nano chop, mass spectrography with gas chromatography, flow cytochemistry and cell sorting, real-time PCR, confocal microscopy and centrifugation (ultra and low-speed) and cell culture. Supporting infrastructures, such as optical and fluorescence microscopes, down to  $-70^{\circ}\text{C}$  chambers and freezers, a dark room and a sterile chamber with laminar flow are also contemplated.

#### *Central Structural and Interface Characterization (CSIC) Laboratory*

The CSIC will incorporate 4 specially designed low noise, shielded rooms, where in-house detailed structural characterization of thin films, interfaces, and nanostructures will be performed. Some of the techniques will be installed are an HRTEM with aberration control (and a possible cryogenic stage) and a dual beam FIB. The installation of an atom probe system is being considered. Two of this low noise shielded rooms are being reserved for special equipment design and test, and for low noise device test.

## **2. Strategic Goals**

When the idea of creating INL was publicly announced for the first time in 2005, it was stated that its mission would be to implement a strong cooperation of both countries in ambitious science and technology joint ventures. So INL aims at being a common point of reference for the excellence groups of the Iberian Peninsula and a key factor in increasing the scientific collaboration between the two countries. On the other hand, most of Iberian groups are working on Nanoscience, only a few of them on Nanotechnology. Similarly to USA, Japan and other European countries, INL also aims at boosting Nanotechnology, leading to practical applications, collaboration with already existing enterprises and the creation of spin-off companies. Obviously, the fundamentals of Nanoscience will be useful for this strategy. Finally, INL will offer new equipment, not yet existing in many of the Portuguese and Spanish laboratories, and will try to complement the already existing instrumentation of both countries.

In summary, it is a strategic goal of the Laboratory to act as a cohesive and strengthening factor in both the Spanish and Portuguese N&N communities and, above all, as a link between them. Furthermore, in its earlier stages, INL will also need their support and help. To fulfil its stated mission, INL must necessarily be perceived by as an impartial and useful entity. With your help we hope to be able to succeed.



Fig 1. A physical model of the future INL campus (from the Basis of Design)

## PHOTOLUMINESCENT MICROPOROUS LANTHANIDE SILICATES AND METAL-ORGANIC FRAMEWORKS

*João Rocha*

*University of Aveiro, CICECO, Department of Chemistry, 3810-193 Aveiro, Portugal*  
[rocha@ua.pt](mailto:rocha@ua.pt)

In the nanotechnology era, although the ‘conventional’ areas of application of zeolites will remain important, microporous solids will find uses in new fields such as optoelectronics. In the early nineties of the last century, zeolite-type silicates built up of transition-metals (mostly Ti) heteropolyhedra, were developed [1]. By the turn of the century, the constituent elements of heteropolyhedral silicates were extended to lanthanides (Ln) and, thus, photoluminescence properties became available [1-3]. The work in the field of ‘bright zeolites’ culminated with the reports of: (i) an intriguing chiral system  $\text{Na}_3[(\text{Y,Ln})\text{Si}_3\text{O}_9]\cdot 3\text{H}_2\text{O}$  for which it was shown that  $\text{Eu}^{3+}$  photoluminescence spectroscopy with excitation by unpolarised light in the absence of an external magnetic field is able to identify enantiomeric domains in chiral frameworks [4]; and (ii)  $\text{K}_7\text{Eu}_3\text{Si}_{12}\text{O}_{32}\cdot 3\text{H}_2\text{O}$ , which possesses isolate  $\text{Eu}^{3+}$  centres and  $\text{Eu}^{3+}\text{—Eu}^{3+}$  dimers and exhibits a remarkably long emission  $^5\text{D}_0$  lifetime of *ca.* 12 ms at 10 K.

With the turn of the century there was a surge of activity on inorganic-organic hybrid solids known as coordination polymers or metal-organic frameworks (MOFs). These materials are of considerable interest because the combination of inorganic and organic fragments produces a large number of new crystal architectures and allows the design of solids with specific functions. Interesting properties which may lead to industrial applications include gas storage and separation, catalysis, guest-exchange and sensors based on optical and magnetic properties. So far, only 10% or so of MOFs are effectively microporous and exhibit zeolite-type behaviour. In particular, very little work is available on microporous photoluminescent MOFs [5,6]. Recently, in collaboration with Corma’s group in Valencia, we reported a new family of magnetic nanoporous MOFs whose quantum yields and efficiencies are the highest reported for solid-state  $\text{Eu}^{3+}$  compounds with organic ligands. An ethanol sensor based on the variation of the fluorescence signal at 619 nm was developed [7].

In this talk I shall show the kaleidoscopic opportunities to engineer photoluminescent centres offered by lanthanide-based microporous silicates and inorganic-organic hybrid MOFs.

### References:

- [1] Rocha, J., Lin, Z., in *Micro- and Mesoporous Mineral Phases, Reviews in Mineralogy and Geochemistry*, Ferraris G. and Merlino S. (eds.), Mineralogical Society of America, Geochemical Society, 2005, Vol 57, Chapter 6, 173.
- [2] Ferreira, A., Ananias, D., Carlos, D., Morais, C. M., Rocha, J., *J. Am. Chem. Soc.*, 125 (2003) 14573.
- [3] Ananias, D., Ferreira, A., Rocha, J., Ferreira, P., Rainho, J.P., Morais, C., Carlos, L.D., *J. Am. Chem. Soc.*, 123 (2001) 5735.
- [4] Ananias, A., Paz, F.A.A., Carlos, L.D., Geraldes, F.G.C., Rocha, J., *Angew. Chem. Int. Ed.*, 45 (2006) 7938.
- [5] Shi, F. N., Cunha-Silva, L., Sá Ferreira, R. A., Mafra, L., Trindade, T., Carlos, L. D., Paz, F. A. A., Rocha, J., *J. Am. Chem. Soc.*, 130 (2008) 150.
- [6] Cunha-Silva, L., Mafra, L., Ananias, D., Carlos, L. D., Rocha, J., Paz, F. A. A., *Chem. Mat.*, 19 (2007) 3527.
- [7] Harbuzaru, B. V., Corma, A., Rey, F., Atienzar, P., Jordá, J. L., García, H., Ananias, D., Carlos L. D. and Rocha, J., *Angew. Chem. Int. Ed.*, 47 (2008) 1080.



## **DIMENSIONALITY EFFECTS IN THE OPTICS OF BN NANOSTRUCTURES: APPLICATIONS FOR OPTOELECTRONIC DEVICES**

*Claudio Attacalite<sup>1</sup>, [Angel Rubio](mailto:angel.rubio@ehu.es)<sup>1</sup>, Ludger Wirtz<sup>2</sup>, Andrea Marini<sup>3</sup>*

<sup>1</sup>*European Theoretical Spectroscopy Facility (ETSF) and Nano bio Spectroscopy Group, Dpto. Física de Materiales, Universidad Pais Vasco, Centro Mixto CSICUPV/EHU 20018 Donostia (Spain). <http://nano-bio.ehu.es>*

<sup>2</sup>*Institute for Electronics, Microelectronics, and Nanotechnology (IEMN), Lille, France*

<sup>3</sup>*Instituto Nazionale per la Fisica della Materia e Dipartimento di Fisica dell'Universita di Roma Tor Vergata Via della Ricerca Scientifica, I-00133 Roma, Italy  
[angel.rubio@ehu.es](mailto:angel.rubio@ehu.es)*

We illustrate the effect of dimensionality and electron-hole attraction in boronitride (BN) compounds. The optical absorption spectra of BN nanotubes are dominated by strongly bound excitons. The absolute position of the first excitonic peak is almost independent of the tube radius and system dimensionality. This provides an explanation for the observed optical gap constancy for different tubes and bulk hexagonal BN. Furthermore, the levels which are responsible for defect-mediated photo-luminescence are shifted by the electric field making BN nanotubes excellent candidates for optoelectronic applications in the UV and below.



## CARBON NANOSTRUCTURES: OPTICAL PROPERTIES FROM TDDFT STUDIES AND COMPLEX MAGNETIC BEHAVIOUR OF SUBSTITUTIONAL TRANSITION METAL IMPURITIES

D.Sánchez-Portal<sup>1,2</sup>

<sup>1</sup>*Centro de Física de Materiales, Centro Mixto CSIC-UPV/EHU,  
Apdo. 1072, 20080 San Sebastián, Spain*

<sup>2</sup>*Donostia Internacional Physics Center (DIPC), Paseo Manuel de Lardizabal, 4, 20018 San  
Sebastián, Spain  
sqbsapod@sc.ehu.es*

We report a theoretical study of substitutional Ni, Co and Fe impurities in graphene. Only Co impurity is magnetic with a moment of  $\sim 1\mu_B$ . Ni substitutional impurities, whose presence in carbon nanotubes has been recently proposed by Ushiro *et al.*[1] from the analysis of extended x-ray absorption fine structure (EXAFS) and x-ray absorption near edge structure (XANES) data, show zero magnetic moment. However, the situation is different, and far more complex, for the Ni substitution in carbon nanotubes. Although the main features of the electronic structure of the Ni defect do not depart strongly from those of the substitutional dopant in graphene, some of the fine details are different leading to the appearance of a magnetic moment. In particular, the positions of some of the defect bands close to the Fermi level show a dependency on the curvature of the tube and the dopant concentration. This gives rise to a complex behavior of the magnetic moment of the Ni defect as a function of these parameters. The magnitude of the magnetic moment shows a complex, non-monotonic behavior as a function of the tube diameter and the impurity concentration (see the Figure below). Non-zero magnetic moments only occur for metallic tubes whereas for semiconducting tubes the magnetic moment remain always zero, like in the case of graphene. This may provide a route to unambiguously identify metallic carbon nanotubes.

In the second part of the talk we briefly present an ab initio study of the optical absorption and dielectric properties of small-diameter carbon nanotubes and other carbon nanostructures using time dependent density functional theory (TDDFT) is presented. The calculations have been performed using the SIESTA program [2]. This code performs standard pseudopotential density functional calculations using a linear combination of atomic orbitals as a flexible basis set. It has been specially optimized for the treatment of very large systems. I have recently participated in the implementation of TDDFT in this program [3]. The scheme used to calculate the optical response in this implementation follows closely the method proposed by Yabana and Bertsch [4]. The idea is to apply an external perturbation to the system at time equal zero. The system is then allowed to evolve by solving the time dependent Kohn-Sham equations. The self-consistent Hamiltonian is computed at each time step and time evolution operator recalculated from it. From the computed time evolution of the density it is possible to obtain information about the dielectric response of the system. Besides the study of the optical properties of carbon nanotubes the method has been recently applied to the study of the electronic stopping in insulators [5].

The work on substitutionally doped carbon nanotubes has been performed in collaboration with E. J. G. Santos, A. Ayuela, S. B. Fagan, J. Mendes Filho, D. L. Azevedo and A. G. Souza Filho

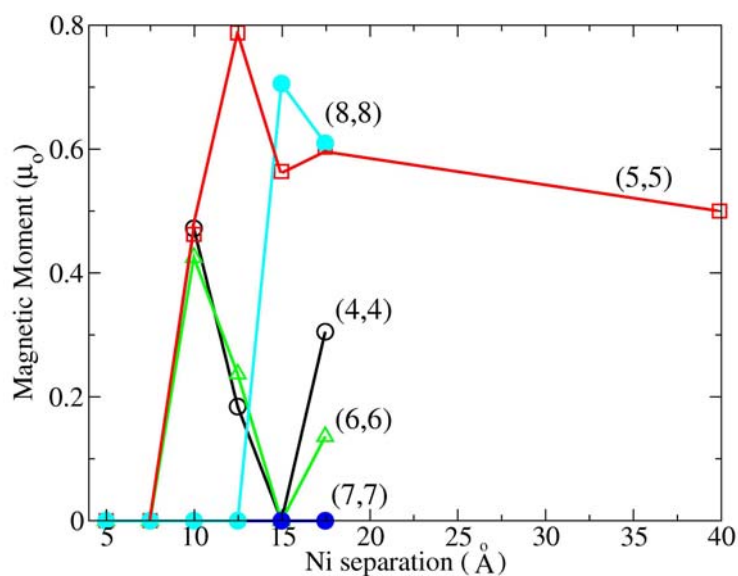


Figure. Magnetic moment associated to a nanotube with a Ni substitutional impurity as a function of the Ni-Ni separation (i.e., size of the supercell used in the calculations) for different metallic armchair tubes.

### References:

- [1] M. Ushiro, K. Uno, T. Fujikawa, Y. Sato, K. Tohji, F. Watari, W.-J. Chun, Y. Koike, and K. Asakura, *Phys. Rev. B* **73**, 144103 (2006)
- [2] A. Tsolakidis, D. Sánchez-Portal, and R. M. Martin, *Phys. Rev. B* **66**, 235416 (2002).
- [3] J. M. Soler, E. Artacho, J. D. Gale, A. García, J. Junquera, P. Ordejón, D. Sánchez-Portal, *J. of Phys.: Cond. Matter* **14**, 2745 (2002), and references therein.
- [4] K. Yabana and G. F. Bertsch, *Phys. Rev. B* **54**, 4484 (1996).
- [5] J. M. Pruneda, D. Sánchez Portal, A. Arnau, J. I. Juaristi, E. Artacho, *Phys. Rev. Lett.* **99**, 235501 (2007)

## MWCNT ACTIVATION AND ITS INFLUENCE ON THE CATALYTIC PERFORMANCE OF PT/MWCNT CATALYSTS FOR SELECTIVE HYDROGENATION

A. Solhy<sup>a</sup>, B. F. Machado<sup>b</sup>, J. Beausoleil<sup>a</sup>, Y. Kihn<sup>c</sup>, F. Gonçalves<sup>b</sup>, M. F. R. Pereira<sup>b</sup>, J. J. M. Órfão<sup>b</sup>, J. L. Figueiredo<sup>b</sup>, J. L. Faria<sup>b\*</sup> and P. Serp<sup>a</sup>

<sup>a</sup>*Laboratoire de Chimie de Coordination UPR CNRS 8241 composante ENSIACET, Toulouse University, 118 route de Narbonne, 31077 Toulouse Cedex 4, FRANCE*

<sup>b</sup>*Laboratório de Catálise e Materiais, Departamento de Engenharia Química, Faculdade de Engenharia, Universidade do Porto, 4200 - 465 Porto – Portugal*

<sup>c</sup>*CEMES-UPR CNRS 8011, 2 rue Jeanne Marvig, 31055 Toulouse, France*

Philippe.Serp@ensiacet.fr

Carbon nanotubes (CNTs) present remarkable intrinsic properties [1], but, for many applications in which they have to interact with or to be integrated in a given system, it is necessary to functionalize their surfaces to obtain higher performances. In particular, even though no specific study has yet appeared on the subject, it has been shown that functionalization should be performed to produce well dispersed supported catalysts [2]. Multi-walled carbon nanotubes were submitted to three activation procedures: nitric acid oxidation, ball-milling and air oxidation. The influence of these treatments on nanotubes surface chemistry and morphology was evaluated by XPS, Raman and infrared spectroscopy, TGA, TPD, nitrogen adsorption and TEM. The three activated materials were used to prepare Pt supported catalysts from the organometallic precursor [Pt(CH<sub>3</sub>)<sub>2</sub>(C<sub>8</sub>H<sub>12</sub>)]. The influence of the activation treatments, together with that of a post-reduction thermal treatment, on the performances of the catalytic systems in the selective hydrogenation of cinnamaldehyde was investigated. It was shown that the best compromise between catalyst activity and selectivity required a low amount of oxygenated groups on the support surface of the final catalyst together with an optimized platinum particle size.

1. Introduction to carbon nanotubes, M. Monthieux, P. Serp, E. Flahaut, C. Laurent, A. Peigney, M. Razafinimanana, W. Bacsa, J.-M. Broto. In, "Springer handbook of nanotechnology" Second revised and extended Edition B. Bhushan (ed.), Springer-Verlag, Heidelberg, Germany, 2007, 43-112.
2. Carbon nanotubes and nanofibers in catalysis, P. Serp, M. Corrias, P. Kalck, Appl. Catal. A, 253, 2003, 337-358.



## MAGNETIC AND STRUCTURAL PROPERTIES OF IRON OXYHYDROXYNITRATE NANOPARTICLES

*N. J. O. Silva<sup>1</sup>, V. S. Amaral<sup>2</sup>, L. D. Carlos<sup>2</sup>, Angel Millán<sup>1</sup>, Fernando Palacio<sup>1</sup>, Benito Rodríguez-González<sup>3</sup>, Luis M. Liz-Marzán<sup>3</sup>, Thelma Berquó<sup>4</sup>, F. Fauth<sup>5</sup>, Verónica de Zea Bermudez<sup>6</sup>*

<sup>1</sup>*Instituto de Ciencia de Materiales de Aragón, CSIC-Universidad de Zaragoza, 50009 Zaragoza, Spain.*

<sup>2</sup>*Departamento de Física and CICECO, Universidade de Aveiro, 3810-193 Aveiro, Portugal.*

<sup>3</sup>*Departamento de Química Física, Universidade de Vigo, 36310 Vigo, Spain.*

<sup>4</sup>*Institute for Rock Magnetism, University of Minnesota, Minneapolis 55455-0128, USA.*

<sup>5</sup>*Labor. Llum Sincrotró, BM16-CRG, c/o ESRF, 6 rue Jules Horowitz, BP220, 38043 Grenoble, France.*

<sup>6</sup>*Departamento de Química, Universidade de Trás-os-Montes e Alto Douro and CQ-VR, Quinta de Prados, Apartado 1013, 5001-911 Vila Real, Portugal.*

[nunojoao@unizar.es](mailto:nunojoao@unizar.es)

Iron oxyhydroxynitrate, with general formula  $\text{FeO}(\text{OH})_{1-x}(\text{NO}_3)_x$  ( $0.2 < x < 0.3$ ), is an ordered precursor of 6-line ferrihydrite in the process of hydrolysis of an iron nitrate salt in aqueous solution [1]. The iron(III) oxyhydroxynitrate was obtained for the first time in the form of a powder consisting of aggregated nanoparticles after freeze drying a Fe(III) nitrate water solution [1,2]. Here we report magnetic and structural properties on iron(III) oxyhydroxynitrate nanoparticles with different average sizes grown in a organic-inorganic hybrid matrix and compare them to those of other iron oxides. The use of a matrix to grow iron(III) oxyhydroxynitrate allowed to access the magnetic properties of the isolated nanoparticles. The first step of the nanohybrids preparation involves the synthesis of a cross-linked organic-inorganic hybrid precursor, similar to the one used in the synthesis of an undoped matrix, termed di-ureasil [3]. In the second step, a solution of iron(III) nitrate nonahydrate, water and ethanol was added to the non-hydrolyzed hybrid precursor. The resulting mixture was then stirred in a sealed flask for a few minutes at RT. After this, the solution was cast into a mould and transferred to an oven at ca. 40 °C during 7 days. Samples were obtained after aging for 3 weeks at ca. 80 °C. Samples were labelled Ih( $x$ ), where  $x$  is the iron mass concentration.

The powder XRD patterns of the two most concentrated samples of Ih nanohybrids (Fig. 1a) show that iron(III) oxyhydroxynitrate nanoparticles were efficiently stabilized in the matrix. Differences between patterns of iron(III) oxyhydroxynitrate and ferrihydrite are apparent: in the iron(III) oxyhydroxynitrate nanoparticles XRD patterns the relative intensity of the double peak at 60-65 °C is the opposite of that of ferrihydrite, and the shoulder appearing at 33 °C in the ferrihydrite nanoparticles is not present in the Ih nanohybrids. TEM images of the Ih(3.8) and Ih(6.5) nanohybrids show the presence of globular-shaped nanoparticles, with diameters of the order of 3 nm. The nanoparticles have nonfaceted and fuzzy edges and the nanoparticles/matrix contrast is low. SAXS patterns of Ih nanohybrids can be modelled as spherical isotropic and diluted Ih nanoparticles dispersed in a homogeneous matrix using GNOM [4]. With this analysis we conclude that the particles size increases with the iron content. The temperature dependence of the dc susceptibility  $\chi$  shows that the Ih nanoparticles are superparamagnetic (Fig. 1b). The zero-field-cooled curves present a maximum at  $T = T_B$  that increases with the iron content (Fig. 1b, inset). This increase agrees qualitatively with the observed size increase, since the anisotropy energy  $E_a$  and therefore  $T_B$  are expected to be related to size by a positive power. Below  $T \approx T_F$ , the  $M(H, T)$  curves of the Ih nanocomposites

show irreversibility, that depends on the sample temperature and field history. Above  $T \approx T_F$ , the  $M(H, T)$  curves of the Ih nanohybrids are reversible, and can be described as having linear and partial saturation components, associated to the antiferromagnetic susceptibility and the uncompensated moment, respectively. For  $T > T_B$ , a paramagnetic-like doublet in the Mössbauer spectra of the Ih nanohybrids is observed, as expected for unblocked superparamagnetic particles. For temperatures below  $T_B$ , the Mössbauer spectrum is magnetically split in a sextet. As observed in the susceptibility,  $T_B$  identified with Mössbauer increases with the iron content. In sample Ih(6.5), the magnetic hyperfine field  $B_{hf}$  at 4.2 K is similar to that previously found for iron(III) oxyhydroxynitrate powders ( $B_{hf} = 450\text{--}460$  kOe [2]), being lower than that of 6-line ferrihydrite. At the same time, the isome shift  $QS$  shows some differences when compared to that usually found in 6-line ferrihydrite ( $-0.06$  mm/s), approaching for that fitted for schwertmannite ( $QS = -0.37$  mm/s at 4.2 K).

## References:

- [1] U. Schwertmann, J. Friedl, and H. Stanjek, *J. Coll. Interface Sci.*, **209** (1999) 215.
- [2] U. Schwertmann, J. Friedl, and G. Pfab, *J. Sol. State Chem.*, **126** (1996) 336.
- [3] V. de Zea Bermudez, L. D. Carlos, and L. Alccer, *Chem. Mater.*, **11** (1999) 569.
- [4] D. Svergun, *J. Appl. Cryst.*, **25** (1992) 495.

## Figures:

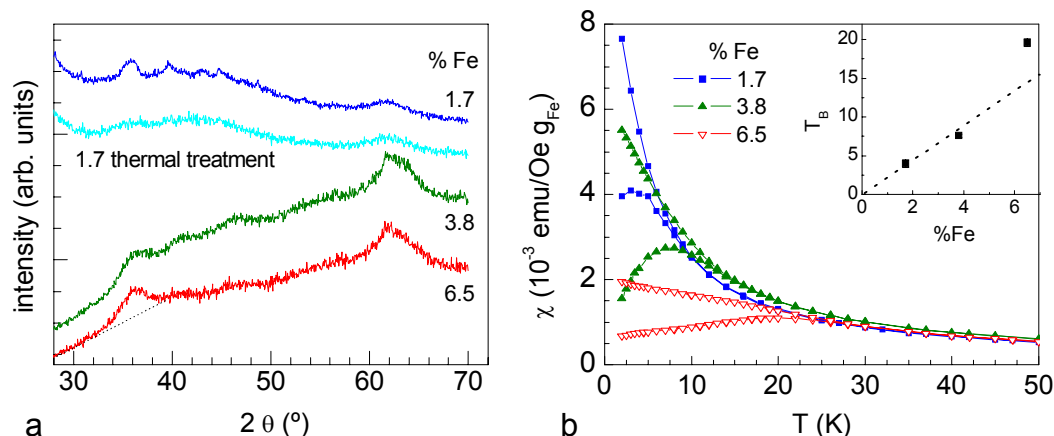


**Fig 1.** a. X-ray diffraction (XRD) patterns of Ih(x) nanohybrids and sample Ih(1.7) after a thermal treatment; b. dc susceptibility  $\chi$  of Ih nanohybrids as a function of temperature. Inset shows the dependence of  $T_B$  with the iron content.

## GRAPHENE ON Ru(0001): SPATIALLY RESOLVED ELECTRONIC STRUCTURE

*A.L. Vázquez de Parga<sup>1</sup>, B. Borca<sup>1</sup>, F. Calleja<sup>1</sup>, M.C.G. Passeggi Jr.<sup>2</sup>, J.J. Hinarejos<sup>1</sup>, F. Guinea<sup>2</sup> and R. Miranda<sup>1,4</sup>*

<sup>1</sup>*Dep. Física de la Materia Condensada, Universidad Autónoma de Madrid, Cantoblanco 28049, Madrid, Spain*

<sup>2</sup>*Laboratorio de Superficies e Interfases, INTEC (CONICET) and UNL, S3000GLN, Santa Fe, Argentina*

<sup>3</sup>*Instituto de Ciencia de Materiales, Consejo Superior de Investigaciones Científicas, Cantoblanco 28049, Madrid, Spain*

<sup>4</sup>*Instituto Madrileño de Estudios Avanzados en Nanociencia (IMDEA Nanociencia), Cantoblanco 28049, Madrid, Spain*

*al.vazquezdeparga@uam.es*

The possibility to produce single layers of graphene [1,2] has opened a fascinating new world of physical phenomena in two dimensions. Graphene has already shown that its charge carriers are massless Dirac fermions [3-7] and that it displays an anomalous integer Quantum Hall Effect [3-5] even at room temperature [8]. While ultra-thin epitaxial films of graphite and even "monolayer-graphite" have been grown on solid surfaces by Chemical Vapor Deposition for quite some time [9], the degree of characterization of the films was hampered by experimental limitations. Systems made up of a few graphene layers have been grown on SiC substrates. Recently it has been claimed that a free standing isolated graphene layer is intrinsically corrugated. Charge inhomogeneities have also been observed in nominally undoped samples. Thus, so far, structural ripples and charge inhomogeneities have been observed separately.

We report on a method to fabricate highly perfect, periodically rippled graphene monolayers and islands on Ru(0001) under Ultra High Vacuum conditions. The graphene layers were produced by thermal decomposition at 1000 K of ethylene molecules pre-adsorbed at 300 K on the sample surface. The epitaxial layer of graphene covers completely the surface of the single-crystal Ru substrate over distances larger than a micron and presents a triangular periodicity of 2.4 nm that is due to the coincidence lattice of graphene and Ru, i.e. the lattice of graphene has a size relation with the underlying Ru lattice that implies that 11 carbon honeycombs (0.246 nm) will adjust almost exactly with 10 Ru-Ru interatomic distances (0.27 nm). The weakly interacting, laterally undistorted graphene structure rides on top of the lattice of the substrate, resulting in some C atoms being slightly higher than others.

The periodic charge inhomogeneities in the graphene layer can be visualized directly in the real space by means of scanning tunnelling microscopy/spectroscopy imaging the spatial distribution of  $dI/dV$  close to the Fermi energy. Fig.1 shows the spatial distribution of the LDOS below and above the Fermi level. The experimental images are in the upper row at the left and the right of the corresponding topographic image. The bright regions correspond to larger LDOS. In our case, the inhomogeneities in the charge distribution are spatially correlated with the ripples in the graphene layer. The reason behind is the periodic modulation of the potential, due to changes in the metallic screening from the substrate.

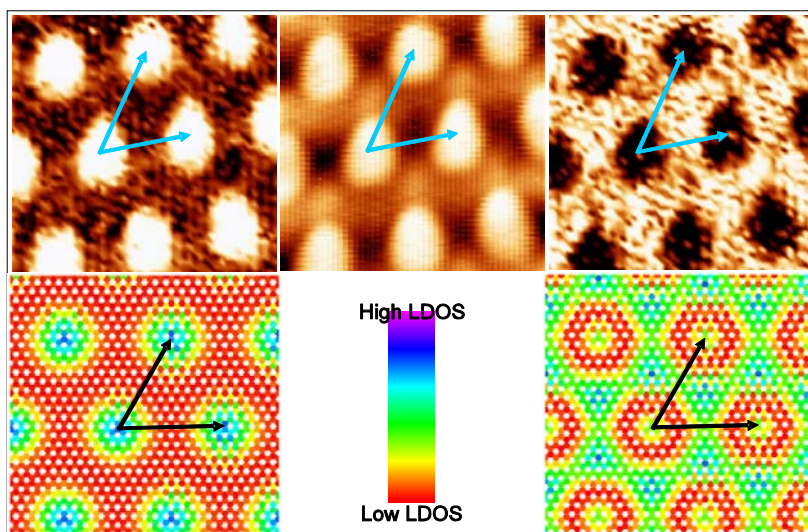
This inhomogeneity can be simulated with a tight-binding model which incorporates a periodic potential associated with the structural ripples that induces a shift of the electronic levels and a corresponding charge transfer from conduction to valence bands for some atoms and the opposite in the others. In agreement with the experiments, the calculations show that

the occupied LDOS is larger on the "high" regions of the superlattice, where the potential is at a minimum, while the empty LDOS is larger at the "low" regions of the graphene layers

### References:

- [1] K.S. Novoselov et al. *Science* **306**, 666 (2004)
- [2] A.K. Geim and K.S. Novoselov, *Nature Mater.* **6**, 183 (2007)
- [3] K.S. Novoselov et al. *Nature* **438**, 201 (2005)
- [4] Y. Zhang et al. *Nature* **438**, 201 (2005)
- [5] K.S. Novoselov et al. *Nature Phys.* **2**, 177 (2006)
- [6] V.P. Gusynin and S.G. Sharapov, *Phys. Rev. Lett.* **95**, 146801 (2005)
- [7] N.M.R. Peres, F. Guinea and A.H. Castro-Neto, **315**, 1379 (2007)
- [8] K.S. Novoselov et al. *Science* **315**, 1379 (2007)
- [9] Ch. Oshima and A. Nagashima, *J. Phys.: Condens. Matter* **9**, 1 (1997)

**Figure 1:** The left and right images in the upper panel are maps of  $dI/dV$  at -100 meV and +200 meV and reflects the spatial distribution of the LDOS below and above the Fermi level, respectively, for an extended graphene layer on Ru(0001). The central image shows the topographic image recorded simultaneously. The lower panel shows the corresponding calculations for the spatially resolved LDOS for a (11x11) periodically corrugated graphene layer.



## ELECTRON ENERGY LOSS SPECTROMETRY IN THE TEM: CHEMICAL INFORMATION AT THE NANOMETER SCALE

*Marc-Georg Willinger*

*University of Aveiro, Chemistry Department, CICECO, 3810-193 Aveiro, Portugal*  
[willinger@ua.pt](mailto:willinger@ua.pt)

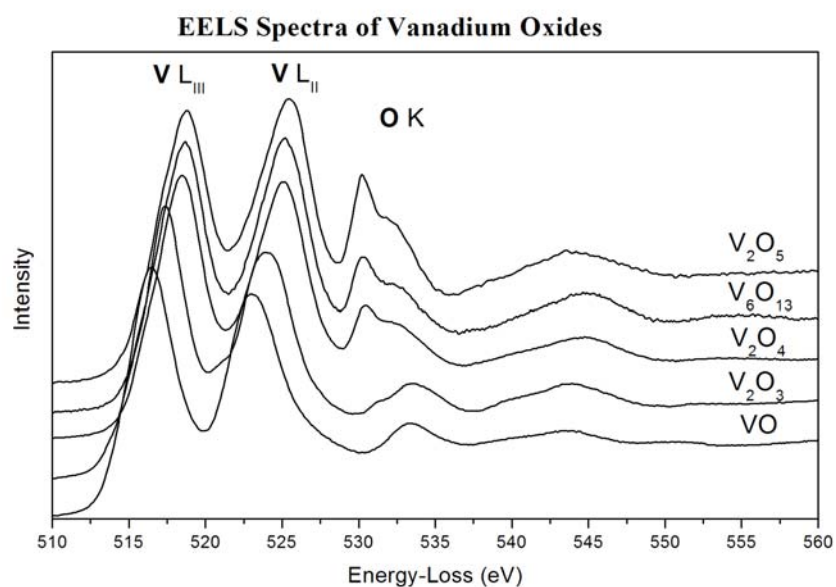
Progress in materials science and nanotechnology are closely connected with the availability of instruments that allow to study the morphology, geometric structure and chemical composition of materials at the nanometer scale. Modern analytical transmission electron microscopes (TEM) certainly fulfil this task in an unsurpassed way. Observation over a large range of magnifications, dark and bright field imaging, electron diffraction, tomography and holography are some of the imaging techniques that can be used in a well equipped analytical TEM. In addition to the imaging capabilities, there is the spectroscopic part and most analytical instruments are equipped with energy dispersive detectors for the detection of characteristic X-rays or electron energy losses caused in inelastic interactions between the probing electrons and the sample material. Especially electron energy loss spectrometry (EELS) is used for the characterization of inelastic scattering processes over a wide energy range, including plasmon and valence band excitations as well as core shell excitations. The spectra can be recorded at high special resolution and provide information about the elemental composition and electronic structure of a material. Due to the high energy resolution, EELS is very sensitive to even slight changes in the electronic structure.

The analytical power obtained by combination of EELS and TEM will be demonstrated for the case of vanadium oxides. Vanadium is able to adapt a wide range of oxidation states ranging from II+ to V+. This makes it an interesting material not only in the field of catalysis but also in energy storage, where vanadium oxides are used for the intercalation of Li ions. The shape and fine structure of the vanadium L and oxygen K edges change in function of the vanadium oxidation state and the geometric arrangement of the oxygen atoms coordinating the vanadium [1] (Fig. 1). This can be used for the identification of the oxidation state of a vanadium oxide species as shown for example in Fig. 2 for the case of a vanadium oxide cluster dispersed on the surface of a multi walled carbon nanotube.

Taking vanadium phosphorous oxides as an example it will further be shown that by the assistance of band structure calculations based on density functional theory and simulated EELS spectra, contributions from differently coordinated atoms to the observed spectrum can be identified [2].

### References:

- [1] C. Hébert, M. Willinger, D.S. Su, P. Pongratz, P. Schattschneider, R. Schlögl, Eur. Phys. J. B. **28** (2002) 407
- [2] M.-G. Willinger, D. S. Su, R. Schlögl, Phys Rev B **71** (2005) 155118.

**Figures:**

**Fig. 1.** Vanadium  $L_{III}$ ,  $L_{II}$  and oxygen K ionization edges recorded for different binary vanadium oxides. Clearly visible are the shift in position and the changes in the intensity ratio of the vanadium L edges as a function of the vanadium oxidation state. The structure of the oxygen K ionization edge also changes drastically when going from  $V_2O_5$  to VO.

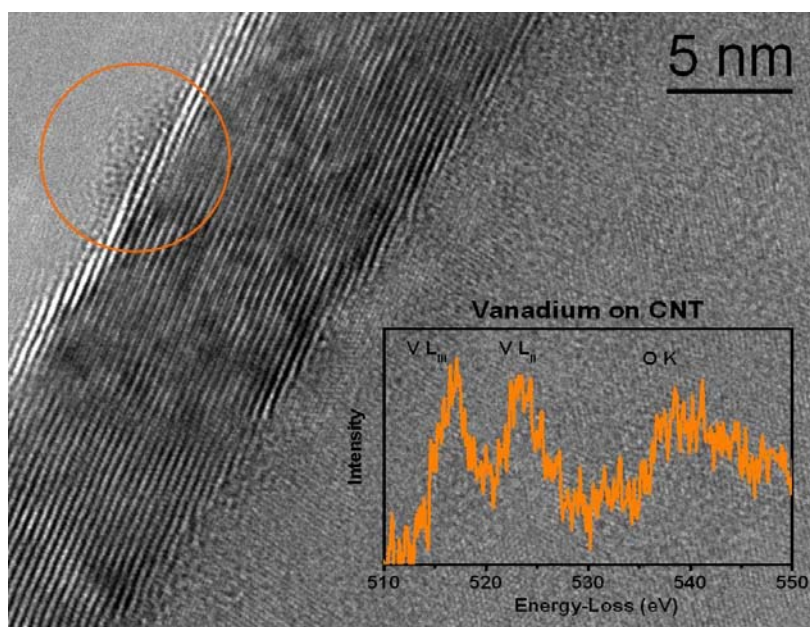


**Fig. 2.** Although the spectrum recorded from the region indicated by the circle is very noisy, the energetic position of the ionization edges allows the assignment of a  $V^{III+}$  oxidation state for the vanadium oxide cluster on the surface of the carbon nanotube.

## SELF-ASSEMBLING AND GUIDED SELF-ORGANIZATION OF OXIDE NANOSTRUCTURES FROM CHEMICAL SOLUTIONS

T. Puig, M. Gibert, J. Zabaleta, N. Mestres, X. Obradors  
Institut de Ciència de Materials de Barcelona, CSIC, 08193 Bellaterra, Spain

The appearance of new functionalities and devices arising from size- and shape-dependent properties has triggered the interest in creating well-defined structures at the nanometric-scale. Self-organizing and self-assembling processes following a bottom-up approach can easily decrease the size limit and also cover cost-effectively much larger surfaces. We present a general methodology for the generation of strain-induced self-assembled oxide nanostructures grown from chemical solutions, a bottom up technique with great potentiality. Control and tuning of morphology, size, distribution and orientation of the resulting interfacial oxide nanostructures through processing parameters like time, atmosphere, temperature is achieved. In particular, special attention is given to the growth of fluorite  $\text{Ce}_{1-x}\text{Gd}_x\text{O}_{2-y}$  (CGO) on perovskite single crystalline substrates in which case the particular orientations of the oxide nanostructures, (011)CGO[1-10]|||(001)ABO<sub>3</sub>[100], (001)CGO[110]|||(001)ABO<sub>3</sub>[100], (011)CGO[1-10]|||(011)ABO<sub>3</sub>[110] controls the different kinetics and make it very suitable for the study of mechanisms leading the evolution of the interfacial nanostructures [1]. The interplay between interfacial energy and strain relaxation energy determine the resulting shape instability giving rise to elongated nanowalls with lateral aspect ratio ( $c$ =long axis/small axis) as large as  $c\sim 35$  (see Figure 1). However, self-organization and localization control of these nanostructures is a complex issue unless they are guided by assisted methodologies. Mechanical modification of the substrate by means of Nanoindentation has been used for assisting the self-organization of  $\text{Ce}_{0.9}\text{Gd}_{0.1}\text{O}_{2-y}$  nanoislands. We will demonstrate that the application of ultra low loads,  $<10$  nN, and deformations  $<100$  nm, on the single crystal perovskite substrate results in the localization and orientation of the  $\text{Ce}_{1-x}\text{Gd}_x\text{O}_{2-y}$  nanowalls along the nanoindented scratches (see Figure 2). The controlled alteration of the relaxation and interfacial energies by the appearance of convex and concave curvatures, are at the origin of the observed CGO localization.

[1] M. Gibert et al., *Advanced Materials*, **19**, 3937 – 3942 (2007)

We acknowledge financial support from MEC (MAT2005-02047, NAN2004-09133-C03-01, MAT2006-26543-E;FPU, Consolider NANOSELCT), Generalitat de Catalunya (Pla de Recerca SGR-0029 and CeRMAE), CSIC(PIF-CANNAMUS) and EU (HIPERCHEM, NESPA)

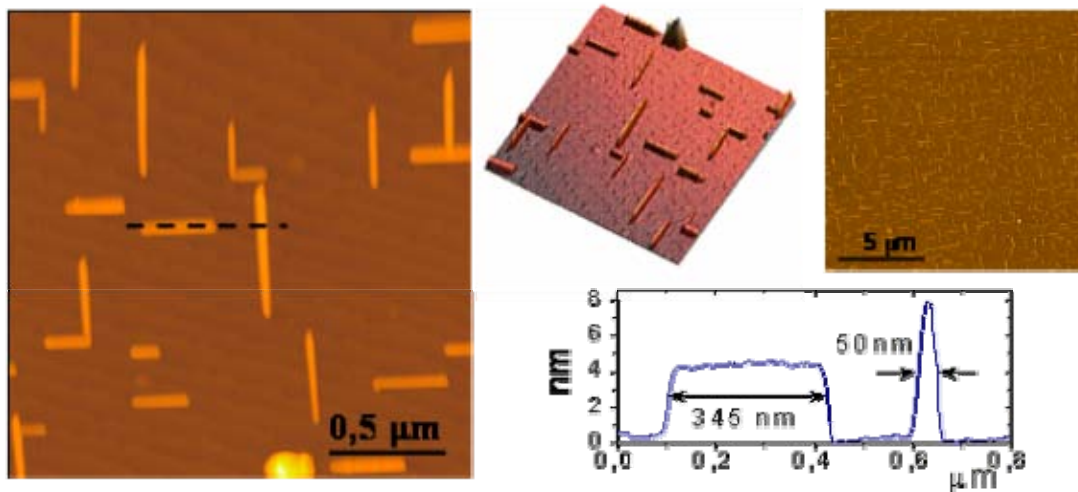


Figure 1. Highly anisotropic self-assembled  $\text{Ce}_{1-x}\text{Gd}_x\text{O}_{2-y}$  nanostructures on  $\text{LaAlO}_3$  prepared from chemical solutions

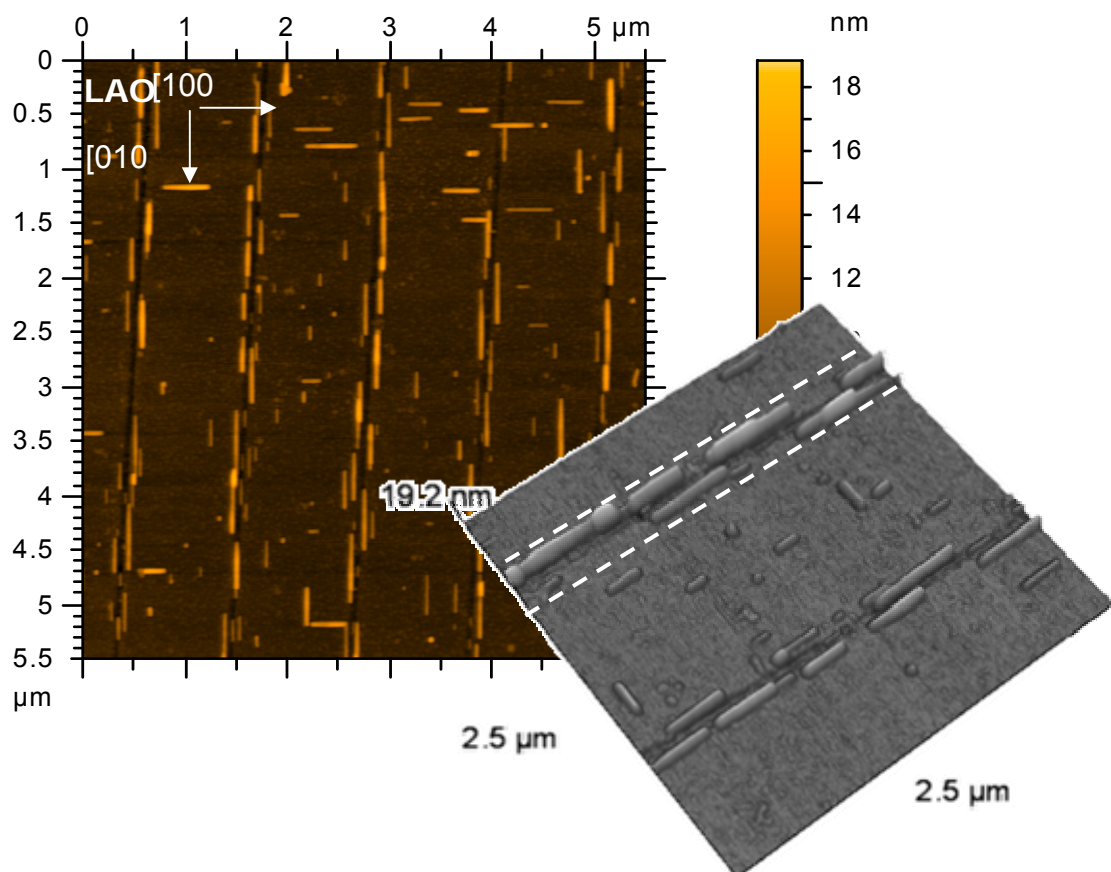


Figure 2.  $\text{Ce}_{0.9}\text{Gd}_{0.1}\text{O}_2$  nanowalls grown on  $\text{LaAlO}_3$  single crystals where controlled scratched deformation by nanoindentation has been previously performed. The localization and orientation of the nanowalls is determined by the nanoindented regions.

## SELF-HEALING COATINGS WITH MULTI-LEVEL PROTECTION BASED ON ACTIVE NANOCONTAINERS

*Mikhail Zheludkevich<sup>1</sup>, Dominik Raps<sup>2</sup>, Alexandre Bastos<sup>2</sup>, Theo Hack<sup>2</sup>, Mario G.S. Ferreira<sup>1</sup>*  
<sup>1</sup>*University of Aveiro, CICECO, Dep. Ceramics and Glass Eng., 3810-193, Aveiro, Portugal*  
<sup>2</sup>*EADS Innovation Works, 81663 Munich, Germany*

[mzheludkevich@ua.pt](mailto:mzheludkevich@ua.pt)

The destructive effect of environment and the corrosion induced degradation are the important problems which determine the service life of many metallic components. The application of organic coatings is the most common and cost effective method of improving protection and durability of metallic structures. However the degradation processes develop faster after disruption of the protective barrier. Therefore an active protection based on “self-healing” of defects in coatings is necessary to provide long-term effect.

The term “self-healing” in materials science means self-recovery of the initial properties of the material after destructive actions of external environment. The same definition can be applied to functional coatings. However, a partial recovery of the main functionality of the material can also be considered as a self-healing ability. Thus, in the case of corrosion protective coatings the term “self-healing” can be interpreted in different ways. The classical understanding of self-healing is based on the complete recovery of the functionalities of the coating due to a real healing of the defect based on the recovery of the coating integrity. However, the main function of anticorrosion coatings is the protection of an underlaid metallic substrate against an environment-induced corrosion attack. Thus, it is not obligatory to recuperate all the properties of the film in this case. The hindering of the corrosion activity in the defect by the coating itself employing any mechanisms can be already considered as self-healing, because the corrosion protective system recovers its main function, namely the corrosion protection, after being damaged.

Development of an active healing mechanism for the polymer coatings becomes an urgent issue for the respective industrial applications. Recently several attempts were made in this field using different protection/healing mechanisms for protective coatings. The first approach consists in introducing organic or inorganic inhibitors to the coating matrix in order to suppress the corrosion processes in the defects [1-3]. Another approach uses incorporation of the microcapsules containing a polymerizable component which is released forming polymer in the growing crack [4].

The present work suggests development of new active multi-level protective systems based on “smart” release nanocontainers incorporated into the polymer coating matrix. The nanocontainer (or nanoreservoir) is a nanosized volume filled with an active substance confined in a porous core and/or a shell which prevents direct contact of the active agent with the adjacent environment. A multi-level self-healing approach will combine - within one system - several damage prevention and reparation mechanisms, which will be activated depending on type and intensity of the environmental impact, as it shown in Figure 1.

Several types of nanoreservoirs of corrosion inhibitors were developed, introduced to the coating system and tested in terms of active corrosion protection. Different approaches of controllable delivery of corrosion inhibitors on demand are discussed here including the oxide and layered double hydroxide (LDH) nanoparticles, the titania nanostructured porous layer obtained by the templating synthesis, and finally “smart” nanocontainers developed using the polyelectrolyte layer-by-layer (LbL) assembled shells which can control the release of the inhibiting species.

The permeation of the polyelectrolyte layer used for creation of nanocontainers shells strongly depends on the different factors. Thus the release of the inhibitor from such a nanoreservoir can be controlled by selection of appropriate external stimuli. The release of inhibitor from polyelectrolyte covered nanocontainers can be triggered by local changes of pH in cathodic and anodic zones of corroding metal. Then the released inhibitor will react with metallic surface stopping the propagation of the corrosion and providing an “intelligent” self-healing effect.

The coatings with the LDH nanocontainers also reveal enhanced long-term corrosion protection in comparison with the undoped films. This effect is obtained due to regulated release of the corrosion inhibitor triggered by the presence of corrosive anions such as chlorides. Moreover LDH nanoparticles developed in this work can play double-effect additionally absorbing aggressive chloride anions and working as nano-traps.

The development of nanocontainers for other levels of protection are in course and is main subject of new FP7 large scale collaborative project MUST.

## References:

- [1] M.L. Zheludkevich, D.G. Shchukin, K.A. Yasakau, H. Möhwald, M.G.S. Ferreira, *Chemistry of Materials*, **19** (2007) 402.
- [2] S.V. Lamaka, M.L. Zheludkevich, K.A. Yasakau, R. Serra, S.K. Poznyak, M.G.S. Ferreira, *Progress in Organic Coatings*, **58** (2007) 127.
- [3] D.G. Shchukin, M.L. Zheludkevich, K.A. Yasakau, S.V. Lamaka, H. Möhwald, M. G.S. Ferreira, *Advanced Materials*, **18** (2006) 1672.
- [4] S. R. White, N. R. Sottos, P. H. Geubelle, J. S. Moore, M. R. Kessler, S. R. Sriram, E. N. Brown, S. Viswanathan, *Nature* **409** (2001) 794.

## Figures:

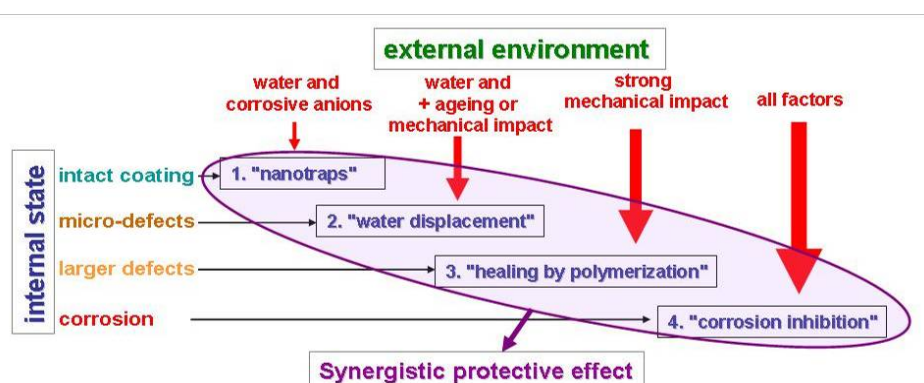


**Figure 1. Illustration of the multi-level protection approach**



## **ORAL CONTRIBUTIONS (PARALLEL SESSIONS)**



## NANOMETRIC AGGREGATES OF A COVALENT PORPHYRIN DIMER FOLLOWED BY FLUORESCENCE CORRELATION SPECTROSCOPY IN AQUEOUS BUFFERED SOLUTION

Suzana M. Andrade,<sup>a</sup> V. Vaz Serra,<sup>b</sup> M.A.F. Faustino,<sup>b</sup> M.G.P.M.S. Neves,<sup>b</sup> J.A.S. Cavaleiro<sup>b</sup>, S.M.B. Costa,<sup>a</sup>

<sup>a</sup>*Centro de Química Estrutural, Complexo I, Instituto Superior Técnico, Av. Rovisco Pais, 1049-001 Lisboa, PORTUGAL*

<sup>b</sup>*Departamento de Química, Universidade de Aveiro, Campus Universitário de Santiago, 3810-193 Aveiro, PORTUGAL*

[suzana.andrade@ist.utl.pt](mailto:suzana.andrade@ist.utl.pt)

The design of covalently linked porphyrins envisages the goal of applying it to molecular photonic devices and artificial biomimetic light-harvesting arrays. Porphyrins are well-known for their tendency to self-aggregate in aqueous solution. The type of self-aggregation can be controlled by a series of factors that include the structure of the porphyrin (substituent groups and coordinated metal ion) and environmental conditions (pH, ionic strength, temperature, cosolvents, etc).

We have recently dealt with the aggregation properties of the anionic water-soluble porphyrin, meso-tetrakis(p-sulfonatophenyl)porphyrin sodium salt TSPP induced at aqueous interfaces. It was shown that under suitable conditions of pH and ionic strength this molecule forms highly ordered molecular J and H aggregates. Interestingly, these aggregates were found to be promoted by interaction with proteins (HSA and BSA) [1], dendrimers [2] and surfactants/lipids [3, 4]. Moreover, it was possible to tune the photophysical properties of the nano-aggregates formed, within these organized systems.

The present work reports the study of the covalent dimer 5-(4-carboxyphenyl)-10,15,20-tris(3-methoxyphenyl)porphyrin with a tyrosine spacer Dim C (Fig. 1) in aqueous solution, at controlled pH and ionic strength using fluorescence techniques. Fluorescence decays obtained in water point to the existence of small undefined porphyrin aggregates which become more organized upon salt addition (5 - 25 mM) and fluorescent particles are detected ( $\tau_f \sim 200$  ps, Fig. 2a).

The characterization of these aggregates was further attempted making use of techniques combining both spatial (imaging) and temporal resolution. In particular, Fluorescence Correlation Spectroscopy (FCS) is a highly sensitive tool to measure concentration and diffusion coefficients from which we may determine binding/dissociation equilibria in the nanomolar range [5]. Based on the latter, a diffusion coefficient of  $D = 6 \pm 1 \mu\text{m}^2\text{s}^{-1}$  (Fig. 3) could be retrieved pointing to nano-aggregates of Dim C in aqueous buffered solution. A decrease in the fluorescence lifetime of Dim C in the presence of cytochrome c occurs indicating a quenching process, possibly due to electron transfer upon binding the dimer to the protein, as the decrease in the difusional time obtained by FCS suggests ( $D \sim 120 \mu\text{m}^2\text{s}^{-1}$ ).

The presence of Brij 35 nonionic micelles clearly destabilizes the porphyrin aggregates by competing hydrophobic interactions leading to incorporation of the porpyrin into the micellar moitie. This is well supported by the increase in the porphyrin lifetime ( $\tau_f \sim 12$  ns; Fig. 2b) similar to that obtained in neat DMSO and the diffusion coefficient calculated agrees well with that of diffusing Brij 35 micelles ( $D \sim 70 \mu\text{m}^2\text{s}^{-1}$ ).

**Acknowledgements:** This work was supported by POCTI/QUI//57387/2004. S.M. Andrade thanks FCT for the award of Post-Doc grant BPD/24367/2005.

## References

- [1] S.M. Andrade, S.M.B. Costa, *Biophys. J.*, 82 (2002) 1607; *ibid. J. Fluoresc.* 12 (2002) 77.  
 [2] P.M.R. Paulo, R. Gronheid, F.C. De Schryver, S.M.B. Costa, *Macromolecules* 36 (2003) 9135  
 [3] S.M. Andrade, S.M.B. Costa, *Chem. Eur. J.* 12 (2006) 1046.  
 [4] S.M. Andrade, R. Teixeira, S.M.B. Costa, A.J.F.N. Sobral, *Biophys. Chem.* 133 (2008) 1.  
 [5] S.M. Andrade, S.M.B. Costa, J.W. Borst, A. van Hoek, A.J.W.G. Visser, *J. Fluoresc.* (2008) 000.

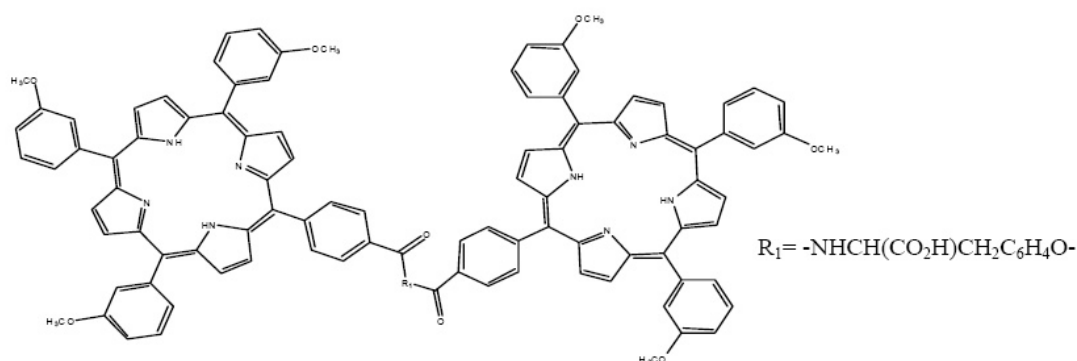


**Figure 1** Scheme of Dim C.

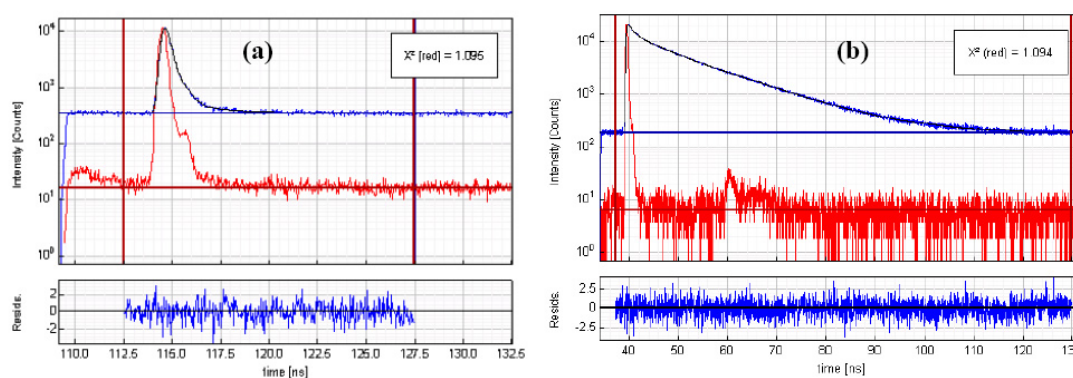


**Figure 2** Fluorescence decays of Dim C in aqueous buffer solution (a) and in the presence of Brij 35 micelles (b).

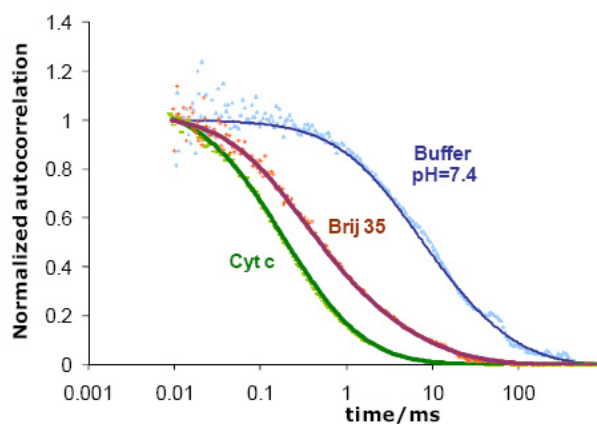


**Figure 3** - Normalized autocorrelation traces (experimental dotted lines; fitting solid lines) of Dim C (70 nM) in aqueous solution (blue) and in the presence of Cyt c (5  $\mu$ M, green) and Brij 35 micelles (1 mM; red).

## NANOTUBE BASED THERMAL MOTORS: SUB-NANOMETER MOTION OF CARGOES DRIVEN BY THERMAL GRADIENTS

*Amelia Barreiro<sup>1</sup>, Riccardo Rurali<sup>2</sup>, Eduardo R. Hernández<sup>3</sup>, Joel Moser<sup>1</sup>, Thomas Pichler<sup>4</sup>, Laszlo Forro<sup>5</sup>, Adrian Bachtold<sup>1</sup>*

<sup>1</sup>*CIN2 Barcelona and CNM-CSIC, Campus UAB, E-08913 Bellaterra, Spain*

<sup>2</sup>*Departament d'Enginyeria Electronica, Campus UAB, E-08913 Bellaterra, Spain*

<sup>3</sup>*Institut de Ciència de Materials de Barcelona, Campus UAB, E-08913 Bellaterra, Spain*

<sup>4</sup>*Faculty of Physics, University of Vienna, Strudlhofgasse 4, 01090 Wien, Austria*

<sup>5</sup>*EPFL, CH-1015 Lausanne, Switzerland*

[amelia.barreiro.icn@uab.es](mailto:amelia.barreiro.icn@uab.es)

There is a growing effort in the scientific community to design and fabricate ever more versatile nanoelectromechanical systems (NEMS). Because carbon nanotubes are very small, mechanically robust and chemically inert, they have attracted considerable interest as NEMS components. In addition, their one-dimensional tubular shape offers a natural track for motion. This tubular shape restricts the motion to only a few degrees of freedom (typically translation or rotation), much as bearings do in every-day machines.

A new generation of nanotube based motors has been envisaged that takes advantage of the atomic corrugation for a new class of tracks [1]. For example, the motion of two coaxial nanotubes relative to one another is given by the track that results from the mutual atomic interaction between the nanotubes. In some cases, the track follows energy minima that can consist of helical orbits ranging from pure rotation to pure translation. In some others, the energy barrier for motion contains local minima and maxima, arranged e.g. as a twisted chess-board like pattern (see some examples in Fig. 1 C-E) [1].

Here we report on an artificial nanofabricated motor (Fig. 1 A,B) in which one short nanotube moves relative to another coaxial nanotube and we present two major advances. First, the atomic interaction between the nanotubes is shown to generate distinct kinds of motion for different devices, namely rotation and/or translation along the nanotube axis. Figure 2 shows an example of a translational motion. Second, we show that the motion is actuated by imposing a thermal gradient along the nanotube, allowing for sub-nanometer displacements. More specifically, the thermal gradient generates a phononic current in one nanotube that hits and drags the second tube. This is, to our knowledge, the first experimental demonstration of displacive actuation at the nanoscale by means of a thermal gradient; we believe that thermal gradient actuation offers many possibilities in the design of novel nanoelectromechanical systems.

### References:

[1] R. Saito, R. Matsuo, T. Kimura, G. Dresselhaus, M.S. Dresselhaus, Chem. Phys. Lett. **348** (2001) 187.

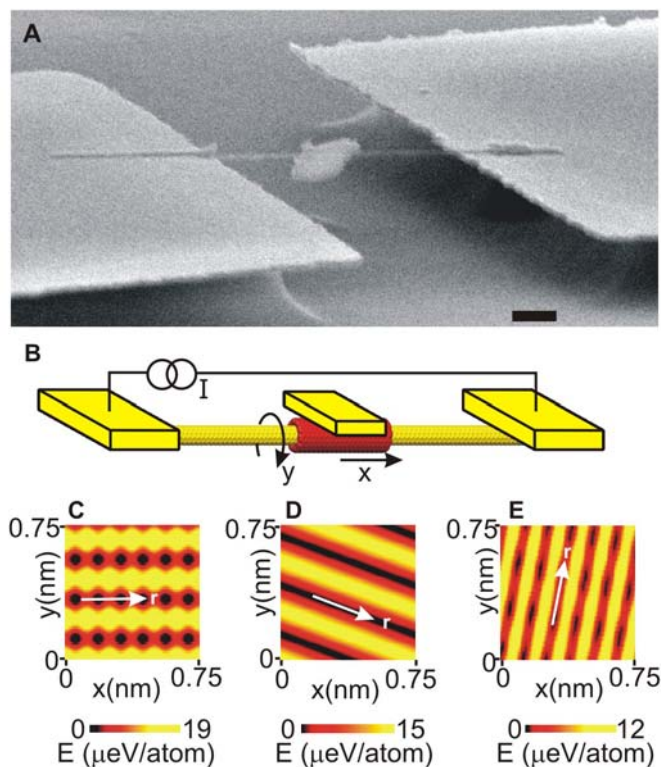
**Figures:**

Fig. 1. Experimental setup. (A) Scanning electron microscope (SEM) image of one device. The scale bar is 300 nm. (B) Schematic of the nanotube motor and its degrees of freedom. The outer (red) nanotube moves with respect to the inner (yellow) nanotube. (C, D, E) Shape of the energy barrier for the relative motion between two coaxial nanotubes, namely (5,5)/(10,10), (29,9)/(38,8) and (27,12)/(32,17), respectively. The diameters of the inner tubes are 0.67, 2.7, and 2.7 nm, respectively. The white arrow indicates the easy axis of motion. The motion is modulated by a series of small periodic barriers in C and E, while vanishingly small friction is expected in D.

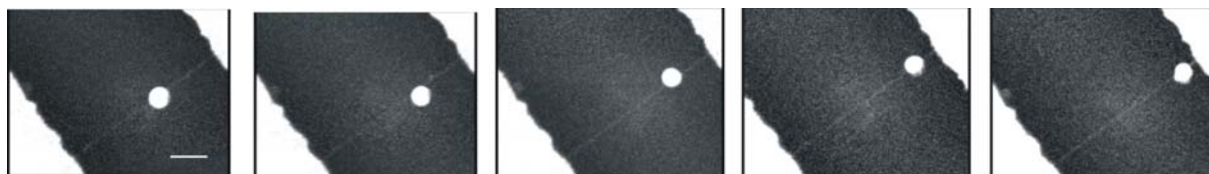


Fig. 2. Translational motion. Top down SEM images where the gold cargo is moving along the nanotube. The motion is actuated by passing a large electrical current through the nanotubes. Note that the driving mechanism for the motion is not due to electromigration, but comes from the thermal gradient along the nanotubes (induced by the electrical current). The metal plate, which initially had a rectangular shape, melted through Joule heating, and became a ball. The scale bar is 400 nm.

## SELF-ASSEMBLED DISORDER

A. Blanco, P.D. García, M. López, R. Sapienza, C. López

[ablanco@icmm.csic.es](mailto:ablanco@icmm.csic.es)

Instituto de Ciencia de Materiales de Madrid (CSIC) and Unidad Asociada  
CSIC-UVigo, C/ Sor Juana Inés de la Cruz 3, 28049 Madrid, Spain.

### Abstract

Self-assembled nanostructures usually develop ordered patterns in three dimensions. Artificial opals are one of such possible arrangements usually forming *fcc* structures with promising photonic properties. Often, and undesirably, unwanted defects are present spoiling the optical properties of such nanostructures: e.g. in thin self-assembled photonic crystals the stacking from one up to four layers of dielectric spheres may arise according to three different arrangements: face-centered cubic, hexagonal close-packed or double hexagonal close-packed (figure 1).<sup>1</sup> On the other hand, and contrary to intuition, the introduction of arbitrarily high amounts of disorder is, in some cases, an equally difficult task but the resulting material presents intriguing new optical properties. We have grown novel nanophotonic materials, *photonic glasses*, which are solid, disordered assembly of monodisperse dielectric spheres.<sup>2</sup> The novelty provided by these structures is the monodispersity of the spheres, which gives rise to a resonant behaviour of diffusion constant and transport mean free path. For the first time, we have measured these macroscopic resonances, as well as the frequency dependence of the energy velocity of the diffused light, which decreases below the group velocity when Mie resonances are excited. Diffusive modes at different frequencies, with different transport properties, appear in photonic glasses, as a result of the collective effect of the single-sphere Mie resonance.<sup>3</sup>

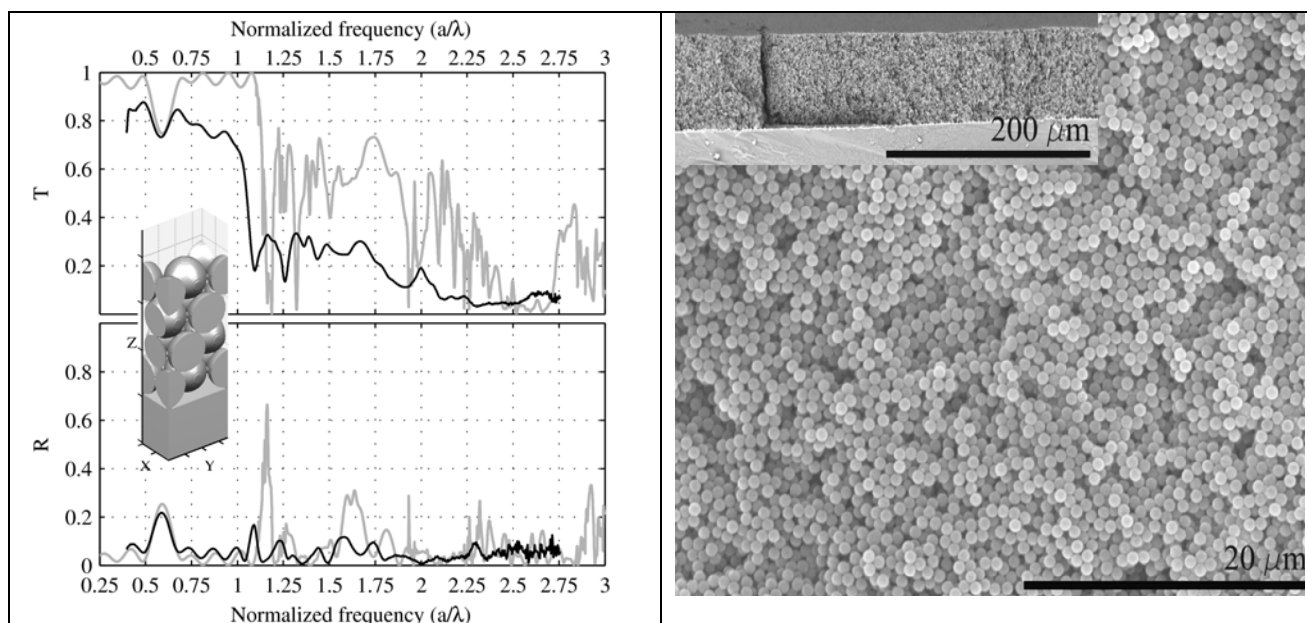


Figure 1. Left: spectra of a four-layer opal arranged in a face centered cubic structure (i.e. with a stacking of the form ABCA). Right:

- 
- <sup>1</sup> X. Checoury, S. Enoch, C. López, and A. Blanco, *Appl. Phys. Lett.* **90**, 161131 (2007)
- <sup>2</sup> P. David García, Riccardo Sapienza, Alvaro Blanco, and Cefe López, *Adv. Mater.* **19**, 2597, (2007)
- <sup>3</sup> R. Sapienza, P. D. García, J. Bertolotti, M. D. Martín, Á. Blanco, L. Viña, C. López, and D. S. Wiersma, *Phys. Rev. Lett.* **99**, 233902 (2007)

## ELECTROSPUN NANOFIBERS AS POTENTIAL REINFORCEMENTS FOR COMPOSITES

J.P. Borges, P.L. Almeida, M.H. Godinho

Departamento de Ciência dos Materiais and CENIMAT/I3N, Faculdade de Ciências e Tecnologia da Universidade Nova de Lisboa, Campus da Caparica, 2829-516 Caparica, Portugal

[jpb@fct.unl.pt](mailto:jpb@fct.unl.pt)

A nanofiber is an elongated and threadlike structure with a diameter in the nanometer range. At this scale several amazing characteristics such as very large surface area to volume ratio (this ratio for a nanofiber can be as large as  $10^3$  times of that of a microfiber), flexibility in surface functionalities, and superior mechanical performance (e.g. stiffness and tensile strength) compared with any other known form of the material. These outstanding properties make the polymer nanofibers to be optimal candidates for many important applications like filtration, protective clothing and biomedical applications [1].

A large number of synthetic and fabrication methods have already been demonstrated for generating nanostructures in the form of fibers [2]. Among these methods, electrospinning is a simple and low-cost method of producing continuous polymeric, ceramic and composite nanofibers [3-5]. Also, electrospinning is able to fabricate various nanofiber assemblies *in situ*. This gives electrospinning an important edge over other larger-scale nanofiber production methods.

Basically in an electrospinning setup a high voltage is applied to a metallic capillary, like a syringe needle, which is attached to a reservoir containing a polymeric solution. Figure 1 shows a schematic illustration of a typical electrospinning setup. Above a critical electrical field the electrostatic force will overcome the surface tension of the solution and a thin jet is ejected from the tip of the capillary. This charged jet will undergo stretching and whipping as a result of the interactions of the external electric field, the viscosity and surface tension of the polymeric solution and many other parameters [6]. This instability causes the fibers to be collected randomly in the form of nonwoven mats. Figure 2 shows a typical SEM image of the nonwoven mat of nanofibers.

In our lab transparency windows were produced using cellulose based nanofibers. These nanofiber mats were used as the liquid crystal alignment layer in these composite electro-optical devices. An increase in transparency and a marked decrease on the operating voltage of these devices was observed as a consequence of the improved interaction of the liquid crystal with the nanofibers.

In the past years a great effort has been made in order to produce highly ordered structures by electrospinning [7]. Different approaches for making parallel electrospun fibers involve either the modification of the collectors or the manipulation of the electric field [2]. These ordered structures can be used for example in the fabrication of electronic and photonic devices [8,9], fiber-reinforced polymer composites[10] and in tissue engineering[11,12].

Up to date, polymer composites reinforced with electrospun nanofibers have been developed mainly for providing some outstanding physical (e.g. optical and electrical) and chemical properties while keeping their appropriate mechanical performance and less work has been done on the development of electrospun polymer nanofiber reinforced composites. First of all, not sufficient quantity of uniaxial and continuous nanofibers has been obtained and could be used as reinforcements. The non-woven or randomly arranged nanofiber mats generally

cannot result in a significant improvement in the mechanical properties of the composites with their reinforcement. Another reason may be that polymers yielding these fibers are generally considered as less suitable for structural enhancement. Although carbon nanofibers are principally achievable from post-processing of electrospun precursor polymer nanofibers such as polyacrylonitrile (PAN) nanofibers [13], these fibers seem to have not been obtained in large quantity of continuous single yarns yet. Thus, extensive work both from the standpoint of nanofiber composite science (fabrication, characterization, modeling and simulation) and from industrial base (applications) viewpoint is necessary in the future.

## References:

- [1] D. Li, Y. Xia, *Adv. Mater.*, **16** (2004), 1151.
- [2] Z.-M. Huang, Y.-Z. Zhang, M. Kotaki, S. Ramakrishna, *Composites Science and Technology*, **63** (2003), 2223.
- [3] A. Greiner, J.H. Wendorff, *Angew. Chem. Int. Ed.*, **46** (2007), 5670.
- [4] See examples, a) D. Li, Y. Xia, *Nano Lett.*, **3**, **555** (2003). b) H. Dai, J. Gong, H. Kim, D. Lee, *Nanotechnology*, **13** (2002), 674.
- [5] D. Li, Y. Wang, Y. Xia, *Nano Lett.*, **3** (2003), 1167.
- [6] A.L. Yarin, S. Koombhongse, D.H. Reneker, *J. Appl. Phys.*, **89** (2001), 3018.
- [7] N.I. Kovtyukhova, T.E. Mallouk, *Chem. Eur. J.*, **8** (2002), 4354.
- [8] Y. Huang, X. Duan, Q. Wei, C.M. Lieber, *Science*, **291** (2001), 630.
- [9] Y. Xia, P. Yang, Y. Sun, Y. Wu, B. Mayers, B. Gates, Y. Yin, F. Kim, H. Yan, *Adv. Mater.*, **15** (2003), 353.
- [10] I.S. Chronakis, *J. Mater. Process. Technol.*, **167** (2005), 283.
- [11] U. Boudriot, R. Dersch, A. Greiner, J.H. Wendorff, *Artif. Organs*, **30** (2006), 785.
- [12] R. Murugan, S. Ramakrishna, *Tissue Eng.*, **12** (2006), 435.
- [13] Y. Wang, S. Serrano, J.J. Santiago-Aviles, *J. Mater. Sci. Lett.*, **21** (2002), 1055.

## Figures:

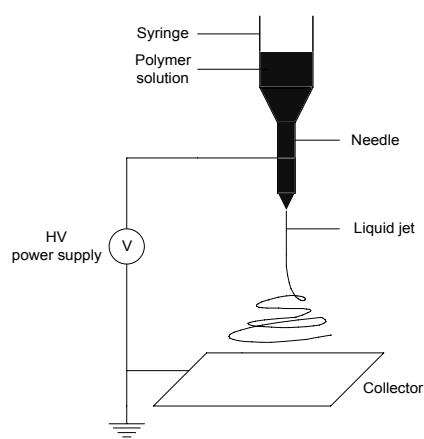


Figure 1 – Schematic illustration of a typical electrospinning setup.

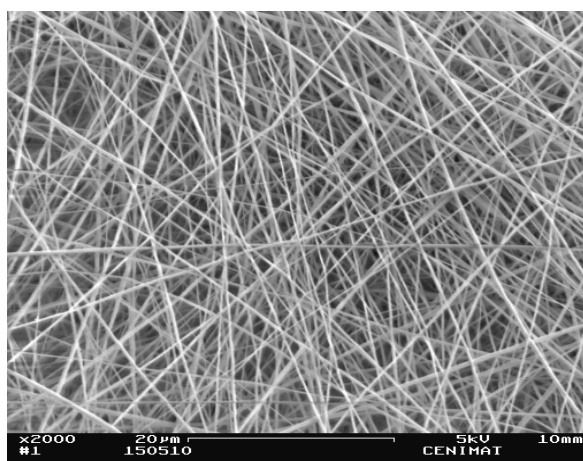


Figure 2 – Typical SEM image of the nonwoven mat of cellulose acetate nanofibers.

Abstract not available

Pedro Brogueira  
Instituto Superior Técnico  
Portugal



## THE ROLE OF POROUS MATERIALS IN THE EFFICIENT STORAGE OF HYDROGEN

*Ernesto Brunet, Carlos Cerro, Olga Juanes and Juan Carlos Rodriguez-Ubis*  
*Department of Organic Chemistry, Faculty of Sciences C-I-207, Universidad Autónoma de Madrid, 28049-Madrid (Spain)*  
[ernesto.brunet@uam.es](mailto:ernesto.brunet@uam.es)

Hydrogen is a very appealing energy vector: the release of its energy does not involve the noxious carbon dioxide. Yet, it is becoming a well known fact by our society that two problems must be solved if hydrogen is to be efficient and safely used as the clean energy carrier of the future: *i*) its environmental-friendly production and *ii*) its safe storage and transportation. Although there are already many reasonably useful technical approaches, neither of the two problems is nowadays at a level of resolution which would make the use of hydrogen routinely possible. Besides, the technical solutions to these problems must be quite robust in order to make a smooth transition to the “hydrogen culture” from the actual fossil-fuel civilization, whose economic moguls are far too powerful to be convincingly counterfeited. Therefore, a lot of research is being performed and even new institutions are being created to accomplish the aforementioned double task. Concerning the second one, hydrogen storage (HS) may be attained by at least four main methods: *i*) in high-pressure cylinders, *ii*) as a liquid in cryogenic tanks, *iii*) in ionic or covalent compounds (chemisorption), and *iv*) by *physisorption* in porous matrices.[1] This communication will give a critical quick view of the visible state-of-the art of the latter method (*physisorption*) and report our approach and progress in the use of porous organic-inorganic solids based in Al and Zr and various phosphonates.

A thorough revision of the literature (Figure 1) shows that the materials with very large specific surface areas (the record is well above 3000 m<sup>2</sup>/g) are not suitable for efficient HS at room temperature and low pressures, as common sense would have been anticipated. The free energy of interaction among the hydrogen molecules and the scarce matter of these systems is very low similarly as it is in an empty cylinder. Therefore, to increase that interaction energy, closer contact H<sub>2</sub>-material and thus much smaller pores are needed. It is now considered that a material bearing micropores or even ultramicropores would be more efficient for HS.[2] Many reported materials fall within this category. However, the average HS capacity (A and B in Figure 1) is around 2 wt% (77K and 1 atm) and a barrier of 3-4 wt% appears to be by far insurmountable. The average enthalpy of interaction H<sub>2</sub>-material is around 6-7 KJ/mol. It seems clear that higher enthalpies are needed (15-20 KJ/mol) to achieve HS at room temperature and atmospheric pressure. It should be noted that a record enthalpy of interaction (17.5 KJ/mol) was reported in faujasite-type (Mg,Na)-Y zeolite[3] but, unfortunately, the HS was low due to a strong entropic compensation. The existence of ions, specially Li<sup>+</sup>, and/or the presence of metals with open coordination sites in microporous organic-inorganic scaffolds are considered quite favourable features to increase HS.[4] Also, the presence of aromatic moieties in these scaffolds, probably with the idea of building kin

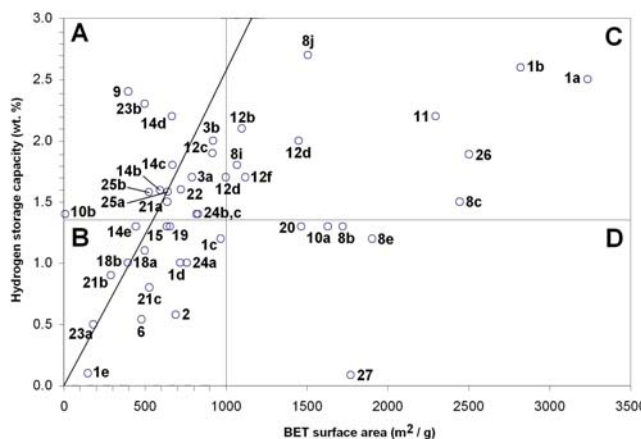


Figure 1

structures to superactivated carbon, graphenes and carbon nanotubes, is also a coveted architectural characteristic.

We are investigating the possibilities that organic-inorganic scaffolds based in phosphonates and Al and Zr have in this field. Although our preliminary results have been only quite modest,[5] we believe that we have a set-up of conceptual and material tools,[6] similar to that reigning organic chemistry, which could lead to the design of an endless number of structures and interesting results. For instance, the use of  $\text{Al}_2(\text{HPO}_3)_x$  ( $\text{C}_{12}\text{H}_8\text{P}_2\text{O}_6$ ) $_{1.5-x/2}$  allows the easy control of the  $\text{HPO}_3$ /diphenylphosphonate ( $\text{C}_{12}\text{H}_8\text{P}_2\text{O}_6$ ) ratio. The resulting materials displayed a good correlation between wt% HS and the  $\text{HPO}_3$  content (UAM-150  $\rightarrow$  152: cf. Figure 2), probably due to the increasing internal area caused by the increment of latter.[7]

The Zr derivatives, in which we have a larger experience, seem to be even much more flexible. Three phases ( $\alpha$ ,  $\gamma$  and  $\lambda$ ; Figure 3) of quite different structures are known for Zr phosphates which easily allow the inclusion of a variety of species, comprising various organic components (carboxylic acids, amines, phosphonates, etc), various phosphorous acids and metal ions. Preliminary results in the building of these structures with the phosphonates of Scheme 1 will be reported in this communication.

## References

- [1] See for example: Zuetzel, A. *Naturwissenschaften* **2004**, *91*, 157-172.
- [2] Bhatia, S. K.; Myers, A. L. *Langmuir* **2006**, *22*, 1688-1700.
- [3] Turnés, G.; Llop, M. R.; Otero, C. *J. Mater. Chem.*, **2006**, *16*, 2884-2885.
- [4] Sun, Q.; Jena, P.; Wang, Q.; Marquez, M. J. *Amer. Chem. Soc.* **2006**, *128*, 9741-9745.
- [5] Brunet, E.; Alhendawi, H. M. H.; Cerro, C.; de la Mata, M.J.; Juanes, O.; Rodríguez-Ubis, J.C. *Angew. Chem. Int. Ed.* **2006**, *45*, 6918-6920.
- [6] Brunet, E.; de la Mata, M.J.; Alhendawi, H. M. H.; Cerro, C.; Alonso, M.; Juanes, O.; Rodríguez-Ubis, J.C. *Chem. Mater.* **2005**, *17*, 1424-1433.
- [7] Brunet, E.; Cerro, C.; Juanes, O.; Rodríguez-Ubis, J.C.; Clearfield, A. *J. Mater. Sci.* **2008**, *43*, 1155-1158

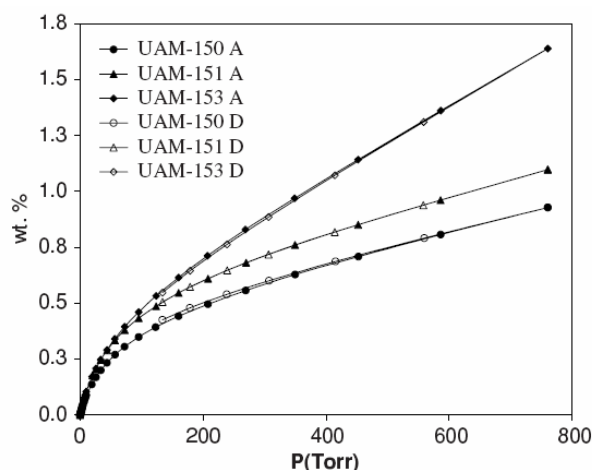


Figure 2

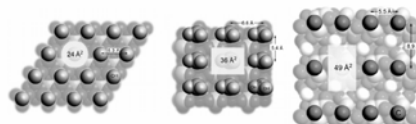
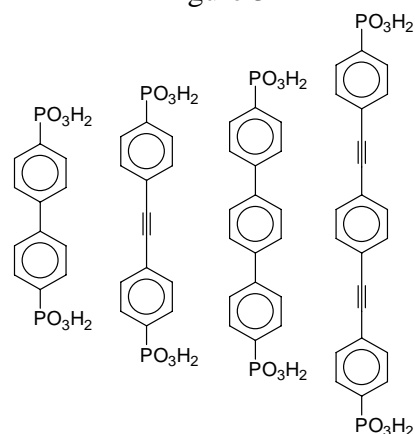


Figure 3



Scheme 1

## INTRODUCTION OF OF POLYPYRROL NANOPARTICLES IN CEMENT PASTE TO IMPROVE THE PHYSICAL PROPERTIES

*Luís Cadillon Costa, François Henry*

<sup>1</sup>*IBN, Departamento de Física, Universidade de Aveiro, Aveiro, Portugal*

<sup>2</sup>*CNRS, Thiais, France*

[kady@ua.pt](mailto:kady@ua.pt)

The introduction of different nanofillers in cements is frequently used to give mechanic reinforcement or flexibility and to hydrophobe the material.

In this work we introduced polypyrrol (PPy) nanoparticles at low concentrations in the cement paste, and we studied their influence in the physical properties of the cement.

The cement powder (CEM I 52.5N) and the desired concentrations of PPy in an aqueous emulsion, were introduced in a reactor and mixed during 5 minutes at 300 r.p.m. The initial water/cement ratio of 0.4 was maintained constant for all the samples.

The complex impedance and admittance was measured during the hardening of the cement, as a function of frequency between 1 Hz and 5 MHz, in order to follow the evolution of electrical properties with the hydration time as well as the effect of the nanoparticles.

Dielectric measurements were carried out using an 850 Stanford Research lock-in amplifier. The method consists in the measuring of the ‘in phase’ and the ‘out of phase’ components of the output signal, and these quantities were then used to calculate the values of effective resistance and capacitance in a parallel RC model of the sample. All the measurements were carried out at constant temperature of 23 °C.

Using the Cole-Cole model of dielectric relaxation [1],

$$Z^*(\omega) = Z_\infty + \frac{Z_0 - Z_\infty}{1 + (i\omega\tau)^\beta}, \quad (1)$$

$$Y^* = i\omega \left[ C_\infty + \frac{C_0 - C_\infty}{1 + (C_0 - C_\infty)/A_0 (i\omega)^\beta} \right] \quad (2)$$

we calculated the relaxation parameters.

In these expressions, which are empirical modifications of the Debye equation [2],  $Z_\infty$  is the high frequency impedance,  $Z_0$  the low frequency impedance,  $\tau$  the relaxation time,  $\beta$  a parameter between 0 and 1 that reflects the homogeneity of the system,  $C_\infty$  the high frequency capacitance and  $C_0$  the low frequency capacitance. An angle of depression can be defined as

$$\alpha = (1 - \beta) \frac{\pi}{2}. \quad (3)$$

and is a measurement of the heterogeneity of the material.

The calculated parameters of the dielectric response had given information about the porosity of the material [3], which was confirmed by the measurement of the contact angle at water.

Figure 1 shows the evolution of the depression angle, during the hardening process, for the cement with several concentrations of PPy nanoparticles. For the higher concentration of nanofillers, the homogeneity, measured by this angle, increases.

**References:**

- [1] K. S. Cole, R. H. Cole, *J. Chem. Phys.*, **9** (1941), 341.  
 [2] P. Debye, *Polar molecules*, Chemical Catalog Company, New York, 1929.  
 [3] F. Henry, M. Reis, L. C. Costa, C. Freire, *Mater. Sci. For.* (submitted).

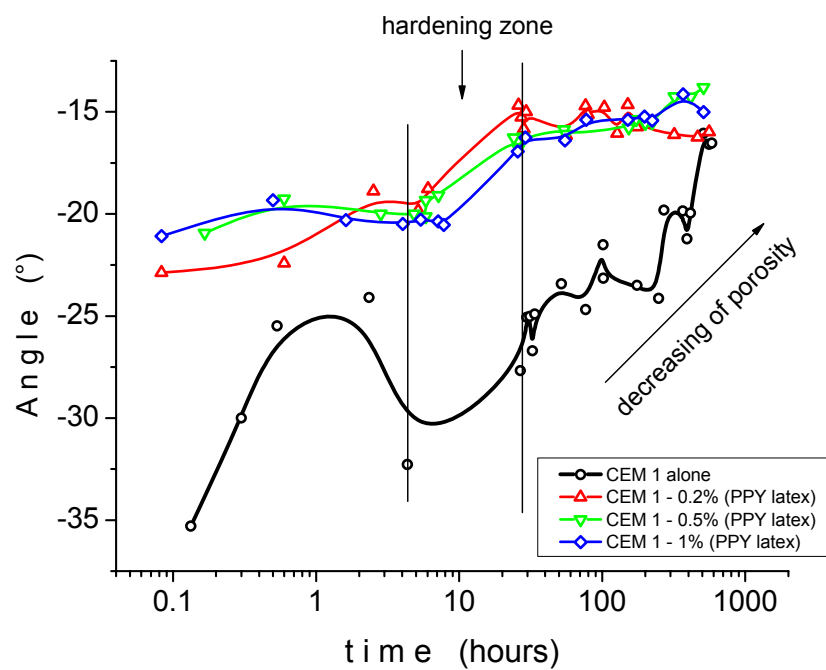
**Figures:**

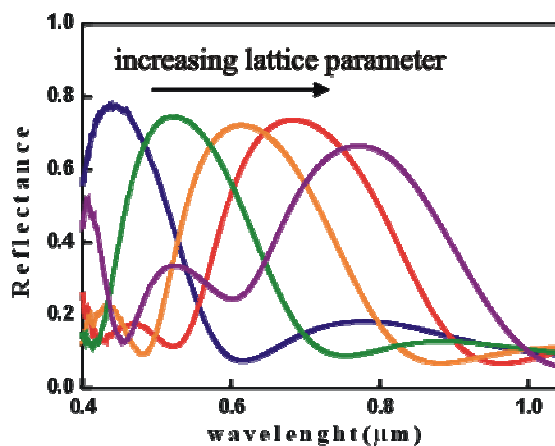
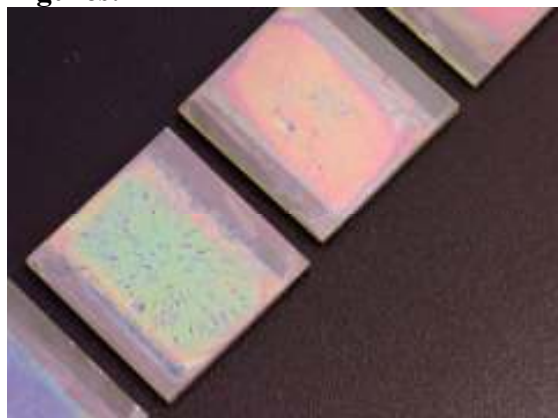
Fig. 1- Depression angle, during the hardening process, for the cement with several concentrations of PPY nanoparticles.

## NANOPARTICLE BASED ONE-DIMENSIONAL PHOTONIC CRYSTALS

*Mauricio E. Calvo, Silvia Colodrero, Manuel Ocaña, Hernán Míguez  
Instituto de Ciencias de Materiales de Sevilla, Américo Vespucio 49 41092, Sevilla, España  
hernan@icmse.csic.es*

Herein we present a synthetic route to build 1D films of  $\text{TiO}_2/\text{TiO}_2$  and  $\text{SiO}_2/\text{TiO}_2$  nanoparticles that display bright structural color, which arises as a result of the periodic modulation of the refractive index. This is achieved by controlling the degree of porosity of each alternate layer through the particle size distribution of the precursor suspensions, which were cast in the shape of a film by spin coating. This method allows tailoring the lattice parameter of the periodic multilayer, thus tuning the Bragg peak spectral position (i.e., its color) over the entire visible region, as it can be seen in the figure 1. In addition, the  $\text{SiO}_2/\text{TiO}_2$  multilayer can be doped optically leading to photonic crystals in which the opening of transmission windows due to the creation of defect states in the gap is demonstrated. The potential of this new type of structures as sensing materials is illustrated by analyzing their specific color changes induced by infiltration of solvents of different refractive index. Moreover, photoelectrochemical measurements show that the  $\text{TiO}_2/\text{TiO}_2$  Bragg mirrors films are conductive and distort the photocurrent response as a result of the interplay between photon and electron transport through them.

**Figures:**





## PREPARING NANOCOMPOSITES VIA MELT PROCESSING: CURRENT DIFFICULTIES AND PERSPECTIVES

*J. A. Covas, F. van Hattum, C. A. Bernardo*  
 I3 / University of Minho, 4800-058 Guimarães, Portugal  
[jcovas@dep.uminho.pt](mailto:jcovas@dep.uminho.pt)

Nanocomposites are expected to exhibit excellent mechanical and thermal properties, even at very low filler contents. In the particular case of Carbon nanotubes, CNTs, Young's modulus, tensile strength and thermal conductivity should reach up to 100, 200 and 2000 times the value of the polymeric matrix, respectively, thus making these materials suitable for sophisticated applications, e.g., in the automotive, aeronautics, textile and medical industries. However, in practice, performances only two or threefold those of the base polymer have been reported [1], this being often attributed to difficulties in preparing sufficiently homogeneous materials. A number of techniques has been used to prepare (reportedly) well dispersed nanocomposites [2,3], including solvent-based (solution/dispersion, followed by sonication), in-situ polymerization, combination of free radical reaction and water-crosslinking reaction, latex technology and melt compounding.

In principle, melt processing is an attractive route to prepare nanocomposites, given the wide range of available shear intensive equipment, its capacity for continuous production with significant output levels and the readiness for scale-up to industrial environment. Co-rotating twin screw extruders seem particularly fit for this purpose, given their flexible construction, adjustable distributive and dispersive mixing characteristics, possibility of combining several operations in a single run (e.g., polymer feeding and melting, CNT feeding, melt mixing, devolatilization, and extrusion) and relatively easy operation. However, and despite the current research on this topic, nanocomposite preparation via melt processing is far from being well understood, conflicting results having been reported.

This work discusses some of the approaches taken by the authors to obtain meaningful compounding-morphology-properties relationships for CNTs / thermoplastic composites. Micro-processing [4] using specially designed equipment (Figure 1 illustrates a micro twin-screw extrusion line, complete with feeding) allows the preparation of composites using very small amounts of CNTs, and thus to investigate topics such as the effect of CNT surface functionalization. On-line sensors [5] (Figure 2) provide the opportunity to follow (via rheological response) the evolution of dispersion along the extruder screw and correlate it with operational variables. Finally, rheometrical set-ups create controlled flow conditions to investigate the effect of extensional flow on dispersion efficiency. In spite of still being far from the ultimate targets, the results obtained so far seem indeed promising.

### References:

1. F. H. Gojny, *Compos. Sci. Tech.*, 64 (2004) 2363-2371
2. F. Hussain, M. Hojjati, M. Okamoto, R. E. Gorga, *J. Compos. Mat.*, 40, 17 (2006) 1511-1575
3. R. Khare, S. Bose, *J. Miner. & Mat. Charact. & Engng*, 4, 1 (2005) 31-46
4. J. A. Covas, C.A. Bernardo, O.S. Carneiro, J.M. Maia, F.W.J. van Hattum, A. Gaspar-Cunha, L.P. Biró, Z.E. Horváth, I. Kiricsi, Z. Kónya, K. Niesz, *J. Polym. Eng.*, 25, 1 (2005) 39-58
5. J. A. Covas, O. S. Carneiro, P. Costa, A. V. Machado, J. M. Maia, *Plast. Rubb. Comp. Macromol. Eng.*, 33, 1, (2004) 55-61

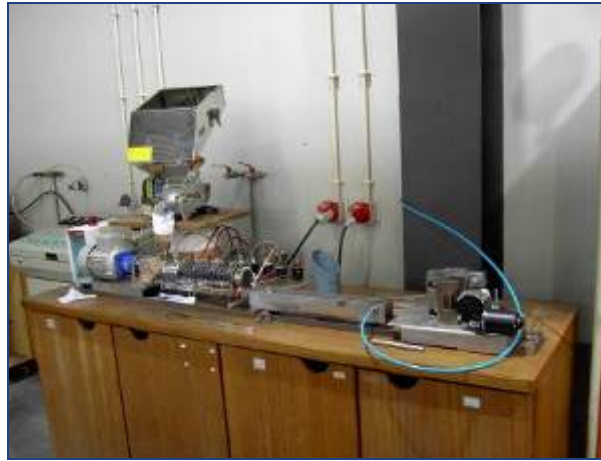


**Figure 1-** Micro-compounding line

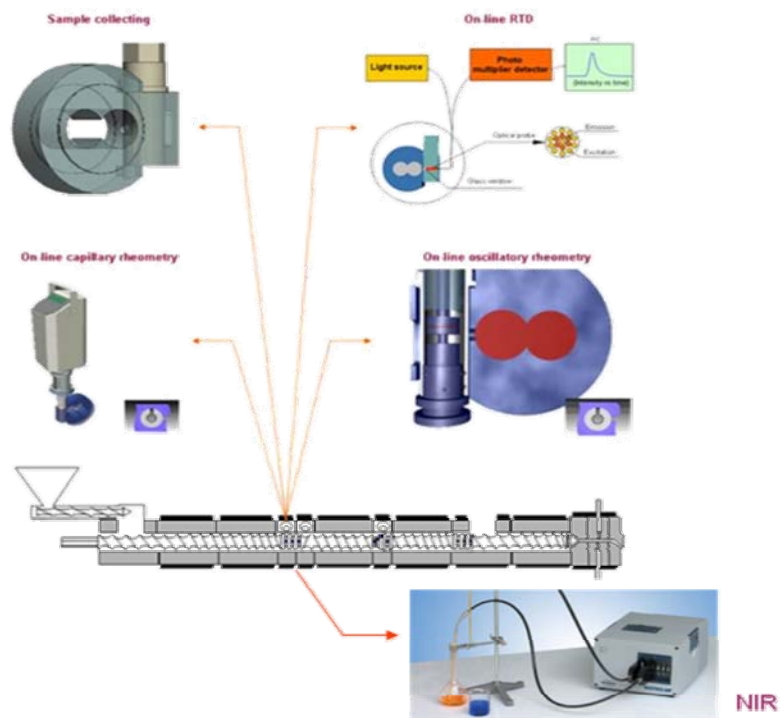


**Figure 2 –** Available on-line instrumentation

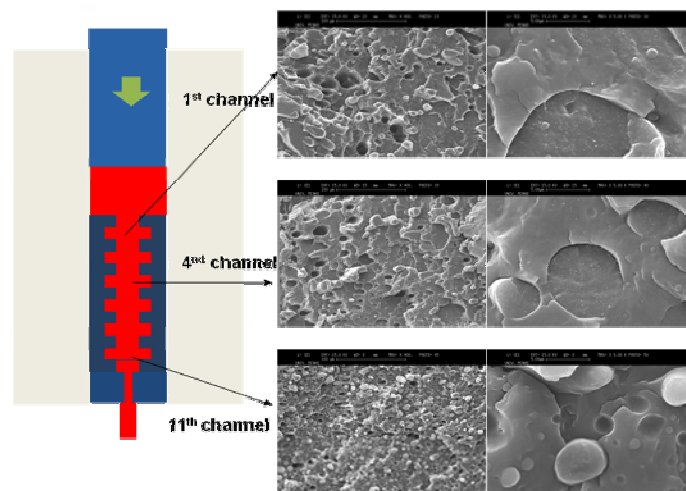


**Figure 3 –** Effect of extensional stresses (induced by repetitive convergent flows) on the dispersion of CNTs in a polymer blend

## NANOSCALE PERIODICITY IN STRIPE-FORMING SYSTEMS AT HIGH TEMPERATURE THE Au/W(110) SYSTEM

*J. de la Figuera, F. Léonard, N. C. Bartelt, R. Stumpf, and K. F. McCarty*

*Instituto de Química-Física "Rocasolano", CSIC, Madrid 28006*

*Universidad Autónoma de Madrid, Madrid 28049*

*Sandia National Laboratories, Livermore, CA 94550*

[juan.delafiguera@iqfr.csic.es](mailto:juan.delafiguera@iqfr.csic.es)

It has been known for many years that self-assembled stress domain patterns can occur on solid surfaces. These patterns arise from the competition between the short-range attractive interaction between atoms, leading to a phase-boundary energy, and a long-range repulsive interaction between boundaries, due to the difference in surface stress between the two phases. This repulsion is mediated by elastic deformations of the substrate. So far, such stress-domain patterns have been observed and quantified in the low-temperature sharp-interface regime, where the interfaces between the two separated phases are abrupt[1, 2]. Theories of pattern formation at crystalline surfaces have focused mainly on this sharp-interface regime[3,4]. These theories predict an exponential dependence of the periodicity of the stress-domain patterns on the strength of the competing interactions. This implies that it should be possible to tune the periodicity over large ranges, but also that the predictive power of the models is limited in the absence of extremely accurate estimates of the interactions. However, as the temperature is increased the amplitude of the modulated pattern decreases. At sufficiently high temperature, the transition to a homogeneous phase occurs. We call this temperature the order-disorder transition (ODT). As the ODT is approached, the interface width is expected to increase, eventually becoming on the order of the stripe periodicity, making the sharp-boundary theory inappropriate. In this paper we present an experimental study of Au on W(110) which shows explicitly this breakdown. We compare the detailed measured temperature dependence with the mean-field theory of the ODT and argue that nanometer-scale periodicities should be much more common than one would expect from the low-T sharp-interface theory.

Experimentally, quantitative observations near the ODT are difficult because thermal fluctuations of boundaries typically destroy the long-range order of the pattern. Here we study stripe formation with long-range order in the system of Au on W(110). As first observed by Duden and Bauer[5, 6], submonolayers of Au on W(110) self-assemble into stripe patterns, which consist of monolayer-thick stripes of condensed-phase Au in coexistence with stripes of a Au adatom gas (see Fig. 1a). Because of strong surface anisotropy, the stripes in this system form along a particular crystallographic direction, [110], and we are able to use low-energy electron microscopy (LEEM) to measure the amplitude (related to the Au density[7]) and wavelength of the pattern as it approaches the ODT. We demonstrate that the amplitude decreases steadily with increasing temperature and vanishes at the ODT. The modulation wavelength also decreases with temperature, depends quadratically on the reduced temperature, but has a finite value of 100 nm at the ODT.

The experimental observations serve as evidence that Au stripes observed on W(110) at high temperature are in the diffuse-interface limit of surface stress domains, with a temperature and coverage dependence qualitatively different from the oft-applied sharp-interface limit. By comparing our results with theoretical calculations of the stripe periodicity, we predict that nanometer-scale stripe patterns should be common near two-dimensional critical points.

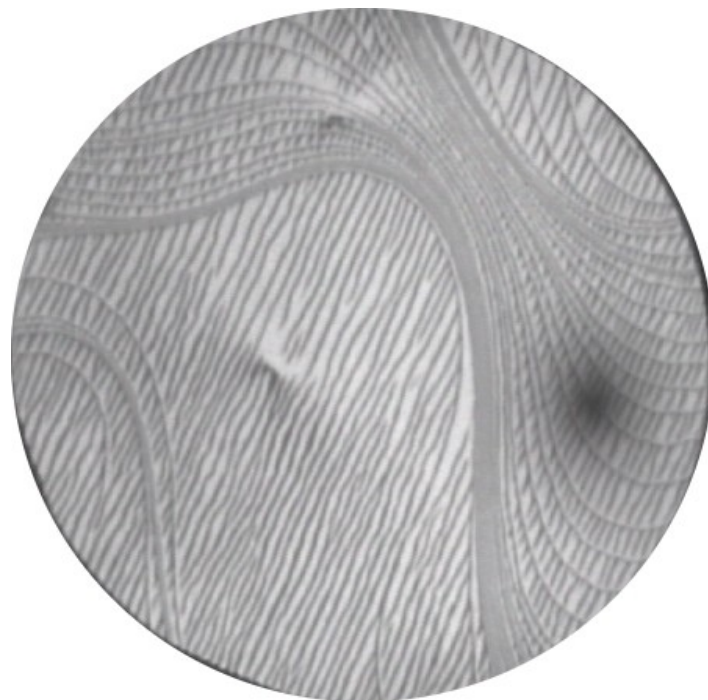
This research was supported by the Office of Basic Energy Sciences, Division of Materials Sciences, U.S. Department of Energy under Contract No. DE-AC04-94AL85000, by the Spanish Ministry of Science and Technology through Project No. MAT2006-13149-C02-02.

### References:

- [1] K. Kern et al., Phys. Rev. Lett. **67** (1991) 855 .
- [2] R. Plass, J. A. Last, N. C. Bartelt, and G. L. Kellogg, Nature **412** (2001) 875.
- [3] O. L. Alerhand, D. Vanderbilt, R. D. Meade, and J. D. Joannopoulos, Phys. Rev. Lett. **61** (1988) 1973.
- [4] V. I. Marchenko, Sov. Phys. JETP **54** (1981) 605.
- [5] T. Duden, Ph.D. thesis, Technischen Universität Clausthal, 1996.
- [6] E. Bauer, in The many facets of metal epitaxy, edited by D. A. King and D. P. Woodruff (Elsevier, Amsterdam, 1997), Vol. 3, Chap. 2, p. 46.
- [7] J. de la Figuera, N. C. Bartelt, and K. F. McCarty, Surf. Sci. **600** (2006) 4062.

### Figures:

The LEEM image shows the W(110) surface with several steps (wavy lines), with monolayer high islands of Au forming a striped pattern on the surface. The field of view is 7  $\mu\text{m}$ .



# COMPRESSED FLUID BASED TECHNOLOGIES FOR THE PREPARATION<sup>39</sup> OF DRUG DELIVERY SYSTEMS

*Elizondo E<sup>1</sup>, Ventosa N<sup>1\*</sup>, Sala S<sup>1</sup>, González D<sup>2</sup>, Blanco-Príeto M.J<sup>2</sup>, Veciana J<sup>1\*</sup>*

<sup>1</sup> *Molecular Nanoscience and Organic Materials Department. Institut de Ciència de Materials de Barcelona (CSIC)-CIBER-BBN, Campus de la UAB s/n 08193-Bellaterra (Barcelona), SPAIN. Phone: 34 93 580 18 53, Fax: 34 93 580 57 29*

<sup>2</sup> *Department of Pharmacy and Pharmaceutical Technology, University of Navarra, Irunlarrea s/n, Pamplona 31080, Spain  
contact e-mail: [vecianaj@icmab.es](mailto:vecianaj@icmab.es), [ventosa@icmab.es](mailto:ventosa@icmab.es)*

From an esthetic perspective, it is attractive to build all desirable pharmacological features of a drug- such as solubility, stability, permeability to biological membranes, and targeting to particular tissues, cells and intracellular compartments- into the drug molecule itself. But it would be simpler and perhaps more powerful to obtain these features by decoupling the biological action of the drug from the other biochemical and physicochemical characteristics that determine these key features of its pharmacology [1]. In agreement with this, the obtaining of new micro- and nanostructured molecular materials, and the understanding of how to manipulate existing materials at nanoscopic level, are playing a crucial role in the fields of drug delivery and clinical diagnostics.

However, in order to be able to commercially exploit the enormous potential of these nanomedicines is necessary the development of efficient and environmental respectful technologies for the manufacturing at industrial scale of these nanostructured materials. Technologies using compressed fluids (CFs) – such as CO<sub>2</sub> – have been proved to be very effective for the straightforward preparation of micro- and nanoparticulated materials, with reproducible supramolecular organization (i.e. crystallinity degree, polymorphic form) [2-7]. Therefore, using compressed solvent media it is often possible to prepare materials with unique physico-chemical characteristics (size, porosity, supramolecular organization, morphology, etc...) unachievable with classical liquid media. Therefore, in this work, we have chosen a CO<sub>2</sub> based process for the preparation of a micro and nanoparticulate material for the treatment of Brucellosis.

Brucellosis is a worldwide zoonosis caused by different species of the genus *Brucella*. The intracellular location of this pathogen, particularly in macrophages, renders treatment difficult since most antibiotics –such as gentamicin- known to be efficient in vitro, do not actively pass through cellular membranes. The enhancement of intracellular penetration by using biodegradable polymers as drug carriers has already been studied [8,9]. Complementary to other conventional methods, compressed fluid techniques have found many useful and sometimes unique applications in the production and processing of such drug delivery systems [10]. In this work, the gentamicin:polymer microparticles were prepared by the method called Precipitation with a Compressed Antisolvent (PCA). In a PCA process a liquid solution is sprayed through a nozzle into a compressed antisolvent, which rapidly diffuses into the sprayed droplets causing the precipitation of the solute. It was proved that by using this PCA process much higher loading factors of the antibiotic were achieved compared to conventional processes for production of nanoparticles. Five different composites were prepared with different proportions between the antibiotic (an inonic complex of gentamicin sulphate and bis(2-ethylhexyl) sulfosuccinate sodium salt (AOT), *GmAOT*) and the biodegradable polymer (poly(methylvinylether/maleic anhydride), *gantrezAN*): 0.09:1, 0.19:1, 0.37:1, 0.67:1, 1:1 (*GmAOT*:*gantrezAN*, w:w) [11].

It was observed that by increasing the amount of antibiotic in the composite, both the morphology and the primary particle size of the resulting nanostructured material changed. In vitro studies were performed in order to check the activity of the composites against the

*Brucella*. All the compositions have shown the same activity as the one observed for the equivalent quantity of gentamicin sulphate. By achieving this high loading factors reduced doses would be needed and therefore, an easier and faster treatment could be provide to the patients.

### References:

- [1] J.A Hubbel, *Science*, **300** (2003) 595.  
 [2] D.W. Matson, J.L. Fulton, R.C. Petersen, R.D. Smith, *Ind. Eng. Chem. Res*, **26**, (1987) 2298.  
 [3] (a) N. Ventosa, S. Sala, J. Veciana, J. Llibre, J. Torres, *Cryst. Growth & Design*, **1** (2001) 299. (b) N. Ventosa, S. Sala, J. Veciana, *J. Supercrit. Fluids*, **26** (2003) 33. (c) M. Gimeno, N. Ventosa, S. Sala, J. Veciana, *Cristal Growth & Design*, **6** (2006) 23.  
 [4] M. Cano-Sarabia, N. Ventosa, S. Sala, C. Patino, R. Arranz, J. Veciana, *Langmuir*, DOI: 10.1021/la7032109  
 [5] E.Weidner, Z. Knez, Z. Novak, PGSS (Particles from gas saturated solutions) a new process for powder generation, in: G. Brunner, M. Perrut, (Ed.), *Proceedings of the third International Symposium on Supercritical Fluids*, **3** (1994) 229.  
 [6] P.M. Gallagher, M.P. Coffey, V.J. Krukons, N. Klasutis, *ACS Symp. Ser.*, **406** (1989) 334.  
 [7] J. Bleich, B.W. Müller, W. Wabmus, *Int. J. Pharm.*, **97** (1993) 111.  
 [8] C. Lecaroz, C. Gamazo, M-J. Blanco-Prieto, *J. Nanosci. Nanotechno*, **6** (2006) 3296.  
 [9] E. Briones, C.I. Colino, José M. Lanao, *J. Controlled Release*, **125** (2007) 210.  
 [10] P. Pathak, M.J. Meziani, Y.-P. Sun, *Expert Opin. Drug. Deliv*, **2** (2005) 747.  
 [11] E. Elizondo, N. Ventosa, S. Sala, J. Veciana, E. Imbuluzqueta, D. Gonzalez, M.J. Blanco-Prieto, C. Gamazo, Patents: P200703314, P200703315. Application date: 7<sup>th</sup> of December of 2007.

### Figures:

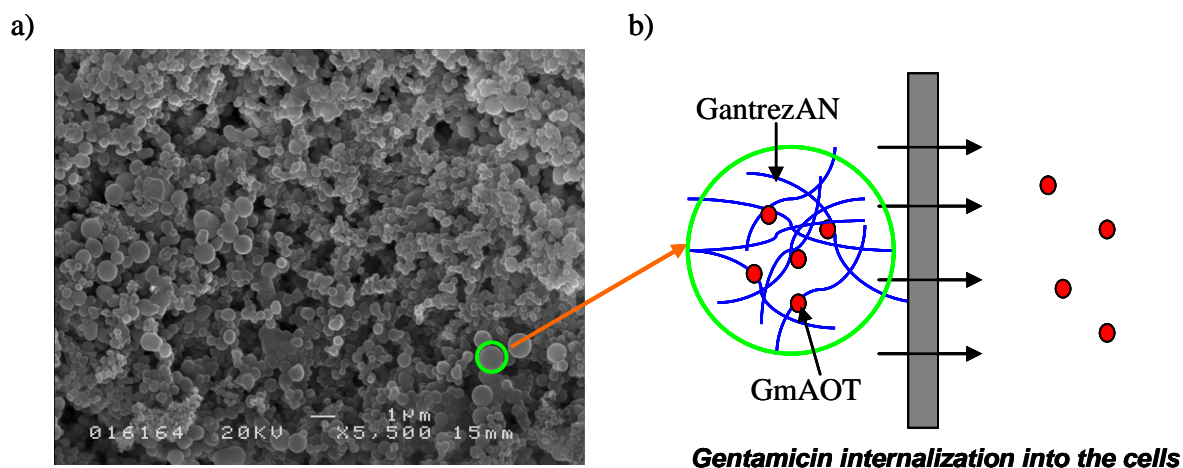


**Figure 1.** a) SEM image of a GmAOT:GantrezAN composite. b) Squeme of the enhanced permeability of gentamicin through cell membranes by using GantrezAN as a carrier.

## PARALLEL NANOGAP FABRICATION WITH NANOMETER SIZE CONTROL USING III-V SEMICONDUCTOR EPITAXIAL TECHNOLOGY

*Iván Fernández-Martínez, Yolanda González, Jose L. Costa-Krämer and Fernando Briones.*

*Instituto de Microelectrónica de Madrid, IMM-CNM-CSIC, Isaac Newton 8 PTM, 28760 Tres Cantos, Madrid, Spain.*

[Contact@E-mail](mailto:ivan@imm.cnm.csic.es) ivan@imm.cnm.csic.es

A reproducible and full-wafer compatible fabrication process for adjustable contact electrodes separated several nanometers is a major technological challenge. Until now, several approaches have been developed [1-6] to achieve a controlled parallel process for patterning multiple nanogaps with controlled sizes. In this letter a novel method for parallel nanogap fabrication using strained epitaxial III-V beams is presented. The process is highly reproducible, allows parallel fabrication and highly accurate gap size control. The beams are fabricated from MBE grown (GaAs/GaP)/AlGaAs strained heterostructures, standard e-beam lithography, and wet etching. During the wet etching process, the relaxation of the accumulated stress at the epitaxial heterostructure produces a controlled beam breakage at the previously defined beam notch. After the breakage, the relaxed strain is proportional to the beam length, allowing nanogap size control. The starting structure is similar to a mechanically adjustable break junction but the stress causing the breakage is, in this case, built-in the beam. This novel technique should be useful for molecular-scale electronics devices.

An array of four beams with different lengths (from 4 to 10  $\mu\text{m}$ ) has been designed and fabricated and it is shown in Fig. 1.a). The formed nanogaps for different cantilever lengths are shown in Fig. 1.b). Fig. 1.c) shows the nanogap size  $d$  as a function of the cantilever length  $L$ . A linear relation is obtained. These results clearly show that the nanogap formation mechanism developed in this work allows us to control the nanogap size by changing the III-V heteroepitaxial beam length, getting nanogap sizes as low as 5 nm.

### References:

- [1] Champagne, A. R.; Pasupathy, A. N; Ralph, D. C. *NanoLetters*, **5** (2005) 305.
- [2] Park, H.; Lim, A. K. L.; Park, J.; Alivisatos, A. P.; McEuen, P. L. *Appl. Phys. Lett.*, **75** (1999) 301.
- [3] Reed, M.A.; Zhou, C.; Muller, C. J.; Burgin, T.P.; Tour, J.M. *Science* **278** (1997) 252.
- [4] Qin, L.; Park, S.; Huang, L.; Mirkin, C. A. *Science* **309** (2005) 113.
- [5] Krahné, R.; Yacoby, A.; Shtrikman, H.; Bar-Joseph, I.; Dadosh, T.; Sperling, J. *Appl. Phys. Lett.* **81** (2002) 730. Maruccio, G.; Marzo, P.; Krahné, R.; Passaseo, A.; Cingolani, R.; Rinaldi, R. *Small* **3** (2007) 1184.
- [6] Johnston, D. E.; Strachan, D. R.; Johnson, A. T. *NanoLetters* **7** (2007) 2774.

**Figures:**

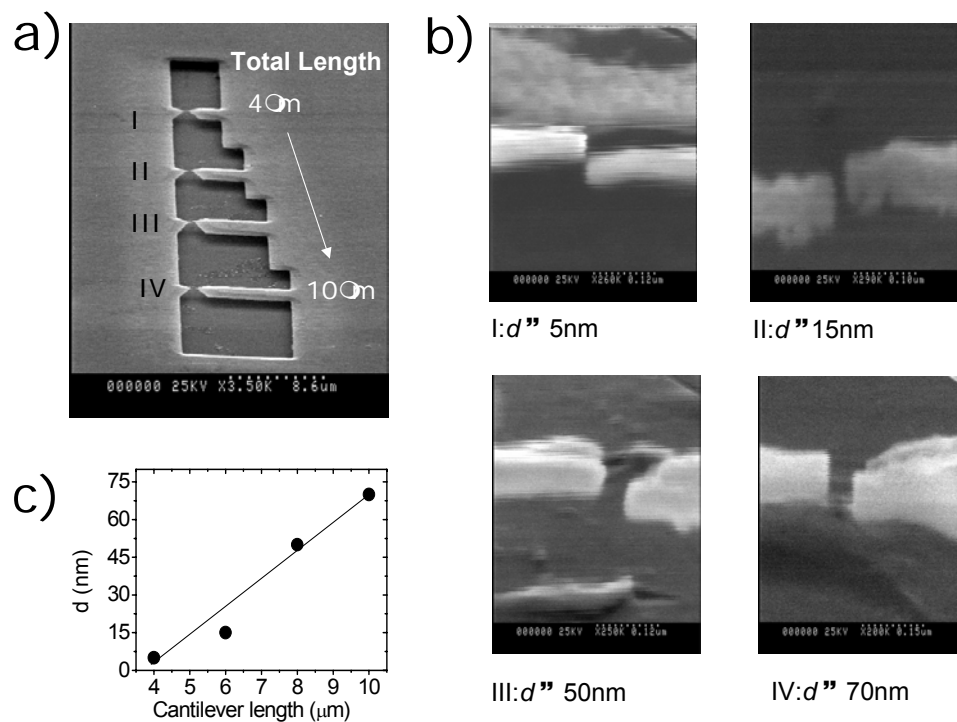


Figure 1) a) Scanning electron microscope image of a four-junction array in which the length of the beam is designed from 4 to 10  $\mu\text{m}$ . The device is tilted 45 degrees during the image acquisition. b) Side view of the different nanogaps that correspond to different beam lengths. The device is tilted 90 degrees during the image acquisition. c) Nanogap size  $d$  as a function of the beam length  $L$ .

## INTERDIGITATED NANO-ELECTRODES FOR SENSING: FABRICATION AND CHARACTERIZATION

Irene Fernandez-Cuesta, Jesús García, Jahir Orozco, César Fernández-Sánchez, Antoni Baldi,  
Xavier Borrísé and Francesc Pérez-Murano

*Centro Nacional de Microelectrónica - Barcelona (CNM-IMB, CSIC)*

[Irene.Fernandez@cnm.es](mailto:Irene.Fernandez@cnm.es)

Interdigitated nanoelectrodes (nIDEs) consist on two arrays of electrodes with comb shape which, under proper bias polarization, can be used for (bio)chemical sensing by measuring the change of impedance or electrochemical current.

In this work we present the fabrication of a complete device, and the first results of its characterization. The device can be used in different configurations: (i) measurement of the electrochemical current generated by chemical reactions occurring in the solution [1], and (ii) study of the impedimetric response of the system when the nature of the solution changes [2] or even further, with the inclusion of nanoparticles in between the digits [3].

### **Fabrication.**

In order to combine micro and nanometer size features, the connection pads and lines are first fabricated by UV lithography, metallization (Ti/Au, 7nm/60nm) and lift-off. Aligning marks have been included in the design of the UV mask for a second lithography level which consist of electron beam lithography to define the digits, followed by metal evaporation and lift off. Figure 1 shows results of the fabrication process: the whole chip, fabricated in gold onto a SiO<sub>2</sub>/Si substrate (a), and a detail of the digits (b), which are 180 nm wide and with a pitch of 230 nm. These devices can be used already for sensing or as the master to fabricate stamps for nanoimprint lithography (NIL). In the second case, a reactive ion etching (RIE) process is performed. Then, the fabrication of subsequent samples is easier and faster, since the two lithography levels (UV and e-beam lithography) are substituted by one single NIL step. Once the electrodes have been fabricated, they are passivated with PMMA, leaving open only the large pads for external connections and the areas with the digits. Then, they are bounded to a printed circuit board (PCB), and encapsulated with *epotec*®. At this point, the sensor is ready to be connected to an external electronic system and the electrodes can be immersed in a liquid media (Figure 1 (c)).

### **Characterization.**

Figure 2(a) shows the first results of electrochemical current measurements. The nIDE was immersed in a solution 1mM of [Fe(CN)<sup>3-</sup>]<sub>6</sub> in KNO<sub>3</sub> (red line). A stabilization potential was applied during the first 30seconds, and then changed to 0V (\*). After the stabilization of the system when V = 0V, the current is due to the reduction processes occurring in the solution. The black line corresponds to the same measure, but in a KNO<sub>3</sub> solution. No electrochemical current is observed after the stabilization in this case. The sensors are being calibrated by adding known concentrations of [Fe(CN)<sup>3-</sup>]<sub>6</sub>, so subsequently can be used to determine the concentration of unknown solutions.

Figure 2(b) corresponds to results of the impedimetric response of the electrodes (total impedance of the media measured as a function of frequency). The electrode was immersed in DI water and then in solutions of NaCl with different concentrations (i.e., the resistivity of the media changes). The figure shows that the change from the low frequency capacity to the high frequency capacity depends on the concentration of Na<sup>+</sup> Cl<sup>-</sup> ions in the aqueous media. Thus, the device can be also calibrated, to be used for sensing. Additional tests performed in liquids

---

\* Fe(CN)<sub>6</sub><sup>3-</sup> + e<sup>-</sup> → Fe(CN)<sub>6</sub><sup>4-</sup>, E<sub>0</sub>=+0.35V

with different permittivities ( $\epsilon_r$ ) have been performed, showing that the higher  $\epsilon_r$  is, the lower the high frequency capacity.

Once the proper response of the sensors has been demonstrated, the devices are being currently used to detect and quantify the presence of insulating nanoparticles (Figure 3). The final goal is to functionalize the nanoparticles to perform specific detection of bioentities: an increase of sensitivity is expected since nIDES would allow the detection of a single nanoparticle. The results will be presented at the conference.

Projects NILSIS and Consolider NanoBioMed are gratefully acknowledged.

## References:

- [1] K. Aoki et al., *J. Electroanal. Chem*, **256** (1988) 269
- [2] R. de la Rica et. al., *Appl. Phys. Lett.* **90**, 174104 (2007)
- [3] L. Malaquin et al. *Nanotechnology*, **16**, (2005) S240–S245

## Figures:

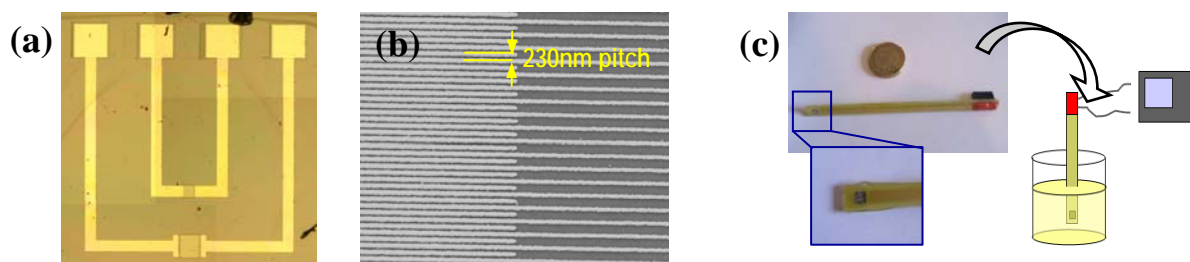


**Figure 1.** (a), optical image of a sensor, fabricated in gold on a  $\text{SiO}_2/\text{Si}$  substrate. The pads are defined by optical lithography, metallization and lift off, and the digits are fabricated in a second step, by e-beam lithography, metallization and lift off. A detail can be seen in the SEM image in (b). (c) once the electrode is fabricated, it is bounded to a PCB and encapsulated, so it can be connected to an external electronic system and the electrodes immersed in a solution, for characterization.

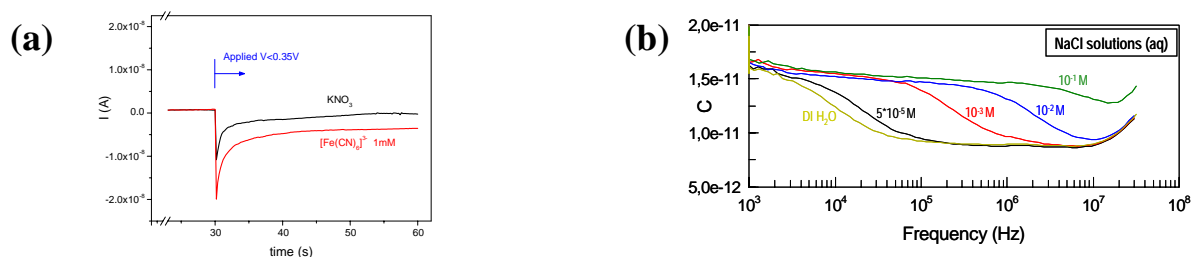


**Figure 2.** (a) **Electrochemical current** measurements, for an applied potential similar to the reduction potential of  $[\text{Fe}(\text{CN})_6]^{3-}$ . When the electrode is immersed in a  $\text{FeCN63-}$  1mM solution, a current due to the electrochemical reaction is measured (red line). For a non-active solution ( $\text{KNO}_3$ ), no current is observed (black line). (b) **Impedimetric characterization:** Dependence of the capacity of the system on the frequency when the electrode is immersed in solutions with different resistivity (i.e., aqueous solutions of NaCl at different concentrations). In this case, the transition from the high frequency capacity to the low frequency one depends on the concentration of ions in the solution.

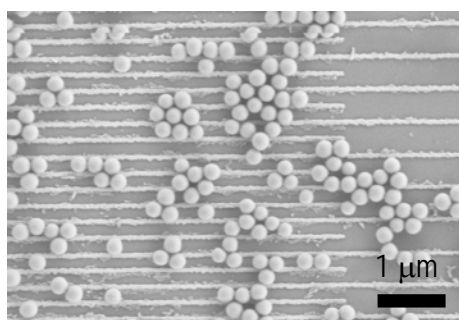


**Figure 3.** SEM image of one of the electrodes (140nm width, 400 nm pitch), where silica nanoparticles (300nm diameter) have been precipitated.

## DNA DETECTION USING AMORPHOUS SILICON SENSORS WITH GOLD NANOPARTICLES

Leonardo Silva<sup>1</sup>, Elvira Fortunato<sup>1</sup>, Hugo Águas<sup>1</sup>, Gonçalo Doria<sup>2</sup>, Pedro Baptista<sup>2</sup>, and Rodrigo Martins<sup>1</sup>

<sup>1</sup>CENIMAT/I3N, Materials Science Department,

<sup>2</sup>CIGMH/SABT, Biotechnology Department, Campus de Caparica, 2829-516 Caparica, Portugal

Tel: +351212948562; Fax: +351212948558

[elvira.fortunato@fct.unl.pt](mailto:elvira.fortunato@fct.unl.pt)

Advances in nanosciences are having a significant impact in many areas of research on nearly every industry. The impact of new nanotechnologies has been particularly large in biodiagnostics, where a number of nanoparticle-based assays have been introduced for biomolecules detection extending the limits of molecular diagnostics to the nanoscale. The applications of nanoparticles have largely focused on DNA-functionalised gold nanoparticles used as the target-specific probes. These gold nanoparticle-based systems can be used for the detection of specific sequences of DNA or RNA. Gold nanoparticles derivatised with thiol modified oligonucleotides complementary to DNA targets - Au-nanoprobes - are used to distinguish fully complementary from mismatched sequences. Here a rapid and inexpensive colorimetric nanoparticle-based method for mismatch detection in DNA using an optoelectronic platform samples is reported [1,2]. The device integrates an amorphous/nanocrystalline biosensor and a light emission source with a gold nanoprobe for specific DNA / RNA detection. This low cost, fast and simple optoelectronic platform permits detection of few picomole of nucleic acid without target or signal amplification making it suitable for application in population diagnostics and in point-of-care hand-held devices.

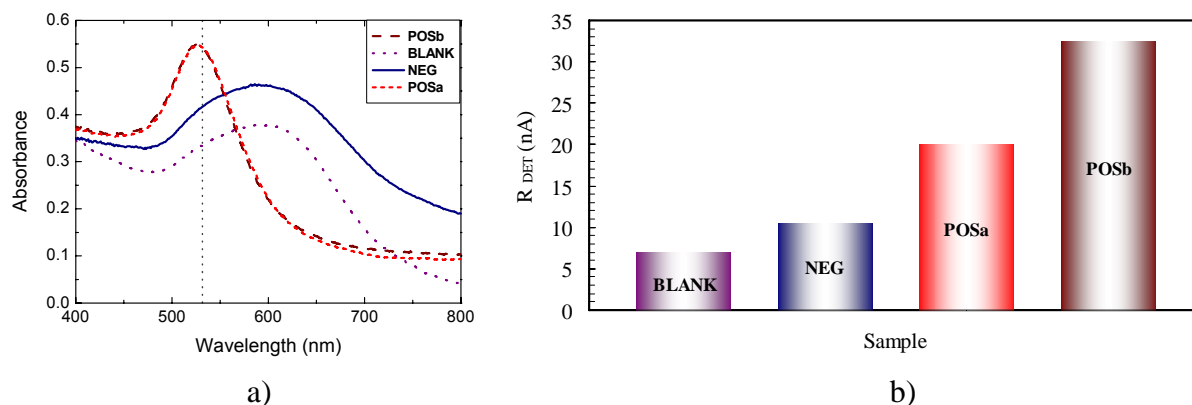


Figure – Comparison between the results obtained by using the conventional method (a) with those ones using the new optoelectronic platform (b), using exactly the same biological samples. The new method besides the DNA identification enables also its quantification (see figure b, POSa and POSb).

[1] R. Martins, P. Baptista, L. Raniero, G. Doria, L. Silva, R. Franco, E. Fortunato, Applied Physics Letters 90 (2007) 023903

[2] Patent pending (September 2006, nº 103 561).



Abstract not available

Paulo Freitas  
INESC-MN, IST and INL  
Portugal



# SINGLE MOLECULE FLUORESCENCE DECAY RATE STATISTICS IN DISORDERED MEDIA

**L. S. Froufe-Pérez<sup>(1,2)</sup>, J. J. Sáenz<sup>(3)</sup> and R. Carminati<sup>(2)</sup>**

(1) Instituto de Ciencia de Materiales de Madrid, Consejo Superior de Investigaciones Científicas, Sor Juana Inés de la cruz, N°3, Cantoblanco, 28049 Madrid, Spain.

(2) Laboratoire Photons et Matière, ESPCI, Centre National de la Recherche Scientifique, 10 rue Vauquelin, 75231 Paris Cedex, France.

(3) Departamento de Física de la Materia Condensada and Instituto "Nicolás Cabrera", Universidad Autónoma de Madrid, Cantoblanco, 28049 Madrid, Spain.

\*Author e-mail address : [luis.froufe@icmm.csic.es](mailto:luis.froufe@icmm.csic.es)

## 1. Introduction

Several powerful optical imaging techniques are based on molecular fluorescence. Single emitters are also key elements in nanophotonics devices. Since the pioneering work of Purcell [1], it has been known that the spontaneous decay rate of a dipolar emitter (atom, molecule, Qdot) is dramatically affected by its environment. When a fluorescent molecule is placed in a complex environment (e.g., cluster, biological system), measurement of *statistical* properties can provide relevant information. This issue has been partially addressed in the literature [2]. In nanoscopic systems (e.g. clusters of nanoparticles) two important contributions are expected: (1) local field effects due to near-field interaction between the emitter and its environment; (2) absorption, which can substantially modify the statistics of the decay rate. In particular, the statistics of the radiative and non-radiative rates are expected to behave differently in the presence of absorption [3].

## 2. Discussion

In this work [4,5], we study the fluorescence rate statistics in a finite size (nanoscopic) random medium (cluster), made of small spherical particles (see the inset in Fig. 1 a). For a given configuration of the system, we calculate numerically the Green tensor of the system. We deduce the spontaneous decay rate  $\Gamma$ , as well the radiative and the non-radiative contributions. Repeating the calculation for the configuration distribution and performing ensemble averages allows to compute the full statistics (probability density, average value, standard deviation). These numerical experiments are used as a basis for a physical discussion.

We focus on the regime in which the statistics is determined by near-field interactions, with negligible multiple scattering. The decay rate statistics is influenced by the local environment of the emitter (i.e. the interaction with the surrounding particles).

In Fig. 1a we show the statistical distribution of the normalized spontaneous decay rate  $\Gamma/\Gamma_0$  obtained from numerical simulations, for a cluster of TiO<sub>2</sub> (Rutile) nanoparticles at an emission wavelength  $\lambda=700\text{nm}$ . At low filling fraction the correlations among particle positions are negligible. It can be seen that, although the average value is close to the one in free-space, the distribution is broad and present a long tail. This is a consequence of the large fluctuations of the local field at the emitter position.

In Fig. 1b we show the distributions functions of the non-radiative decay rate. As can be seen, for different levels of absorption (determined by the imaginary part of the dielectric constant of the particles), the shape of the distributions remains invariant when the non-radiative decay rate is scaled by the imaginary part of the dielectric constant. Hence, the average value (inset Fig. 1b) and fluctuations of  $\Gamma^{\text{NR}}$  scales linearly with  $\epsilon''$ .

In the case of small clusters compared to the emission wavelength, and low filling fraction, a simple analytical model reproduces with great detail the numerical calculations. It can be shown that the standard deviation, normalized to the averaged modification of the decay rate (Fig. 2a) presents two well defined regimes. For low absorption level fluctuations are controlled by near-field scattering, while for higher degrees of absorption, fluctuations reach a regime controlled by non-radiative coupling, although the apparent quantum yield is still high (Fig. 2b). Also fluctuations and angular correlations of the emitted intensity pattern can be obtained within this framework. It will be shown how statistical properties of the emitted light intensity and its emission rate strongly depend on the optical and structural properties of the close neighborhood of the emitter at

the nanoscale. And, interestingly, the fluctuations of the decay rate depend dramatically on the statistical properties of the orientation of the emitter [5]. Hence we could take advantage of this behavior to obtain information of the local environment of the emitter at the nanoscale.

### 3. Conclusions

In summary, we have studied the statistics of the spontaneous decay rates in disordered nanoscopic clusters using both numerical simulations and a simple analytical model. Our results show that such statistics carry useful information about the local structure of the environment at the nanometer scale, even in the presence of absorption. This paves the way towards new imaging techniques in complex media at the nanometer scale.

### 4. References

- [1] E.M. Purcell, "Spontaneous emission probabilities at radio frequencies", *Phys. Rev.* **69**, 681 (1946).
- [2] W. Guo, "Spontaneous emission of an excited atom in a random absorbing medium", *Phys. Rev. A*, **69**, 043802 (2004).
- [3] R. Carminati, J. J. Greffet, C. Henkel, and J. M. Vigoureux, "Radiative and non-radiative decay of a single molecule close to a metallic nanoparticle", *Opt. Comm.* **261**, 368 (2006).
- [4] L. S. Froufe-Pérez, R. Carminati and J. J. Saenz, "Fluorescence decay rate statistics of a single molecule in a disordered cluster of nanoparticles", *Phys. Rev. A*, **76**, 013835 (2007).
- [5] L. S. Froufe-Pérez and R. Carminati, "Lifetime fluctuations of a single emitter in a disordered nanoscopic system: The influence of the transition dipole orientation", in press *Physica. Status Solidi (a)* (2008).

### 2. Figures

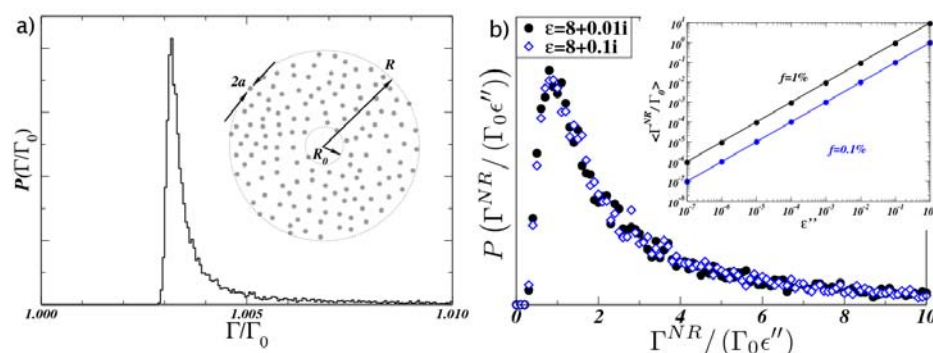


Fig.1. a) Statistical distribution of the normalized spontaneous decay rate  $\Gamma/\Gamma_0$  for a cluster of non-absorbing nanoparticles. Particle radius  $a=2.5\text{nm}$ , dielectric constant  $\epsilon=8$ , cluster radius  $R=54\text{nm}$ , volume fraction  $f=1\%$ . Inset: geometry of the system. The emitter is placed at the center of the cluster, and is surrounded by a spherical exclusion volume of radius  $R_0=5\text{nm}$ . b) Statistical distribution of the non-radiative decay rate  $\Gamma^{\text{NR}}$  (normalized by  $\epsilon''\Gamma_0$ ) for a cluster of absorbing nanoparticles. The dielectric constant is  $\epsilon=8+i\epsilon''$ , with  $\epsilon''=10^{-2}$  (circles) and  $\epsilon''=10^{-1}$  (diamonds). Inset: Averaged value of the normalized non-radiative decay rate  $\langle\Gamma^{\text{NR}}/\Gamma_0\rangle$  versus the imaginary part of the dielectric constant of the particles, for  $f=0.1\%$  and  $f=1\%$ . Symbols: numerical calculation. Solid lines: analytical model.

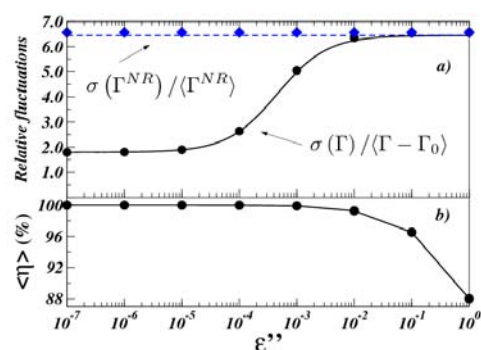


Fig. 2. a) Normalized standard deviation of the decay rate  $\sigma(\Gamma)/\langle\Gamma-\Gamma_0\rangle$  versus the imaginary part of the dielectric constant of the particles. Symbols: numerical calculation. Solid line: analytical model. Dashed line: analytical model for the normalized standard deviation of the non-radiative rate  $\sigma(\Gamma^{\text{NR}})/\langle\Gamma^{\text{NR}}\rangle$ . b) averaged apparent quantum yield  $\langle\eta\rangle$  (the intrinsic quantum yield of the emitter is assumed to be unity).  $f=0.1\%$ , other parameters as in Fig. 1.

*Daniel Garcia-Sanchez*,<sup>1,2</sup> *Alvaro San Paulo*,<sup>2</sup> *Arend M. van der Zande*,<sup>3</sup> *Maria Jose Esplandiu*,<sup>1</sup> *Benjamin Lassagne*,<sup>1,2</sup> *Francesc Perez-Murano*,<sup>2</sup> *Laszlo Forró*,<sup>4</sup> *Albert Aguasca*,<sup>5</sup> *Paul L. McEuen*<sup>3</sup> and *Adrian Bachtold*<sup>1,2</sup>

<sup>1</sup>CIN2 Barcelona Campus UAB, E-08913 Bellaterra, Spain. <sup>2</sup>CNM-CSIC Campus UAB, E-08913 Bellaterra, Spain. <sup>3</sup>Cornell Center for Materials Research, Cornell University, Ithaca, NY 14853, USA. <sup>4</sup>EPFL, CH-1015 Lausanne, Switzerland. <sup>5</sup>Universitat Politècnica de Catalunya, Barcelona, Spain.

[daniel.garcia.icn@uab.es](mailto:daniel.garcia.icn@uab.es)

Carbon nanotubes are often recognized as the ultimate material for high-frequency mechanical resonators. For instance, nanotube resonator devices hold promise for ultralow mass detection or quantum electromechanical experiments. However, the detection of the mechanical vibrations remains very challenging. We have developed a novel detection method for nanotube vibrations, which is based on atomic force microscopy [1]. This method enables the detection of resonances up to 3.1 GHz with subnanometer resolution in vibration amplitude as shown in figure 1. Importantly, it allows the imaging of the mode-shape for the first, second and third eigenmodes, as shown in figure 2.

We have also applied this method to study suspended graphene sheets [2]. As shown in figure 3, we have found a new class of exotic nanoscale vibration eigenmodes not predicted by the elastic beam theory, where the amplitude of vibration is maximum at the free edges. The edge modes are frequently, but not always, observed in resonators for which the suspended sheet displays local buckling. To understand the relationship between local buckling and the edge modes, we have calculated the effect of strain with simulations based on the finite element method. Figure 3 shows that the resonance frequencies and shape modes of the model are in reasonable agreement with the measurements.

Simulations based on the finite element method show that these edge eigenmodes are the result of non-uniform stress, which is generated during fabrication. The shape of these exotic eigenmodes and the corresponding stress must be taken into account in future experiments and applications, such as the determination of the Young's modulus[3] and the accurate calibration of mass, force, or charge sensing[4-6]. It may also be possible to manipulate the eigenmode shape by varying the strain during measurements via electrostatic tuning[4].

## References:

- [1] D. Garcia-Sanchez *et al.*, Phys. Rev. Lett., **99** (2007), 085501.
- [2] D. Garcia-Sanchez *et al.*, Submitted.
- [3] I.W. Frank *et al.*, J. of Vac. Sci. And Tech. B, **25** (2007) 2558.
- [4] Bunch, J.S. et al. Science, **315** (2007) 490.
- [5] H. Craighead, Nature Nanotech. **2** (2007), 18.
- [6] J. Tamayo, *et al.* Appl. Phys. Lett. **89**, (2006) 224104.

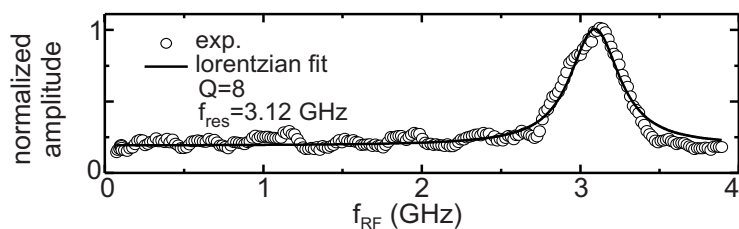
**Figures:**

Figure 1. Resonance peak of the fundamental eigenmode for a 265 nm long MWNT resonator.

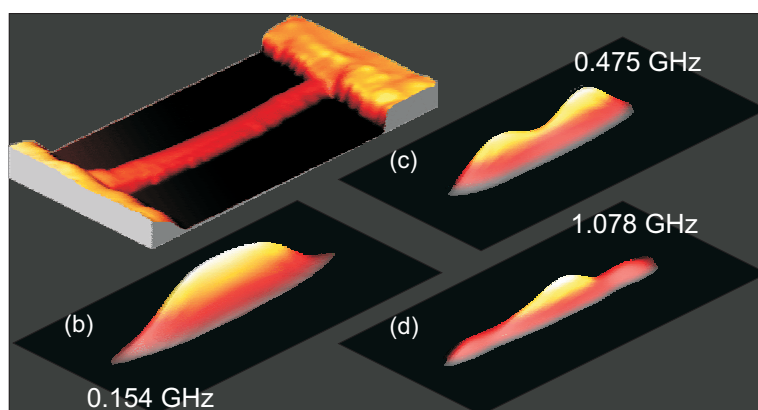


Figure 2. (a) Topography and (b)-(d) vibration images for a 770 nm long MWNT resonator. The images (b), (c), (d) correspond to the first, second and third eigenmodes.

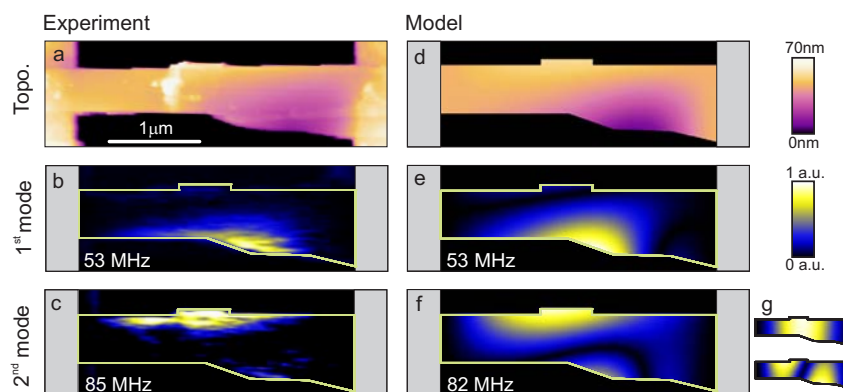


Figure 3. Graphene resonator with local buckling. (a) Measured topography. (b) Shape of the first eigenmode (raw data). (c) Shape of the second eigenmode (raw data). (d) Topography obtained using FEM simulations on a stressed graphene sheet. (e) Shape of the first eigenmode using FEM simulations. (f) Shape of the second eigenmode using FEM simulations. (g) Shape of the two first eigenmodes using FEM simulations without any stress. The resonance frequencies are 17 and 46 MHz.

## SERS ON FUNCTIONALIZED SILVER NANOSTRUCTURES: TOWARDS THE DETECTION OF SINGLE MOLECULES IN HOT SPOTS

*José V. García-Ramos, L. Guerrini, C. Domingo and S. Sánchez-Cortés*  
*Instituto de Estructura de la Materia. CSIC, Serrano, 121, Madrid, Spain*  
[jvicentegr@iem.cfmac.csic.es](mailto:jvicentegr@iem.cfmac.csic.es)

The optical properties of metallic Nanoparticles have a big scientific and technological importance. Such properties are determined by the Localized Surface Plasmons (LSP) the nanoparticles (NPs) support, which strongly depend on the NPs size and shape. The resonant excitation of the LSP leads to enormous enhancement of the electromagnetic field in close proximity of the NPs which originates a very important enhancement in the cross sections of SERS technique (Surface Enhanced Raman Scattering). This is the reason of the high sensitivity of this technique which, together with its ability to provide accurate structural information, makes it suitable to be employed as a molecular sensing technique. The possibility of controlling the LSP, tailoring the NPs morphology, pushes ahead the investigation of new methods of production of metallic NPs. Besides, they can be functionalized to improve their properties and increase their selectivity, consequently enlarging their applications.

In general the molecules active in SERS show some affinity for the metal resulting in the necessary approach to the surface. However many other molecules, whose trace detection is of great interest, do not present this affinity and their SERS signal is not detectable. The important environmental contaminants polycyclic aromatic hydrocarbons (PAHs) belong to the last group of molecules. Nonetheless it has been shown that by modifying properly the chemical properties of the metal surface it is possible to augment drastically the approaching of these pollutants to the metallic substrate<sup>1-3</sup>, then their SERS sensing being feasible.

At the same time it is generally accepted that the possibility of single molecule detection (SMD) depends on the existence of interparticle gaps where the main part of the electromagnetic field intensification occurs<sup>4,5</sup>. One usually refers to these special regions of the metallic surface as *hot spots* (HS). Aggregated colloids are the main source for SMD<sup>6</sup> but the fabrication of such HS escapes from the experimental control in macro conditions. Thus, the molecules adsorbed on the metal surface may effectively play a crucial role in the formation of these HS<sup>7,8</sup>.

We have employed three Viologen Dications (VGD), specifically paraquat (PQ), diquat (DQ) and lucigenin (LG), for the functionalization of silver colloidal nanoparticles (Ag NPs). VGD are able both to form charge transfer (CT) complexes with electron donor species such as PAHs<sup>9</sup> and interact strongly with the metal surface. In particular their bifunctional nature makes them able to induce the formation of HS. Thus VGD act simultaneously as HS builders and as molecular hosts in the detection of analytes to the highly sensitive region of the so-formed HS. The three VGD considered were selected because of their different structure regarding the extension of the aromatic part and the position of N atoms included.

The LG functionalization provided the most powerful VGD-NPs sensor system: we have reported the SERS detection of pyrene (PYR) down to nanomoles through spectra obtained employing the colloidal suspension (macro Raman) and in the zeptomol regime for spectra products of single aggregate of NPs (micro Raman). Furthermore we concluded that the LG-

NPs sensor system presents the ability to improve at the same time its stability (increased CT contribution and tighter bridging between LG and the two silver particle constituting the dimer) when interacting with the target molecule PYR.

### Acknowledgements

Authors acknowledge grants FIS2007-63065 from Dirección General de Investigación, Ministerio de Educación y Ciencia (Spain) and Comunidad Autónoma de Madrid project MICROSERES number S-0505/TIC 0191 for financial support. L.G. acknowledges CSIC for the I3P fellowship co-founded by the European Social Fund.

### References

- [1]. Leyton, P.; Sanchez-Cortes, S.; Garcia-Ramos, J.V.; Domingo, C. ; Campos-Vallette, M.M.; Saitz, C.; Clavijo, R.E. *J. Phys. Chem. B* **2004**, 108, 17484.
- [2]. Leyton, P.; Sanchez-Cortes, S.; Garcia-Ramos, J.V.; Domingo, C. ; Campos-Vallette, M.M.; Saitz, C. *Appl. Spectrosc.* **2005**, 59, 1009.
- [3]. Guerrini, L.; García- Ramos, J.V.; Domingo, C.; Sanchez-Cortes, S. *Langmuir* **2006**, 22, 10924.
- [4]. Otto, A. *J. Raman Spectrosc.* **2006**, 37, 937.
- [5]. Le Ru, E. C.; Etchegoin, P. G.; Meyer, M. *J. Chem. Phys.* **2006**, 125, 204701.
- [6]. Aroca, R. *Surface-enhanced Vibrational Spectroscopy*, John Wiley & Sons: Chichester, 2006
- [7]. Anderson, D. J.; Moskovits, M. *J. Phys. Chem.* **2006**, 110, 13722.
- [8]. Lee, S. J.; Morrill, A. R.; Moskovits, M. *J. Am. Chem. Soc.* **2006**, 128, 2200.
- [9]. Wiley: New York, 1998 Monk, P. *The Viologens: Physicochemical Properties, Synthesis and Applications of the Salts of 4,4'-Bipyridine*.

## HIGH MOBILITY INDIUM ZINC OXIDE DEPOSITED BY RF MAGNETRON SPUTTERING AT ROOM TEMPERATURE

*G. Gonçalves, E. Elangovan, P. Barquinha, L. Pereira, R. Martins, E. Fortunato*  
 CENIMAT/I3N, Materials Science Department, Campus de Caparica, 2829-516 Caparica,  
 Portugal

Tel: +351212948562; Fax: +351212948558

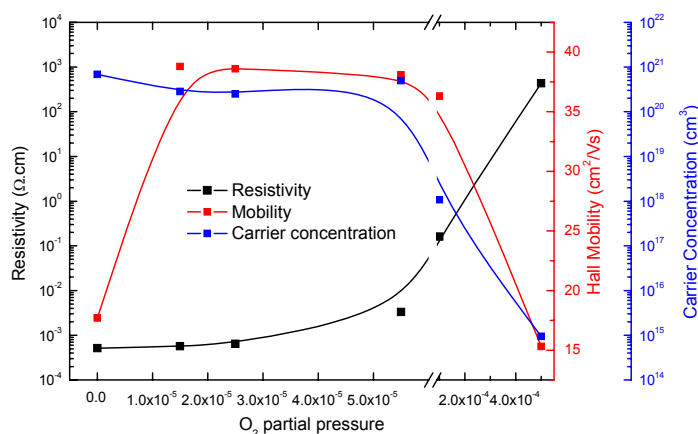
*gpg@fct.unl.pt*

Transparent conducting oxide (TCO) with optical transmission exceeding 80 % in the visible region (550 nm) and resistivity less than  $10^{-3}$   $\Omega\text{cm}$  have been widely used in a variety of applications, for more than a half-century. More recently, they become the subject of intense investigation for applications as transparent electrodes for optoelectronic devices like flat panel displays, solar cells to organic light emitting diodes. Most of the previous research on TCOs has been focused on indium tin oxide (ITO) and fluorine tin oxide (FTO).

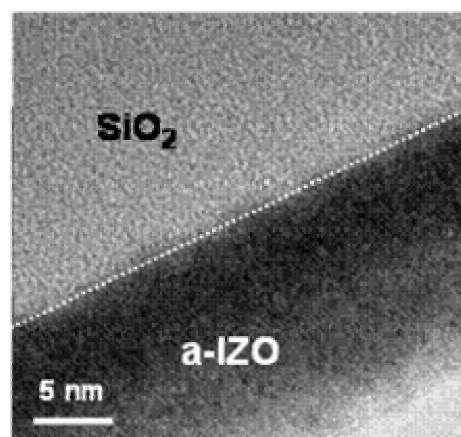
The TCOs most widely used for display applications are crystalline indium tin oxide (c-ITO), amorphous indium tin oxide (a-ITO), and amorphous indium zinc oxide (a-IZO). The most common method for the deposition of these TCOs is DC/RF magnetron sputter deposition.

In general, ITO is deposited from sintered ceramic  $\text{In}_2\text{O}_3$  targets containing between 3 and 10 wt%  $\text{SnO}_2$  while IZO targets contain 7-10 wt%  $\text{ZnO}$ . At present, crystalline ITO deposited onto substrates heated to 250-350 °C offers the lowest resistivity currently available ( $1\text{-}3 \times 10^{-4}$   $\Omega\text{cm}$ ). Two alternatives to c-ITO that may be processed at room temperature are a-ITO and a-IZO. Both of these amorphous materials have slightly inferior electrical transport properties compared to c-ITO but, they are, in some applications, favoured over crystalline ITO because they offer improved lithographic line definition due to the more controllable wet-etch characteristics of the amorphous phase. In addition, a-IZO offers the advantage of not requiring the addition of oxygen to the sputter gas since the optimum resistivity is at or near zero oxygen partial pressure.

In this paper we present some of the the morphological, electrical and optical properties of a-IZO thin films as well as its applications to optoelectronic devices with improved performances like: transparent TFTs, electrochemical devices and PLEDs.



Dependence of the electrical resistivity, carrier concentration and carrier mobility of a-IZO films as a function of oxygen partial pressure.



TEM cross section of an amorphous oxide semiconductor (indium zinc oxide) deposited onto  $\text{SiO}_2$  by rf magnetron sputtering at room temperature. The electron Hall mobility is  $60 \text{ cm}^2/\text{Vs}$ .



## TUNABLE FABRY-PEROT OPTICAL FILTER WITH A RESONANT CAVITY BASED ON A PIEZOELECTRIC POLYMER

*B. Silva\**, *J.G. Rocha\**, *A. J. Ferreira\*\**, *S.Lanceros-Mendez\*\** and *G.Minas\**

*\*Universidade do Minho, Dept. de Electrónica Industrial, 4800-058 Guimarães, Portugal*

*\*\*Universidade do Minho, Dept de Física, Campus de Gualtar, 4710-057 Braga, Portugal*

*gerardo@dei.uminho.pt*

This article describes a tunable Fabry-Perot optical filter with its resonant cavity based on a piezoelectric polymer, for application in the biochemical analysis of biologic fluids. The filter is composed by two thin-films of silver -mirrors- located parallel one to the other and separated by a nanometer size thin polymer film of poly(vinilidene fluoride), PVDF, in its  $\beta$ -phase. When applying an electrical voltage to the mirrors, the thickness of the polymer changes, changing the distance between the mirrors and thus modifying the response of the filter. The lack of parallelism in conventional Fabry-Perot filters is solved with this approach, once the changes in polymer, reflecting variations at a molecular level, are uniform in the whole area. Therefore, this filter provides the selection of a wide range of wavelengths allowing the use of a conventional white light as source, and avoiding the use of monochromatic sources that increase substantially the price of the analysis devices and consequently the cost of the analysis.

The analysis of biological fluids has shown to be a very important factor in the detection and/or treatment of illnesses. For that reason, it is usual a doctor to prescribe, periodically, clinical analysis to the patients for routine diagnosis. Normally the analyses are performed in central laboratories dislocated from the doctor's office, being their results available only some hours or even days later. Due to this situation, the doctor cannot make a reliable diagnosis to the patient in useful time and, moreover, the analysis system becomes expensive and uncomfortable [1, 2]. In order to avoid the drawbacks existing in conventional analysis devices, it has been developed small portable and easy of use devices that provide higher comfort to the patient.

The filter that is presented here constitutes one of the three parts of a clinical analysis microlaboratory, whose working principle is based on the spectrophotometric analysis of biological fluids for measuring the concentration of several biomolecules that are present in those fluids. Each biomolecule presents a maximum value of absorbance when excited by a light at a specific wavelength. The concentration of each biomolecule in the biological fluid is directly related with the value of the absorbance [3, 4].

The referred microlaboratory is composed by three parts. The first one is a microchannel system in which the samples and reagents are placed, and includes microreservoirs where each sample is tested (Fig. 1a). The second part contains optical detectors and their readout electronics, which are usually manufactured in CMOS (Fig. 1b). The third part contains the optical filtering system, which selects the wavelength that corresponds to the biomolecule into analysis (Fig. 1c). The tunable optical filter presented in this article has the main goal of simplifying the third part of the microlaboratory, replacing the array of non-tunable optical filters already implemented by our group (Fig.1c) [5].

The fabrication of the filter is based on thermal evaporation and spin coating techniques. In a first step, a silver mirror was deposited on a glass substrate, whose only function here is to

serve as physical support to the filter. In the next step a nonmeter size thin polymer film was spin-coated on top of the silver thin-film already deposited and poled. Finally, the second thin-film of silver was deposited on the polymer film. Fig. 2 shows a picture of the filter.

### Acknowledgements:

Work supported by the Portuguese Science Foundation (grant PTDC/BIO/70017/2006).

### References:

- [1] S. K. Strasinger and M. S. Di Lorenzo, *Urianalysis and Body Fluids*, 4th ed., F. A. Davis Company, Philadelphia, PA. 2001.
- [2] C. Pinheiro, J. G. Rocha, L. M. Gonçalves, S. Lanceros-Mendez and G. Minas, *A tunable Fabry-Perot optical filter for application in biochemical analysis of human's fluids*, in ISIE IEEE, Montréal, Québec, Canada, pp. 2778-2783, July 9-12, 2006.
- [3] *Biochemical and Organic Reagents*, Sigma, 2002.
- [4] G. Minas, R. F. Wolffenbuttel and J. H. Correia, *A Lab-on-a-Chip for Spectrophotometric Analysis of Biological Fluids*. In *Lab-on-a-Chip*, The Royal Society of Chemistry, **5**, (2005), pp. 1303-1309.
- [5] G. Minas, R. F. Wolffenbuttel and J. H. Correia, *An array of highly selective Fabry-Perot optical-channels for biological fluids analysis by optical absorption using white light source for illumination*. In *Journal of Optics A*, IOP, **8** (2006), pp. 272-278.

### Figures:

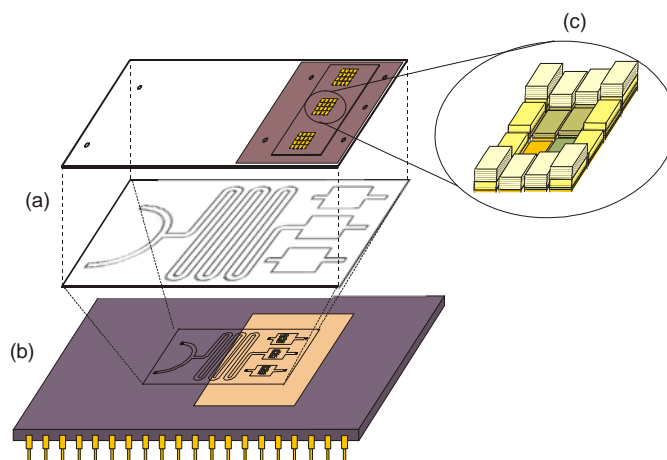


Fig.1: Schematic representation of the lab-on-a-chip structure; a) microchannel system, b) optical detectors and their readout electronics; c) optical filter array.

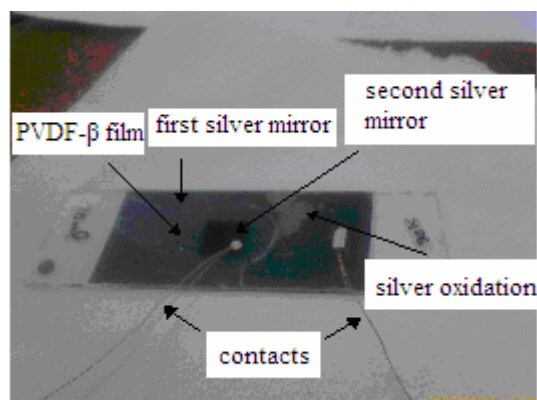


Fig.2: Tunable Fabry-Perot Optical filter prototype.

## POLYMER BASED ELECTRO-ACTIVE MICRO- AND NANO-COMPOSITES

**J. Gomes<sup>1,2</sup>, D. Miranda,<sup>1</sup> S. E. Fernandes<sup>1</sup>, J. Serrado Nunes<sup>1</sup>, P. Costa<sup>1</sup>, S. Firmino Mendes<sup>1</sup>,  
C.M. Costa<sup>1,2</sup>, V. Sencadas<sup>1</sup>, S. Lanceros-Méndez\*<sup>1</sup>**

<sup>1</sup>Dept. de Física, Universidade do Minho, Campus de Gualtar, 4710-057 Braga, Portugal,

<sup>2</sup>CeNTI, Center for Nanotechnology and Smart Materials, Rua Fernando Mesquita 2785, 4760-034, Famalicão, Portugal

\*lanceros@fisica.uminho. pt

### Abstract

Polymeric materials filled with micro and nanoparticles have been widely investigated in the last few years. Till recently, mainly the mechanical reinforcement effect of these nanofillers was highlighted. Nowadays, several composites and nano-composites of electroactive polymers have been investigated due to their potential applications. In this way, carbon nanotubes/ polymer nanocomposites with high dielectric constant; electroactive polymers with metallic nanoparticles in order to tune electro-optic properties, magnetostrictive nanoparticles inducing magnetoelectric response, and the introduction of ceramic microparticles to tune dielectric and piezoelectric properties have been investigated. [1]

In this work several nanocomposites of carbon nanofibers, magnetic nanoparticles and ceramic micro-particle with electroactive PVDF have been prepared by a solution method with *N, N*-dimethylformamide for different wt% concentration of the fillers. The crystalline phase of the matrix was the non-polar  $\alpha$ -PVDF. Further, the nanocomposites are uniaxially stretched in order to achieve the phase transformation to polar  $\beta$ -phase within the polymeric matrix.

The general issues related to the processing of the electroactive composites such as dispersion, stretching and poling will be presented and discussed. The influence of the amount of crystalline part of the polymer, morphological properties, macroscopic mechanical and electrical properties and thermal stability of the composites were studied.

SEM micrographs of the samples show that the composites crystallise in a spherulitic structure, similar to the one of pure  $\alpha$ -PVDF [1]. AFM micrographs also show the crystalline spherulitic structure with randomly distributed nanoparticles. (Figure 1)

The insertions of nanofillers also have a significant effect on the elastic modulus, electrical properties and electro-optical properties of the composites with respect to the polymer matrix. As an example, the elastic modulus of the PVDF-CNF composites nearly doubles for a small incorporation of CNF (lower than 1%) and remains almost constant for higher concentrations.

The  $\alpha$  to  $\beta$  phase transformation in order to get the electroactive  $\beta$ -phase of the polymer was studied for the nanocomposites and it was concluded that the maximum amount of  $\beta$ -phase is obtained by stretching ratios of 5 or more at a temperature of 80 °C [1-3] (Fig. 2).

In order to achieve the desired electromechanical, magnetoelectric and electro-optical properties, the composites have to be poled (Figure 3 and 4). The poling behaviour of the polymer matrix nanocomposites, and the selection of the poling method, is also evaluated taking into account the poling behaviour of the ferroelectric PVDF-matrix.

The general issues related to the processing of the electroactive composites such as dispersion, stretching and poling will be presented and discussed. The influence of these parameters on some key macroscopic properties such as the electrical and mechanical properties will be also presented.

Particular attention will be drawn on the stretching and poling process necessary to achieve

polar  $\beta$ -phase within the polymeric matrix, as this critical step shows specific issues within the different nanocomposites.

### Acknowledgements

Authors want to express their thanks to *Solvay* and *Applied Sciences, Inc.*, for the excellent material provided and to *Portuguese Foundation for Science Technology – FCT* for financial support (Grant POCI/CTM/ 59425/2004). V. Sencadas acknowledges the FCT for the PhD Grant (SFRH/BD/16543/2004).

### References

- [1] Sencadas V, Moreira VM, Lanceros-Mendez S, Pouzada AS, Gregório Filho R, *Mat. Sci. Forum* Vol. 514-116, 872-876, 2006.
- [2] Sencadas V, Lanceros-Mendéz S, Gregorio Jr. R, submitted to *Acta Materialia*, 2008
- [3] Nam Y, Kim W, Cho Y, Chae D, Kim G, Hong S, Hwang S, Hong S, *Macromolecular Symposium*, 249-250, 478-484, 2007.

### Figures:

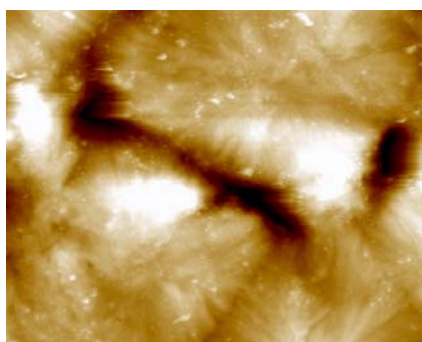


Figure 1. AFM images of the spherulitic structure with with randomly distributed nanoparticles

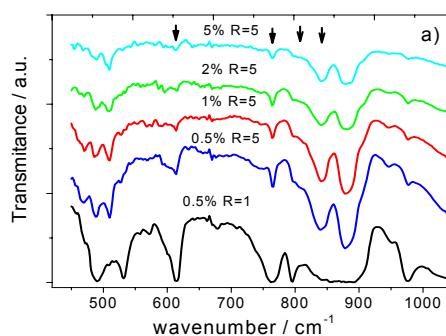


Figure 2. FTIR spectra of PVDF-CNF nanocomposites with different CNF concentrations.

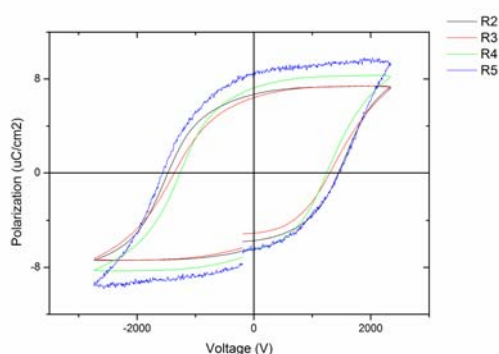


Figure 3. Hysteresis loops for different stretching ratios R2-R5.

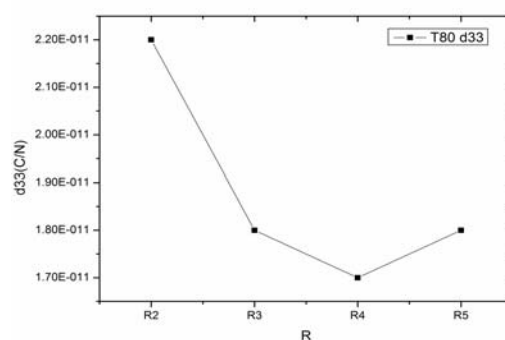


Figure 4.  $d_{33}$  coefficient for different stretching ratios R2-R5 in a sample stretched at a temperature of 80 °C.

## INTEGRATED PLATFORM FOR STEM CELLS SEPARATION/COUNTING

*J.Loureiro, S.Cardoso, C.L.Silva, J.M.Cabral, P.P.Freitas*  
*INESC-MN, Rua Alves Redol, Lisboa, Portugal*  
[jloureiro@inesc-mn.pt](mailto:jloureiro@inesc-mn.pt)

Hematopoietic stem/progenitor cells (HSC) have vast potential for use in medical applications (such as bone marrow transplantations) and the separation of these cells from blood has an important role in the stem cells research [1]. However, the most usual techniques, (MACS™) and (FACS), have some drawbacks like being cell-losing or very time-consuming.

This work is in the area of nanobioengineering, combining a cross-disciplinary approach of nanotechnology, bioseparation engineering and hematology with a common goal: the separation, purification and monitoring of HSC *in vitro*.

Until now a device based on magnetophoresis has been developed using microfluidics and in-situ magnetic fields (up to 6kA/m), generated by metallic lines, in order to separate stem cells from blood in a more efficient and easy way [2], [3], [4], [5]. In the same device Spin Valve sensors are used to measure the efficiency of the separation (by counting the cells as they are separated).

The geometry of the separator makes it possible to change only the path of specific stem cells, that are magnetically labeled with 50nm magnetic beads functionalized with monoclonal antibodies (MAbs), instead of separating all the magnetic elements in the fluid (which is vital to keep count of the stem cells).

The fluidic system consists in 2 micro-channels (150µm wide, 14µm thick and 40µm apart) joined over several gaps of 2.5mm and disposed in an “H”-type geometry (fig.1 and fig.2). The laminar flow is generated in the y-direction along both channels, from the inlet to the outlet. The fluidic system is bonded to the separator platform which consists in two successive lines (7µm wide and 500nm thick), deviated from the y-direction by an angle of 5 degrees, starting in one channel and ending in the other one. At the end of each metallic line there are 3 SV in each channel to count the cells that have been separated and those that might fail to be separated [6],[7].

To prove the concept and test the design, preliminary tests were made passing 2µm magnetic particles through the channels. These particles ( $\chi=0.22$  and  $\rho=1.1 \times 10^3$  kg/m<sup>3</sup>) feel a magnetic force of 9.5pN, when passing over the metallic lines (due to a magnetic field of 6kA/m and a gradient of  $2.2 \times 10^6$  kA/m, when applying 100mA), which force them to be deviated in the x-direction. With velocities flow rates around 30nL/min, particles were observed to follow the line path, moving from the beginning of the line (in the first channel) until the end of it (in the second channel) (fig.3). When any particle fail to feel the first line (due to agglomeration for e.g.) it can be separated when passing over the next line. These measurements were made for a concentration of  $1 \times 10^5$  particles/µl to make the optical inspection easier. The real experiment will be made with human hematopoietic stem/progenitor cells (CD34<sup>+</sup> enriched cells), from umbilical cord blood samples.

### References:

- [1] - "Ex-vivo expansion of hematopoietic stem cells in bioreactors", Cabral, J.M. (2001) *Biotechnology Letters* 23, 741-751.
- [2] – “Flow through, Immunomagnetic Cell Separation”, J.J.Chalmers, M.Zborowski, L.Sun and L.Moore, in *Biotechnol. Prog.* 1998, 14, 141-148
- [3]– “Separations based on magnetophoretic mobility”, M. Zborowski, L.Moore, P.Stephen Williams and J.J.Chalmers, in *Separation Science and Technology*, vol.37, No.16, pp.3611-3633, 2002

- [4] – “Continuous sorting of magnetic cells via on-chip free-flow magnetophoresis”, N.Pamme and C.Wilhelm, Lab-Chip, 2006, 6, 974-980
- [5] – “Analytical model for the magnetic field and force in a magnetophoretic microsystem”, E.P.Furlani and Y.Sahoo, in J.Phys. D: Appl. Phys. 39 (2006) 1724-1732
- [6]- “Flow Velocity Measurement In Microchannels Using Magnetoresistive Chips”, H.A. Ferreira, D. L. Graham, P. Parracho, V. Soares, and P.P.Freitas, IEEE Trans Magn., vol.40, pp. 2652-2654, July 2004.
- [7]- “Magnetoresistive sensors”, P.P Freitas, R.Ferreira, S.Cardoso and F.Cardoso, in J.Phys.: Condens. Matter 19, N16 (23 April 2007), 165221 (21pp)

### Figures:

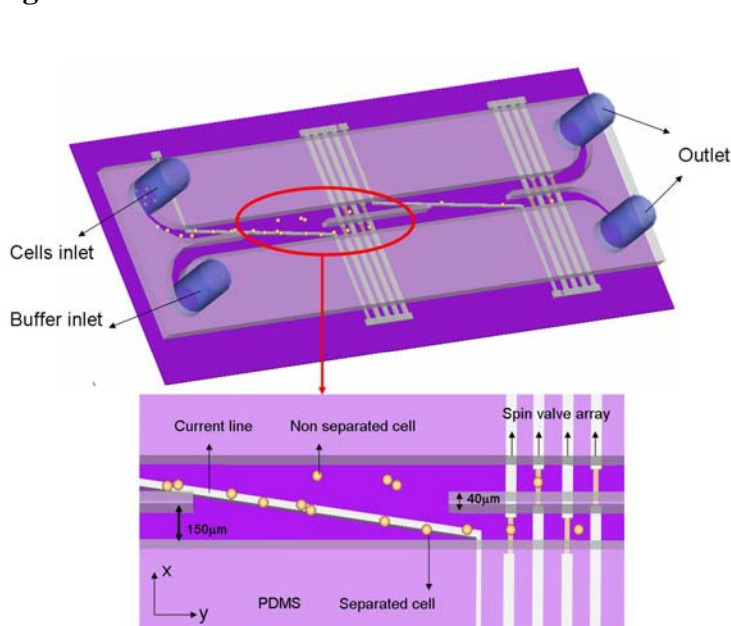


Fig1: “H-type” fluidic platform, allowing stem cells to be separated from one channel to the other due to the magnetic field created by the oblique current lines. Each channel has spin valves at the end to count the cells

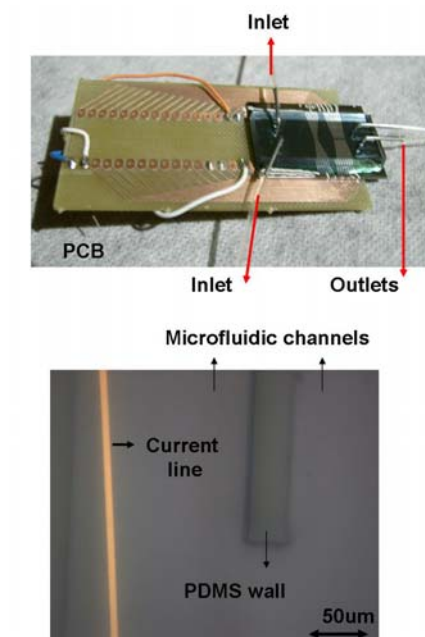


Fig2: Real chip mounted on a PCB to allow electrical measurements (top); Microscope image of the microfluidic system showing the current line near the gap between both channels

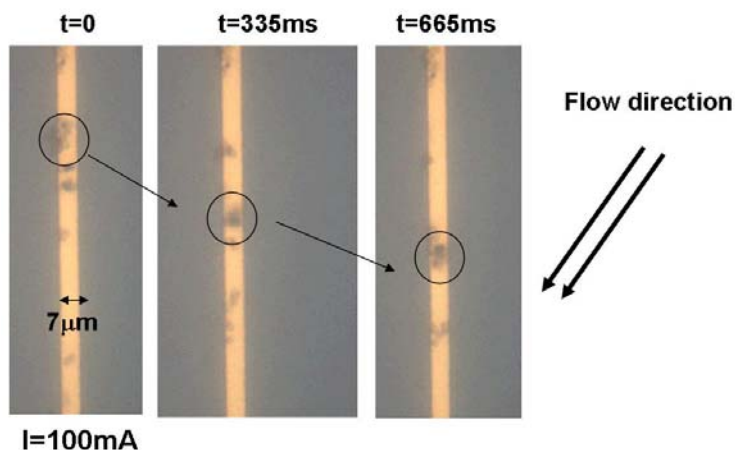


Fig3: Time evolution of the  $2\mu\text{m}$  particles position due to the fluid velocity and the magnetic field created by the current line (when applying 100mA) during the separation. These particles were moving over the line with a velocity around  $75\mu\text{m/s}$ .

## DIRECT NUMERICAL SIMULATION OF CARBON NANOFIBRE COMPOSITES UNDER SHEAR FLOW

M. Yamanoi, João M. Maia

I3N – Institute for Nanostructures, Nanomodeling and Nanofabrication  
IPC – Institute for Polymers and Composites, University of Minho, Portugal  
Campus de Azurém 4800-058 Guimarães, Portugal  
yamanoi@dep.uminho.pt; jmaia@dep.uminho.pt

The mechanical and transport properties of carbon nanofibres, CNF, in combination with their low production costs make them a promising material for use in polymer composites. However, the level of these properties is largely dependent on the fibres' dispersion state and aspect ratio, which, in turn, depend on the processing history of the composites. Due to strong Van der Waals interactions, CNFs tend to agglomerate, reducing their effectiveness in polymer composites. Applied shear during processing can break up the agglomerates and disperse the CNFs, but excessive shear can lead to fibre breakage, which negatively affects final properties. It is therefore crucial to 'tailor' the level of shear to obtain good dispersion, without fibre length reduction.

The current work studies the effect of simple shear flows (dominant in typical polymer processes) on the dispersion state of CNF composites and consists in a direct simulation method based on the Particle Simulation Method developed by Yamamoto et al. [1] to analyze fiber dispersed systems. In the present work fibers are modelled as a series of connected spheres, with stretching force, torsion and bending torques being considered. Also studied is the effect of van der Waals interactions on the state of aggregation of the nanofibres. In addition our code allows the simulation of the effects of both near-field and far-field hydrodynamic interactions with relatively short computational times [2], collision interactions [3] and fibre orientation [4]. The method is a very powerful one, currently allowing the semi-quantitative prediction of the dynamics of the fibre suspensions as well as the correct prediction of the kinematics, including some previously unexplained orientation effects observed experimentally.

This work focuses on the flocculation structures that form under shear flows for different fiber flexibilities. Thus, Young moduli,  $E$ , of 6, 60, and 600 G Pa were selected for flexible, semi-flexible, and rigid fibers, respectively. Table 1 shows details of the model nano-fiber composites.

Volume fraction, $\phi$	0.01
Radius of fiber, $a$	25 nm
Aspect ratio	20
Number of fiber	50
Shear rate, $\dot{\gamma}$	10
Viscosity of matrix, $\eta_0$	1000 Pa·s
Young modulus, $E$	6, 60, 600GPa

Table 1: Materials parameters used for simulation.

The randomly oriented, perfectly dispersed, no contact between fibers state shown in the figure 3 was used as an initial condition for the simulations. Figure 4 shows the snapshots of fiber structures of (a)  $E= 6$  GPa, (b)  $E= 60$  GPa, and (c)  $E= 600$  GPa under simple shear flows. Figure 4a shows small round flocculation, consisting of a few fibers. There is not only flocculation but also isolated S-shaped fibers that tumble periodically along their axis. Figure 4b shows cylindrical flocculation from many fibers, with the bundles essentially aligned in the vorticity

direction. Figure 4c shows flocculation parallel to the flow direction, with percolation conditions occurring. The percolation volume fraction threshold for rigid fibers of aspect ratio 20 is 0.0415 [6]. Although the present simulation is for a volume fraction 0.01, which is less than the threshold, it is conceivable that VDW interactions effectively decrease it, thus allowing percolation to occur. The behaviors shown in Figures 4b and 4c have also been observed experimentally [5].

Figure 5 shows the orientation of fibers under simple shear flows. At strain  $\gamma = 0$ , the components of orientation  $a_{xx}$ ,  $a_{yy}$ ,  $a_{zz}$  are 0.33, from which it is obvious that the initial state is an isotropically oriented one. After the application of the flow field, the maximum oriented state is achieved for every case at a strain  $\gamma$  around 20. After that, differences are observed, with both Figure 5a and 5b showing that  $a_{xx}$  decreases and  $a_{yy}$  and  $a_{zz}$  are gradually increasing (at strain 200  $a_{yy}$  and  $a_{zz}$  are almost equal).

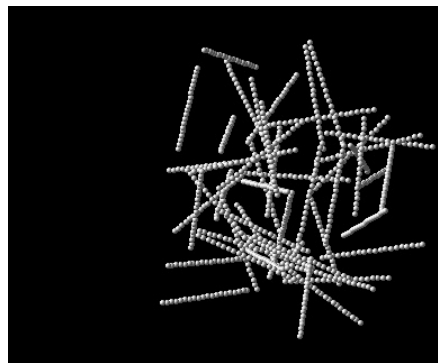
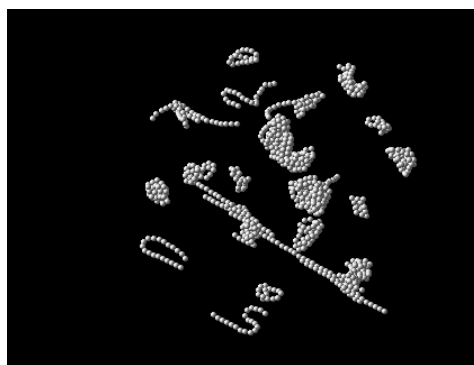
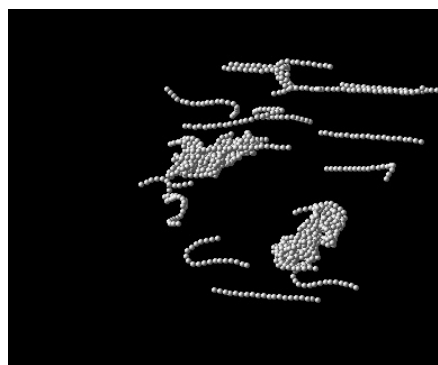


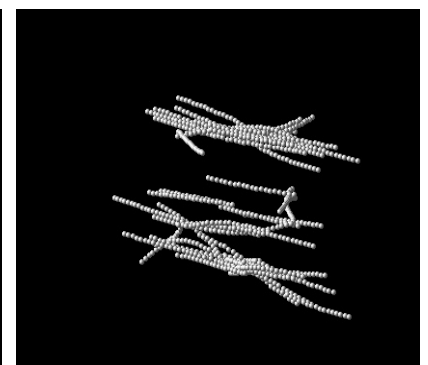
Figure 1: Initial condition



(a)  $E= 6$  GPa



(b)  $E= 60$  GPa



(c)  $E= 600$  GPa

Figure 2: Aggregated structures of nano-fibers at  $\gamma=200$  under simple shear flows.

## REFERENCES

- [1] S. Yamamoto and T. Matsuoka, J. Chem. Phys. 98, 644, 1993.
- [2] L. Durlafsky, J. F. Brady and G. Bossis, J. Fluid Mech. 180, 21, 1987.
- [3] S. Yamamoto and T. Matsuoka, J. Chem. Phys. 102, 2254, 1995.
- [4] S. G. Advani and C. L. Tucker III, J. Rheol. 31, 751-784, 1987.
- [5] A. W. K. Ma, M. R. Mackley and A. A. Rahatekar, Rheol. Acta. 46, 979, 2007.
- [6] E. J. Garboczi, K. A. Snyder, J. F. Douglas and M. F. Thorpe, Phys. Rev. E 52, 819, 1995.

**PREFERENTIAL NUCLEATION, MOLECULAR DISTORTION, CHARGE TRANSFER, AND ELASTIC EFFECTS IN THE SELF-ASSEMBLY OF TCNQ ON Cu(100)**

*Christian Urban*<sup>1</sup>, *Marta Trelka*<sup>1</sup>, *David Écija*<sup>1</sup>, *Roberto Otero*<sup>1,2</sup>, *Rodolfo Miranda*<sup>1,2</sup>,  
*Luis Sánchez*<sup>3</sup>, *Nazario Martín*<sup>2,3</sup>,  
*Yang Wang*<sup>4</sup>, *Manuel Alcamí*<sup>4</sup>, *Fernando Martín*<sup>4</sup>,  
*José M. Gallego*<sup>5</sup>

<sup>1</sup> *Dpto. de Física de la Materia Condensada, Universidad Autónoma de Madrid, Cantoblanco, 28049-Madrid, Spain*

<sup>2</sup> *Instituto Madrileño de Estudios Avanzados en Nanociencia (IMDEA-Nanociencia), Cantoblanco, 28049-Madrid, Spain*

<sup>3</sup> *Departamento de Química. Universidad Autónoma de Madrid. Cantoblanco, 28049 - Madrid. Spain*

<sup>4</sup> *Departamento de Química Orgánica. Universidad Complutense de Madrid. Cantoblanco, 28040 - Madrid. Spain*

<sup>5</sup> *Instituto de Ciencia de Materiales de Madrid - CSIC, Cantoblanco, 28049-Madrid, Spain*  
[josemaria.gallego@uam.es](mailto:josemaria.gallego@uam.es)

It is well known that the 2D self-assembly of organic molecules on solid surfaces is the result of a combination of molecule-molecule and molecule-substrate interactions. However, due to the large number of factors involved (which can include charge transfer between the molecule and the substrate, changes in the molecular conformation, the combination of weak noncovalent forces, like van der Waals or dispersive forces, with stronger ones, like hydrogen bonding or even covalent bonding), there are few cases where the surface arrangement of the molecule is completely understood. In this work we report on the self-assembly of TCNQ when vapour-deposited in UHV conditions on Cu(100), as studied with a combination of STM experiments and DFT calculations, which has allowed us to get a complete picture of the system, even although TCNQ is a strong electron acceptor, and then it is expected to interact strongly with the Cu surface.

The STM results show that submonolayer amounts of TCNQ grow epitaxially on Cu(100), with an almost rectangular lattice, although forming four different domains on the surface (Fig. 1). Taking into account the size of the molecule, and the angular orientation of the molecular main axis with respect to the substrate, these domains can be explained by assuming that the molecule rotates on the surface until the four N atoms are on bridge positions of the Cu atomic lattice (Fig 2). In addition, the theoretical calculations show that the Cu-N bonding changes the molecular conformation: the N atoms are closer to the Cu surface than the rest of the molecule (Fig. 3), while at the same time the Cu surface is noticeably distorted.

The self-assembly of the molecule is also the result of a combination of forces. Along one direction of the overlayer unit cell, the molecular arrangement comes dictated mainly by dispersive and van der Waals forces, in combination with elastic effects that produce the dislocations visible on the STM images. Along the other direction, on the other hand, the intermolecular interaction is mediated through the substrate, involving charge transfer and surface distortion.

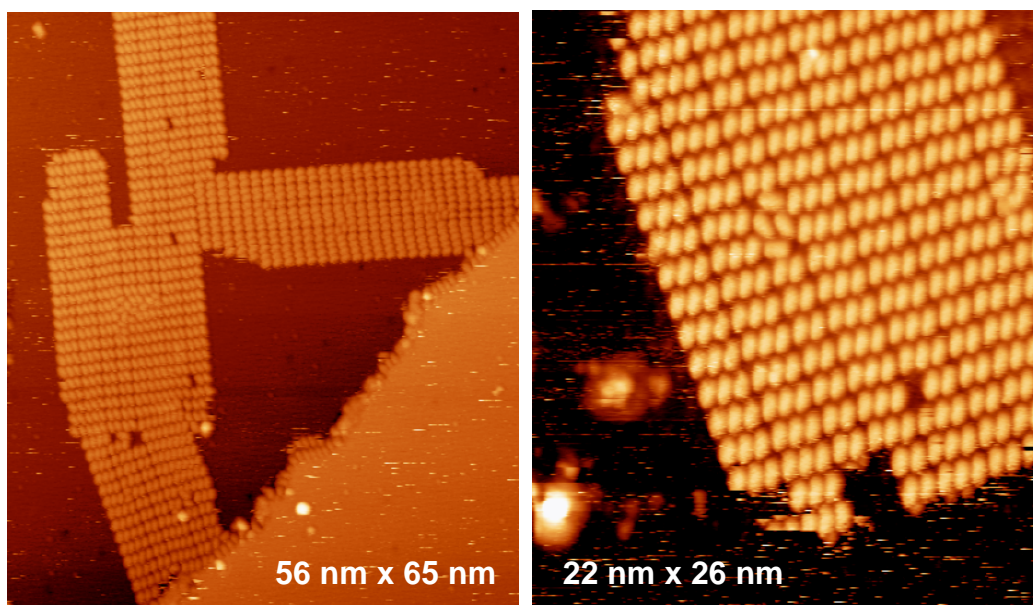


**Figure 1:** STM image of the Cu(100) surface after depositing  $\sim 0.4$  ML of TCNQ.

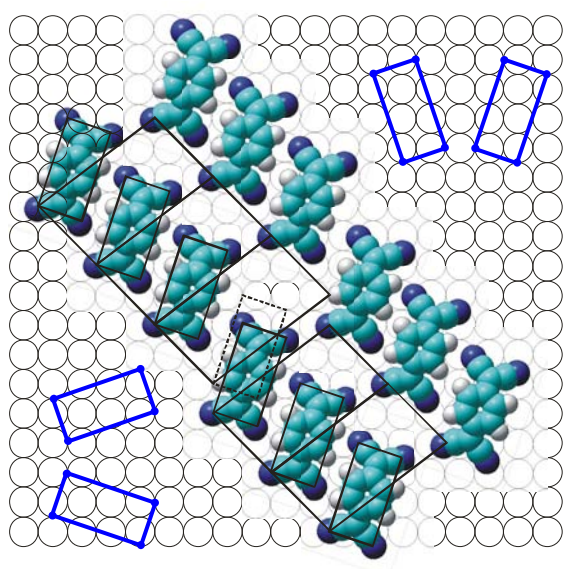


**Figure 2:** Proposed model of the TCNQ lattice on Cu(100), showing the surface unit cell and the molecular orientation. The blue rectangles show the four different orientations of the molecule with respect to the substrate.

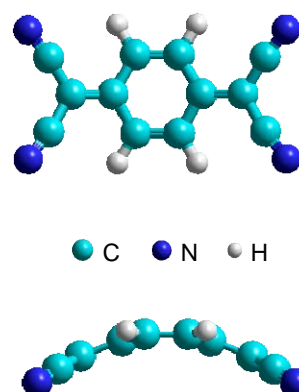


**Figure 3:** Top and lateral view of the calculated conformation of TCNQ when adsorbed on the Cu(100) surface.

## SILVER NANOPARTICLES AND GOLD METALLODENDRIMERS: FROM MOLECULAR PRECURSORS TO NANOMATERIALS

Eduardo J. Fernández,<sup>a</sup> Jorge García-Barrasa,<sup>a</sup> Antonio Laguna,<sup>b</sup> José M. López de Luzuriaga,<sup>a</sup> Miguel Monge,<sup>a</sup> M. Elena Olmos,<sup>a</sup> Eva Sánchez-Forcada,<sup>a</sup> and Carmen Torres<sup>c</sup>

<sup>a</sup>Departamento de Química. Universidad de La Rioja. Grupo de Síntesis Química de La Rioja, UA-CSIC. Madre de Dios 51. E-26006 Logroño (Spain)

<sup>b</sup>Departamento de Química Inorgánica. Instituto de Ciencias de Materiales de Aragón. Universidad de Zaragoza-CSIC. E-50009 Zaragoza (Spain)

<sup>c</sup>Departamento de Agricultura y Alimentación. Universidad de La Rioja. Madre de Dios 51. E-26006 Logroño (Spain)  
*miguel.monge@unirioja.es*

The increased interest in the synthesis of new metal-based nanomaterials stems from the fact that new electronic, optical or magnetic properties can be reached at this length scale. These properties can be tuned depending on the size and the shape of the new nanomaterials. By the use of our experience in gold and silver organometallic and coordination chemistry we have carried out the synthesis of metal nanoparticles and nanometer sized metallodendrimers through chemical methods.

The first research line makes use of the organometallic silver precursor [Ag(C<sub>6</sub>F<sub>5</sub>)] that under mild conditions and in the presence of stabilizers, permits the synthesis of small size silver nanoparticles. This *organometallic method* leads to Ag nanoparticles stabilized in different substrates such as organic ligands (amines), polymers (PVP, cellulose acetate) or inorganic SiO<sub>2</sub> (see Figure 1). Moreover, alkylamine capped silver nanoparticles (ca. 10 nm) display high antimicrobial activity against some representative microorganisms.[1]

We have also focused on the synthesis and study of a series of gold metallodendrimers. These new materials are based on PPI or PAMAM dendrimers functionalized with peripheral PPh<sub>2</sub> groups what permits the coordination of Au(I) fragments. Depending on the dendrimer generation it is possible to design new complexes from the molecular level to the nanoscale. For example, when the periphery of the dendrimer is grafted with Au(I)-thiolate units luminescent metallodendrimers can be obtained (see Figure 2).[2]

### References:

[1] E. J. Fernández, C. Torres, J. M. López de Luzuriaga, M. Monge, J. García-Barrasa, Spanish Patent P200700456, 2007.

[2] E. J. Fernández, A. Laguna, J. M. López de Luzuriaga, M. Monge, M. Montiel, M. E. Olmos, R. C. Puelles, E. Sánchez-Forcada, *Eur. J. Inorg. Chem.* (2007) 4001-4005.

**Figures:**

**Figure 1.** Transmission electron micrographs (a and c) of different magnifications and, particle size distribution (b) of HDA capped Ag nanoparticles.

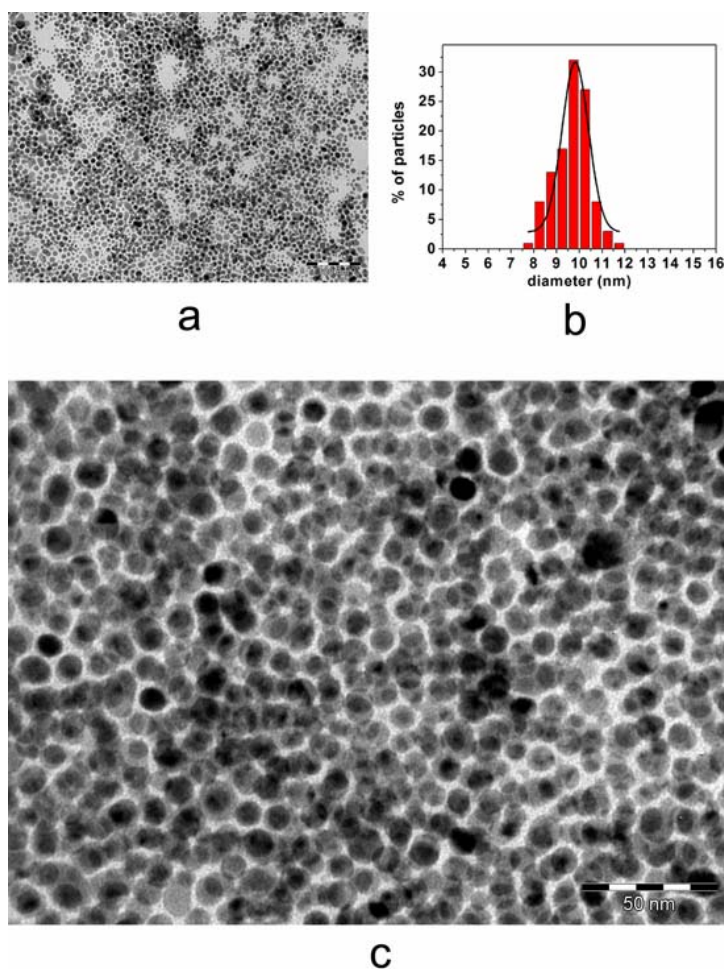
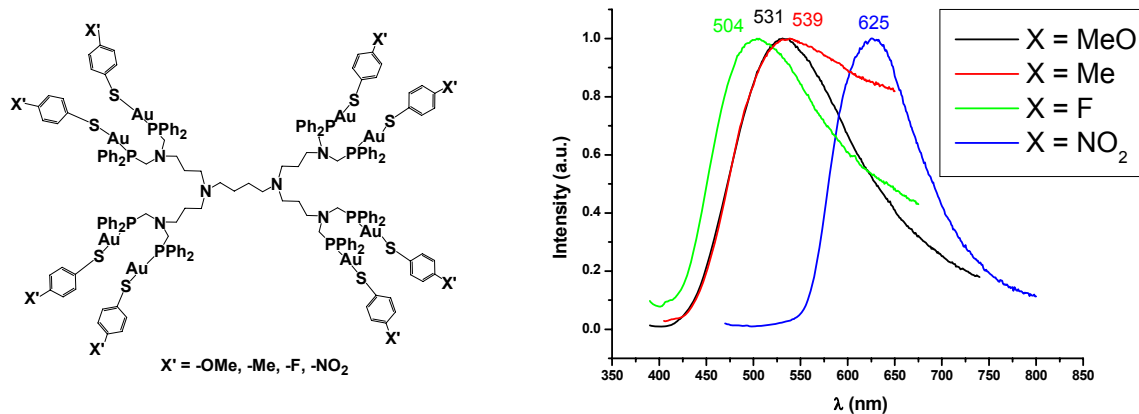


**Figure 2.** Octanuclear phosine thiolate gold dendrimers with different 4-substituted benzenethiolates and emission spectra in solid state at 77 K.



## BIODEGRADABLE POLYMERIC MICROFIBRES REINFORCED WITH NANOFIBRES FOR BIOMEDICAL APPLICATIONS

*E.D. Pinho<sup>1,2,\*</sup>, A. Martins<sup>1,2</sup>, J.V. Araújo<sup>1,2</sup>, R.L. Reis<sup>1,2</sup>, N.M. Neves<sup>1,2</sup>*

<sup>1</sup>*3B's Research Group – Biomaterials, Biodegradables and Biomimetics, Department of Polymer Engineering, University of Minho, Campus de Gualtar, 4710-057 Braga, Portugal;*

<sup>2</sup>*IBB – Institute for Biotechnology and Bioengineering, Braga, Portugal\**

[epinho@dep.uminho.pt](mailto:epinho@dep.uminho.pt)

In the biomaterials field, nanofibre based structures and its composites are promising materials to produce scaffolds. The enhanced physicochemical properties and its structure being similar to the architecture of the extracellular matrix (ECM) may solve the major challenge of tissue engineering, which is obtaining the appropriate scaffold [1].

The main purpose of this work was to develop a novel composite structure which combines polymeric microfibres reinforced by nanofibres. This combination was obtained by melting extrusion of a synthetic biodegradable polymer, poly(butylene succinate) (PBS) (99,95% wt), reinforced with chitosan nanofibre meshes (0.05% wt). The chitosan meshes, composed by randomly aligned nanofibres, were produced by electrospinning technique (Figure 1a)). Longitudinal and cross sections of reinforced microfibres were observed by scanning electron microscopy (Figure 1b)).

The tensile mechanical properties revealed that the introduction of the reinforcement into the microfibres increased the tensile modulus to  $553.2 \pm 48.4$  MPa. This improvement is around 70%, considering that the tensile modulus of microfibres without nanofibre reinforcement was  $327.8 \pm 35.3$  MPa (Figure 2 and Table1).

The various structures were subjected to swelling and degradation tests upon immersion in an isotonic saline solution at 37°C. The presence of chitosan nanofibres in the microfibres also enhanced the water uptake in up to 10% (Figure 3), caused by the higher hydrophilicity of the chitosan nanofibre meshes.

The combination of good mechanical properties and enhanced degradability of the developed structures is believed to have great potential for the production of 3D fiber mesh scaffolds, to be applied in the field of Tissue Engineering and Regenerative Medicine.

### References:

[1] Lutolf, M.P., Hubbell, J.A., “Synthetic biomaterials as instructive extracellular microenvironments for morphogenesis in tissue engineering”, *Nature Biotechnology*, **23**, 2005, 47-55.

### Figures:

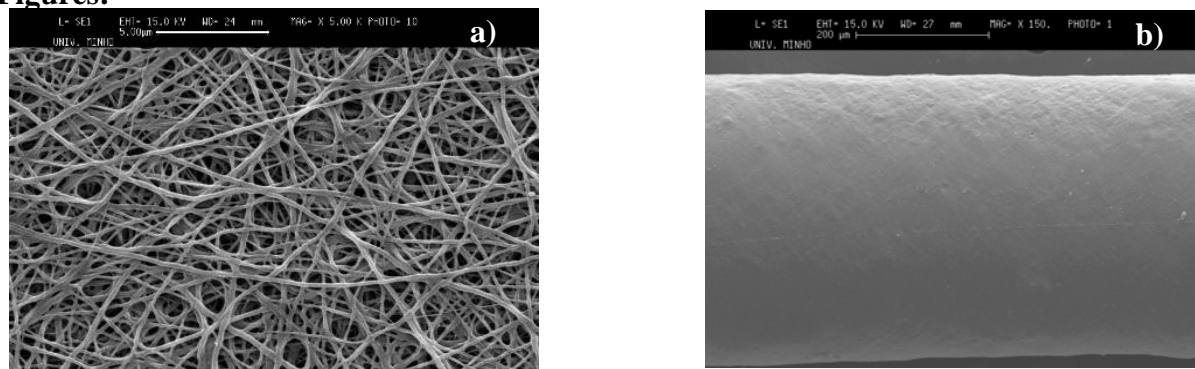


Figure 1- a) SEM micrograph of an electrospun Chitosan nanofibre meshes (x5000) and b) PBS microfibre (x150)

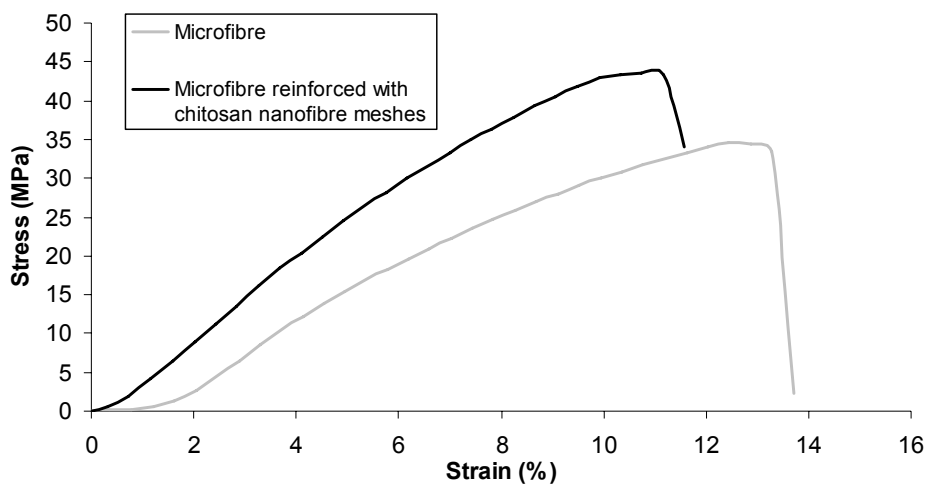


Figure 2 - Tensile stress-strain of chitosan microfibrils with and without chitosan nanofibre meshes reinforcements.

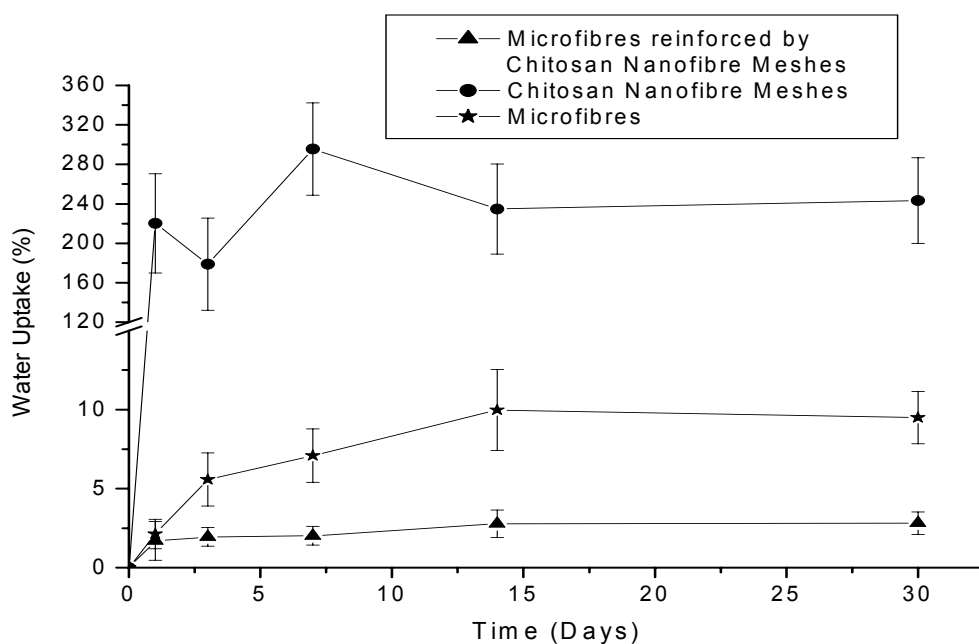


Figure 3 - Water uptake of the microfibrils reinforced by chitosan nanofibre meshes, chitosan nanofibre meshes and microfibrils, during the periods of immersion in isotonic saline solution.

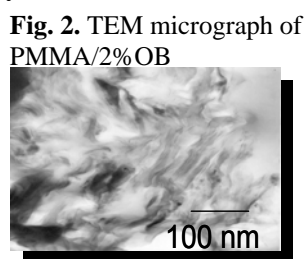
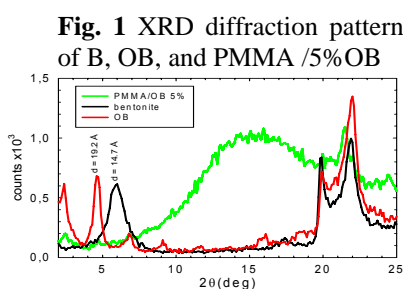
Table 1 - Tensile properties of microfibrils with and without chitosan nanofibres reinforcement.

Materials	Tensile Stress (MPa)	Tensile Modulus (MPa)	Tensile Strain (%)
<b>Microfibrils</b>	$30.6 \pm 7.2$	$327.8 \pm 35.3$	$11.6 \pm 2.3$
<b>Microfibrils reinforced with chitosan nanofibre meshes</b>	$35.4 \pm 6.4$	$553.2 \pm 48.4$	$10.7 \pm 0.9$

## PMMA-ORGANO BENTONITE NANOCOMPOSITES FROM THE EXFOLIATION-ADSORPTION TECHNIQUE AND THEIR CHARACTERIZATION BY FTIR, XRD, TEM, TSDC AND DSC.

*Norkis Salazar Serge*<sup>1</sup>, *Nery Suárez*<sup>2</sup>, *José Luis Feijoo*<sup>3</sup>, *María Hernández*<sup>2</sup>  
<sup>1</sup>Departamento de Química, <sup>2</sup>Departamento de Física, <sup>3</sup>Departamento de Materiales  
 Universidad Simón Bolívar, Caracas, Venezuela  
[nsalazar@usb.ve](mailto:nsalazar@usb.ve), [nsuarez@usb.ve](mailto:nsuarez@usb.ve), [jfeijoo@usb.ve](mailto:jfeijoo@usb.ve), [mahernan@usb.ve](mailto:mahernan@usb.ve)

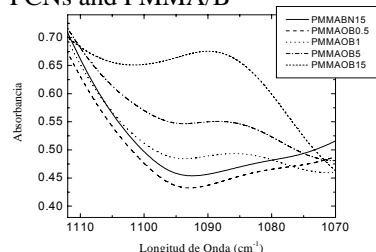
This work is related to the preparation of polymer-clay nanocomposites (PCNs) by the exfoliation-adsorption technique, from atactic poly(methyl methacrylate) (PMMA) in solution, using Bentonite (B) as a layered-silicate natural clay. To optimize the intercalation of B with PMMA, it has been organically modified (OB) with a quaternary ammonium salt that helps the interchange of cations, and thus converting its hydrophilic surface to an organophilic one. An investigation of the morphology and molecular motions or dynamics of the net polymer film as well as the PCN final films was performed by X-ray diffraction (XRD), Transmission Electron Microscopy (TEM), Infra-Red Spectroscopy (IR), Thermally Stimulated Depolarization Currents (TSDC), and Differential Scanning Calorimetry (DSC) techniques. One of our interests was to discuss the solvent influence on the polymeric matrix. Herein, comparative studies of the effects of different solvents on the thermal and dielectric properties of the net PMMA films are reported. Four solvents were used to prepare the films, toluene, dichlorometane, tetrahydrofuran and acetone.



In Figure 1, XRD diffraction patterns (using Cu Kalfa radiation), reports the spacing between ordered layers of clay via the presence of the  $d_{100}$  or basal spacing. The original B exhibits a peak associated with a spacing of 14.7 Å, whereas the expanded OB shows a value of 19.2 Å. The absence of this basal peak suggests a high dispersion of clay platelets (exfoliation) in the PMMA/OB with 5% OB. The broad peak at around  $15^\circ = 2\theta$  is due to the amorphous hallow of the atactic PMMA nanocomposite. The efficiency of the intercalation can be also check by TEM microphotographs. Figure 2 clearly shows that the OB layers are mainly exfoliated in the PMMA/OB with 2% OB.

The efficiency of the intercalation can be also check by TEM microphotographs. Figure 2 clearly shows that the OB layers are mainly exfoliated in the PMMA/OB with 2% OB.

**Fig. 3** FTIR curves of PMMA/OB PCNs and PMMA/B



The FTIR spectra of the Si-O stretching region are shown in Figure 3 for PMMA/OB with varying % OB concentration, and PMMA with 15% of natural B. The graph shows the presence of a peak with increasing intensity and slight shift of its maximum towards higher  $\lambda^{-1}$  position as the OB content increases. The absence of this peak in the PMMA/B sample corroborates their previous assignation to Si-O groups [1] interacting with polymer molecules. The significant changes of this peak with the OB content obviously reflect the variation in the distribution of environments of the Si-O bonds, providing also an indication of the increasing overall degree of intercalation/exfoliation.

Figure 4 shows the dielectric spectra of the PMMA films prepared with the different solvents and the compressed molded sample. It displays a series of well established intrinsic relaxation signals [2], i.e.,  $\gamma$  (methyl groups),  $\gamma'$  (adsorbed polar water molecules),  $\beta$  (carboxymethyl side

groups flip),  $\beta'$  (postulated as a main chain rearrangement accompanying the side group flip, characterized as a rotation around the local chain axis), and long-range conformational change of the polymer backbone. (A) displays the secondary relaxations whose intensity and profile vary with the selected solvent. The glass transition is shown at higher temperatures (B) as a huge peak, with intensity and temperature position ( $T_g$ ) variations among the different solvents. The whole spectra of the cast samples exhibit evident intensity attenuation as compared to the molded film. A lower value of  $T_g$  is also a common feature among the cast samples. Comparable  $T_g$  trends have been obtained by DSC technique. Traces of the different solvents are expected to reside in relatively strong binding sites [2], e.g., hydrogen bonded to C=O groups. The measured amount of the remanent acetone, dichlorometane, toluene, and tetrahydrofuran solvents, obtained by NMR, is 0.30, 0.40, 9.00, and 14.00% respectively. The samples with higher solvent contents exhibit lower  $T_g$  values. The retained solvent molecules, trapped inside the PMMA films, affect the dynamics of the segmental and the localized dielectric relaxations. This effect differs in function of the nature and the amount of the solvent, and it could be partly explained by acid-base interactions between PMMA and the solvents [3].

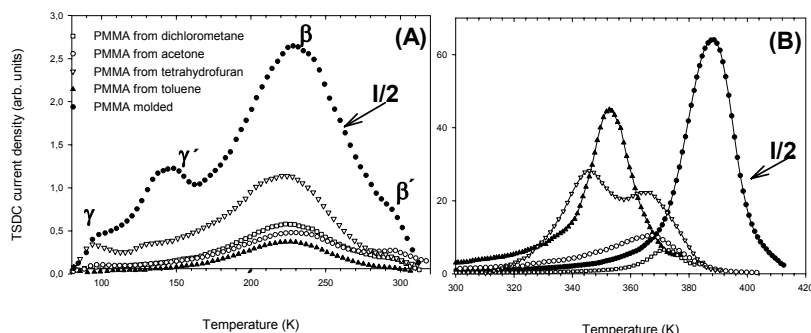
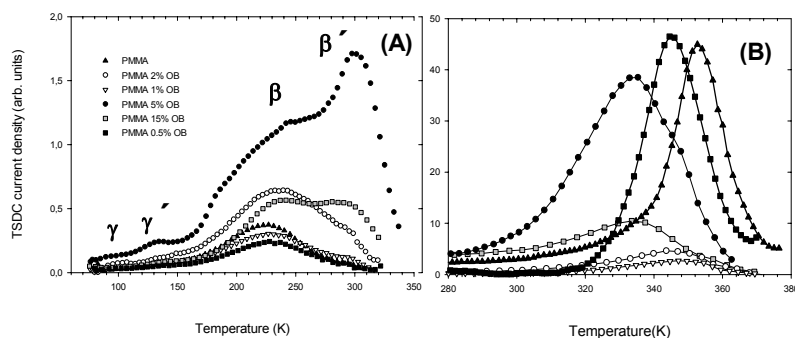


Figure 5 (A) shows that, on increasing the OB content the intensity of the low temperature relaxations decreases in the sample with 0.5% OB, increases up to 5% OB, and then drops again at 15% OB. A positive high-temperature shift of the low temperature spectra is observed in the samples with 2, 5, and 15% OB. This shift, related with the enhancement of the  $\beta'$  process, could be explained by the increased exfoliation, as it increases the rotational mobility of the PMMA chains [4]. Figure 5 (B) shows that the temperature position of the dielectric manifestation of the glass transition is a decreasing function of the OB content. Similar  $T_g$  decreasing trend was obtained by DSC. This behavior is consistent with previous results [4-5] and have been rationalized assuming that the layered silicates reduce the intermolecular (cooperative) domain size, which increases with the exfoliation. However, as the layered silicate/polymer interactions could restrict segmental mobility, the outcome should be a “tug-of-war”, where the influence of these opposite effects must be accounted for.

**Fig. 5** Low temperature (A), and High temperature (B) TSDC spectra of PMMA/OB PCNs.



**References:**

- [1] K. C. Cole, *Macromolecules*, **41**(3) (2008) 834-843.
- [2] I. M. Kalogeras, E. R. Neagu, and A. Vassilikou-Dova; *Macromolecules* **37**, (2004)1042-1053.
- [3] S. Bistac, J. Schultz, *Mat. Sci. & Eng.*, **31** (1997) 347-350.
- [4] R. Davis, A. J. Bur, M. McBrearty, Y. Lee, J. W. Gilman, and P. R. Start; *Polymer* **45**, (2004) 6487-6493.
- [5] J. Mijovic, H. Lee, J. Kenny, and J. Mays, *Macromolecules*, **39**(6), 2006) 2172-2182.

## RHEOLOGICAL STUDIES ON POLYMERIC NANOPARTICLE DISPERSIONS STABILIZED BY A POLYFRUCTOSE-DERIVATIVE SURFACTANT

*Marc Obiols-Rabasa<sup>1</sup>, Jordi Esquena<sup>1,\*</sup>, Conxita Solans<sup>1</sup>, Jérémie Nestor<sup>1</sup>, Bart  
Levecké<sup>2</sup>, Karl Booten<sup>2</sup>, Tharwat F. Tadros<sup>3</sup>*

<sup>1</sup> CSIC - Institut d'Investigacions Químiques i Ambientals de Barcelona (IIQAB),  
CIBER-BBN, Jordi Girona 18-26, 08034 Barcelona, Spain

<sup>2</sup> Orafti, Bio Based Chemicals, Aandorenstraat 1, B-3300 Tienen, Belgium

<sup>3</sup> 89 Nash Grove Lane, Wokingham, Berkshire, RG40 4HE, UK

\* [jemqci@iiqab.csic.es](mailto:jemqci@iiqab.csic.es)

The preparation of stable concentrated dispersions of latex particles is a very important subject due to technological interest in many applications. In this context, nonionic graft copolymer surfactants are commonly used because of their adsorption onto the particles forming strong steric barriers, highly insensitive to both temperature and electrolyte. We have studied a graft copolymer surfactant, consisting of an inulin (polyfructose) backbone on which several alkyl groups are randomly grafted [1]. The alkyl groups provide the anchor points for attachment at the solid/liquid interface, leaving the polyfructose loops in contact to the external aqueous solution. Previous results showed that particles covered by this surfactant possess very good stability at high electrolyte concentration [2, 3]. Colloidal dispersions stabilized by this inulin-derivative surfactant remain with no flocculation at high electrolyte ( $\text{Na}_2\text{SO}_4$ ) concentration such as  $1.5 \text{ mol}\cdot\text{dm}^{-3}$  [3] (Figure 1).

In the present work, a rheological behaviour study of polystyrene (PS) latex particles sterically stabilized with the polyfructose-derivative surfactant was carried out. The results of steady-state shear stress as a function of shear rate showed that could be used for determining the adsorbed layer thickness of the hydrophobically modified inulin polymeric surfactant. The surfactant layer thickness was determined by comparison of experimental data with the Dougherty-Krieger theoretical curve, which describes the relative viscosity as a function of the volume fraction assuming hard sphere systems [4]. The results proved that a graft copolymer layer was adsorbed onto the polystyrene particles reducing the maximum volume fraction from  $\phi = 0.6$  assuming randomly packed hard spheres down to  $\phi = 0.505$  (Figure 2). From these measurements, an adsorbed graft polymeric surfactant layer thickness of approximately  $9.6 \pm 2 \text{ nm}$  was calculated. Moreover, viscoelastic measurements showed a change from mainly viscous to predominantly elastic response at low effective volume fraction,  $\phi_{\text{eff}} = 0.24$ . The latter indicates strong hydration of the polyfructose loops and tail, providing very strong steric repulsion, which indicates that soft interactions are present between the particles containing adsorbed surfactant.

The results of the layer thickness determination by rheology were consistent with those obtained in previous layer thickness determination studies carried out by means of Dynamic Light Scattering (DLS) [2] and Atomic Force Microscopy (AFM) [5]. Studies by DLS were carried out by post-adding the polymeric surfactant to a surfactant-free PS dispersion. The results showed an adsorbed layer thickness of approximately 10 nm. AFM measurements were carried out by means of a modified

atomic force microscope apparatus [6]. The steric repulsions between two layers of the polymeric surfactant adsorbed onto a hydrophobic sphere and a plate were measured. The results showed that high steric repulsion was present even at high electrolyte concentration when approaching the two adsorbed layers. From these measurements, an adsorbed surfactant layer thickness of 9 nm approximately was obtained, confirming the rheological determinations.

### References:

- [1] Stevens, C.V., Meriggi, A., Peristeropoulou, M., Christov, P.P., Booten, K., Levecke, B., Vandamme, A., Pittevels, N., Tadros, Th.F., *Biomacromolecules* **2**, 2001, 1256-1259
- [2] Esquena, J., Dominguez, F.J., Solans, C., Levecke, B., Booten, K., Tadros, Th.F., *Langmuir* **25**, 2003, 10463
- [3] Nestor, J., Esquena, J., Solans, C., Levecke, B., Booten, K., Tadros, Th.F., *Langmuir* **21**, 2005, 4837-4841
- [4] Tadros, Th.F., *Adv. Colloid Interface Sci.* **108-109**, 2004, 227-258
- [5] Nestor, J., Esquena, J., Solans, C., Luckham, P.F., Musoke, M., Levecke, B., Booten, K., Tadros, Th.F., *J. Colloid Interface Sci.* **311**, 2007, 430-437
- [6] Braithwaite, G.J.C., Howe, A., Luckham, P.F., *Langmuir* **12**, 1996, 4224

### Figures:

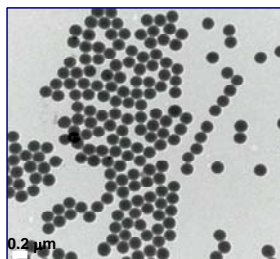


Figure 1. Polystyrene latex particles obtained by Transmission Electron Microscopy (TEM)

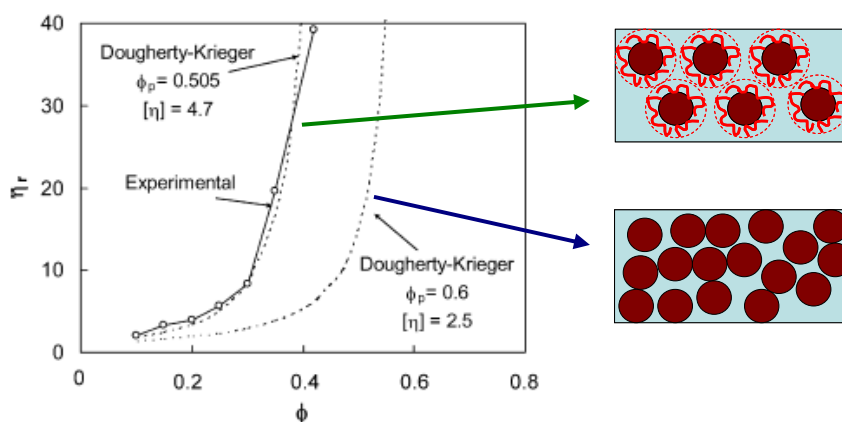


Figure 2. Relative viscosity as a function of particle volume fraction

## 1D ZnO CHAINS AS THE SPINAL CORD OF ADSORBED METALLOPORPHYRIN NANOTUBES LINKED BY WATER LIGANDS

*Marta Trelka<sup>1</sup>, Christian Urban<sup>1</sup>, Celia Rogero<sup>2</sup>, Eva Mateo<sup>2</sup>, Paula de Mendoza<sup>3</sup>, Wang Yang<sup>4</sup>, Iñaki Silanes<sup>5</sup>, Manuel Alcamí<sup>4</sup>, Andrés Arnau<sup>5</sup>, José Ángel Martín Gago<sup>2,6</sup>, Fernando Martín<sup>4</sup>, Antonio Echavarren<sup>3</sup>, José María Gallego<sup>6</sup>, Roberto Otero<sup>1</sup> & Rodolfo Miranda<sup>1,7</sup>*

<sup>1</sup> *Dep. de Física de la Materia Condensada & Instituto Nicolás Cabrera, Universidad Autónoma de Madrid, Campus de Cantpoblanco, 28049 Madrid, Spain*

<sup>2</sup> *Centro de Astrobiología (CSIC-INTA), 28850 Madrid, Spain*

<sup>3</sup> *Institut Català d'Investigació Química, 43007 - Tarragona, Spain*

<sup>4</sup> *Dep. de Química, Universidad Autónoma de Madrid, Campus de Cantpoblanco, 28049 Madrid, Spain*

<sup>5</sup> *Donostia International Physics Center (DIPC) and Departamento de Física de Materiales and Unidad de Física de Materiales, E- 20018 San Sebastian, Spain*

<sup>6</sup> *Instituto de Ciencia de Materiales de Madrid - CSIC, 28049 Madrid, Spain*

<sup>7</sup> *Instituto Madrileño de Estudios Avanzados en Nanociencia (IMDEA-Nanociencia), Madrid 28049, Spain*

[roberto.otero@uam.es](mailto:roberto.otero@uam.es)

Zinc oxide is a technologically attractive material due to its unique piezoelectric and optoelectronic properties. In recent years a very intense activity has been directed towards the fabrication of ZnO nanowires for applications such as room-temperature, ultra-violet lasing, field-effect transistors, chemical and biochemical sensors, etc. The growth of such nanowires is usually carried out by vapour-liquid-solid method, in which liquid droplets of surfactant direct the growth of the ZnO nanowire. The width of the resulting nanowire is thus determined by the size of the surfactant droplets, usually no smaller than 50 nm [1].

On the other hand, it is well known that 1D structures made out of face-to-face stacked metallomacrocycles can be stabilized by ligand coordination between the metal centres. For example, Ru and Os porphyrins can form long 1D, conductive polymers in which pyrazine ligands bridge the metal centres in neighbouring porphyrins. The resulting structure can thus be regarded as a nanotube in which an organic outer scaffolding protects an inner, strictly 1D metal-ligand spinal cord [2].

In this work we describe the formation of long 1D ZnO chains as spinal cords of self-assembled Zn-porphyrin nanotubes created by deposition of aquo(tetramesitylporphyrinato)zinc(II) (H<sub>2</sub>O-ZnTMP) on noble-metal surfaces. Our low-temperature Scanning Tunnelling Microscopy (STM) experiments reveal that the deposition of H<sub>2</sub>O-ZnTMP on Au(111) and Cu(100) leads to the formation of long 1D tube-like structures, which are not found upon deposition of the metal-free H<sub>2</sub>TMP. Moreover, the nanotubes are also disrupted upon annealing to temperatures in which the H<sub>2</sub>O ligands detach from the Zn atoms, as monitored by X-Ray Photoemission Spectroscopy (XPS). Density Functional Theory (DFT) calculations also support this view, yielding binding energies of about 0.7 eV per monomer due to the presence of the water links, whereas in the absence of water ligands the attractive interaction energy between the ZnTMP units is negligible.

This work demonstrates that coordination bonds can be preserved upon sublimation and surface adsorption, opening new ways to steer the coordinative co-polymerization of adsorbed species by deposition of supramolecular units that already contain some of the coordination bonds to be found in the desired final product. We have shown that this method can be used to grow 1D metalloporphyrin coordination copolymers with a ZnO spinal cord with potential applications in molecular optoelectronic devices such as optoelectronic gates.

## References:

- [1] Z. L- Wang, J. Phys.: Condens. Matter, **16** (2004) R829.  
 [1] J. P. Collman, J. T. McDevitt, G. T. Yee, et al., Proc. Natl. Acad. Sci. USA, **83** (1986) 4581.

## Figures:

**Figure 1.** Stick-and-ball model of the Zn porphyrin used in this study.

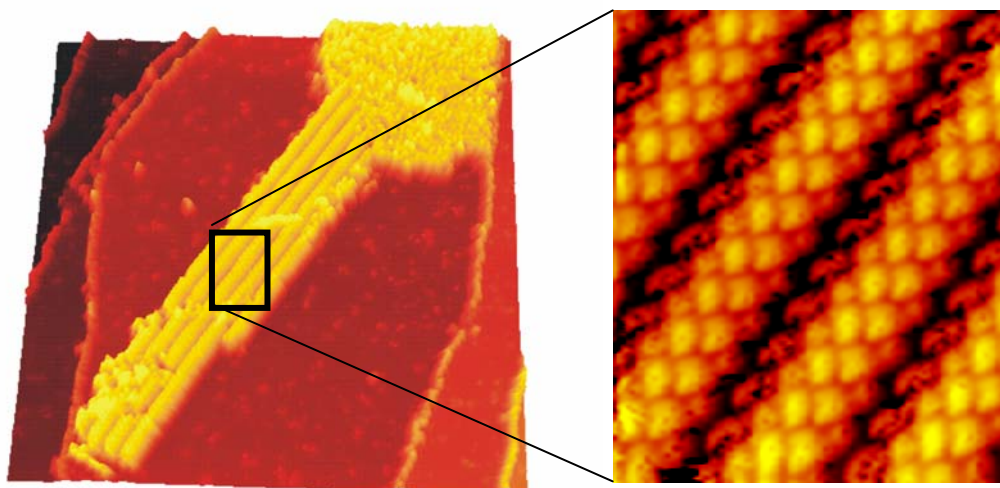
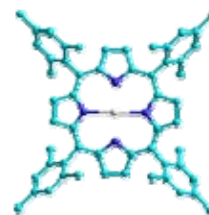
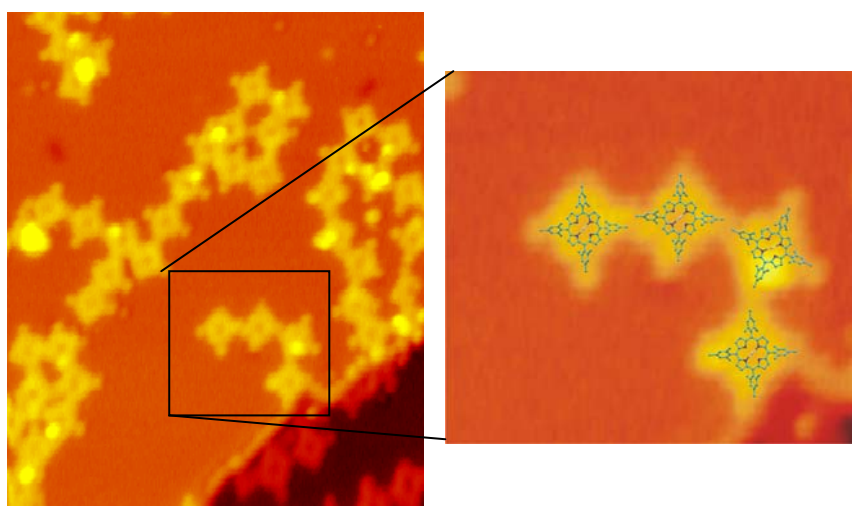


**Figure 2.**  $98.4 \times 98.4$  nm<sup>2</sup> STM image of long tubes coexisting with disorder after depositing ZnTMP on Cu(100) and a zoom-in showing the spiral shape of the tubes

**Figure 3.**  $21 \times 25$  nm<sup>2</sup> STM image showing individual flat lying ZnTMP molecules on Cu(100) after annealing the tubes to 500 K.



## PROTEIN NANOPARTICLES FOR MOLECULAR THERAPY: MOLECULAR CONSTRUCTION OF SIVp17/HIV1p6 NANOPARTICLES AND ASSEMBLY IN ANIMAL CELL CULTURES

*Luísa Pedro, Sandra S. Soares, Guilherme N.M. Ferreira*

*IBB-Institute for Biotechnology and Bioengineering*

*Centre for Molecular and Structural Biomedicine*

*University of Algarve, Campus Gambelas, 8005-139 Faro, Portugal*

[lpedro@ualg.pt](mailto:lpedro@ualg.pt)

Protein nanoparticles, such as Virus-like particles (VLPs), are becoming promising agents to delivery molecular therapy agents. A nanoparticle was constructed by fusion of the SIV (Simian Immunodeficiency Virus) p17 matrix protein with the HIV-1 (Human Immunodeficiency Virus Type 1) p6 protein with the goal transport of therapeutically agents to specifically targeted cells [1]. We have previously shown that the chimeric p17/p6 protein assembles from 293T cells as fully membrane encapsulated particle with 80 nm and an average of 7700 protein subunits. The intent of this construction is to enable particle engineering based on molecular assembly strategies in order to incorporate selected targeting motifs and particular therapeutic agents. The particles are assembled in animal cell culture upon transiently transfecting the cells with three different vectors one of which encodes the main structural protein of the nanoparticles - the fusion protein p17/p6. The affinity recognition of p6 protein with specific motives included in HIV-1 Vpr protein is then explored to enable the incorporation into the assembling nanoparticles of specific biomolecules linked to such motives. This is demonstrated by construction a fusion protein containing Vpr and EGFP. Co-transfecting animal cells with this vector and the vector encoding p17/p6 results in the assembly of nanoparticles associated with EGFP which is inside the assembled nanoparticles.

This communication addresses the steps involved in the molecular construction, assembly and characterization of such nanoparticles as well as the attempts to their optimization in animal cell cultures.

### References:

[1] Costa, M.J.L., Pedro, L., Matos, A.P.A., Aires-Barros, M.R., Belo, J.A., Gonçalves, J., Ferreira, G.N.M., *Biotechnol. Appl. Biochem.*, 48 (2007), 35.

### Acknowledgments:

The authors thank to Portuguese Foundation for Science and Technology (FCT) the financial support through the research project POCI/BIO/62476/2004 and the grants SFRH/BD/36674/2007 and SFRH/BPD/30290/2006.



## STANDARDIZATION ON NANOTECHNOLOGIES. THE AENOR SPANISH GROUP GET15 AND ITS ROLE WITHIN ISO AND CEN

\* *Emilio Prieto*<sup>1</sup>, \*\* *Javier García*<sup>2</sup>

\* *Centro Español de Metrología (CEM), Alfar, 2, Tres Cantos, 28760 Madrid, Spain*

\*\* *Asociación Española de Normalización (AENOR), Génova, 6, 28004 Madrid, Spain*

<sup>1</sup>[eprieto@cem.mityc.es](mailto:eprieto@cem.mityc.es), <sup>2</sup>[jgarcia@aenor.es](mailto:jgarcia@aenor.es)

Standards are ubiquitous (covering many different areas), virtually invisible to “the man in the street” – there are over 15,000 International Standards, many with multiple parts, but are absolutely critical to our modern way of life – covering things such as CDs/DVDs, internet protocols, credit cards, pin numbers, quality and environmental management.

Standardization in nanotechnology should help to ensure that nanotechnology is developed and commercialised in an open, safe and responsible manner by supporting safety testing, legislation and regulation, public and environmental safety, commercialisation and procurement, patenting and IPR, communication about the benefits, opportunities and potential problems associated with nanotechnologies.

In 1999, the Interagency Working Group on Nanotechnology workshop concluded that:

“Nanotechnology will only become a coherent field of endeavour through the confluence of three important technological streams:

- New and improved control of the size and manipulation of nanoscale building blocks;
- New and improved characterization (spatial resolution, chemical sensitivity, etc) of materials at the nanoscale;
- New and improved understanding of the relationship between nanostructure and properties and how these can be engineered”

without forgetting safety and consumer acceptance.

Currently, some of the main challenges in nanotechnology standardization are:

- Internationally agreed terminology/definitions.
- Internationally agreed protocols for toxicity testing of nanoparticles.
- Standardized protocols for evaluating environmental impact of nanoparticles.
- Methods of test suitable for nanoscale devices and nanoscale dimensions.
- Development and/or standardization on measurement techniques and instruments.
- New calibration procedures and certified references materials for validation of test instruments at the nanoscale.
- Standards for multifunction nanotechnology systems and devices.

To give an answer to such challenges, ISO TC 229 and CEN TC 352 were created, following also other mirror Committees at national level in all countries members of ISO and/or CEN, as for instance the AENOR GET15 Group in Spain.

Today, Standardization in the field of nanotechnologies includes either or both of the following:

- Understanding and control of matter and processes at the nanoscale, typically, but not exclusively, below 100 nanometres in one or more dimensions where the onset of size-dependent phenomena usually enables novel applications;
- Utilizing the properties of nanoscale materials that differ from the properties of individual atoms, molecules, and bulk matter, to create improved materials, devices, and systems that exploit these new properties.

Specific tasks include developing standards for terminology and nomenclature; metrology and instrumentation, including specifications for reference materials; test methodologies; modelling and simulation; and science-based health, safety, and environmental practices.

The importance, structure, works in progress and for the future within these international (ISO and CEN) and national (GET 15) Committees are presented in detail in this talk.

## NON-AQUEOUS SOL-GEL ROUTES APPLIED TO ATOMIC LAYER DEPOSITION

*E. Rauwel<sup>1</sup>, G. Clavel<sup>1</sup>, M.-G. Willinger<sup>1</sup>, P. Rauwel<sup>2</sup>, F. Ducroquet<sup>3</sup>, N. Pinna<sup>1</sup>*

*1 - Department of Chemistry and CICECO, University of Aveiro, 3810-193 Aveiro*

*2 - Department of Ceramics and CICECO, University of Aveiro, 3810-193 Aveiro*

*3 - Minatec-IMEP, 3 Parvis Louis Néel, BP 257, 38016 Grenoble*

Usually traditional Atomic Layer Deposition (ALD) processes use aqueous sol-gel routes for oxide thin film growth. Typically, transition metal precursors (halides, alkoxide or amide) are reacted with an oxidizing agent (e.g. water, radical oxygen or ozone). More specifically the reaction of such metal complexes with water leads, upon hydrolysis and condensation, to the formation of a metal oxide thin film. The films grown by this traditional way are amorphous; hence a post-synthetic heat treatment is generally required to induce the desired crystallization in order to improve the quality of the film. They also contain large amounts of undesired impurities ranging from unreacted carbon species to halides. Furthermore, as water is a strong oxidizing agent at the typical ALD range of deposition temperatures (200-400 °C) some substrates (e.g. Silicon) are rapidly oxidized. In fact, metal oxide thin films grown on silicon always present a non-negligibly thick oxidized interface layer (silica or silicates) in between the silicon and the deposited metal oxide which usually hinders microelectronic applications.

Many solutions are presently proposed to overcome these problems, like using new metal organic precursors [1,2] or by the utilization of plasma during the deposition process.

Recently various non-aqueous sol-gel routes were proposed for the formation of metal oxide nanoparticles [3,4] and hybrid materials [5] in solution. They proved to be powerful alternatives, especially because they have the capacity to overcome the main drawbacks of traditional sol-gel routes. However, only a few non-aqueous routes were applied to ALD. The most successful were the ones reported on the reaction of metal alkoxides with metal halides [6] and the formation of silica and silicates [7, 8].

In this work we present a novel non-aqueous approach applied to ALD [9] leading to the formation of high quality metal oxide thin films. Moreover, this approach demonstrates a real ability to reduce the oxide interlayer in the case of deposition on silicon substrates. This process enables to grow metal oxides coating at temperatures as low as 50 °C on various supports including monocrystalline substrates, carbon nanotubes, organic fibers, etc. The characterization of these films will be presented together with their possible formation mechanism.

### References:

- [1] A. C. Jones, et al. *Chem. Vap. Dep.* **2006**, 12, 83.
- [2] J. Niinistö, et al. *Chem. Mater.* **2007**, 19, 3319.
- [3] N. Pinna, M. Niederberger, *Angew. Chem. Int. Ed.* **2008**, DOI: 10.1002/anie.200704541
- [4] M. Niederberger, G. Garnweitner, N. Pinna, G. Neri, *Prog. Solid State Chem.* **2005**, 33, 59.
- [5] N. Pinna, *J. Mater. Chem.* **2007**, 17, 2769.
- [6] M. Ritala, K. Kukli, A. Rahtu, P. I. Raisanen, M. Leskela, T. Sajavaara, J. Keinonen, *Science* **2000**, 288, 319.
- [7] R. G. Gordon, J. Becker, D. Hausmann, S. Suh, *Chem. Mater.* **2001**, 13, 2463.
- [8] D. Hausmann, J. Becker, S. L. Wang, R. G. Gordon, *Science* **2002**, 298, 402.
- [9] E. Rauwel, G. Clavel, M.-G. Willinger, P. Rauwel, N. Pinna, *Angew. Chem. Int. Ed.* **2008**, DOI: 10.1002/anie.200705550



## NOVEL TOOLS FOR NANOPROTOTYPING USING DUALBEAM™ FIB/SEM

*Steve Reyntjens, Laurent Roussel, Oliver Wilhelmi*

*FEI Company, Achtseweg Noord 5, 5600 KA Eindhoven, The Netherlands*

[steve.reyntjens@fei.com](mailto:steve.reyntjens@fei.com)

The potential of focused ion beam equipment for prototyping of micromechanical structures has been recognized and described in the past [1]. Until recently, this potential has mostly been exploited using case-specific deposition and milling geometries and design/fabrication strategies that were tailored to individual designs [2]. This way of working limits the design complexity because of the limited amount of milling/deposition operations that can be done in a practical and timely fashion.

Traditional microelectronics design as well as EBL (electron beam lithography) typically use advanced CAD packages to layout complex two-dimensional geometries. The design is often presented in the form of a GDS-II file. We have recently introduced a turnkey solution for translating these GDS-II designs into native FIB (focused ion beam) and DualBeam format: this software module is called “GDStoDB”. The conversion is done in a way that enables a reliable transfer of the design onto the substrate material. Recent investigations have shown that this is not straightforward [3, 4], as the end result may depend strongly on the exposure strategy: the ion beam current, scanning trajectory and speed, as well as single-pass versus multipass exposure must all be taken into account. The new software module allows the translation of a two-dimensional design into individual dwell points for the ion beam, relying on traditional FIB-based parameters such as “overlap” and “depth” and taking proper exposure strategies into account. Combining this with the excellent ion beam quality enables the quick and elegant realization of complex designs, from virtually any layout editor.

An example is shown in Figure 1, which shows a simple split-ring resonator. This design was realized in a Au layer on a glass substrate. The total width of the U-shape is around 300 nm, with the legs well below 100 nm. It is realised by cutting out a relatively large field of tens of micrometers around it (rather than milling the U-shape, all the surrounding material is milled while the U-shape remains unaffected in the middle). The required layout is easily drawn in a CAD package, and conversion into dwell points using the “GDStoDB” tool results in a single file containing the complete design, ready for direct execution on the DualBeam instrument. Since the scanning strategy is optimized for FIB, the shape will be reproduced in a reliable manner, avoiding artifacts that may result from a typical EBL exposure strategy (single pass).

We see applications of this design-and-prototype technique in MEMS (post-processing, mechanical tuning), micro-optics and microphotonics, micro- and nanofluidics, nanoimprint template fabrication, and other fields of nanotechnology fabrication.

### References:

- [1] S Reyntjens, R Puers, J. Micromech. Microeng, **11** (2001) 287
- [2] Morita *et al*, J. Vac. Sc. Technol., **B 21** (6), (2003) 2737
- [3] D J Stokes, O Wilhelmi, S Reyntjens, L Roussel, Proc. CIASEM Peru (2007)
- [4] P M Nellen, V Callegari, R Broennimann, Microel. Engineering **86** (2006) 1805

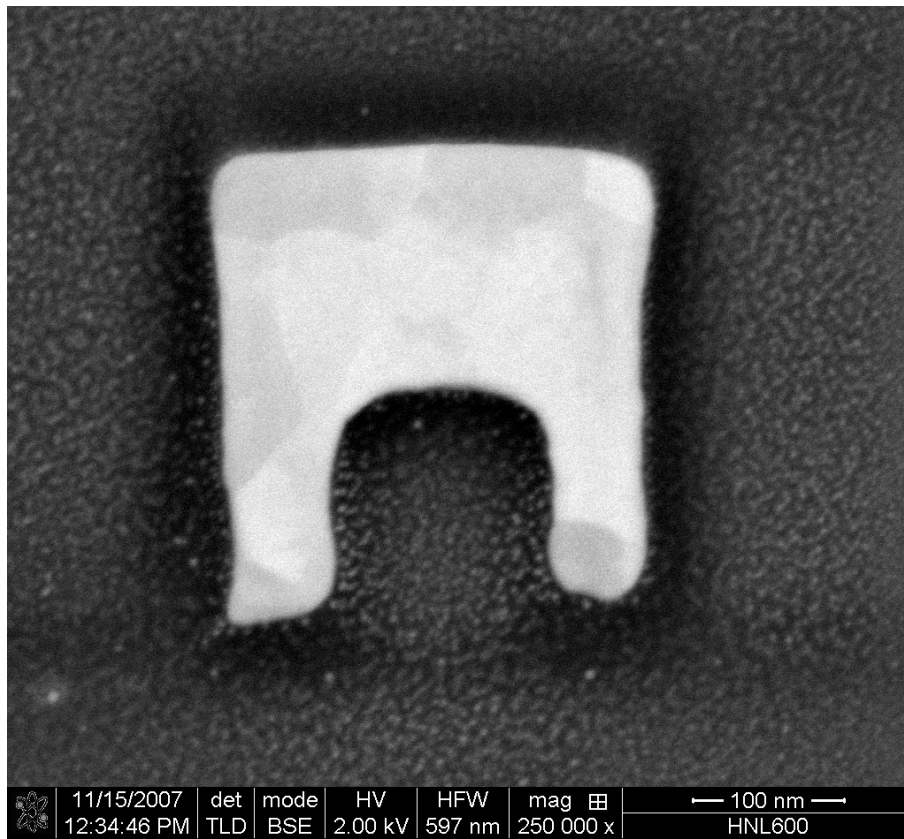
**Figures:**

Figure 1: Close-up of split-ring resonator, fabricated by FIB-milling a thin Au layer around a U-shaped resonator, on a glass substrate

## NANOBIOTECHNOLOGY AND NANOMEDICINE IN SPAIN

Prof. Dr. Josep Samitier

*CIBER-Bioengineering-Biomaterials and Nanomedicine,  
Spanish Technology Platform on Nanomedicine  
Institute for Bioengineering of Catalonia - University of Barcelona, Barcelona (Spain)*

### Abstract

Spain presents a lag with the European Union in terms of R & D in both total investments relative to GDP and company involvement in the financing of such investment. Spanish companies' research shortfall suggests that they fail to develop know-how of their own and, moreover, they are failing to take advantage of the technology generated by public research centres. This makes it essential to increase the critical mass and research excellence of our Science and Technology System. To meet these challenges, the Spanish government started in 2005, the INGENIO 2010 program, to maintain and improve existing R & D and Innovation programs and to focus significant resources on new strategic initiatives.

The INGENIO 2010 programme aims to achieve a gradual focus of these resources on strategic actions to meet the challenges faced by the Spanish Science and Technology System. This gradual focus will be achieved by allocating a significant portion of the minimum annual increase of 25% in the national R & D and Innovation budget to strategic initiatives grouped in three major lines of action:

- The CENIT Program (National Strategic Technological Research Consortiums) to stimulate R & D and Innovation collaboration among companies, universities, public research bodies and centres, scientific and technological parks and technological centres. The CENIT program co-finance major public-private research activities. These projects will last a minimum of 4 years with a minimum annual budgets of 5 million euros, where i) a minimum of 50% will be funded by the private sector, and ii) at least 50% of the public financing will go to public research centres or technological centres.
- The CONSOLIDER Program to reach critical mass and research excellence. CONSOLIDER Projects offers long-term (5-6 years), large scale (1-2 million euros) financing for excellent research groups and networks. Research groups may present themselves in all areas of know-how of the National R & D and Innovation Program.
- The CIBER (virtual research institute) promote high quality research in Biomedicine and Health Sciences in the National Health Care System and the National R & D System, with the development and enhancement of Network Research Structures.

In addition to these three main programs, support actions to increase Human resources creating new stable research positions and a strategic scientific and technological infrastructures program to ensure the availability and renewal of scientific and technological equipment and the promotion of scientific and technological parks linked to Universities and public research bodies, are also included in the Ingenio 2010 initiative.

As an example of the Spanish nanobio and nanomedicine structures, three main structures exist in this moment devoted to improve the collaboration at national level and promote collaborations at international level.

The “nanobiomed” consolidator consortium integrated by 60 researchers from 7 research institutes and universities. The main research activities are based on the use of nanoparticles for drug delivery, biosensors and enhanced MRI contrast.

The Spanish Technology Platform on NanoMedicine (STPNM) is a joint initiative between Spanish industries and research centres working on nanotechnologies for medical applications

The CIBER BBN is one of the new CIBER consortiums existing in the country that was created under the leadership of Instituto de Salud Carlos III (ISCIII) to encourage quality research and the critical mass of researchers in the field of Biomedicine and Healthcare Sciences. The scientific areas comprised within the CIBER-BBN are: Bioengineering and biomedical imaging, Biomaterials and tissue engineering and Nanomedicine, and the Center’s research is focused on the development of prevention, diagnostic and follow-up systems and on technologies related to specific therapies such as Regenerative Medicine and Nanotherapies. The CIBER-BBN is formed by 49 research groups, 46 of which are full members and 3 of which are associates

In summary, the evolution of this new research structures confirms that the nanobiotechnology and nanomedicine is a research priority in Spain and that exists a potentially strong sector to be developed in the next years.

## **DOMINO PROJECT: A CHALLENGING ADVENTURE FOR THE SPANISH INDUSTRY INTO THE NANOWORLD**

**J. Santarén**  
**R&D Department, TOLSA S.A.**

DOMINO is an acronym in Spanish, that stands for “Desarrollo y Obtención de Materiales Innovadores con Nanotecnología Orientada” (Development and Obtention of Materials with Innovation and Nanotechnologically Oriented). The DOMINO project has been undertaken by a consortium of 16 Spanish innovative companies from different industrial sectors, with the collaboration of 13 research institutions, with the aim of developing new and improved nanomaterials-based products.

The project has a duration of 4 years, starting January 2007, with a total budget of 28,5 million Euros. This singular project was selected in the second call for proposals launched by CDTI (Centre for the Development of Industrial Technology) in 2006 within the CENIT programme, included in the Spanish INGENIO 2010 initiative started in 2005. One of the objectives of this initiative is to foster cooperation between companies and research institutions in large integrated and long term projects of industrial research, with challenging objectives aiming to technological breakthroughs. The projects in the CENIT programme shall focus on increasing the scientific-technological capabilities of Spanish companies and should allow to generate new knowledge in priority areas with high future economic potential. The generated knowledge should be useful in the development of new products, processes or services, to allow increasing the Spanish industry competitiveness.

The high interest generated by CENIT programme is proved by the fact that 42 proposals with the participation of 531 companies were submitted in this second call for proposals, and eventually only 15 projects were selected.

The DOMINO consortium is composed by Tolsa, Acciona Infraestructuras, Grupo Antolín, Bioker Research, Caiba, Cray Valley Ibérica, Cristalerías Mataró, Grupo General Cable Sistemas, Industrias Murtra, Keraben, Líneas y Cables, Linpac Plastics Pravia, Moldeo y Diseño, Plastic Omnium Equipamientos Exteriores, Grupo Repol and Sistemas y Procesos Avanzados. The Spanish research institutions participating in the project are Aimplas, Ainia, Cidaut, Fundación Agustín de Betancourt, Inasmet, Institute for Ceramic and Glass (ICV), Institute of Material Science of Madrid (ICMM), Institute of Polymer Science and Technology (ICTP), National Coal Institute (INCAR), Labein, University of Alicante, Complutense University of Madrid and University de Zaragoza.

The ultimate objective of the project is the development of new nanostructured materials for new products with improved properties and enhanced performances for different industrial markets, including automotive, packaging, textiles, electricity and electronics, aeronautics, aerogenerators, environment sector, ceramics, glass, building and coatings. Some of them are traditional sectors with great economical interest in Spain, which are currently threatened by global competitors, particularly from Far East. The development of innovative products with differential properties is essential to improve the competitiveness of DOMINO partners in their markets thereby ensuring their survival.

Two of the few Spanish companies who are carrying out research to develop new nanomaterials are participating in this project: Tolsa and Grupo Antolin. Grupo Antolin, is researching on carbon nanofibers and has developed proprietary technology to manufacture this type of nanomaterial, which is only produced by four other companies in the world. Grupo Antolin is currently the only European company able to manufacture carbon nanofibres in a economically feasible way. Tolsa is developing nanomaterials based on sepiolite, a very uncommon clay with a needle-like morphology. These nanomaterials include sepiolite-based nanoclays and nanoclays functionalized with metal nanoparticles and nano-oxides. Although there are currently a few companies producing nanoclays based on layered silicates, Tolsa is the only company that is producing nanosepiolite products.

The partners in the DOMINO consortium are working closely on the research and development of new nanostructured materials based on polymers, ceramics, glass and cements, with the following general objectives:

- To develop new nanomaterials based on carbon nanofibers and sepiolite nanoclays, and
- To obtain structural and functional nanocomposites with improved performance and properties, including mechanical and thermal properties, electrical conductivity, fire retardancy, corrosion resistance, durability, and recyclability.

These new materials will allow to obtain:

- Lighter and more resistant automotive components with improved surface finish and easier recyclability
- Plastic pieces with improved mechanical and thermal performance.
- Food packaging for increased shelf life of foods and beverages.
- Textiles with increased durability, hygiene and fire resistance.
- Ceramics materials with electrical conductivity, improved mechanical performance, hardness and new esthetical effects.
- New technical glasses
- New materials for more efficient and healthy buildings

In summary, the companies of the DOMINO project place a big bet on the future of nanotechnology, that will allow to ensure their competitiveness in a increasingly competitive market and will improve the technological level of the Spanish industry in a strategic area with great economic potential.

## INTERFACE ANALYSIS TECHNIQUES ON NANOSCALE DIMENSION IN FLEXIBLE SOLAR CELLS

Schwarz, R. Ayouchi, C. Casteleiro

*Instituto Superior Técnico, Departamento de Física, Av. Rovisco Pais 1, P-1049-001, Lisboa, Portugal*

G.M. Junior, M. Ribeiro, P. Alpuim

*University of Minho, Department of Physics, P-4800-058 Guimarães, Portugal*

**Basic idea:** This work concerns the study of interface properties in thin film devices on a nanometer depth scale. Several analysis techniques are employed and correlated:

- photocapacitance spectroscopy [1],
- stress measurement at the interface,
- interface recombination by steady-state and transient grating techniques (SSPG, TG),
- photoluminescence (PL), and
- correlation between interface light scattering and the open-circuit voltage  $V_{oc}$ .

As a typical example we consider a tandem structure of an amorphous silicon based thin film solar cell consisting of nano-structured ZnO window layer, followed by a p-i-n a-Si:H solar cell deposited at the amorphous-to-microcrystalline transition (polymorphous), and terminating in a hydrogenated microcrystalline silicon bottom p-i-n cell. The three regions are tailored for best performance in the UV, visible, and IR spectral range, respectively. The whole structure is deposited on a flexible polymeric substrate [2].

**Techniques:** The flexible substrate is critical in two respects: first, the surface roughness of the ZnO contact layer (including ZnO quantum dots as shown in Fig. 1) which is helpful for improving the solar cell efficiency through light scattering may be responsible for creation of detrimental interface trap states. Secondly, a flexible substrate imposes mechanical constraints on the contact layer that may deteriorate the quality of its interface to the semiconductor film. Photocapacitance spectroscopy is sensitive to non-radiative recombination introduced by additional interface states and to the local electric field distribution near the heterostructure interface. Cells will be inserted in a four-point bending jig and their I-V characteristics under fixed illumination will be recorded as a function of the applied bending moment that will induce strain in a controlled manner in the devices. The degradation of solar cell performance, reflected in its  $V_{oc}$ ,  $I_{sc}$  and fill factor values, will be studied as a function of the number of load-unload cycles applied in the four-point bending geometry. Comparison of photocapacitance measurement results performed before and after mechanical stressing of the device will elucidate about the extent of the damage in the interface ZnO/a-Si:H caused by strain [3].

**Technology:** We have previously used photocapacitance spectroscopy to study the local defect creation in irradiated amorphous silicon-based p-i-n detectors [1]. Here we extend this technique to study thin film solar cells deposited on ZnO-coated flexible substrates (PI and PEN). The p-i-n structures were deposited by RF-PECVD and HW-CVD at particularly low substrate temperature

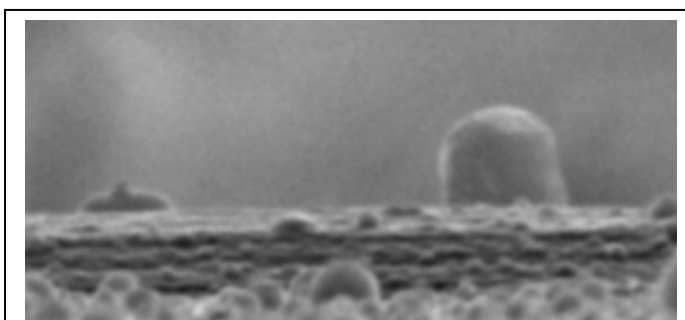


Figure 1: ZnO quantum dot on catalytic Au layer

of 150 °C. Hydrogen dilution was varied between 50 and 98 %. One of the contact layers used was polycrystalline ZnO prepared from sintered oxide targets by pulsed laser deposition (PLD). The photocapacitance measurements were done under HeNe laser illumination at a modulation frequency up to 1 MHz, as a function of voltage bias, and under different white light bias conditions. Enhanced recombination is seen by both the reduction of the photocapacitance signal and by faster capacitance decay in pulsed mode. The spatial resolution under focused laser light is limited ultimately by lateral carrier diffusion.

**Scientific relevance:** The analysis with photocapacitance spectroscopy has several innovative aspects: First, it is an alternative to the usual laser-beam-induced photocurrent measurements (LBIC) to study solar cell quality. Secondly, the technique is sensitive to both interface defects and interface electric field profiles between the ZnO contact layer and the p-i-n solar cell structure. Finally, by scanning a focused laser beam across the cell we obtain a topological image of defect regions of the solar cell.

The 4-point bending technique allows the application of pure bending to the specimen under study, if it is placed between the two inner loading points. It is possible to apply tensile or compressive strain just by placing the device in the convex or concave surface upon bending. The effect on solar cell performance of the cracks that will develop perpendicular to the substrate and through the solar cell thickness under positive strain and the eventual recover of device performance under negative strain will be measured. The combination of this technique with the photocapacitance spectroscopy will allow to assess the relative importance of the mechanically damage in the bulk of the device and in the interface with ZnO.

**Conclusions:** Spectrally and spatially resolved photocapacitance measurements, stress measurement at heterointerface, the correlation between interface recombination, open-circuit voltage and photoluminescence yield give a comprehensive picture of the interface quality between a conductive transparent oxide layer and a thin film solar cell. As an example we studied a typical solar cell structure composed of ZnO/a-Si:H on polymer substrate. A lateral spatial resolution of a few tens of microns is achieved when scanning across the cell surface. The depth resolution obtained by wavelength selection is of nanometer scale in the interface region.

#### **References:**

- [1] C. Casteleiro, R. Schwarz, A. Maçarico, J. Martins, M. Vieira, F. Wuensch, M. Kunst, E. Morgado, P. Stallinga, H. Gomes, “*Spatially-Resolved Photocapacitance Measurements to Study Defects in a-Si:H Based p-i-n Particle Detectors*”, to be published in *Thin Solid Films* (2008).
- [2] S.A. Filonovich, P. Alpuim, L. Rebouta, J.-E. Bourée, Y. M. Soro, “*Amorphous and nanocrystalline silicon solar cells deposited by HWCVD and rf-PECVD on plastic substrates at 150°C*”, *Journal of Non-Crystalline Solids*, in print (2008).
- [3] P. Alpuim, S. Lanceros-Mendez, V. Sencadas, M. Andrade, S.A. Filonovich, “*Piezo-Resistive Properties Of Nanocrystalline Silicon Thin Films Deposited On Plastic Substrates By Radio-Frequency And Hot-Wire Chemical Vapor Deposition*”, *Thin Solid Films*, 515 (19), 7658 (2007).

## **NANOMECHANICAL DEVICES: ULTRASENSITIVE SENSORS OF MOLECULAR RECOGNITION AND CONFORMATIONAL CHANGES OF BIOMOLECULES.**

*Javier Tamayo, Johann Mertens, Daniel Ramos, María Arroyo and Montserrat Calleja  
Institute of Microelectronics of Madrid (IMM-CNM, CSIC), Isaac Newton 8 (PTM), Tres  
Cantos, 28760 Madrid, Spain  
[jtamayo@imm.cnm.csic.es](mailto:jtamayo@imm.cnm.csic.es)*

In the last years, a large variety of ultrasensitive nanomechanical sensors that have been developed and used as biological sensors. The results demonstrate that rapid detection of biomolecules with high sensitivity and specificity without need of sample pre-treatment and labeling with fluorescent dyes. The applications range from protein and DNA detection to detection of single pathogens. This technology has the potential to revolutionize the fields of molecular biology and preventive medicine. However, it is still needed a major multidisciplinary convergence and development of nanofabrication techniques, measurement schemes, theory, large scale integration of nanodevices, optical and electrical components & microfluidics. In addition, all of these high cost developments must lead to a final technology suitable for mass production at low cost. Here, we present results in several of the battle fronts described above faced in collaboration with several multidisciplinary scientific and industrial partners. The results can be split into dynamic and static modes nanomechanical sensors. In the dynamic mode, the nanomechanical structure resonates at its natural frequency, which sensitively changes when the resonator interacts with the biomolecules present in the sample [1,2]. In the static mode, it is monitored the deflection of a cantilever which changes as a consequence of the surface stress originated from molecular adsorption.

### **Dynamic Nanomechanical Biosensors**

In order to develop nanomechanical devices for ultrasensitive pathogen detection, we have measured the effect of the bacteria adsorption on the resonant frequency of microcantilevers as a function of the adsorption position and vibration mode [3,4]. The resonant frequencies were measured from the Brownian fluctuations of the cantilever tip. We found that the sign and amount of the resonant frequency change is determined by the position and extent of the adsorption on the cantilever with regard to the shape of the vibration mode [5,6]. To explain these results, a theoretical one-dimensional model is proposed. We obtain analytical expressions for the resonant frequency that accurately fits the data obtained by the finite element method. More importantly, the theory data shows a good agreement with the experiments. Our results indicate that there exist two opposite mechanisms that can produce a significant resonant frequency shift: the stiffness and the mass of the bacterial cells. The combination of high vibration modes and the confinement of the adsorption to defined regions of the cantilever allow detection of single bacterial cells by only measuring the Brownian fluctuations, i.e., without any use of external energy. These results are relevant in order to obtain reproducible and sensitive nanomechanical sensors. The results of this study have been applied for a new design of arrays of nanomechanical resonators, with a volume of about  $10^4$  times smaller for ultrasensitive detection of nucleic acids. The fabricated arrays have alternate nanomechanical resonators with different sensitized regions to obtain a double signature of the target based on the mass and stiffness of the molecule. We have been able to detect DNA hybridization at the level of few femtograms in air and without any external excitation, which implies one of the highest sensitivities obtained in these conditions.

## **Static Nanomechanical Biosensors**

We show two relevant applications of nanomechanical biosensors: functional genomics and bionanomachines. In the first case, we show that adsorption of water on highly-packed self-assembled monolayers of single stranded (ss) DNA has an extraordinary effect on the intermolecular interactions. We have followed the process by measuring the nano-scale bending that a silicon microcantilever, on which the ssDNA monolayer is attached, experiences under controlled relative humidity. More importantly, the hydration-induced tension undergoes dramatic changes when the monolayer interacts with either complementary or single mismatched ssDNA targets. The analysis of the results suggests that the tension of the nucleic acid films is mainly governed by the hydration forces originated in the intermolecular channels. The discovered phenomena open the door for the development of a novel label-free DNA biosensor with specificity to single mutations and a sensitivity of at least ten times higher than the label-dependent DNA microarrays [7]. In the second case, bionanomachines such as chaperonins are immobilized on the cantilever. The conformational changes driven by the ATP hydrolysis lead to measurable cantilever fluctuations. This technique can provide new insight about the dynamics of molecular motors that have been elusive so far.

D.R. acknowledges the fellowship funded by the Autonomic Community of Madrid. This research was supported by Spanish Ministry of Science under grant No. TEC2006-10316 and by Autonomic Community of Madrid under grant No. 200550M056.

### **References:**

- [1] J. Tamayo, *Nature Nanotechnology* **2** (2007) 342.
- [2] J. Tamayo, M. Calleja, D. Ramos and J. Mertens, *Physical Review B* **76** (2007) 180201(R).
- [3] D.Ramos, J.Tamayo, J. Mertens, M. Calleja and A. Zaballos, *Journal of Applied Physics* **100** (2006) 106105.
- [4] D. Ramos, J. Tamayo, J. Mertens, M. Calleja, L.G. Villanueva and A. Zaballos, *Nanotechnology* **19** (2008) 035503.
- [5] J. Tamayo, D. Ramos, J. Mertens and M. Calleja, *Applied Physics Letters* **89** (2006) 224104.
- [6] H. Craighead, *Nature Nanotechnology* **2** (2007) 18.
- [7] J. Mertens, C. Rogero, M. Calleja, D. Ramos, C. Briones, J.A. Martín-Gago and J. Tamayo, submitted.

## NANOANTENNAS - CONTROLLING SINGLE MOLECULE EXCITATION AND EMISSION

Tim H. Taminiou, Fernando D. Stefani, Daan Brinks, Lars Neumann & Niek van Hulst\*

ICFO – the Institute of Photonic Sciences

Mediterranean Technology Park, 08860 Castelldefels (Barcelona), Spain

\*ICREA - Inst. Catalana de Recerca i Estudis Avancats, 08015, Barcelona, Spain

e-mail: [Niek.vanHulst@ICFO.es](mailto:Niek.vanHulst@ICFO.es)

Antennas have been used for over a century to control the emission and reception of radio and microwave radiation. An optical equivalent is of great interest as it will enable unique nano-scale control of both the absorption and emission of single molecules[1]. Here we will discuss results obtained by reversible coupling single molecules to an optical monopole antenna (shown in figure 1), precisely tuned to resonance [2]. It is shown that under illumination a locally enhanced field is created leading to increased excitation. The field is confined within 25 nm. The antenna effectively focuses optical energy far below the diffraction limit and is used as a high-resolution optical microscope with single molecule sensitivity (figure 1).

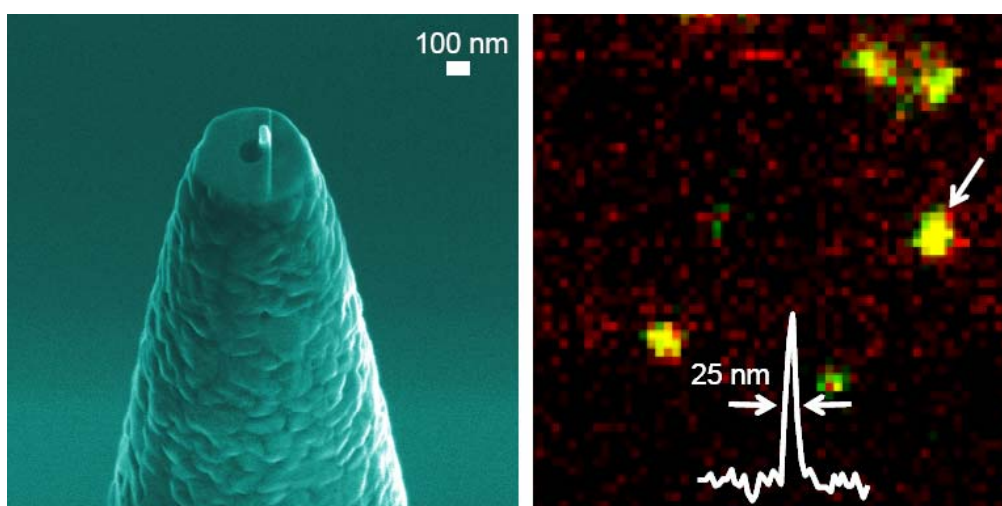


*Figure 1. Left: Optical monopole antenna. Right: Single molecule fluorescence at 25 nm resolution.*

In emission, the radiative properties of a molecule, e.g. the excited state lifetime [3] and emission spectrum [4], can be manipulated. We experimentally demonstrate control of polarization [5] and emission direction of a single molecule by an optical antenna [6]. It is shown how the emission is determined by the antenna design regardless of the orientation of the molecule. This directly reveals the role of the plasmon resonance in the emission process and provides a clear guideline to arbitrarily direct single-molecule emission with optical antennas, an interesting prospect for efficient nano-sized sensors and light sources.

Inspired by these initial results we now explore the limits of the nanoantenna probes. Several aspects are under study to enhance and localize the optical field: metal, shape, antenna configuration, fabrication method, etc.

*Metal:* Aluminum is a relatively good electrical conductor in the optical regime, with very short skin depth and suitable for sharp tip definition. However, other less perfect conductors, such as silver and gold, display stronger plasmon resonances with potentially stronger field enhancement for nanoantennas.

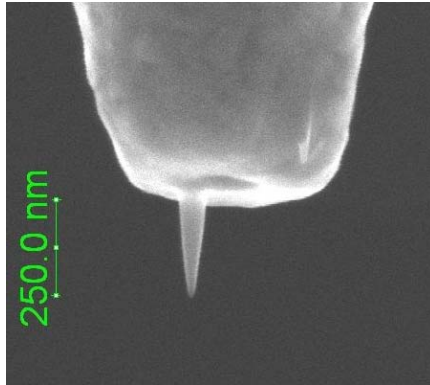


*Figure 2:*  
*E-beam deposited nano-antenna.*  
*Material: Platinum*

*Shape:* The field enhancement of a resonant antenna and its decay length are roughly inversely related to the radius of curvature of the antenna apex, making small radii of curvature a must. Beyond sharp tip also gap antennas are an interesting alternative to increase the local field further.

*Fabrication:* Our monopole nanoantennas have been fabricated using FIB milling. Shape, sharpness and size of the antennas are limited to 10-20 nm by the finite resolution of the ion beam. Moreover, the optical properties of the antennas are affected by gallium ions that are implanted during the FIB milling, and the evaporation process that leaves the metal in small crystalline clusters on the scale of the antenna dimensions instead of a smooth layer. A good alternative is given by metal deposition assisted by a focused electron beam. We show how e-beam fabrication shows much narrower, sharper and smoother antennas.

In this presentation we will show recently fabricated nanoantenna probes, calculations for different materials and configurations and experimental data on antenna performance.

- [1] J.-J. Greffet, *Science* **308**, 1561 (2005).
- [2] T. H. Taminiau, R. J. Moerland, F. B. Segerink, L. Kuipers, N. F. van Hulst, *Nano Lett.* **7**, 28 (2007).
- [3] S. Kuhn *et al.*, *Phys. Rev. Lett.* **97**, 017402 (2006).
- [4] J. S. Biteen *et al.*, *Appl. Phys. Lett.* **88**, 131109 (2006).
- [5] R. J. Moerland, T. H. Taminiau, L. Novotny, N. F. van Hulst, L. Kuipers, *Nano Lett.* **8**, 606 (2008).
- [6] T. H. Taminiau, F.D. Stefani, N.F. van Hulst, *Nature Photonics* **2** (April 2008).

## SCANNING NANO-METROLOGY OF ULTRA THIN FILMS

*V.Khosla, I.Hermann, N.Gitis, M.Vinogradov*  
*CETR, 1715 Dell Avenue, Campbell, CA, USA*  
[info@cetr.com](mailto:info@cetr.com)

Traditional techniques of tribological and mechanical characterization of coatings are limited to friction, wear and scratch tests on a micro-level with balls or pins having much larger sizes, and loads-displacements much larger, than the film thickness. Lately-popular nano-indentation allows for testing of thinner films, but its pressure distribution is concentrated under (in the front of) the indenter and thus makes it vulnerable to substrate effects for ultra-thin films, while ultra-shallow depths would require unachievable-yet resolution of tip and system calibration. Common AFM-based techniques use smaller tips and displacements, but limited to nano-dimensional and topographic characterization of surfaces.

Moreover to detect the nano-non-homogeneities, a high-resolution surface mapping is required. Use of traditional nano-indentation for surface mapping is limited by the duration of a required series of numerous indents and their spacial resolution (the minimum space between indents is typically three times the diameter of the tip, or over 100 nm, to avoid the effect of the preceding indent). This makes nano-indentation unsuitable for studies of local nano-defects, or non-homogeneity

To overcome the shortcoming of traditional nano indenter a novel new tool, nano analyzer, was developed. It measures scratch-hardness of ultra shallow films where the pressure distribution (still in the front of the indenter) in the same surface layer where the indenter is sliding. As post-scratch detection of the shallow nano-scratches is challenging, it utilizes the same tip for both scratching and nano-imaging for nano-scratch-hardness testing of ultra-thin films. And to detect homogeneity of films the tool uses technique of nano-mapping, where a diamond nano-tip is vibrating in a tapping mode, frequency and phase of its vibrations are monitored and analyzed, and simultaneous topographical and stiffness (Young's modulus) maps of surface are produced with nano-resolution in both vertical and horizontal directions (Figure 1). Thus a novel new technique nano-analyzer enables effective quantitative tribo-mechanical characterization of ultra-thin films.

Examples of the nano-analysis of various thin hard films are discussed in detail (Figure 4). The paper also discusses mechanical property analysis of bump like structures under different loading conditions (figure 2,3). The tool is used to indent a bump and then do non destructive nano mapping of cracks Young's modulus. This paper compares touches on the fundamental constraints of the current techniques, and throws light on new technologies.

### REFERENCES

1. D. Tabor (1996). Indentation hardness: Fifty years on. - Philosophical Magazine A, V. 74, No 5, pp. 1207-1212.

2. Nano and Micro Indentation and Scratch Tests of Mechanical Properties of Metals Dr. Norm Gitis, Dr. Ilja Hermann, Dr. Suresh Kuiry and Vishal Khosla

Figures

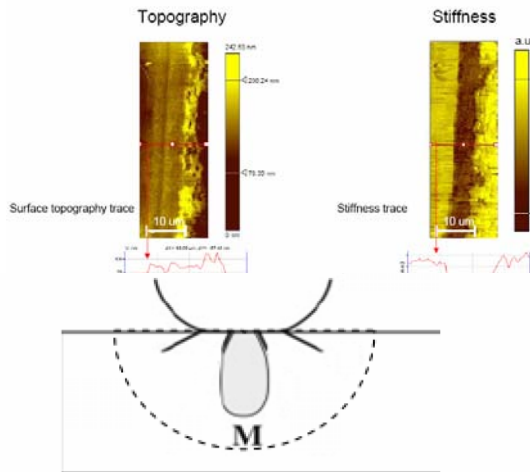


Figure 1. Topographical and stiffness map by Nano-analyzer NA-1

Figure 2. Cracks propagation mechanism when indenting on top of a bump

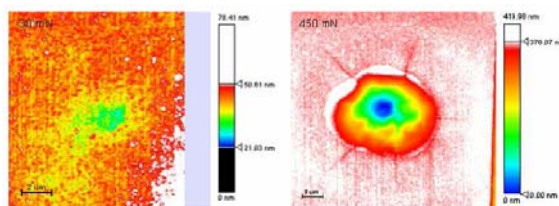


Figure 3. Results obtained after indenting a bump. Mechanism shown at different load with modulus mapping of the surface after the indent.

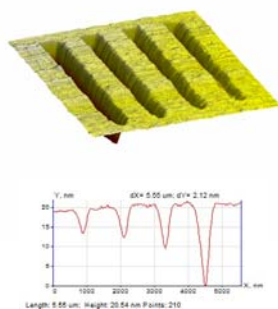


Figure 4 Ultra Shallow scratches in order of nm to find the scratch hardness of the low k materials



## INDEX POSTERS

### SESSION PA / SESSION PB

**Session A (PA)** is dedicated to students and **Session B (PB)** to seniors (Doctors)

**Only posters submitted by fully registered (payment processed) participants are listed below. Last update (04-04-2008)**

(Please, find your final **poster number** by looking up your name in the **Author Index** displayed in the Registration Area and the Poster Exhibition Area.)



Presenting Author	Country	Topic	Poster Title
<b>Alphabetical Order (Session PA / Session PB)</b>			
<b>Aguilar-Caballos</b>	Maria-Paz	Spain	NanoBiotechnology / Nanomedicine
Nanostructures as analytical tools in bioassays			
<b>Albuquerque</b>	Rita	Portugal	NanoChemistry
The influence of Ag <sub>2</sub> S percentage on the photoactivity of TiO <sub>2</sub> /Ag <sub>2</sub> S nanocomposites			
<b>Albuquerque</b>	Rita	Portugal	NanoBiotechnology / Nanomedicine
Optimization and characterization of amorphous/nanocrystalline biosensors for DNA detection using gold nanoparticles			
<b>Alcami</b>	Manuel	Spain	NanoChemistry
Understanding the Supramolecular Self-Assembly of the Fullerene Derivative PCBM on Au(111) Surface			
<b>Alegre</b>	Daniel	Spain	NanoMaterials
Properties of single-crystalline ZnO nanodots and highly-textured ZnO films grown by electrochemistry			
<b>Alija</b>	Alejandro	Spain	Nanomagnetism
Ratchet effects on domain wall motion in Co-Si amorphous films with arrays of asymmetric holes: experiments and theoretical simulations			
<b>Alonso</b>	Javier	Spain	Nanomagnetism
Study of the influence of the interactions in the magnetic behaviour of Fe-Ag thin films above the percolation limit			
<b>Alpuim</b>	Pedro	Portugal	NanoBiotechnology / Nanomedicine
ultra-sensitive shape sensor test structures based on piezo-resistive doped nanocrystalline silicon			
<b>Amaral</b>	Joao	Portugal	Nanomagnetism
Magnetic studies of mechanically alloyed metastable fcc Fe <sub>23</sub> Cu <sub>77</sub> : superferromagnetism with bimodal cluster size distribution.			
<b>Andrade</b>	Suzana M	Portugal	NanoChemistry
Nanometric aggregates of a covalent porphyrin dimer followed by Fluorescence Correlation Spectroscopy in aqueous buffered solution			
<b>Anson</b>	Alejandro	Spain	NanoMaterials
Separation of Argon and Oxygen by Adsorption on a Titanosilicate Molecular Sieve			
<b>Arroyo Cardoso</b>	Filipe	Portugal	NanoBiotechnology / Nanomedicine
Increasing the sensitivity of magnetoresistive-based biochips			
<b>Azevedo</b>	Nuno	Portugal	NanoBiotechnology / Nanomedicine
Development and application of peptide nucleic acids (PNA) for the rapid identification of microorganisms by fluorescence in situ hybridization (FISH)			
<b>Barbosa</b>	Hélder	Portugal	Simulation at the Nanoscale
Simulation in Organic Nanoelectronics: from Single Molecule to Thin Film			
<b>Barreiro</b>	Amelia	Spain	Nanotubes
Nanotube based thermal motors: sub-nanometer motion of cargoes driven by thermal gradients			
<b>Barroca</b>	Nathalie	Portugal	SPM
Poly(L-lactic)acid as stimulator of bone growth: Piezo-force microscopy study of the local piezoelectric properties			
<b>Batista</b>	Carlos	Portugal	NanoMaterials
VO <sub>2</sub> -Based Thermochromic Thin Films for Energy Efficient Windows			
<b>Bechir</b>	Anamaria	Romania	NanoBiotechnology / Nanomedicine
Biotechnologies for obtaining new pharmaceutical formulations based on mixtures of type I non-denatured fibrillar collagen gels and extracts from marine algae with applications in nanomedicine			
<b>Bernacka-Wojcik</b>	Iwona	Portugal	NanoBiotechnology / Nanomedicine
Nanostructural semiconducting photocatalysts for medical applications			
<b>Bouju</b>	Xavier	France	Other
How does pentagonal molecules self-assemble on a six-fold symmetry surface? The case of penta-tert-butyl-corannulene molecule on Cu(111)			

<b>Brunet</b>	Ernesto	Spain	NanoChemistry	The Role of Porous Materials in the Efficient Storage of Hydrogen
<b>Burzuri</b>	Enrique	Spain	Nanomagnetism	How well aligned are the magnetic anisotropy axes in crystals of Mn12 molecular nanomagnets? An angle-dependent ac susceptibility study
<b>Bystrov</b>	Vladimir	Portugal	NanoMaterials	Composite nano-biomaterials based on polyvinylidene fluoride copolymers
<b>Cabrera</b>	Lourdes	Spain	NanoMaterials	Conductive Polymers with Embedded Magnetite Nanoparticles: Synthesis and Characterization
<b>Cadillon Costa</b>	Luís	Portugal	NanoMaterials	Introduction of polypyrrol nanoparticles in cement paste
<b>Calvo</b>	Mauricio	Spain	Nanophotonics	Nanoparticle based One-Dimensional Photonic Crystals
<b>Carabineiro</b>	Sonia	Portugal	NanoChemistry	Preparation of gold nanoparticles on several supports and their use for the oxidation of carbon monoxide
<b>Carbonera</b>	Chiara	Spain	Nanomagnetism	Fabrication of nanospheres from Mn12 acetate SMM: do the chemical properties of the original cluster show changes?
<b>Carretero Genevrier</b>	Adrián	Spain	Nanotubes	Single-Crystalline La0.7Sr0.3MnO3 Nanowires Grown by Template Directed Chemical Solution Synthesis
<b>Carvalho</b>	Oscar	Portugal	Nanotubes	Mechanical and fatigue properties of sintered Nanotube-based functionally graded materials
<b>Carvalho Miranda</b>	Maria Adelaide	Portugal	NanoChemistry	Gold Anisotropic Nanoparticles: Syntehsis and Characterization
<b>Castillejos</b>	Eva	France	Nanotubes	Strategies for the Selective Confinement of Nanoparticles in the inner cavity of Multi-Walled Carbon Nanotubes
<b>Castro-Garcia</b>	Socorro	Spain	NanoMaterials	Magnetocapacitive response in Fe3O4 nanoparticles
<b>Cerqueira</b>	Mariana	Portugal	NanoBiotechnology / Nanomedicine	Influence of Patterned Electrospun Nanofiber Meshes on Human Dermal Fibroblasts, Keratinocytes and Adipose Stem Cells Behaviour
<b>Chaves Romero</b>	Ferney A.	Spain	NanoElectronics	Analytic Model of Quantum Electrostatic Potential in Double-Gate MOSFETs
<b>Chiorcea-Paquim</b>	Ana-Maria	Portugal	NanoMaterials	Atomic force microscopy and electrochemical studies of palladium nanoparticles and nanowires electrodeposited onto carbon electrode surfaces
<b>Comenge</b>	Joan	Spain	NanoBiotechnology / Nanomedicine	Addressing the Immune System: Macrophages Responses Towards Au Nanoparticle Conjugates
<b>Costa Martins</b>	Rui	Portugal	NanoBiotechnology / Nanomedicine	Cellular Automata Model for Controlling Supercooling: NanoBioTechnology Perspective into CryoPreservation of Living Tissues
<b>Cunha</b>	Cristiana	Portugal	NanoBiotechnology / Nanomedicine	Targeting nanoprobe for early invasive cancer cells using Hereditary Diffuse Gastric Cancer (HDGC) as a model.
<b>De Teresa Noguerras</b>	Jose Maria	Spain	NanoMaterials	In-situ STEM investigation of thin films in a dual-beam equipment
<b>del Castillo</b>	Javier	Spain	Nanophotonics	Structural characterization and luminescent study of transparent nanostructured Eu3+ doped sol-gel derived SiO2-PbF2 glass-ceramics
<b>del Castillo</b>	Javier	Spain	Nanophotonics	SiO2-CeF3:Eu3+ nano-glass-ceramics prepared by sol-gel method. Structural and Optical Characterization

<b>Doria</b>	Gonçalo	Portugal	NanoBiotechnology / Nanomedicine	Revealing the mechanism of SNP detection with gold nanoprobess by non-cross-linking aggregation
<b>Eaton</b>	Peter	Portugal	SPM	Atomic Force Microscopy and Fluorescence Microscopy of Malarial Hepatocytes
<b>El-Hawi</b>	Nancy	France	NanoChemistry	A novel method of synthesis of silica nanoparticles in alcoholic organic medium
<b>Elizondo Sáez de Vicuña</b>	Elisa	Spain	NanoBiotechnology / Nanomedicine	Compressed Fluid Based Technologies for the Preparation of Drug Delivery Systems
<b>Farjas Silva</b>	Jordi	Spain	NanoMaterials	Restricted epitaxial growth during thermal crystallization of nanocrystalline silicon: experiments and modeling
<b>Fernandes</b>	João	Portugal	SPM	Atomic force microscopy of the antibacterial effects of chitosans on Bacillus cereus (and its spores)
<b>Fernandes</b>	Francisco	Spain	NanoMaterials	Structural and functional properties of gelatin-clay nanocomposites
<b>Fernández</b>	Iván	Spain	NEMS / MEMS	Parallel nanogap fabrication with nanometer size control using III-V semiconductor epitaxial technology
<b>Fernandez-Cuesta</b>	Irene	Spain	NanoBiotechnology / Nanomedicine	Interdigitated nanoelectrodes for sensing: fabrication and characterization
<b>Ferreira</b>	Paula	Portugal	NanoElectronics	Synthesis and electric properties of nanoporous BaTiO <sub>3</sub>
<b>Ferreira</b>	María Rute	Portugal	NanoMaterials	Self-photopatternable di-ureasil-zirconium oxo-clusters organic-inorganic hybrids for low cost integrated optical substrates
<b>Ferreira</b>	Carla	Portugal	NanoChemistry	Functionalized nano-microstructures to combat biofouling of industrial surfaces
<b>Figueiredo</b>	Hugo	Portugal	NanoChemistry	Modified electrode based on Zeolite-encapsulated Cr(III) complex
<b>Figueiredo Lopes</b>	Luís M.	Portugal	NanoChemistry	Ruthenium Complexes Encapsulated in Nanostructured Sol-gel Silica Matrices
<b>Fortunato</b>	Elvira	Portugal	NanoBiotechnology / Nanomedicine	DNA detection using amorphous silicon sensors with gold nanoparticles
<b>Fuss</b>	Martina	Spain	SPM	Theory of Topography and Recognition Imaging by Dynamic Force Microscopy
<b>Garcia-Ramos</b>	Jose V	Spain	NanoChemistry	SERS on Functionalized Silver Nanostructures: Towards the Detection of Single Molecules in Hot Spots
<b>Garcia-Sanchez</b>	Daniel	Spain	NEMS / MEMS	Mechanical detection of the vibrations of Carbon Nanotube and Graphene Resonators
<b>Gauffre</b>	Fabienne	France	NanoMaterials	New strategies of colloidal stabilization of nanoparticles for applications in aqueous media
<b>Gil</b>	Marta	Spain	NanoMaterials	Synthesis and characterization of modified ordered mesoporous materials
<b>Gomes</b>	Joana	Portugal	NanoBiotechnology / Nanomedicine	Nanoencapsulation of bioactive compounds
<b>Gomes</b>	Inês	Portugal	NanoBiotechnology / Nanomedicine	Probing the Surface Properties of Cytochromes c/Gold Nanoparticles Complexes
<b>Gomes</b>	João	Portugal	Nanotubes	Carbon Nanofibre-poly(vinylidene fluoride) nanocomposite: effect of the carbon nanofibres concentration on the a to b phase transformation and the degree of crystallinity
<b>Gomes Coutinho</b>	Paulo José	Portugal	NanoMaterials	TiO <sub>2</sub> and CdS nanoparticles obtained from soft templating methods

<b>Gómez de Pedro</b>	Sara	Spain	NanoChemistry	Synthesis of nanoparticles in microfluidic devices based on the LTCC technology
<b>Goncalves</b>	Luis	Portugal	NEMS / MEMS	Thermoelectric thin-films for microcoolers and energy scavenging microsystems
<b>González</b>	Mónica	Spain	NanoBiotechnology / Nanomedicine	Non-specific adsorption of biomolecules on single-walled carbon nanotubes
<b>Gonzalez Fernandez</b>	Africa	Spain	NanoBiotechnology / Nanomedicine	ROS induction and cytotoxicity of inorganic nanoparticles in human cells
<b>González-Díaz</b>	Juan B.	Spain	Nanophotonics	Surface plasmon resonance effects on the magneto-optical response of noble-metal ferromagnet nanodisks.
<b>Gonzalez-Dominguez</b>	Jose Miguel	Spain	NanoChemistry	Carbon nanotubes dispersion towards polymer integration
<b>Griol</b>	Amadeu	Spain	Nanophotonics	Experimental realization of a high efficient coupling technique for SOI devices based on inverted tapers and V-grooves integration
<b>Guedes</b>	Andre	Portugal	Nanomagnetism	Hybrid Magnetoresistive/MEMS devices for 1/f noise reduction
<b>Guerrero Ramírez</b>	Luis Guillermo	Spain	NanoMaterials	Synthesis of nano-structured copolymeric hydrogels based on N-Isopropyl acrylamide (NIPA) by Microemulsion Polymerization
<b>Hervías Sarasqueta</b>	Xabier	Spain	NanoMaterials	Study of drug release on smart nano-sized hydrogels based on N-isopropyl acrylamide by High Performance Liquid Chromatography
<b>Hortigüela</b>	María Jesús	Spain	NanoMaterials	Enzymatic Synthesis of Amorphous Calcium Phosphate-Chitosan Nanocomposites and its Processing into Hierarchical Structures
<b>Hungerford</b>	Graham	Portugal	NanoBiotechnology / Nanomedicine	Sol-gel derived biocompatible glasses towards bone implant integration
<b>Jaafar</b>	Miriam	Spain	SPM	True variable field magnetic force microscopy for nanostructures characterization
<b>Jiménez</b>	David	Spain	NanoElectronics	Electrical characteristics of graphene based transistors
<b>Kahn</b>	Myrtil	France	NanoChemistry	Experimental evidence of the existence in solution of organizations of ZnO nanoparticles synthesized by organometallic method using dynamic light scattering
<b>Kaltzakorta</b>	Idurre	Spain	Other	synthesis and characterization of silica microcapsules containing organic compounds of different viscosity
<b>Köber</b>	Mariana	Spain	NanoBiotechnology / Nanomedicine	Opto-magnetic detection of dimer formation of superparamagnetic Fe <sub>3</sub> O <sub>4</sub> nanoparticles in liquids. Application to a molecular recognition transducer.
<b>Lajos</b>	Gejza	Spain	NanoBiotechnology / Nanomedicine	Surface-enhanced Fluorescence and Raman Scattering Study of Antitumoral Drug Hypericin: An Effect of Aggregation and Self-spacing Depending on pH
<b>Lamela</b>	Jorge	Spain	Nanophotonics	SNOM study of periodically poled ferroelectric domains in LiNbO <sub>3</sub> , LiTaO <sub>3</sub> and Ba <sub>2</sub> Nb <sub>5</sub> O <sub>15</sub> crystals
<b>Lanceros-Mendez</b>	Senentxu	Portugal	Nanophotonics	Tunable Fabry-Perot Optical Filter with a Resonant Cavity
<b>Leitao</b>	Diana	Portugal	NanoMaterials	Py antidot thin films: a transport and magnetic characterization as a function of temperature
<b>Lermo Soria</b>	Anabel	Spain	NanoMaterials	Electrochemical immunosensing of folic acid based on improved nanostructured transducer

<b>Liebana</b>	Susana	Spain	NanoMaterials	Electrochemical biosensing in food for pathogenic bacteria based on nanostructured transducers
<b>Lingenfelder</b>	Magali	Germany	SPM	Tuning the expression of supramolecular chirality by molecular footprint engineering on metal surfaces
<b>Lopez</b>	Hender	Spain	Simulation at the Nanoscale	Spin Dependent Injection Model for Monte Carlo Device Simulation
<b>López Ramírez</b>	María Rosa	Spain	NanoChemistry	A SERS study of charge-transfer processes in the Raman spectrum of the benzoate anion adsorbed on silver nanostructures
<b>López-Ruiz</b>	Román	Spain	Nanomagnetism	Influence of stress and size over the magnetic response of nickel nanowires
<b>Loureiro</b>	Joana	Portugal	NanoBiotechnology / Nanomedicine	Integrated platform for Stem Cells separation/counting
<b>Lugo</b>	Nayar	Spain	NanoMaterials	Pure copper deformed by equal-channel angular pressing (ECAP)
<b>Macedo</b>	Rita	Portugal	Nanomagnetism	Nano-Sized MgO-based Magnetic Tunnel Junctions fabricated by e-beam lithography combined with chemical-mechanical polishing
<b>Machado</b>	Bruno	Portugal	Nanotubes	Liquid-Phase Hydrogenation of Unsaturated Aldehydes: Enhancing Selectivity of MWCNT Catalysts by Thermal Activation
<b>Maia</b>	João	Portugal	Simulation at the Nanoscale	Direct Numerical Simulation of Carbon Nanofibre Composites Under Shear Flow
<b>Malainho</b>	Eva	Portugal	NanoMaterials	Modelling of the Optical Spectra of CVD-deposited Silicon Films for Solar Cell Applications
<b>Marín</b>	Sergio	Spain	NanoBiotechnology / Nanomedicine	Electrochemical genosensors labelled with cds qds
<b>Maris</b>	Maria	Romania	NanoBiotechnology / Nanomedicine	Preliminary studies concerning the rheological stability of certain pharmaceutical formulations with controlled action in the field of nanomedicine
<b>Marques</b>	Leonel	Portugal	NanoMaterials	In situ diffraction study of high-pressure transformation of C60 to disordered sp <sup>2</sup> -carbon
<b>Martín</b>	Iñigo	Spain	Nanotubes	Carbon nanotubes growth from L-type and AlPO <sub>4</sub> -5 zeolites by thermal chemical vapour deposition
<b>Martinez de Baroja</b>	Natalia	Spain	NanoBiotechnology / Nanomedicine	Nanobiosensor for glucose based on chemically modified glucose oxidase labelled to magnetic nanoparticles
<b>Martinez Perez</b>	Maria Jose	Spain	Nanomagnetism	Size-dependent magnetic properties of magnetoferritin
<b>Martinez Rincon</b>	Marta	Spain	NanoChemistry	Electrochemical Synthesis of Magnetite Nanoparticles Coated of Methylene Blue
<b>Martins</b>	Verónica	Portugal	NanoBiotechnology / Nanomedicine	Biological detection limit of a GMR-based biochip for pathogenic analysis
<b>Martins</b>	Manuel	Portugal	Nanophotonics	Quantum dots/polymer-nanocomposites for luminescent optical fiber probes
<b>Martins</b>	Albino	Portugal	NanoBiotechnology / Nanomedicine	Electrospun Nanofibrous Structures as Scaffolds for Connective Tissues Regeneration
<b>Martins</b>	Ana João	Portugal	NanoMaterials	Hydrophobic-hydrophilic properties of titanium dioxide thin films
<b>Matos</b>	Henrique	Portugal	NanoBiotechnology / Nanomedicine	Particle Formation by Supercritical Fluid-Assisted Processes
<b>Miranda</b>	Rodolfo	Spain	NanoChemistry	Preferential nucleation, molecular distortion, charge transfer, and elastic effects in the self-assembly of TCNQ on Cu(100)

<b>Molina</b>	Luis M.	Spain	NanoChemistry	Ab initio studies of direct propene epoxidation at oxide-supported gold clusters and nanoparticles
<b>Monge</b>	Miguel	Spain	NanoChemistry	Silver nanoparticles and gold metallodendrimers: from molecular precursors to nanomaterials
<b>Monteiro</b>	Fernando	Portugal	NanoBiotechnology / Nanomedicine	A 3D type I Collagen / hydroxyapatite nanoparticles composite for bone regeneration
<b>Moreno</b>	César	Spain	SPM	Reversible Bipolar Resistive Switching La <sub>1-x</sub> Sr <sub>x</sub> MnO <sub>3-d</sub> thin films by C-SFM
<b>Moros</b>	María	Spain	NanoBiotechnology / Nanomedicine	Cell response against water stable magnetic nanoparticles obtained by thermal decomposition procedure
<b>Neves</b>	Nuno	Portugal	NanoBiotechnology / Nanomedicine	Z-axis (depth) control of cell spreading on micropatterned surfaces
<b>Neves</b>	Márcia	Portugal	NanoMaterials	Photoluminescent di-ureasil hybrids containing CdSe/ZnS quantum dots
<b>Niehus</b>	Manfred	Portugal	Nanophotonics	Exploration of laser induced gratings coupled to surface plasmon polaritons
<b>Nobre</b>	Sónia	Portugal	Nanophotonics	Eu(III) -based organic/inorganic lamellar hybrids self-directed assembled
<b>Obiols-Rabasa</b>	Marc	Spain	NanoMaterials	Rheological studies on polymeric nanoparticle dispersions stabilized by a polyfructose-derivative surfactant
<b>Otero Martin</b>	Roberto	Spain	NanoChemistry	1D ZnO Chains as the Spinal Cord of Adsorbed Metalloporphyrin Nanotubes Linked by Water Ligands
<b>Otero Martin</b>	Roberto	Spain	NanoMaterials	Molecular conformation, organizational chirality, and Fe metallation of mesotetramesitylporphyrins on Cu(100)
<b>Pacios</b>	Merce	Spain	Nanotubes	Amperometric (bio)sensors based on carbon nanotubes
<b>Paulo</b>	Pedro	Portugal	Simulation at the Nanoscale	Molecular Dynamics Simulations of Porphyrin-Dendrimer Systems: Towards Modelling Electron-Transfer in Solution
<b>Paulo</b>	Pedro	Portugal	NanoBiotechnology / Nanomedicine	Individual Detection of Gold Nanoparticles in Liquid using Photothermal Correlation Spectroscopy
<b>Pedro</b>	Luísa	Portugal	NanoBiotechnology / Nanomedicine	Protein nanoparticles for molecular therapy: Molecular construction of SIVp17/HIV1p6 nanoparticles and assembly in animal cell cultures
<b>Peláez</b>	Samuel	Spain	Simulation at the Nanoscale	Tailoring mechanical properties at the nanoscale: the dependence of Young's modulus of nanowires on the shape and axial orientation.
<b>Pellejero</b>	Ismael	Spain	NEMS / MEMS	A Comparison of Zeolites and Polymers used as sensitive layers in microcantilever-based gas sensors
<b>Peña</b>	Diego	Spain	NanoChemistry	Bottom-up approach to nanographenes via arynes
<b>Pereira</b>	Andre	Portugal	NanoMaterials	Heat Generation in Tunnel Junctions for Current-written Pinned Layer
<b>Pérez de Luque</b>	Alejandro	Spain	NanoBiotechnology / Nanomedicine	Nanoparticles in agriculture: development of smart delivery systems for plant research
<b>Pérez López</b>	Briza	Spain	NanoBiotechnology / Nanomedicine	Nanostructured biosensors for the analysis of phenolic compounds
<b>Perez Murano</b>	Francesc	Spain	NEMS / MEMS	Nanomechanical resonators integrated on CMOS defined by electron beam lithography
<b>Pérez Rafael</b>	Sandra	Spain	NanoBiotechnology / Nanomedicine	Characterization of MWCNT/PS/antibody membrane prepared by phase inversion method for biosensing applications

<b>Picas</b>	Laura	Spain	SPM	AFM characterization of supported planar bilayers of the inner membrane of Escherichia coli
<b>Pinho</b>	Sonia	France	Other	Hybrid nanoparticles for MRI and photoluminescence imaging applications in cells tracking
<b>Pinho</b>	Elisabete	Portugal	NanoMaterials	Biodegradable Polymeric Microfibres Reinforced with Nanofibres for Biomedical Applications
<b>Pinna</b>	Nicola	Portugal	NanoMaterials	Nanostructured Materials from Non-Aqueous Sol-Gel Approaches: Optical, Magnetic and Gas Sensing Properties
<b>Pinto</b>	Sara	Portugal	NanoMaterials	Ge nanocrystals embedded in alumina for non volatile memory applications
<b>Pires</b>	Liliana R.	Portugal	NanoBiotechnology / Nanomedicine	Chitosan nanoparticles for the delivery of genes toward tissue regeneration
<b>Prada</b>	Marta	United States	NanoElectronics	Relaxation and Decoherence in Two-electron Silicon Quantum Dots
<b>Prieto</b>	Emilio	Spain	Other	EMRP Research Project: Traceable characterization of nanoparticles
<b>Prieto</b>	Emilio	Spain	Other	EMRP Research Project: New traceability routes for nanometrology
<b>Proença</b>	Mariana	Portugal	Nanotubes	Ordered Assembly of Oxide Nanotubes in a Porous Alumina Membrane
<b>Puertas</b>	Sara	Spain	NanoBiotechnology / Nanomedicine	Biofunctionalitation of Magnetic Nanoparticles for Immunomagnetic Biosensors
<b>Quaresma</b>	Pedro	Portugal	NanoChemistry	Sonochemical formation of gold nuclei on magnetite nanoparticles and growth to a core-shell system
<b>Querejeta</b>	Ana	Spain	NanoChemistry	Tunable hydrothermal synthesis of BaMnO <sub>3</sub> nanocrystals
<b>Quintanilla</b>	Marta	Spain	NanoMaterials	Optical characterization of up-conversion properties of fluorescent NaYF <sub>4</sub> :Er,Yb nanocrystals
<b>Ramalho</b>	Ruben	Portugal	NanoBiotechnology / Nanomedicine	Electric alignment of microtubules on a microfabricated surface: micron-level control
<b>Ramos</b>	Daniel	Spain	NEMS / MEMS	Origin of the response of nanomechanical resonators to bacteria adsorption
<b>Rauwel</b>	Erwan	Portugal	NanoChemistry	Non-Aqueous Sol-Gel Routes Applied to Atomic Layer Deposition
<b>Reguera</b>	Javier	Spain	NanoMaterials	Influence of the molecular architecture on the self-assembly of pH- and temperature sensitive elastin-like block-copolymers.
<b>Rei</b>	Ana	Portugal	NanoMaterials	Production and characterization of nanostructured biosensors
<b>Retolaza</b>	Aritz	Spain	NanoBiotechnology / Nanomedicine	Protein patterning by Thermal Nanoimprint Lithography on functionalized polymers
<b>Ribeiro</b>	Sidney J.L.	Brazil	NanoMaterials	Bacterial cellulose based OLED's
<b>Rocha</b>	Sandra	Portugal	NanoBiotechnology / Nanomedicine	Peptide Encapsulation in Polyelectrolyte Nanocapsules
<b>Rodas</b>	Yolanda	Spain	NanoChemistry	Zeolite-based microreactors
<b>Rodrigues</b>	Rogério	Portugal	NanoBiotechnology / Nanomedicine	Qualitative and Quantitative Analysis of Biorecognition in Piezoelectric Biosensors
<b>Rodrigues</b>	João	Portugal	NanoChemistry	Molecular Materials Based on Organometallic Compounds
<b>Rodríguez Abreu</b>	Carlos	Spain	NanoChemistry	In-situ synthesis of nanoparticles using lyotropic liquid crystals
<b>Rodríguez Cantó</b>	Pedro Javier	Spain	Simulation at the Nanoscale	Modeling and Investigation of the ester cleavage in modern Photoresists materials

<b>Rodríguez-Vazquez</b>	María J.	Spain	NanoChemistry	Synthesis, characterization and stability of carboxylate-modified silver clusters powders dispersible in water
<b>Ruiz de Luzuriaga</b>	Alaitz	Spain	NanoMaterials	Synthesis of single-chain polymeric nanoparticles by a combination of RAFT polymerization and “click” chemistry techniques
<b>Sahagun</b>	Enrique	Spain	SPM	Adhesion hysteresis in Dynamic Atomic Force Microscopy
<b>Sainz</b>	Miguel	Spain	NanoMaterials	Customised nanocomposites based on rubber matrices for high demand applications.
<b>Salazar</b>	Norkis	Venezuela	NanoMaterials	PMMA-Organic Bentonite Nanocomposites from The Exfoliation-Adsorption Technique and Their Characterization by FTIR, XRD, TEM, TSDC and DSC.
<b>Salsamendi</b>	Maitane	Spain	NanoElectronics	New nanostructured multichromic materials for electrooptical devices
<b>Sanchez Ordoñez</b>	Samuel	Spain	Nanotubes	Characterization and enhancement of electrochemical properties of MWCNT/polysulfone composite modified screen-printed electrodes
<b>Sardon</b>	Haritz	Spain	NanoChemistry	Stability of triethoxysilane terminated waterborne polyurethane nanoparticles
<b>Schwarz</b>	Reinhard	Portugal	Nanophotonics	Interface analysis techniques on nanoscale dimension in flexible solar cells
<b>Segura</b>	Juan José	Spain	SPM	Water/L-alanine interactions: hydrophilicity vs hydrophobicity
<b>Sencadas</b>	Vitor	Portugal	NanoMaterials	Processing and characterization of nano composites of poly (vinilidene fluoride) doped with silver nano-particles
<b>Serra</b>	Ricardo	Portugal	NanoMaterials	Surface tailoring of coil coating using nanostructured films obtained by plasma polymerization of organosilanes precursors
<b>Sevillano</b>	Ignacio	Spain	Nanomagnetism	Synthesis and characterization of Zn nanoferrites
<b>Sirbu</b>	Rodica	Romania	NanoBiotechnology / Nanomedicine	Study concerning the nanobiotechnology of obtaining of collagen gels from marine fish skin and your rheological characterisation for using in dental medicine
<b>Soares</b>	Pedro	Portugal	NanoMaterials	Production and characterization of nanocomposite amorphous carbon thin films
<b>Sporer</b>	Christian	Spain	NanoBiotechnology / Nanomedicine	Novel Anionophores for Biosensor applications- Characterisation of Imidazolium Protophanes and Cyclophanes on Gold Surfaces
<b>Stanescu</b>	Iuliana Mihaela	Romania	SPM	TEM studies of crystalline hydroxyl and fluoro-apatite in bone tissues
<b>Stauber</b>	Tobias	Portugal	NanoMaterials	Optical conductivity of graphene beyond the Dirac cone approximation
<b>Tamayo</b>	Javier	Spain	NanoBiotechnology / Nanomedicine	Nanomechanical Devices: Ultrasensitive sensors of molecular recognition and conformational changes of biomolecules.
<b>Tejedor Busquets</b>	Robert	Spain	NanoMaterials	Mechanical Properties of Nanocrystalline and Ultrafine Grained Steel Obtained by Mechanical Milling
<b>Tolosa Ruiz</b>	Ángel	Spain	NanoMaterials	Powder coatings: a study of properties by addition of nanoresins.
<b>Tomás</b>	Helena	Portugal	NanoBiotechnology / Nanomedicine	PAMAM dendrimers used as vectors for gene delivery into Mesenchymal Stem Cells
<b>Torcal-Milla</b>	Francisco J.	Spain	Simulation at the Nanoscale	Interfero-diffractive linear optical encoder with nanometric resolution

<b>Torres</b>	Francesc	Spain	NEMS / MEMS	Measurement of Repulsive Casimir Forces Using MEMS Structures
<b>Tristany</b>	Mar	France	NanoChemistry	Synthesis of Ruthenium and Platinum Nanoparticles Stabilized by Heavily Fluorinated Compounds (Mar TRISTANY)
<b>Valencia Alvarez</b>	Jose Luis	Spain	SPM	Monte-Carlo uncertainty evaluation of transfer standards for atomic force microscopy
<b>Vasconcelos</b>	Helena	Portugal	NanoMaterials	New dye sensitized nano semiconductors in water purification with solar light
<b>Vaz Osorio</b>	Inês	Portugal	NanoChemistry	Silver nanowires: photocatalytic synthesis and characterization
<b>Vieira</b>	Ana Catarina	Portugal	NanoMaterials	Age-hardening effect on the properties and nanostructure of functionally graded Al alloy – SiCp composites
<b>Vieira</b>	Milena	Portugal	Other	Production of Apatite-like Lanthanum Silicate thin film electrolytes by oxidation of La-Si sputtered thin films
<b>Xiao</b>	Jun	USA	NanoMaterials	Scanning Nano-Metrology of ultra thin films
<b>Yagüe</b>	Clara	Spain	NanoBiotechnology / Nanomedicine	Synthesis and functionalization of silica nanoparticles with hydrophilic or hydrophobic groups
<b>Yasakau</b>	Kiryl	Portugal	SPM	A study of the localized corrosion behavior of metals by AFM/SKPFM technique



**Session PA (109)**

Presenting Author	Country	Poster Title	
<b>TOPIC: NanoBiotechnology / Nanomedicine</b>			
<b>Albuquerque</b>	Rita	Portugal	Optimization and characterization of amorphous/nanocrystalline biosensors for DNA detection using gold nanoparticles
<b>Arroyo Cardoso</b>	Filipe	Portugal	Increasing the sensitivity of magnetoresistive-based biochips
<b>Bernacka-Wojcik</b>	Iwona	Portugal	Nanostructural semiconducting photocatalysts for medical applications
<b>Cerqueira</b>	Mariana	Portugal	Influence of Patterned Electrospun Nanofiber Meshes on Human Dermal Fibroblasts, Keratinocytes and Adipose Stem Cells Behaviour
<b>Comenge</b>	Joan	Spain	Addressing the Immune System: Macrophages Responses Towards Au Nanoparticle Conjugates
<b>Cunha</b>	Cristiana	Portugal	Targeting nanoprobe for early invasive cancer cells using Hereditary Diffuse Gastric Cancer (HDGC) as a model.
<b>Doria</b>	Gonçalo	Portugal	Revealing the mechanism of SNP detection with gold nanoprobe by non-cross-linking aggregation
<b>Elizondo Sáez de Vicuña</b>	Elisa	Spain	Compressed Fluid Based Technologies for the Preparation of Drug Delivery Systems
<b>Fernandez-Cuesta</b>	Irene	Spain	Interdigitated nanoelectrodes for sensing: fabrication and characterization
<b>Gomes</b>	Inês	Portugal	Probing the Surface Properties of Cytochromes c/Gold Nanoparticles Complexes
<b>González</b>	Mónica	Spain	Non-specific adsorption of biomolecules on single-walled carbon nanotubes
<b>Köber</b>	Mariana	Spain	Opto-magnetic detection of dimer formation of superparamagnetic Fe <sub>3</sub> O <sub>4</sub> nanoparticles in liquids. Application to a molecular recognition transducer.
<b>Lajos</b>	Gejza	Spain	Surface-enhanced Fluorescence and Raman Scattering Study of Antitumoral Drug Hypericin: An Effect of Aggregation and Self-spacing Depending on pH
<b>Loureiro</b>	Joana	Portugal	Integrated platform for Stem Cells separation/counting
<b>Marín</b>	Sergio	Spain	Electrochemical genosensors labelled with cds qds
<b>Martinez de Baroja</b>	Natalia	Spain	Nanobiosensor for glucose based on chemically modified glucose oxidase labelled to magnetic nanoparticles
<b>Martins</b>	Verónica	Portugal	Biological detection limit of a GMR-based biochip for pathogenic analysis
<b>Martins</b>	Albino	Portugal	Electrospun Nanofibrous Structures as Scaffolds for Connective Tissues Regeneration
<b>Moros</b>	María	Spain	Cell response against water stable magnetic nanoparticles obtained by thermal decomposition procedure
<b>Pedro</b>	Luísa	Portugal	Protein nanoparticles for molecular therapy: Molecular construction of SIVp17/HIV1p6 nanoparticles and assembly in animal cell cultures
<b>Pérez López</b>	Briza	Spain	Nanostructured biosensors for the analysis of phenolic compounds
<b>Pérez Rafael</b>	Sandra	Spain	Characterization of MWCNT/PS/antibody membrane prepared by phase inversion method for biosensing applications
<b>Pires</b>	Liliana R.	Portugal	Chitosan nanoparticles for the delivery of genes toward tissue regeneration
<b>Puertas</b>	Sara	Spain	Biofunctionalization of Magnetic Nanoparticles for Immunomagnetic Biosensors
<b>Ramalho</b>	Ruben	Portugal	Electric alignment of microtubules on a microfabricated surface: micron-level control

<b>Rodrigues</b>	Rogério	Portugal	Qualitative and Quantitative Analysis of Biorecognition in Piezoelectric Biosensors
<b>Yagüe</b>	Clara	Spain	Synthesis and functionalization of silica nanoparticles with hydrophilic or hydrophobic groups

### TOPIC: NanoChemistry

<b>Albuquerque</b>	Rita	Portugal	The influence of Ag <sub>2</sub> S percentage on the photoactivity of TiO <sub>2</sub> /Ag <sub>2</sub> S nanocomposites
<b>Carvalho Miranda</b>	Maria Adelaide	Portugal	Gold Anisotropic Nanoparticles: Synthesis and Characterization
<b>El-Hawi</b>	Nancy	France	A novel method of synthesis of silica nanoparticles in alcoholic organic medium
<b>Ferreira</b>	Carla	Portugal	Functionalized nano-microstructures to combat biofouling of industrial surfaces
<b>Figueiredo</b>	Hugo	Portugal	Modified electrode based on Zeolite-encapsulated Cr(III) complex
<b>Gómez de Pedro</b>	Sara	Spain	Synthesis of nanoparticles in microfluidic devices based on the LTCC technology
<b>Gonzalez-Dominguez</b>	Jose Miguel	Spain	Carbon nanotubes dispersion towards polymer integration
<b>Martinez Rincon</b>	Marta	Spain	Electrochemical Synthesis of Magnetite Nanoparticles Coated of Methylene Blue
<b>Quaresma</b>	Pedro	Portugal	Sonochemical formation of gold nuclei on magnetite nanoparticles and growth to a core-shell system
<b>Querejeta</b>	Ana	Spain	Tunable hydrothermal synthesis of BaMnO <sub>3</sub> nanocrystals
<b>Rodas</b>	Yolanda	Spain	Zeolite-based microreactors
<b>Rodríguez-Vazquez</b>	María J.	Spain	Synthesis, characterization and stability of carboxylate-modified silver clusters powders dispersible in water
<b>Sardon</b>	Haritz	Spain	Stability of triethoxysilane terminated waterborne polyurethane nanoparticles
<b>Vaz Osorio</b>	Inês	Portugal	Silver nanowires: photocatalytic synthesis and characterization

### TOPIC: NanoElectronics / Molecular Electronics

<b>Chaves Romero</b>	Ferney A.	Spain	Analytic Model of Quantum Electrostatic Potential in Double-Gate MOSFETs
<b>Salsamendi</b>	Maitane	Spain	New nanostructured multichromic materials for electrooptical devices

### TOPIC: Nanomagnetism

<b>Alija</b>	Alejandro	Spain	Ratchet effects on domain wall motion in Co-Si amorphous films with arrays of asymmetric holes: experiments and theoretical simulations
<b>Alonso</b>	Javier	Spain	Study of the influence of the interactions in the magnetic behaviour of Fe-Ag thin films above the percolation limit
<b>Amaral</b>	Joao	Portugal	Magnetic studies of mechanically alloyed metastable fcc Fe <sub>23</sub> Cu <sub>77</sub> : superferromagnetism with bimodal cluster size distribution.
<b>Burzuri</b>	Enrique	Spain	How well aligned are the magnetic anisotropy axes in crystals of Mn <sub>12</sub> molecular nanomagnets? An angle-dependent ac susceptibility study

<b>Guedes</b>	Andre	Portugal	Hybrid Magnetoresistive/MEMS devices for 1/f noise reduction
<b>López-Ruiz</b>	Román	Spain	Influence of stress and size over the magnetic response of nickel nanowires
<b>Macedo</b>	Rita	Portugal	Nano-Sized MgO-based Magnetic Tunnel Junctions fabricated by e-beam lithography combined with chemical-mechanical polishing
<b>Martinez Perez</b>	Maria Jose	Spain	Size-dependent magnetic properties of magnetoferritin

<b>TOPIC: NanoMaterials</b>			
<b>Alegre</b>	Daniel	Spain	Properties of single-crystalline ZnO nanodots and highly-textured ZnO films grown by electrochemistry
<b>Batista</b>	Carlos	Portugal	VO <sub>2</sub> -Based Thermochromic Thin Films for Energy Efficient Windows
<b>Cabrera</b>	Lourdes	Spain	Conductive Polymers with Embedded Magnetite Nanoparticles: Synthesis and Characterization
<b>Fernandes</b>	Francisco	Spain	Structural and functional properties of gelatin-clay nanocomposites
<b>Gil</b>	Marta	Spain	Synthesis and characterization of modified ordered mesoporous materials
<b>Guerrero Ramírez</b>	Luis Guillermo	Spain	Synthesis of nano-structured copolymeric hydrogels based on N-Isopropyl acrylamide (NIPA) by Microemulsion Polymerization
<b>Hervías Sarasqueta</b>	Xabier	Spain	Study of drug release on smart nano-sized hydrogels based on N-isopropyl acrylamide by High Performance Liquid Chromatography
<b>Hortigüela</b>	María Jesús	Spain	Enzymatic Synthesis of Amorphous Calcium Phosphate-Chitosan Nanocomposites and its Processing into Hierarchical Structures
<b>Leitao</b>	Diana	Portugal	Py antidot thin films: a transport and magnetic characterization as a function of temperature
<b>Lermo Soria</b>	Anabel	Spain	Electrochemical immunosensing of folic acid based on improved nanostructured transducer
<b>Liebana</b>	Susana	Spain	Electrochemical biosensing in food for pathogenic bacteria based on nanostructured transducers
<b>Lugo</b>	Nayar	Spain	Pure copper deformed by equal-channel angular pressing (ECAP)
<b>Malainho</b>	Eva	Portugal	Modelling of the Optical Spectra of CVD-deposited Silicon Films for Solar Cell Applications
<b>Martins</b>	Ana João	Portugal	Hydrophobic-hydrophilic properties of titanium dioxide thin films
<b>Obiols-Rabasa</b>	Marc	Spain	Rheological studies on polymeric nanoparticle dispersions stabilized by a polyfructose-derivative surfactant
<b>Pereira</b>	Andre	Portugal	Heat Generation in Tunnel Junctions for Current-written Pinned Layer
<b>Pinto</b>	Sara	Portugal	Ge nanocrystals embedded in alumina for non volatile memory applications
<b>Quintanilla</b>	Marta	Spain	Optical characterization of up-conversion properties of fluorescent NaYF <sub>4</sub> :Er,Yb nanocrystals
<b>Reguera</b>	Javier	Spain	Influence of the molecular architecture on the self-assembly of pH- and temperature sensitive elastin-like block-copolymers.
<b>Rei</b>	Ana	Portugal	Production and characterization of nanostructured biosensors

<b>Ruiz de Luzuriaga</b>	Alaitz	Spain	Synthesis of single-chain polymeric nanoparticles by a combination of RAFT polymerization and “click” chemistry techniques
<b>Sencadas</b>	Vitor	Portugal	Processing and characterization of nano composites of poly (vinilidene fluoride) doped with silver nano-particles
<b>Serra</b>	Ricardo	Portugal	Surface tailoring of coil coating using nanostructured films obtained by plasma polymerization of organosilanes precursors
<b>Soares</b>	Pedro	Portugal	Production and characterization of nanocomposite amorphous carbon thin films
<b>Tejedor Busquets</b>	Robert	Spain	Mechanical Properties of Nanocrystalline and Ultrafine Grained Steel Obtained by Mechanical Milling
<b>Vieira</b>	Ana Catarina	Portugal	Age-hardening effect on the properties and nanostructure of functionally graded Al alloy – SiCp composites

### TOPIC: Nanophotonics

<b>González-Díaz</b>	Juan B.	Spain	Surface plasmon resonance effects on the magneto-optical response of noble-metal ferromagnet nanodisks.
<b>Lamela</b>	Jorge	Spain	SNOM study of periodically poled ferroelectric domains in LiNbO <sub>3</sub> , LiTaO <sub>3</sub> and Ba <sub>2</sub> Nb <sub>5</sub> O <sub>15</sub> crystals
<b>Martins</b>	Manuel	Portugal	Quantum dots/polymer-nanocomposites for luminescent optical fiber probes
<b>Nobre</b>	Sónia	Portugal	Eu(III) -based organic/inorganic lamellar hybrids self-directed assembled

### TOPIC: Nanotubes

<b>Barreiro</b>	Amelia	Spain	Nanotube based thermal motors: sub-nanometer motion of cargoes driven by thermal gradients
<b>Carretero Genevrier</b>	Adrián	Spain	Single-Crystalline La <sub>0.7</sub> Sr <sub>0.3</sub> MnO <sub>3</sub> Nanowires Grown by Template Directed Chemical Solution Synthesis
<b>Carvalho</b>	Oscar	Portugal	Mechanical and fatigue properties of sintered Nanotube-based functionally graded materials
<b>Machado</b>	Bruno	Portugal	Liquid-Phase Hydrogenation of Unsaturated Aldehydes: Enhancing Selectivity of MWCNT Catalysts by Thermal Activation
<b>Martín</b>	Iñigo	Spain	Carbon nanotubes growth from L-type and AlPO <sub>4-5</sub> zeolites by thermal chemical vapour deposition
<b>Pacios</b>	Merce	Spain	Amperometric (bio)sensors based on carbon nanotubes
<b>Sanchez Ordoñez</b>	Samuel	Spain	Characterization and enhancement of electrochemical properties of MWCNT/polysulfone composite modified screen-printed electrodes

### TOPIC: NEMS / MEMS

<b>Fernández</b>	Iván	Spain	Parallel nanogap fabrication with nanometer size control using III-V semiconductor epitaxial technology
<b>Garcia-Sanchez</b>	Daniel	Spain	Mechanical detection of the vibrations of Carbon Nanotube and Graphene Resonators
<b>Goncalves</b>	Luis	Portugal	Thermoelectric thin-films for microcoolers and energy scavenging microsystems
<b>Pellejero</b>	Ismael	Spain	A Comparison of Zeolites and Polymers used as sensitive layers in microcantilever-based gas sensors

<b>Ramos</b>	Daniel	Spain	Origin of the response of nanomechanical resonators to bacteria adsorption
--------------	--------	-------	--

### TOPIC: Scanning Probe Microscopies (SPM)

<b>Fernandes</b>	João	Portugal	Atomic force microscopy of the antibacterial effects of chitosans on <i>Bacillus cereus</i> (and its spores)
<b>Fuss</b>	Martina	Spain	Theory of Topography and Recognition Imaging by Dynamic Force Microscopy
<b>Jaafar</b>	Miriam	Spain	True variable field magnetic force microscopy for nanostructures characterization
<b>Moreno</b>	César	Spain	Reversible Bipolar Resistive Switching La <sub>1-x</sub> Sr <sub>x</sub> MnO <sub>3-d</sub> thin films by C-SFM
<b>Picas</b>	Laura	Spain	AFM characterization of supported planar bilayers of the inner membrane of <i>Escherichia coli</i>
<b>Sahagun</b>	Enrique	Spain	Adhesion hysteresis in Dynamic Atomic Force Microscopy
<b>Segura</b>	Juan José	Spain	Water/L-alanine interactions: hydrophilicity vs hydrophobicity
<b>Stanescu</b>	Iuliana Mihaela	Romania	TEM studies of crystalline hydroxyl and fluoro-apatite in bone tissues
<b>Yasakau</b>	Kiryl	Portugal	A study of the localized corrosion behavior of metals by AFM/SKPFM technique

### TOPIC: Simulation at the Nanoscale

<b>Barbosa</b>	Hélder	Portugal	Simulation in Organic Nanoelectronics: from Single Molecule to Thin Film
<b>Lopez</b>	Hender	Spain	Spin Dependent Injection Model for Monte Carlo Device Simulation
<b>Peláez</b>	Samuel	Spain	Tailoring mechanical properties at the nanoscale: the dependence of Young's modulus of nanowires on the shape and axial orientation.
<b>Torcal-Milla</b>	Francisco J.	Spain	Interfero-diffractive linear optical encoder with nanometric resolution

### TOPIC: Other

<b>Kaltzakorta</b>	Idurre	Spain	synthesis and characterization of silica microcapsules containing organic compounds of different viscosity
<b>Pinho</b>	Sonia	France	Hybrid nanoparticles for MRI and photoluminescence imaging applications in cells tracking
<b>Vieira</b>	Milena	Portugal	Production of Apatite-like Lanthanum Silicate thin film electrolytes by oxidation of La-Si sputtered thin films

<b>Session PB (87)</b>			
<b>Presenting Author</b>	<b>Country</b>	<b>Poster Title</b>	
<b>TOPIC: NanoBiotechnology / Nanomedicine</b>			
<b>Aguilar-Caballos</b>	Maria-Paz	Spain	Nanostructures as analytical tools in bioassays
<b>Alpuim</b>	Pedro	Portugal	ultra-sensitive shape sensor test structures based on piezo-resistive doped nanocrystalline silicon
<b>Azevedo</b>	Nuno	Portugal	Development and application of peptide nucleic acids (PNA) for the rapid identification of microorganisms by fluorescence in situ hybridization (FISH)
<b>Bechir</b>	Anamaria	Romania	Biotechnologies for obtaining new pharmaceutical formulations based on mixtures of type I non-denatured fibrillar collagen gels and extracts from marine algae with applications in nanomedicine
<b>Costa Martins</b>	Rui	Portugal	Cellular Automata Model for Controlling Supercooling: NanoBioTechnology Perspective into CryoPreservation of Living Tissues
<b>Fortunato</b>	Elvira	Portugal	DNA detection using amorphous silicon sensors with gold nanoparticles
<b>Gomes</b>	Joana	Portugal	Nanoencapsulation of bioactive compounds
<b>Gonzalez Fernandez</b>	Africa	Spain	ROS induction and cytotoxicity of inorganic nanoparticles in human cells
<b>Hungerford</b>	Graham	Portugal	Sol-gel derived biocompatible glasses towards bone implant integration
<b>Maris</b>	Maria	Romania	Preliminary studies concerning the rheological stability of certain pharmaceutical formulations with controlled action in the field of nanomedicine
<b>Matos</b>	Henrique	Portugal	Particle Formation by Supercritical Fluid-Assisted Processes
<b>Monteiro</b>	Fernando	Portugal	A 3D type I Collagen / hydroxyapatite nanoparticles composite for bone regeneration
<b>Neves</b>	Nuno	Portugal	Z-axis (depth) control of cell spreading on micropatterned surfaces
<b>Paulo</b>	Pedro	Portugal	Individual Detection of Gold Nanoparticles in Liquid using Photothermal Correlation Spectroscopy
<b>Pérez de Luque</b>	Alejandro	Spain	Nanoparticles in agriculture: development of smart delivery systems for plant research
<b>Retolaza</b>	Aritz	Spain	Protein patterning by Thermal Nanoimprint Lithography on functionalized polymers
<b>Rocha</b>	Sandra	Portugal	Peptide Encapsulation in Polyelectrolyte Nanocapsules
<b>Sirbu</b>	Rodica	Romania	Study concerning the nanobiotechnology of obtaining of collagen gels from marine fish skin and their rheological characterisation for using in dental medicine
<b>Sporer</b>	Christian	Spain	Novel Anionophores for Biosensor applications- Characterisation of Imidazolium Protophanes and Cyclophanes on Gold Surfaces
<b>Tamayo</b>	Javier	Spain	Nanomechanical Devices: Ultrasensitive sensors of molecular recognition and conformational changes of biomolecules.
<b>Tomás</b>	Helena	Portugal	PAMAM dendrimers used as vectors for gene delivery into Mesenchymal Stem Cells

<b>TOPIC: NanoChemistry</b>			
<b>Alcami</b>	Manuel	Spain	Understanding the Supramolecular Self-Assembly of the Fullerene Derivative PCBM on Au(111) Surface

<b>Andrade</b>	Suzana M	Portugal	Nanometric aggregates of a covalent porphyrin dimer followed by Fluorescence Correlation Spectroscopy in aqueous buffered solution
<b>Brunet</b>	Ernesto	Spain	The Role of Porous Materials in the Efficient Storage of Hydrogen
<b>Carabineiro</b>	Sonia	Portugal	Preparation of gold nanoparticles on several supports and their use for the oxidation of carbon monoxide
<b>Figueiredo Lopes</b>	Luís M.	Portugal	Ruthenium Complexes Encapsulated in Nanostructured Sol-gel Silica Matrices
<b>Garcia-Ramos</b>	Jose V	Spain	SERS on Functionalized Silver Nanostructures: Towards the Detection of Single Molecules in Hot Spots
<b>Kahn</b>	Myrtil	France	Experimental evidence of the existence in solution of organizations of ZnO nanoparticles synthesized by organometallic method using dynamic light scattering
<b>López Ramírez</b>	María Rosa	Spain	A SERS study of charge-transfer processes in the Raman spectrum of the benzoate anion adsorbed on silver nanostructures
<b>Miranda</b>	Rodolfo	Spain	Preferential nucleation, molecular distortion, charge transfer, and elastic effects in the self-assembly of TCNQ on Cu(100)
<b>Molina</b>	Luis M.	Spain	Ab initio studies of direct propene epoxidation at oxide-supported gold clusters and nanoparticles
<b>Monge</b>	Miguel	Spain	Silver nanoparticles and gold metallodendrimers: from molecular precursors to nanomaterials
<b>Otero Martin</b>	Roberto	Spain	1D ZnO Chains as the Spinal Cord of Adsorbed Metalloporphyrin Nanotubes Linked by Water Ligands
<b>Peña</b>	Diego	Spain	Bottom-up approach to nanographenes via arynes
<b>Rauwel</b>	Erwan	Portugal	Non-Aqueous Sol-Gel Routes Applied to Atomic Layer Deposition
<b>Rodrigues</b>	João	Portugal	Molecular Materials Based on Organometallic Compounds
<b>Rodríguez Abreu</b>	Carlos	Spain	In-situ synthesis of nanoparticles using lyotropic liquid crystals
<b>Tristany</b>	Mar	France	Synthesis of Ruthenium and Platinum Nanoparticles Stabilized by Heavily Fluorinated Compounds (Mar TRISTANY)

### TOPIC: NanoElectronics / Molecular Electronics

<b>Ferreira</b>	Paula	Portugal	Synthesis and electric properties of nanoporous BaTiO <sub>3</sub>
<b>Jiménez</b>	David	Spain	Electrical characteristics of graphene based transistors
<b>Prada</b>	Marta	United States	Relaxation and Decoherence in Two-electron Silicon Quantum Dots

### TOPIC: Nanomagnetism

<b>Carbonera</b>	Chiara	Spain	Fabrication of nanospheres from Mn <sub>12</sub> acetate SMM: do the chemical properties of the original cluster show changes?
<b>Sevillano</b>	Ignacio	Spain	Synthesis and characterization of Zn nanoferrites

### TOPIC: NanoMaterials

<b>Anson</b>	Alejandro	Spain	Separation of Argon and Oxygen by Adsorption on a Titanosilicate Molecular Sieve
<b>Bystrov</b>	Vladimir	Portugal	Composite nano-biomaterials based on polyvinylidene fluoride copolymers

<b>Cadillon Costa</b>	Luís	Portugal	Introduction of polypyrrol nanoparticles in cement paste
<b>Castro-Garcia</b>	Socorro	Spain	Magnetocapacitive response in Fe <sub>3</sub> O <sub>4</sub> nanoparticles
<b>Chiorcea-Paquim</b>	Ana-Maria	Portugal	Atomic force microscopy and electrochemical studies of palladium nanoparticles and nanowires electrodeposited onto carbon electrode surfaces
<b>De Teresa Noguerras</b>	Jose Maria	Spain	In-situ STEM investigation of thin films in a dual-beam equipment
<b>Farjas Silva</b>	Jordi	Spain	Restricted epitaxial growth during thermal crystallization of nanocrystalline silicon: experiments and modeling
<b>Ferreira</b>	María Rute	Portugal	Self-photopatternable di-ureasil-zirconium oxo-clusters organic-inorganic hybrids for low cost integrated optical substrates
<b>Gauffre</b>	Fabienne	France	New strategies of colloidal stabilization of nanoparticles for applications in aqueous media
<b>Gomes Coutinho</b>	Paulo José	Portugal	TiO <sub>2</sub> and CdS nanoparticles obtained from soft templating methods
<b>Marques</b>	Leonel	Portugal	In situ diffraction study of high-pressure transformation of C <sub>60</sub> to disordered sp <sup>2</sup> -carbon
<b>Neves</b>	Márcia	Portugal	Photoluminescent di-ureasil hybrids containing CdSe/ZnS quantum dots
<b>Otero Martin</b>	Roberto	Spain	Molecular conformation, organizational chirality, and Fe metallation of mesotetramesitylporphyrins on Cu(100)
<b>Pinho</b>	Elisabete	Portugal	Biodegradable Polymeric Microfibres Reinforced with Nanofibres for Biomedical Applications
<b>Pinna</b>	Nicola	Portugal	Nanostructured Materials from Non-Aqueous Sol-Gel Approaches: Optical, Magnetic and Gas Sensing Properties
<b>Ribeiro</b>	Sidney J.L.	Brazil	Bacterial cellulose based OLED's
<b>Sainz</b>	Miguel	Spain	Customised nanocomposites based on rubber matrices for high demand applications.
<b>Salazar</b>	Norkis	Venezuela	PMMA-Organo Bentonite Nanocomposites from The Exfoliation-Adsorption Technique and Their Characterization by FTIR, XRD, TEM, TSDC and DSC.
<b>Stauber</b>	Tobias	Portugal	Optical conductivity of graphene beyond the Dirac cone approximation
<b>Tolosa Ruiz</b>	Ángel	Spain	Powder coatings: a study of properties by addition of nanoresins.
<b>Vasconcelos</b>	Helena	Portugal	New dye sensitized nano semiconductors in water purification with solar light
<b>Xiao</b>	Jun	USA	Scanning Nano-Metrology of ultra thin films

<b>TOPIC: Nanophotonics</b>			
<b>Calvo</b>	Mauricio	Spain	Nanoparticle based One-Dimensional Photonic Crystals
<b>del Castillo</b>	Javier	Spain	SiO <sub>2</sub> -CeF <sub>3</sub> :Eu <sup>3+</sup> nano-glass-ceramics prepared by sol-gel method. Structural and Optical Characterization
<b>del Castillo</b>	Javier	Spain	Structural characterization and luminescent study of transparent nanostructured Eu <sup>3+</sup> doped sol-gel derived SiO <sub>2</sub> -PbF <sub>2</sub> glass-ceramics
<b>Griol</b>	Amadeu	Spain	Experimental realization of a high efficient coupling technique for SOI devices based on inverted tapers and V-grooves integration
<b>Lanceros-Mendez</b>	Senentxu	Portugal	Tunable Fabry-Perot Optical Filter with a Resonant Cavity
<b>Niehus</b>	Manfred	Portugal	Exploration of laser induced gratings coupled to surface plasmon polaritons
<b>Schwarz</b>	Reinhard	Portugal	Interface analysis techniques on nanoscale dimension in flexible solar cells

<b>TOPIC: Nanotubes</b>			
<b>Castillejos</b>	Eva	France	Strategies for the Selective Confinement of Nanoparticles in the inner cavity of Multi-Walled Carbon Nanotubes
<b>Gomes</b>	João	Portugal	Carbon Nanofibre-poly(vinylidene fluoride) nanocomposite: effect of the carbon nanofibres concentration on the a to b phase transformation and the degree of crystallinity
<b>Proença</b>	Mariana	Portugal	Ordered Assembly of Oxide Nanotubes in a Porous Alumina Membrane

<b>TOPIC: NEMS / MEMS</b>			
<b>Perez Murano</b>	Francesc	Spain	Nanomechanical resonators integrated on CMOS defined by electron beam lithography
<b>Torres</b>	Francesc	Spain	Measurement of Repulsive Casimir Forces Using MEMS Structures

<b>TOPIC: Scanning Probe Microscopies (SPM)</b>			
<b>Barroca</b>	Nathalie	Portugal	Poly(L-lactic)acid as stimulator of bone growth: Piezo-force microscopy study of the local piezoelectric properties
<b>Eaton</b>	Peter	Portugal	Atomic Force Microscopy and Fluorescence Microscopy of Malarial Hepatocytes
<b>Lingenfelder</b>	Magalí	Germany	Tuning the expression of supramolecular chirality by molecular footprint engineering on metal surfaces
<b>Valencia Alvarez</b>	Jose Luis	Spain	Monte-Carlo uncertainty evaluation of transfer standards for atomic force microscopy

<b>TOPIC: Simulation at the Nanoscale</b>			
<b>Maia</b>	João	Portugal	Direct Numerical Simulation of Carbon Nanofibre Composites Under Shear Flow
<b>Paulo</b>	Pedro	Portugal	Molecular Dynamics Simulations of Porphyrin-Dendrimer Systems: Towards Modelling Electron-Transfer in Solution
<b>Rodríguez Cantó</b>	Pedro Javier	Spain	Modeling and Investigation of the ester cleavage in modern Photoresists materials

<b>TOPIC: Other</b>			
<b>Bouju</b>	Xavier	France	How does pentagonal molecules self-assemble on a six-fold symmetry surface?The case of penta-tert-butyl-corrannulene molecule on Cu(111)
<b>Prieto</b>	Emilio	Spain	EMRP Research Project: New traceability routes for nanometrology
<b>Prieto</b>	Emilio	Spain	EMRP Research Project: Traceable characterization of nanoparticles





## **LIST OF PARTICIPANTS**

## **ALPHABETICAL ORDER**

**Nanospain2008 Participants (329)**



## PARTICIPANTS

Only participants fully registered (payment done) appear in this list

**Registered Participants: 329 - last update: April 04, 2008**

Last Name	Name	Institution	Country
<b>Aguilar-Caballeros</b>	Maria-Paz	University of Córdoba	Spain
<b>Aimé</b>	Jean-Pierre	C'Nano GSO	France
<b>Albuquerque</b>	Rita	University of Lisbon	Portugal
<b>Alcami</b>	Manuel	Universidad Autónoma de Madrid	Spain
<b>Alegre Castro</b>	Daniel	Instituto de Microelectrónica de Madrid-CSIC	Spain
<b>Alegret</b>	Salvador	Universitat Autònoma de Barcelona	Spain
<b>Alija</b>	Alejandro	Universidad de Oviedo	Spain
<b>Almeida</b>	Antonio	Universidade de Lisboa	Portugal
<b>Alonso</b>	Javier	Universidad del País Vasco	Spain
<b>Alpuim</b>	Pedro	Universidade do Minho	Portugal
<b>Amantia</b>	David	LEITAT Technological Center	Spain
<b>Amaral</b>	Joao	Universidade de Aveiro-CICECO	Portugal
<b>Anamaria</b>	Bechir	University of Constanza	Romania
<b>Andrade</b>	Suzana M	Instituto Superior Técnico	Portugal
<b>Ansón</b>	Alejandro	Instituto de Carboquímica-CSIC	Spain
<b>Ares</b>	Pablo	Nanotec Electrónica S.L.	Spain
<b>Arroyo Cardoso</b>	Filipe	INESC-MN	Portugal
<b>Artacho</b>	Emilio	University of Cambridge	UK
<b>Azevedo</b>	Nuno	Institute for Biotechnology and Bioengineering	Portugal
<b>Baptista</b>	Pedro	CIGMH/DCV - FCT/UNL	Portugal
<b>Barbosa</b>	Hélder	University of Minho	Portugal
<b>Barreiro</b>	Amelia	Institut Català de Nanotecnologia	Spain
<b>Barroca</b>	Natália	University of Aveiro - CICECO	Portugal
<b>Batista</b>	Carlos	University of Minho	Portugal
<b>Berger</b>	Andreas	Asociación CIC nanoGUNE	Spain
<b>Bergmans</b>	Robbert	NMi Van Swinden Laboratorium	Delft
<b>Bernacka-Wojcik</b>	Iwona	CEMOP/UNINOVA	Portugal
<b>Bernard</b>	Charlotte	C'Nano GSO	France
<b>Bernardo</b>	Carlos A.	International Iberian Nanotechnology Laboratory	Portugal
<b>Blanco</b>	Alvaro	ICMM-CSIC	Spain
<b>Blick</b>	Robert H.	University of Wisconsin-Madison	USA
<b>Bonafos</b>	Caroline	CEMES/CNRS	France
<b>Borges</b>	João	Universidade Nova de Lisboa	Portugal
<b>Borrisé</b>	Xavier	CNM-IMB, CSIC	Spain
<b>Boujou</b>	Xavier	C'NanoGSO - CEMES-CNRS	France
<b>Bozi</b>	Daniel	DIPC	Spain
<b>Bravo</b>	Ernesto	SODENA	Spain
<b>Bravo</b>	Javier	SODENA	Spain
<b>Briones</b>	Fernando	Instituto de Microelectrónica de Madrid-CSIC	Spain
<b>Broqueira</b>	Pedro	Instituto Superior Técnico	Portugal
<b>Brown</b>	Ross	IPREM6ECP	France
<b>Brunet</b>	Ernesto	Universidad Autónoma de Madrid	Spain
<b>Burzuri</b>	Enrique	Instituto de Ciencia de Materiales de Aragón	Spain
<b>Bystrov</b>	Vladimir	Universidade de Aveiro-CICECO	Portugal
<b>Cabrera</b>	Lourdes	Universidad Autónoma de Madrid	Spain
<b>Cadillon Costa</b>	Luís	University of Aveiro	Portugal
<b>Calvo</b>	Mauricio	Instituto de Ciencias de los Materiales de Sevilla	Spain
<b>Campillo</b>	Igor	Asociación CIC nanoGUNE	Spain
<b>Carabineiro</b>	Sónia	Laboratório de Catálise e Materiais/FEUP	Portugal
<b>Caraiane</b>	Aurelia	University of Constanta	Romania
<b>Carbonera</b>	Chiara	Instituto de Ciencia de Materiales de Aragón	Spain

Last Name	Name	Institution	Country
Carcedo	Laura	Centro Español de Metrología	Spain
Carlos	Luís	University of Aveiro	Portugal
Carretero	Adrián	ICMAB - CSIC	Spain
Carvalho	Oscar	Universidade do Minho	Portugal
Castillejos	Eva	LCC CNRS	France
Castro-García	Socorro	University of A Coruña	Spain
Cerqueira	Mariana	Universidade do Minho	Portugal
Chacon	Carmen	Phantoms Foundation	Spain
Chaves Romero	Ferney A.	Universidad Autónoma de Barcelona	Spain
Chiorcea-Paquim	Ana-Maria	Universidade de Coimbra	Portugal
Clavel	Guyhaine	University of Aveiro	Portugal
Comenge Farre	Joan	Institut Català de Nanotecnologia	Spain
Correia	Antonio	Phantoms Foundation	Spain
Correia Quaresma	Pedro	REQUIMTE-Universidade do Porto	Portugal
Costa Martins	Rui	University of Minho	Portugal
Costa-Krämer	José Luís	Instituto de Microelectrónica de Madrid-CSIC	Spain
Covas	José	I3N/University of Minho	Portugal
Cruz	Fernando	Imperial College London	UK
Cruz	M-Eugenia	INETI	Portugal
Cunha	Cristiana	INEB/IPATIMUP	Portugal
Cussó	Fernando	Universidad Autónoma de Madrid	Spain
Daniel da Silva	Ana Luisa	University of Aveiro and CICECO	Portugal
Danti	Josep	INDRA	Spain
de Carvalho Miranda	Maria Adelaide	REQUIMTE-Universidade do Porto	Portugal
de la Figuera	Juan	Instituto de Química-Física Rocasolano	Spain
De la Fuente	Jesús M.	Instituto de Nanociencia de Aragón	Spain
De Teresa Nogueras	José Maria	Instituto de Ciencia de Materiales de Aragón	Spain
de Torres	Esther	Midatech Biogune S.L.	Spain
del Castillo Vargas	Javier	Universidad de la Laguna	Spain
Delville	Marie-Helene	ICMCB/CNRS	France
Diez	Dionisio	MAB Industrial, S.L.U	Spain
Donaire	Manuel	Universidad Autónoma de Madrid	Spain
Doria	Gonçalo	CIGMH/DCV & REQUIMTE/DQ - FCT/UNL	Portugal
Douglas	Trevor	Montana State University	USA
Dubegny	Christophe	Schaefer Techniques	France
Eaton	Peter	Universidade do porto	Portugal
El Hawi	Nancy	LPCNO - INSA Toulouse	France
Elizondo Sáez de Vicuña	Elisa	ICMAB - CSIC	Spain
Farjas Silva	Jordi	Universitat de Girona	Spain
Fernandes	Francisco	ICMM - CSIC	Spain
Fernandes	João	Escola Superior de Biotecnología - UCP	Portugal
Fernández	Claudio	Fundación Lurederra	Spain
Fernández	Rafael	Nanotec Electrónica S.L.	Spain
Fernández	Iván	Instituto de Microelectrónica de Madrid-CSIC	Spain
Fernández	Maite	Phantoms Foundation	Spain
Fernández Barquin	Luís	CITIMAC	Spain
Fernández-Cuesta	Irene	Centro Nacional de Microelectrónica	Spain
Ferreira	Carla	University of Porto	Portugal
Ferreira	José	Instituto Superior Técnico	Portugal
Ferreira	Paula	University of Aveiro and CICECO	Portugal
Ferreira	Rute	University of Aveiro-CICECO	Portugal
Ferreira	Tânia	Universidade Minho	Portugal
Figueiredo Lopes	Luís M.	Instituto Superior Técnico	Portugal
Fortunato	Elvira	FCT-UNL/CENIMAT-I3N	Portugal
Franco	Ricardo	REQUIMTE/DQ - FCT/UNL	Portugal
Freitas	Paulo	INESC-MN, IST and INL	Portugal

Last Name	Name	Institution	Country
<b>Froufe</b>	Luís	ICMM - CSIC	Spain
<b>Fujita</b>	Daisuke	National Institute for Materials Science	Japan
<b>Fuss</b>	Martina	Instituto de Microelectrónica de Madrid-CSIC	Spain
<b>García</b>	Daniel	Institut Català de Nanotecnologia	Spain
<b>García Barrientos</b>	Africa	Midatech Biogune S.L.	Spain
<b>García Lastra</b>	Juan María	Universidad del País Vasco	Spain
<b>García Mendoza</b>	Rubén Antonio	Universidad Politécnica de Madrid	Spain
<b>García-Martín</b>	Antonio	Instituto de Microelectrónica de Madrid-CSIC	Spain
<b>García-Mochales</b>	Pedro	Universidad Autónoma de Madrid	Spain
<b>García-Ramos</b>	José V.	Instituto de Estructura de la Materia. CSIC	Spain
<b>Gauffre</b>	Fabienne	University of Toulouse	France
<b>Gil</b>	Adriana	Nanotec Electrónica S.L.	Spain
<b>Gil</b>	Marta	Instituto de Nanociencia de Aragón	Spain
<b>Gomes</b>	Inês	Universidade Nova de Lisboa	Portugal
<b>Gomes</b>	Joana	FEUP	Portugal
<b>Gomes</b>	João	CENTI	Portugal
<b>Gomes</b>	Maria	University of Minho	Portugal
<b>Gomes Coutinho</b>	Paulo José	University of Minho	Portugal
<b>Gómez</b>	Eva	Nanotec Electrónica S.L.	Spain
<b>Gómez de Pedro</b>	Sara	Universitat Autònoma de Barcelona	Spain
<b>Gonçalves</b>	Gonzalo	FCT-UNL/CENIMAT-I3N	Portugal
<b>Gonçalves</b>	Luis	Universidade do Minho	Portugal
<b>González</b>	Cristina	Alava Ingenieros/ Medida y Calibración	Spain
<b>González</b>	José Miguel	Instituto de Carboquímica-CSIC	Spain
<b>González</b>	Mónica	Instituto de Carboquímica-CSIC	Spain
<b>González Fernández</b>	Africa	Universidad de Vigo	Spain
<b>González Jorge</b>	Higinio	Laboratorio Oficial de Metroloxía de Galicia	Spain
<b>González-Díaz</b>	Juan Bautista	Instituto de Microelectrónica de Madrid-CSIC	Spain
<b>Gourdon</b>	André	CNRS CEMES	France
<b>Grazu Bonavia</b>	Maria Valeria	Instituto de Nanociencia de Aragón	Spain
<b>Griol</b>	Amadeu	Nanophotonics Technology Center	Spain
<b>Guari</b>	Yannick	Institut Charles Gerhardt Montpellier	France
<b>Guedes</b>	André	INESC-MN	Portugal
<b>Guerrero Ramírez</b>	Luís Guillermo	Universidad del País Vasco	Spain
<b>Hanbucken</b>	Magrit	Direction Générale de la Recherche et de l'Innovation (DGRI)	France
<b>Hernández Borrell</b>	Jordi	University of Barcelona	Spain
<b>Hernández-Palacios</b>	Martin	Aliter	Spain
<b>Hervías Sarasqueta</b>	Xabier	Universidad del País Vasco	Spain
<b>Hortigüela</b>	María Jesús	ICMM - CSIC	Spain
<b>Hungerford</b>	Graham	Universidade do Minho	Portugal
<b>Huntzinger</b>	Jean-Roch	Université Montpellier 2 / GES	France
<b>Imaz</b>	Inhar	Nanosfun- Institut català de nanotecnologia	Spain
<b>Jaafar</b>	Miriam	ICMM-CSIC	Spain
<b>Jaque Rechea</b>	Francisco	Universidad Autónoma de Madrid	Spain
<b>Jiménez</b>	David	Universitat Autònoma de Barcelona	Spain
<b>Kahn</b>	Myrtil	CNRS	France
<b>Kaltzakorta</b>	Idurre	LABEIN-TECNALIA	Spain
<b>Kholkin</b>	Andrei	Universidade de Aveiro	Portugal
<b>Kippenberg</b>	Tobias J.	Max-Planck Institute of Quantum Optics	Germany
<b>Kläui</b>	Mathias	University of Konstanz	Germany
<b>Köber</b>	Mariana	Instituto de Microelectrónica de Madrid-CSIC	Spain
<b>Lajos</b>	Gejza	Safarik University	Slovakia
<b>Lalo</b>	Helene	LAAS-CNRS	France
<b>Lamela Prieto</b>	Jorge	Universidad Autónoma de Madrid	Spain
<b>Lanceros-Mendez</b>	Senentxu	Universidade do Minho	Portugal
<b>Laranjeira</b>	Pedro	Dias de Sousa S.A.	Portugal

Last Name	Name	Institution	Country
Laukhina	Elena	CIBER-BBN/ICMAB-CSIC	Spain
Lecommandoux	Sebastien	LCPO, University of Bordeaux	France
Leitao	Diana	IFIMUP	Portugal
Lermo	Anabel	Universitat Autònoma de Barcelona	Spain
Liebana Girona	Susana	Universitat Autònoma de Barcelona	Spain
Lingenfelder	Magalí	Max Planck institute for solid state research	Germany
López	Hender	Universitat Autònoma de Barcelona	Spain
López Ramírez	María Rosa	Universidad de Málaga	Spain
López Vázquez de Parga	Amadeo	Universidad Autónoma de Madrid	Spain
López-Ruiz	Román	Instituto de Ciencia de Materiales de Aragón	Spain
Loureiro	Joana	INESC_MN / IST	Portugal
Lugo Chacón	Nayar Adolfo	Universidad Politécnica de Cataluña	Spain
Macedo	Rita	INESC-MN	Portugal
Machado	Bruno	Laboratório de Catálise e Materiais/FEUP	Portugal
Maestu	Ceferino	Universidad Politecnica de Madrid	Spain
Maia	Joao	University of Minho	Portugal
Malainho	Eva	Universidade do Minho	Portugal
Malta	Oscar L.	Universidade de Pernambuco	Brazil
Maria	Maris	University of Constanza	Romania
Marín	Sergio	Institut Catala de Nanotecnología	Spain
Marques	Leonel	University of Aveiro and CICECO	Portugal
Martín	Iñigo	Centro Nacional de Microelectrónica	Spain
Martínez	Elena	Institut de Bioenginyeria de Catalunya (IBEC)	Spain
Martínez	María Teresa	Instituto de Carboquímica-CSIC	Spain
Martínez de Baroja	Natalia	Instituto de Nanociencia de Aragón	Spain
Martínez de Morentin	Luís	Fundación Lurederra	Spain
Martínez Pérez	Maria José	Instituto de Ciencia de Materiales de Aragón	Spain
Martínez Rincón	Marta	Universidad Autónoma de Madrid	Spain
Martins	Albino	Universidade do Minho	Portugal
Martins	Ana João	University of Minho	Portugal
Martins	Manuel	University of Aveiro	Portugal
Martins	Pedro	Universidade do Minho	Portugal
Martins	Verónica	Instituto Superior Técnico - CEBQ	Portugal
Mas Torrent	Marta	ICMAB - CSIC	Spain
Maspoch	Daniel	Nanosfun- Institut català de nanotecnologia	Spain
Matos	Henrique	Instituto Superior Técnico	Portugal
Melo	Luís	Fundação para a Ciência e a Tecnologia	Portugal
Melo	Luís F.	University of Porto	Portugal
Merino	Santos	Fundación TEKNIKER	Spain
Miles	Mervyn	University of Bristol	UK
Mina Rosales	Alejandra	Universidad Politécnica de Madrid	Spain
Miranda	Rodolfo	Universidad Autónoma de Madrid	Spain
Mocanu	Valentin	University of Constanta	Romania
Molina	Luís M.	Universidad de Valladolid	Spain
Monge	Miguel	Universidad de La Rioja	Spain
Monteiro	Fernando	INEB- Instituto de Engenharia Biomédica	Portugal
Moreno	Cesar	ICMM - CSIC	Spain
Moreno Llombart	Consuelo	AIDO	Spain
Moros	Maria	Instituto de Nanociencia de Aragón	Spain
Neves	Márcia	Universidade de Aveiro - CICECO	Portugal
Neves	Nuno	University of Minho	Portugal
Niehus	Manfred	ISEL/DEETC	Portugal
Nobre	Sónia	University of Aveiro-CICECO	Portugal
Obiols-Rabasa	Marc	IIQAB - CSIC	Spain
Ordoñez	Luís	Telstar Instrumat S.L.	Spain
Otero Martín	Roberto	IMDEA - Universidad Autónoma de Madrid	Spain

Last Name	Name	Institution	Country
Pacios Pujadó	Mercè	Universitat Autònoma de Barcelona	Spain
Paiva	Maria Conceição	Universidade do Minho	Portugal
Paulo	Pedro	Centro de Química Estrutural - Instituto Superior Técnico	Portugal
Pedro	Luisa	University of Algarve	Portugal
Peláez Machado	Samuel	ICMM-CSIC	Spain
Pelaz	Beatriz	Instituto de Nanociencia de Aragón (INA)	Spain
Pellejero Alcázar	Ismael	Instituto de Nanociencia de Aragón	Spain
Penedo García	Marcos	Instituto de Microelectrónica de Madrid-CSIC	Spain
Peña	Diego	Universidad Santiago de Compostela	Spain
Pereira	Andre	IFIMUP	Portugal
Pereira	Sergio	University of Aveiro-CICECO	Portugal
Peres	Ivone	FEUP	Portugal
Pérez de Luque	Alejandro	Institute of Sustainable Agriculture, CSIC	Spain
Pérez López	Briza	Institut Catala de Nanotecnología (ICN)/UAB	Spain
Pérez Rafael	Sandra	Universitat Autònoma de Barcelona	Spain
Pérez-Murano	Francesc	Centro Nacional de Microelectrónica	Spain
Picas	Laura	University of Barcelona	Spain
Pinho	Elisabete	3B's Research Group	Portugal
Pinho	Sonia	ICMCB/CNRS and University of Aveiro	France
Pinna	Nicola	University of Aveiro	Portugal
Pinto	Sara	Universidade do Minho	Portugal
Pires	Liliana	INEB - Instituto de Engenharia Biomédica	Portugal
Pitães Figueiredo	Hugo Sérgio	Universidade do Minho	Portugal
Pitarke	José Maria	CIC nanoGUNE	Spain
Prada	Marta	University of Wisconsin - Madison	USA
Prieto	Emilio	Centro Español de Metrología	Spain
Proença	Mariana	IFIMUP	Portugal
Puertas	Sara	Instituto de Nanociencia de Aragón	Spain
Querejeta Fernández	Ana	Universidad Complutense de Madrid	Spain
Quintanilla Morales	Marta	Universidad Autónoma de Madrid	Spain
R.P. Queiroz	Maria João	Universidade do Minho	Portugal
Ramalho	Ruben	Instituto Superior Técnico	Portugal
Ramon-Laca	Joaquin	Phantoms Foundation	Spain
Ramos Vega	Daniel	Instituto de Microelectrónica de Madrid-CSIC	Spain
Rauwel	Erwan	University of Aveiro-CICECO	Portugal
Reguera Gomez	Javier	Universidad de Valladolid	Spain
Rei	Ana	Universidade do Minho	Portugal
Retolaza	Aritz	Fundación TEKNIKER	Spain
Reyntjens	Steve	FEI Company	Netherlands
Ribeiro	Sidney J.L.	Instituto de Química- UNESP	Brazil
Rivas	José	International Iberian Nanotechnology Laboratory - INL	Portugal
Rivaya	Alfonso	BIOMETA	Spain
Rocha	Joao	University of Aveiro-CICECO	Portugal
Rocha	Sandra	FEUP	Portugal
Rodas Expósito	Yolanda	Chemical Engineering and Environment Technology	Spain
Rodica	Sirbu	University of Constanza	Romania
Rodrigues	João	Universidade da Madeira	Portugal
Rodrigues	Rogério	IBB/CBME - Universidade do Algarve	Portugal
Rodrigues da Graca	Anabela	ESTeSL	Portugal
Rodríguez	Ángel	Universidad Politécnica de Cataluña	Spain
Rodríguez Abreu	Carlos	IIQAB - CSIC	Spain
Rodríguez Cantó	Pedro Javier	Nanophotonics Technology Center	Spain
Rodríguez-Vázquez	María J.	Universidad de Santiago de Compostela	Spain
Roldan	José Luís	Phantoms Foundation	Spain

Last Name	Name	Institution	Country
Rubio	Angel	Universidad del País Vasco (UPV)	Spain
Ruiz de Luzuriaga	Alaitz	Cidetec/Nuevos materiales	Spain
Sáenz	Juan José	Universidad Autonoma de Madrid	Spain
Sahagun	Enrique	Universidad Autónoma de Madrid	Spain
Sainz	Miguel	Fundacion Lurederra	Spain
Sala	Mar	TELSTAR INSTRUMAT, S.L.	Spain
Salazar Serge	Norkis	Universidad Simón Bolívar	Venezuela
Salgado Amaro	Mariana	Universidade do Minho	Portugal
Salsamendi	Maitane	Cidetec/Nuevos materiales	Spain
Samitier Marti	Samitier Marti	IBEC	Spain
Sampaio Ribeiro de Abreu	Renato Danton	ESTeSL	Portugal
Sánchez	Samuel	Universitat Autònoma de Barcelona	Spain
Sánchez Portal	Daniel	DIPC	Spain
Santaren	Julio	TOLSA S.A.	Spain
Sardon	Haritz	Universidad del País Vasco	Spain
Schwarz	Reinhard	Instituto Superior Técnico	Portugal
Segura	Juan José	Institut Català de Nanotecnologia	Spain
Sencadas	Vitor	Universidade do Minho	Portugal
Serp	Philippe	LCC CNRS	France
Serra	Ricardo	University of Aveiro	Portugal
Serrano	Soraya	Phantoms Foundation	Spain
Sevillano Alaejo	Ignacio	Universidad Politécnica de Madrid	Spain
Silva	Nuno Joao	Instituto de Ciencia de Materiales de Aragón	Spain
Silva Alburquerque	Paula Cristina	ESTeSL	Portugal
Simões	Sandra	INETI - UNFAB	Portugal
Soares	Pedro	Universidade do Minho	Portugal
Soares	Sandra	IBB/CBME - Universidade do Algarve	Portugal
Solans Marsà	Conxita	IIQAB - CSIC	Spain
Sporer	Christian	Institute for Bioengineering of Catalonia (IBEC)	Spain
Stadler	Hartmut	VEECO INSTRUMENTS GmbH	Germany
Stanescu	I. Mihaela	University of Constanta	Romania
Stauber	Tobias	Universidade do Minho	Portugal
Tamayo	Javier	Instituto de Microelectrónica de Madrid-CSIC	Spain
Tejedor Busquets	Robert	Universitat Politècnica de Catalunya	Spain
Tolosa Ruiz	Angel	AIDO	Spain
Tomás	Helena	Universidade da Madeira	Portugal
Torcal-Milla	Francisco J.	Universidad Complutense de Madrid	Spain
Torres	Francesc	Universitat Autònoma de Barcelona	Spain
Trindade	Isabel	IN and IFIMUP	Portugal
Tristany	Mar	Laboratoire de Chimie de Coordination du CNRS	France
Valencia Álvarez	José Luís	Laboratorio Oficial de Metroloxía de Galicia	Spain
Van Hulst	Niek	ICFO-Institut de Ciències Fotòniques	Spain
Vasconcelos	Helena	Universidade dos Açores	Portugal
Vaz Osorio	Inês	REQUIMTE-Universidade do Porto	Portugal
Veciana	Jaume	ICMAB - CSIC	Spain
Ventosa	Nora	ICMAB - CSIC	Spain
Vermelhudo	Vitor	SECIL-C <sup>a</sup> Geral de Cal e Cimento S.A.	Portugal
Vieira	Ana Catarina	University of Minho	Portugal
Vieira	Milena	School of Technology and Management of the Polytechnic	Portugal
Vieira	Teresa	ICEMS-Departamento de Engenharia Mecânica	Portugal
Willinger	Marc-Georg	University of Aveiro-CICECO	Portugal
Xiao	Jun	CETR	USA
Yagüe	Clara	Instituto de Nanociencia de Aragón	Spain
Yasakau	Kirył	University of Aveiro	Portugal

<b>Last Name</b>	<b>Name</b>	<b>Institution</b>	<b>Country</b>
<b>Zabaleta Llorens</b>	Jone	ICMAB - CSIC	Spain
<b>Zheludkevich</b>	Mikhail	Universidade de Aveiro - CICECO	Portugal





# NANOSPAIN 2008

Braga (Portugal) April 14-18, 2008  
Nanolberian Conference

In collaboration with:



Red Española de Nanotecnología  
Spanish Nanotechnology Network



Parque Científico de Madrid - Pabellon C - 1ªPlanta  
Ctra Colmenar Viejo Km 15  
Campus de Cantoblanco - Universidad Autónoma de Madrid  
28049 Madrid, Spain  
Fax: +34 91 4973471  
E-mail: [antonio@phantomsnet.net](mailto:antonio@phantomsnet.net)  
WEB: <http://www.phantomsnet.net>



International Iberian Nanotechnology Laboratory

FCT Fundação para a Ciência e a Tecnologia  
MINISTÉRIO DA CIÊNCIA, TECNOLOGIA E ENSINO SUPERIOR Portugal

